Ethynyl[2.2]paracyclophanes–
building blocks for carbon rich compounds

Von der Gemeinsamen Naturwissenschaftlichen Fakultät
der Technischen Universität Carolo-Wilhelmina
zu Braunschweig

zur Erlangung des Grades eines
Doktors der Naturwissenschaften
(Dr. rer. nat.)

genehmigte
D i s s e r t a t i o n

von
Heino Hinrichs
aus Aurich

1. Referent: Prof. Dr. H. Hopf
2. Referent: Prof. Dr. L. Ernst
eingereicht am: 27.01.2005
mündliche Prüfung (Disputation) am: 30.03.2005

2005

Teilergebnisse aus dieser Arbeit wurden mit Genehmigung der Gemeinsamen Naturwissenschaftlichen Fakultät, vertreten durch den Mentor der Arbeit, in folgenden Beiträgen vorab veröffentlicht:

Publikation:

L. Bondarenko, I. Dix, H. Hinrichs, H. Hopf, Ethynyl[2.2]paracyclophanes - New Building Blocks for Molecular Scaffolding, *Synthesis* **2004**, 2751-2759.

Tagungsbeiträge:

H. Hinrichs, H. Hopf, M. M. Haley, Synthesis of 4,5-Diethynyl[2.2]paracyclophane (Poster) International Symposium of Novel Aromatic Compounds (ISNA) 2001, San Diego (2001).

H. Hinrichs, J. Marsden, H. Hopf, M. M. Haley, π-π-Wechselwirkungen in Paracyclophan-Dehydrobenzannulenen (Poster) GDCh Jahrestagung 2003, München (2003).

H. Hinrichs, H. Hopf, M. M. Haley, π-π-Interactions in [2.2]Paracyclophane/Dehydro-benzannulenes (Vortrag, Poster) JCF-Frühjahrssymposium 2004, Heidelberg (2004).

H. Hinrichs, H. Hopf, M. M. Haley, Ethynyl[2.2]paracyclophanes as building blocks for carbon rich compounds (Poster) 14. Vortragstagung der Liebig-Vereinigung für Organische Chemie der Gesellschaft Deutscher Chemiker (ORCHEM 2004), Bad Nauheim (2004).

Die vorliegende Arbeit wurde in der Zeit von Oktober 2000 bis September 2004 am Institut für Organische Chemie der Technischen Universität Braunschweig unter der Leitung von Prof. Dr. H. Hopf angefertigt.

I wish to express my sincere gratitude to Prof. Dr. Henning Hopf for his supervision, support and encouragement throughout this research. Without his ideas, remarks, advice and endless interest, this study could not have been carried out and completed.

I am very grateful to Prof. Michael M. Haley for the research opportunity he gave me during my short visit in Eugene, Oregon. I also wish to thank him for his advice, ideas, valuable discussions and remarks.

I offer my sincere thanks to Prof. Dr. P. G. Jones and Dr. I. Dix for the X-ray structure analyses; Ms. P. Holba-Schulz for high resolution and 2D NMR spectra; Ms. K. Kadhim for UV and IR spectra; Dr. U. Papke and Ms. D. Döring for MS spectra, Dr. T. Beuerle for GC/MS analyses; Dr. M. Nimz from GBF Braunschweig Stöckheim for MALDI TOF mass spectrometry and Dr. J. Grunenberg and Prof. Dr. R. Herges for molecular modeling studies.

I am very grateful to Prof. Dr. L. Ernst and Dr. K. Ibrom for many valuable discussions about the NMR spectra and the iterative analyses of the bridge protons of **56**, **98**, **99**, **111**, **144** and **153**. Furthermore, I am thankful to Prof. Dr. L. Ernst for agreeing to be the co-referee of my thesis.

I thank all the group members of Prof. Dr. H. Hopf and Dr. U. Jahn.
I also thank all the members of the Haley group who made my time in Oregon very enjoyable.

To my parents

and

Mădălina

Table of Contents

1 Introduction

Since the isolation of benzene ([6]annulene, **1**) by Faraday in 1825[1], chemists are interested to understand the unusual chemical properties of this hydrocarbon. The next higher vinylog, [8]annulene (1,3,5,7-cyclooctatetraene, **2**) was synthesized in 1911 by Willstätter in minute amounts by a lengthy synthetic sequence, making comprehensive studies of the chemical behavior impossible.[2] In 1940, Reppe and coworkers discovered that acetylene can be cyclotetramerized to **2** in the presence of catalytic amounts of nickel(II) salts. It was shown that **2** has a boat like structure **3** and behaves as a typical cyclopolyolefin and not like an aromatic molecule.[3, 4]

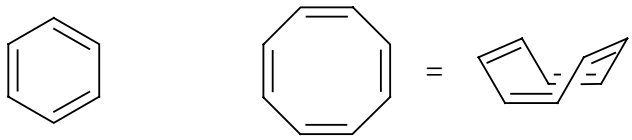

1 **2** **3**

Figure 1: [6]- and [8]annulene.

One way to planarize **3** is the replacement of a double by a triple bond leading to cyclooctatrieneyne (**5**). This hydrocarbon was synthesized by Krebs from bromocyclooctatetraene (**4**) by treatment with potassium *tert*-butoxide.[5] Unfortunately, **5** was too reactive to measure its NMR spectra. But the intermediate formation was proven by trapping with tetraphenylcyclopentadienone and decarbonylation to the Diels-Alder adduct **6**.

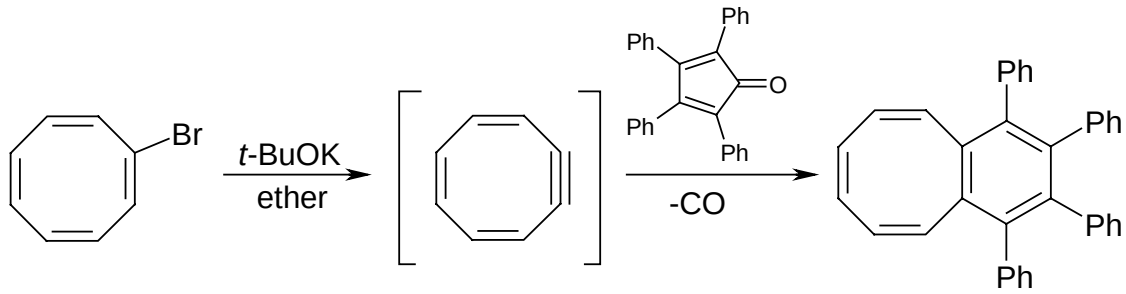

4 **5** **6**

Scheme 1: Synthesis of a planar derivative of cyclooctatetraene by Krebs.[5]

Stabilizing the dehydroannulene by annelation with benzene rings gave the relatively unstable, but planar hydrocarbon **8** which was subjected to ^{1}H NMR analysis, indicating that **8** is a paratropic hydrocarbon.[6]

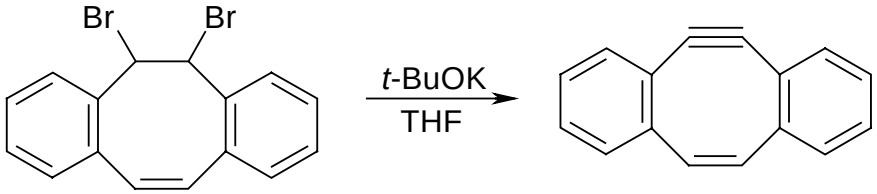

7 **8**

Scheme 2: Synthesis of dibenzodehydro[8]annulene (8).[6]

In the late 1950s, Eglinton and coworkers described novel carbocyclic products (dehydrobenzoannulenes, DBAs) like **9**, obtained by oxidative coupling of terminal acetylenes.[7] Later, the authors showed that the initially assumed structure **9**, proposed on the basis of strain considerations, was incorrect; instead the strained dimer **10** has been formed.[8, 9]

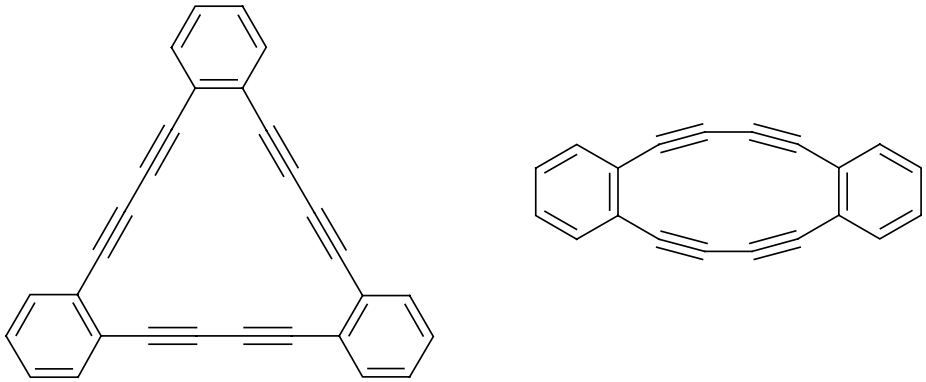

9 **10**

Figure 2: Dehydrobenzoannulenes reported by Eglinton.[7]

In those days, terminal acetylenes were usually obtained by conversion of two-carbon side chains using methods that include halogenation/dehalogenation of vinyl- or acetylarenes (Scheme 3). Alternatively, carbon chains were introduced into the aromatic ring by Vilsmeier and related processes.

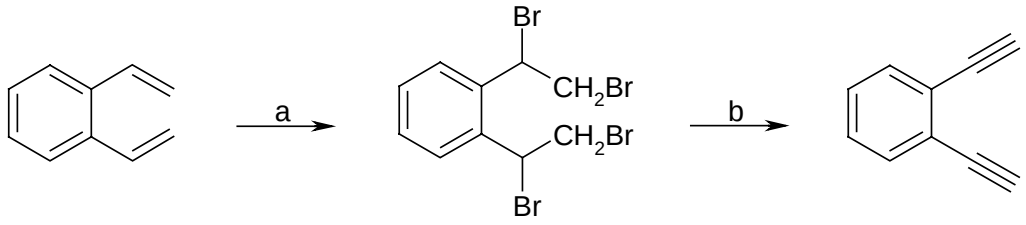

11 **12** **13**

(a) Br_2, CCl_4; (b) *t*-BuOK, *t*-BuOH; *t*-BuOK, benzene

Scheme 3: Synthesis of *ortho*-diethynylbenzene from divinyl precursors.

The driving force for the synthesis of DBAs in the next 20 years was the question of ring currents in those macrocyclic systems.

The first *meta*-substituted DBA **18** was synthesized in 1974 by Staab and Neunhoeffer using the Stephens-Castro coupling of 3-ethynyl-iodobenzene (**16**) in the critical step (Scheme 4).[10] This intermediate was prepared from the acetyl precursor **14** as also summarized in Scheme 4.

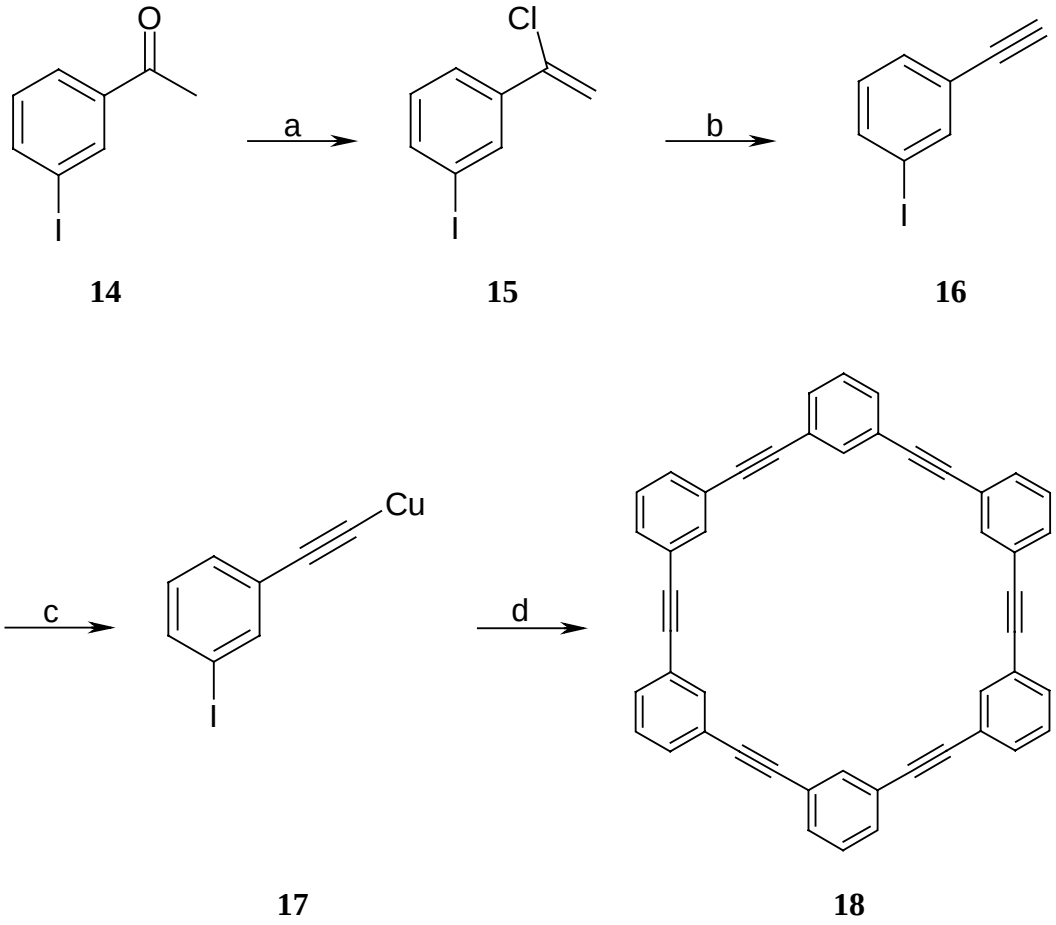

14 **15** **16**

17 **18**

(a) PCl_5; (b) *t*-BuOK, *t*-BuOH; (c) CuCl, NH_3, H_2O, EtOH; (d) pyridine, Δ

Scheme 4: Synthesis of DBA **18** by Staab and Neunhoeffer.[10]

In 1980, Sonogashira reported a convenient synthesis of ethynylarenes by Pd-catalyzed cross-coupling of bromo- or iodoarenes with trimethylsilylacetylene (TMSA).[11] This method has become the keystep for the construction of ethynylated arenes and the resulting DBAs ever since.

Beginning in the early 1990s, a renewed interest in the field of annulene chemistry could be noted because these hydrocarbons became important substrates in material science applications such as nonlinear optical behavior,[12] polymerization to tubular polymers[13] or even explosions to furnish carbon nanostructures.[14]

In 1997, 40 years after Eglinton's later corrected report of the synthesis of **9**, Haley and coworkers have synthesized this molecule by intramolecular ring closure of **21** (Scheme 5).[15]

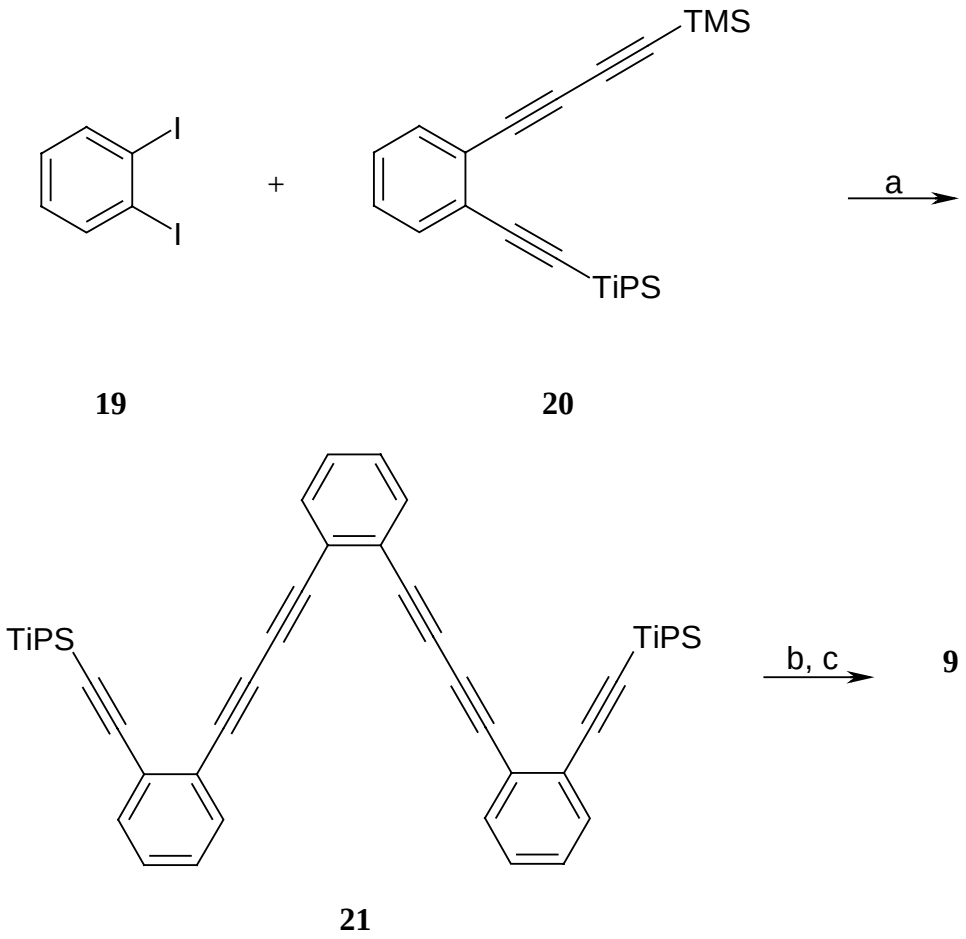

(a) KOH, H_2O, $Pd(PPh_3)_4$, $PdCl_2(PPh_3)_2$, CuI, NEt_3, THF; (b) Bu_4NF, EtOH, THF; (c) $Cu(OAc)_2 \cdot H_2O$, pyridine, CH_3OH

Scheme 5: Synthesis of DBA **21** by intramolecular ring closure acc. by Haley et al.[15]

Due to the instability of terminal diacetylenes, an *in situ* deprotection/alkynylation procedure was developed by Haley. Under pseudo high dilution conditions, the more labile TMS group was removed from 1-[(triisopropylsilyl)-ethynyl]-2-(4-trimethylsilyl-buta-1,3-diynyl)benzene (**20)** *in situ* using KOH, and the resultant butadiyne was coupled with 1,2-diiodobenzene (**19**) under otherwise typical Sonogashira conditions. Protodesilylation of **21** with TBAF followed by oxidative dimerization with $Cu(OAc)_2$ in pyridine gave the [18]annulene **9**.

Compared to organic dehydroannulenes, much less is known about systems that incorporate organometallic fragments. These compounds are on the one hand interesting from their spectroscopic viewpoint, on the other, they offer a high potential in material

science, for example the synthesis and application of metal containing nanostructures. Bunz and coworkers have synthesized systems incorporating metal organic complexes like bis(trimethylsilyl)cyclobutadiene-(cyclopentadienyl-cobalt) **24** (Scheme 6).[16]

Reaction of cyclobutadiene **22** with 1-chloro-4-trimethylsilylbuten-3-yne (**175**) under Pd/Cu catalysis in piperidine furnished the cyclobutadiene complex **23**. Deprotection with K_2CO_3 followed by oxidative cyclization with $Cu(OAc)_2$ in acetonitrile gave the CpCo(cyclobutadieno)-fused dehydroannulene **24** in 74% yield.

Surprisingly, ^{1}H NMR studies suggest that the fused cyclobutadiene complex might be more aromatic than benzene. This postulate is based on Scott's and Günther's [17] model for the determination of aromaticity by regarding the chemical shifts and $^3J_{HH}$ coupling constants of the vinylic protons in an annulene.

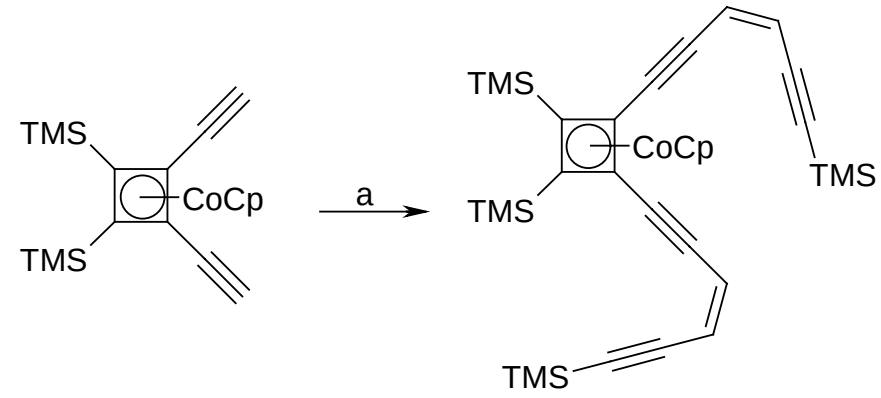

22 **23**

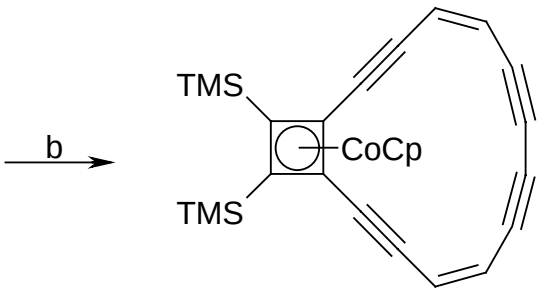

24

(a) 1-chloro-4-trimethylsilylbuten-3-yne (**175**), $Pd(PPh_3)_4$, CuI, piperidine; (b) [i] K_2CO_3; [ii] $Cu(OAc)_2$, CH_3CN

Scheme 6: Synthesis of dehydrobenzoannulenes containing metal complexes acc. by Bunz et al.[16]

With tetra(ethynyl)cyclobutadiene-(cyclopentadienyl-cobalt) (**25**) or bis(ethynyl)-ferrocene (**27**), other interesting complexes like **26** or **28** have been synthesized by comparable routes (Scheme 7).[18, 19]

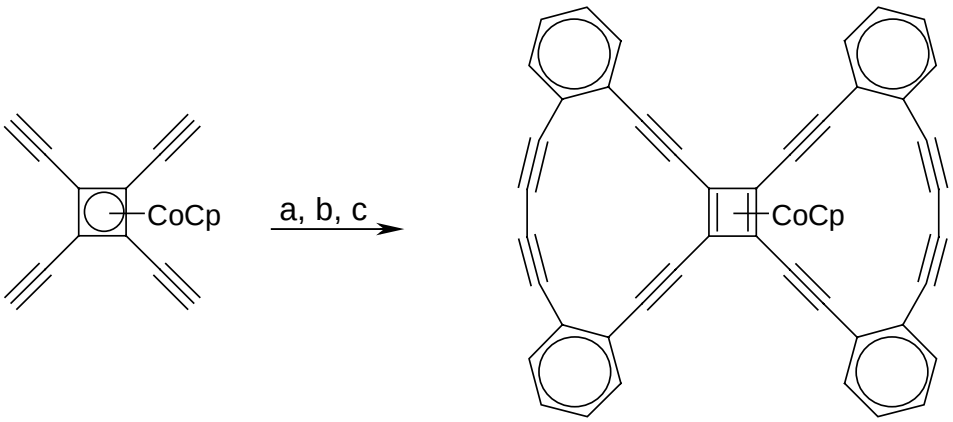

25 **26**

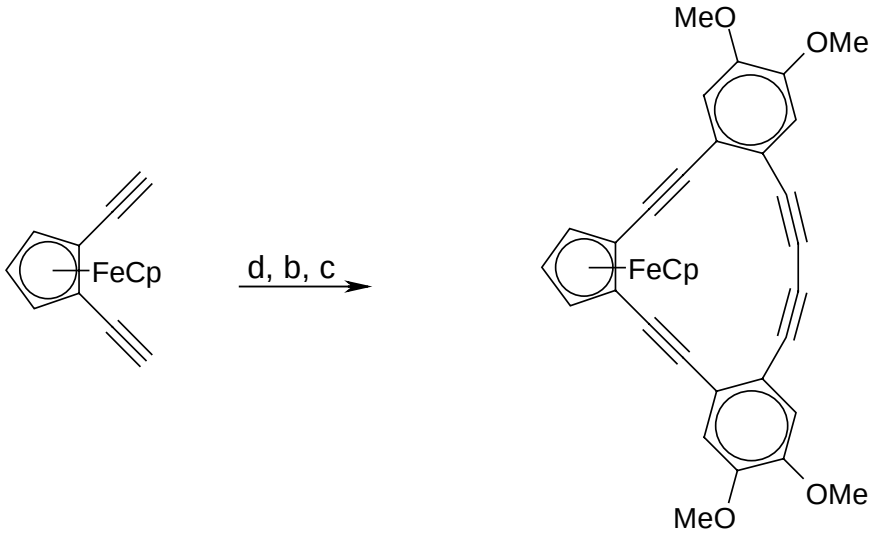

27 **28**

(a) 2-(trimethylsilylethynyl)iodobenzene, $Pd(PPh_3)_2Cl_2$, CuI, piperidine;
(b) K_2CO_3, THF, methanol; (c) $Cu(OAc)_2$, CH_3CN; (d) 3,4-dimethoxy-5-(trimethylsilylethynyl)iodobenzene, $Pd(PPh_3)_2Cl_2$, CuI, amine

Scheme 7: Other dehydrobenzoannulenes containing metal containing subunits.

Twisted cyclophynes (Figure 3) with *para*-bridged central benzene rings such as **29** or the *meta*- bridged derivatives **30** and **31** were synthesized by Fallis and coworkers using Pd- and Cu- mediated cross coupling reactions.[20, 21] The *meta*-bridged isomers do not interconvert because of steric hinderence. Another interesting three-dimensional macrocycle is **32**, synthesized by Rubin and coworkers.[22] In the ion cyclotron mass spectrum, dehydrogenation down to $[C_{60}H_{14}]^-$ was observed.

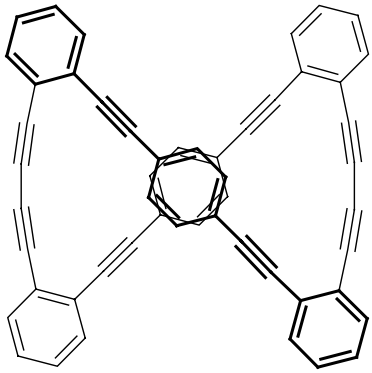

29

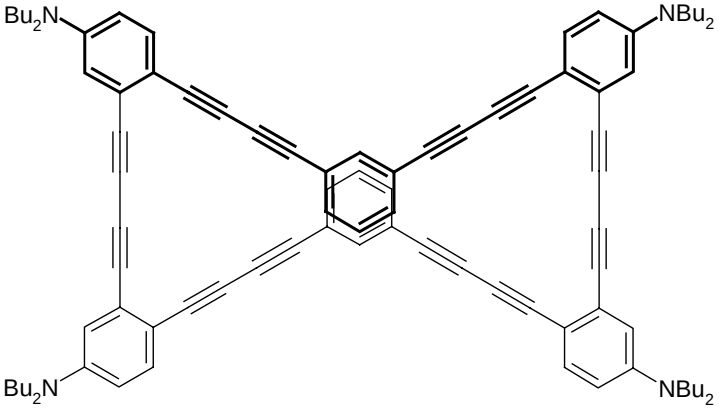

30

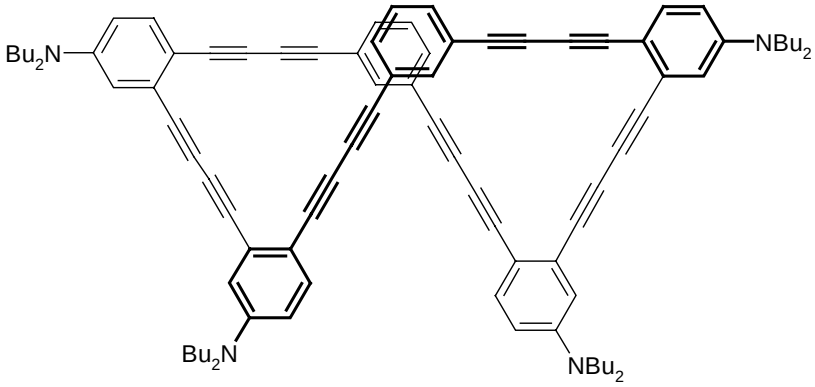

31

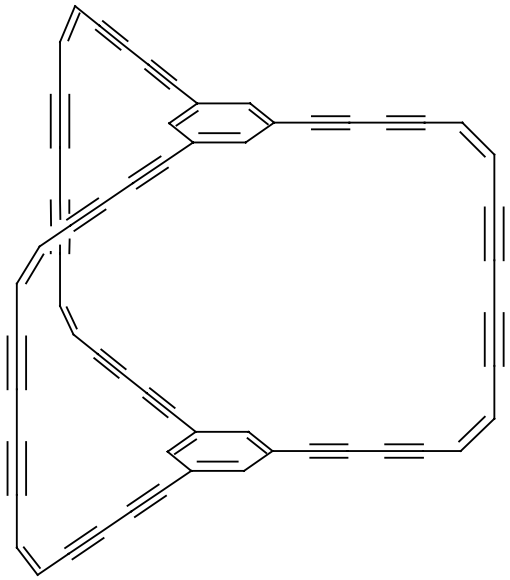

32

Figure 3: Three dimensional cyclophynes synthesized in the groups of Fallis[20, 21] and Rubin et al.[22]

A structurally completely different class of hydrocarbons, which were studied to understand aromaticity, are the cyclophanes especially derivatives of [2.2]paracyclophane (**36**). Traces of this bridged aromatic compound were first isolated in 1949 by Brown and Farthing from pyrolysis products of *p*-xylene (**33**) (Scheme 8).[23]

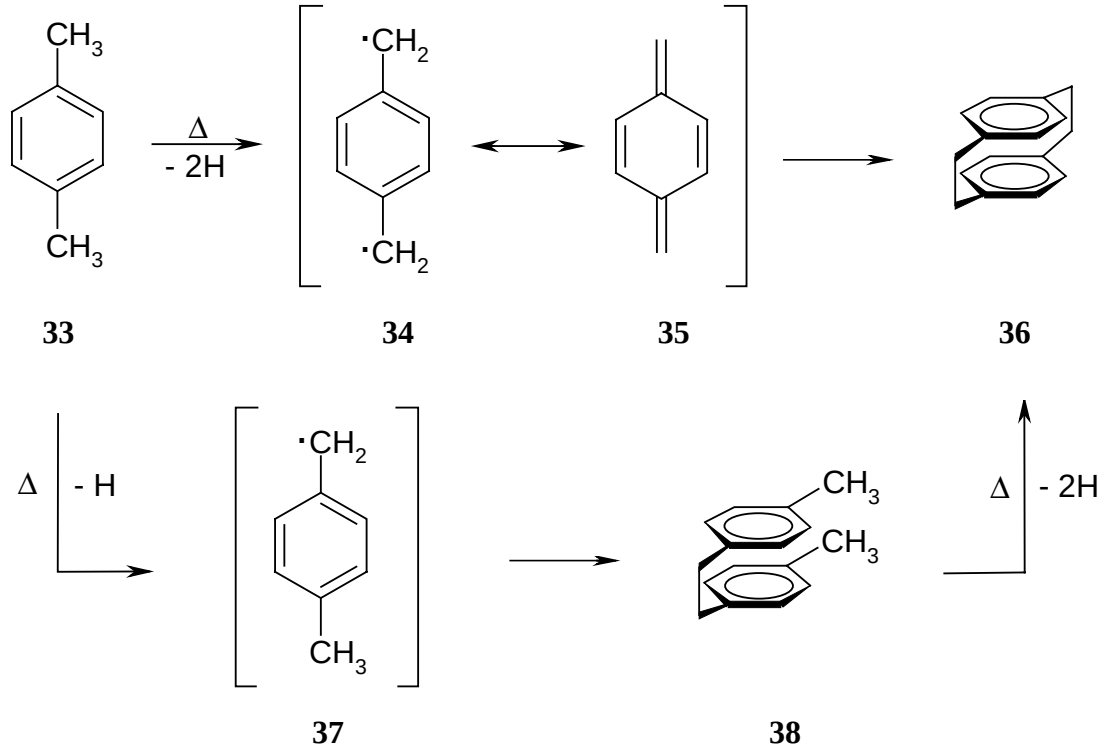

Scheme 8: Synthesis of [2.2]paracyclophane by Brown and Farthing.[23]

The formation of **36** presumably is initiated by abstraction of two hydrogen atoms from *p*-xylene (**33**) to provide the diradical **34**. Out of its mesomeric form, *p*-xylylene (**35**), it could dimerize to **36**. The alternative is a stepwise process *via* the radical **37** which can dimerize to 4,4'-dimethylbibenzyl (**38**). Final dehydrogenation and cyclization of **38** could also lead to [2.2]paracyclophane (**36**).

Two years after the first isolation, Cram and Steinberg presented the first directed route to **36** by Wurtz coupling of 4,4'-dibromomethylbibenzyl (**41**) generated by bromomethylation of bibenzyl (**40**, Scheme 9).[24]

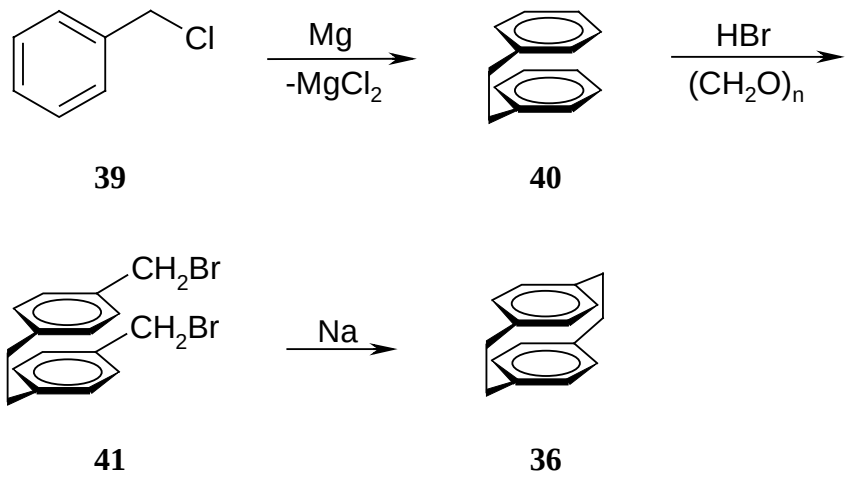

Scheme 9: Synthesis of [2.2]paracyclophane by Cram and Steinberg.[24]

A preparatively more satisfactory method using the dimerization of *p*-xylylenes was discovered by Winberg and Fawcett in 1960.[25] 1,6-Hofmann elimination of *p*-methyl-benzyltrimethylammonium hydroxide (**42**) leads to **35**, which again dimerizes to **36** in yields up to 20% (Scheme 10).

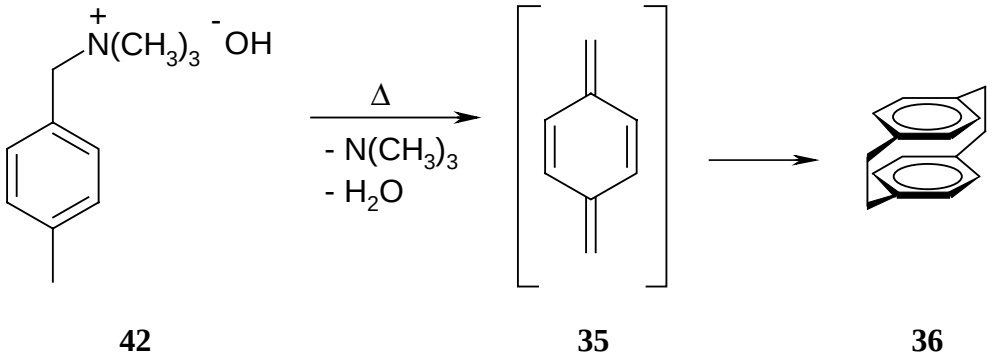

Scheme 10: Synthesis of [2.2]paracyclophane by Winberg and Fawcett.[25]

The dithiacyclophane route (Scheme 11) developed independently by Vögtle[26], Boekelheide[27] and Staab[28] provides in the first step a less strained intermediate, **45**, in which the two benzene rings are already arranged in parallel orientation. By photolytic sulfur extrusion or sulfone pyrolysis of the sulfone **46**, [2.2]paracyclophane (**36**) can be obtained in up to 80% yield.

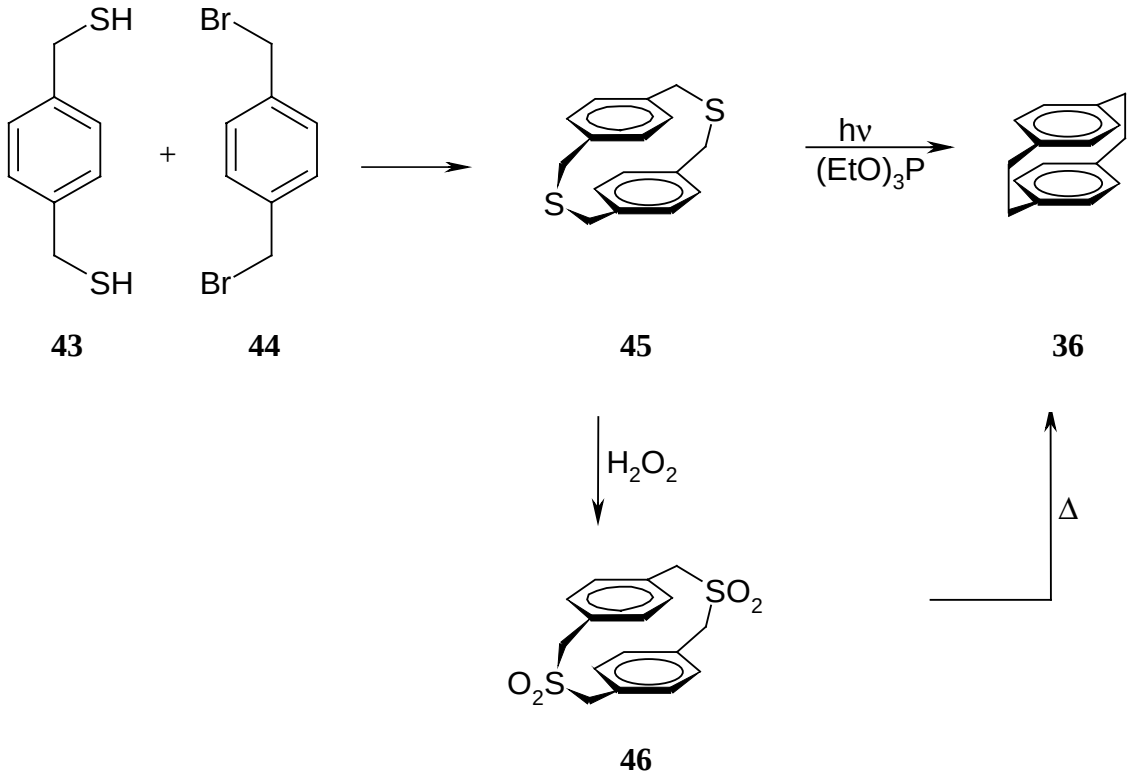

43 **44** **45** **36**

46

Scheme 11: Synthesis of [2.2]paracyclophane (**36**) by the dithiacyclophane route.[26, 27, 28]

The Diels-Alder approach (Scheme 12), developed by Hopf and coworkers from 1972 onwards, was a new method to synthesize functionalized [2.2]paracyclophanes.[29]

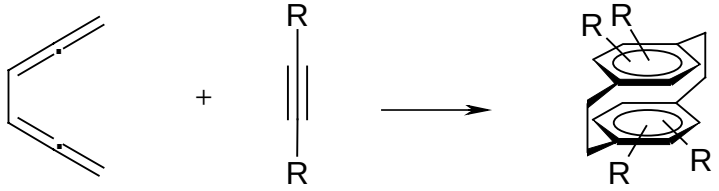

47 **48** **49**

Scheme 12: Hopf's synthesis of functionalized [2.2]paracyclophanes by Diels-Alder approach.[29]

The diene **47** can be prepared by converting propargylbromide into its Grignard reagent, formation of an organocuprate intermediate by transmetallation with cuprous chloride and reacting the cuprate with a second equivalent propargylbromide. In this reaction, propargylallene is formed as side product. The alkynes **48** have to be activated by electron-withdrawing groups. With monosubstituted dienophiles, mixtures of all possible four regioisomers are usually obtained, symmetrical substituted dienophiles lead to 4,5,12,13-tetrasubstituted [2.2]paracyclophanes.

The reason why [2.2]paracyclophanes are interesting compounds for understanding the concept of aromaticity are their unusual structural features such as the nonplanarity and

the small distance between the benzene rings, causing electronic interactions between the aromatic decks. The first X-ray structure analysis of **36** was carried out in 1953 by Brown, showing a boat type deformation of the arene rings.[30]

Numerous studies about the synthesis and chemical behavior of [*m.n*]paracyclophanes were performed in the early 1950s by Cram and coworkers.[24, 31]

In his first paper regarding "Macro Rings", Cram already discussed some expected chemical properties of small [*m.n*]paracyclophanes such as directive and activating or deactivating effects by substituents. Other interesting aspects covered the forces between the aromatic decks by introduction of electron releasing groups in one ring and electron withdrawing groups in the other.[24] In the twelfth paper on "Macro Rings" Cram discussed "Stereochemical Consequences of Steric Compression in the Smallest Paracyclophane".[31 i)] In this article, the synthesis and complete resolution of [2.2]paracyclophane carboxylic acid is also described. In 1969 (35th communication on Macro Rings), Cram described intramolecular effects like the *pseudo-gem* effect, one of the most important effects in paracyclophane chemistry.[32]

The combination of the two classes of hydrocarbons, the annulenes and the [2.2]paracyclophanes should give rise to so called [2.2]paracyclophane/dehydrobenzoannulene hybrids (PC/DBAs). With these systems, it should be possible to learn more about electronic interactions in aromatic systems. The first published example was the *pseudo-ortho* derivative of 1,2:9,10-dibenzo-5,6-[2.2]paracyclophano-3,7,11,13-tetradehydro[14]annulene (**52**), synthesized in a cooperation between the groups of Hopf and Haley by Pd-catalyzed cross coupling reaction of 4,16-diethynyl-[2.2]paracyclophane (**50**) with 2-(trimethylsilylethynyl)iodobenzene to the open tetraacetylene **51,** followed by *in situ* deprotection and oxidative cyclization to **52** (Scheme 13).[33] The bathochromic shift of **52** relative to the broken analogue **51** in the electronic absorption spectra suggests global transannular delocalization throughout the conjugated macrocycle *via* through-space electronic delocalization in the cyclophane.

Since these were only singular results it appeared desirable to extend the experimental basis and initiate a systematic effort aimed at general routes to these novel hydrocarbons. The corresponding preparative efforts providing the model systems **53**, **54** and **55** are described in this dissertation.

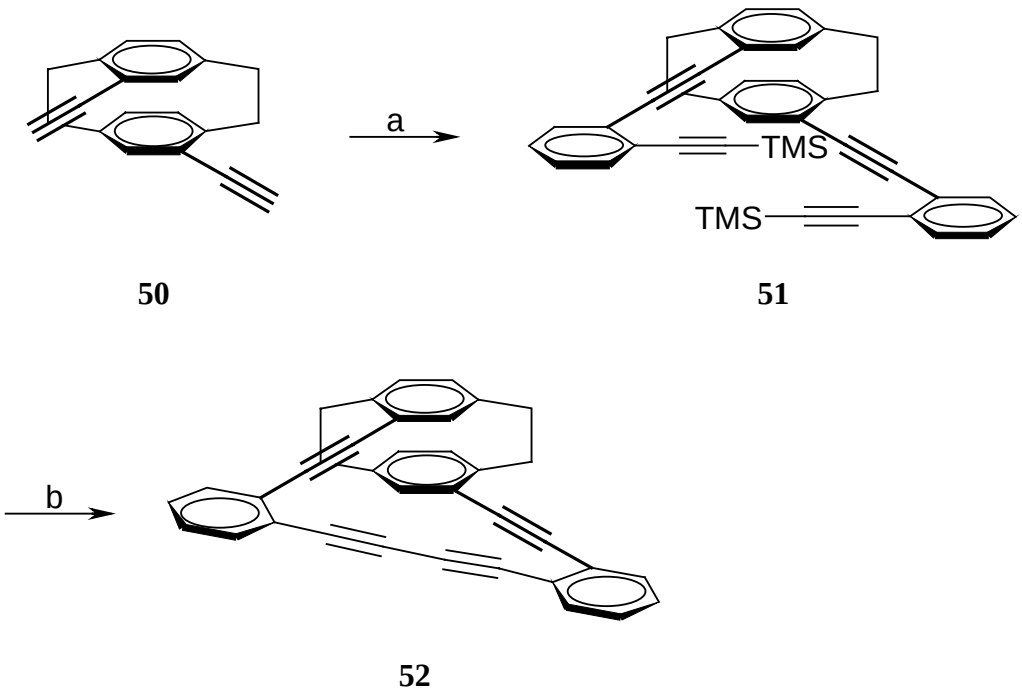

50 **51**

52

(a) 2-(trimethylsilylethynyl)iodobenzene, $Pd(PPh_3)_4$, CuI, NEt_3, THF; (b) K_2CO_3, CuCl, $Cu(OAc)_2$, pyridine, CH_3OH

Scheme 13: Synthesis of the first PC/DBA hybrid by Hopf, Haley et al.[33]

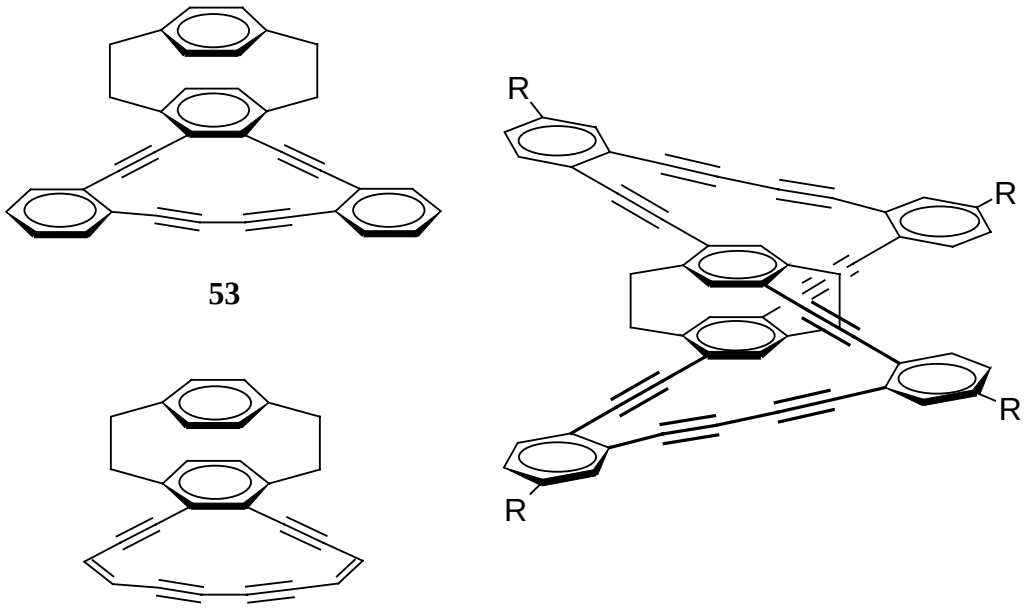

53

54 **55**

Figure 4: PC/DBAs synthesized in this work.

2 Retrosynthetic Analysis

In principle, the [2.2]paracyclophane/dehydrobenzoannulene **53** can be synthesized by two different routes, by intramolecular (Scheme 14) or by intermolecular cyclization (Scheme 15).

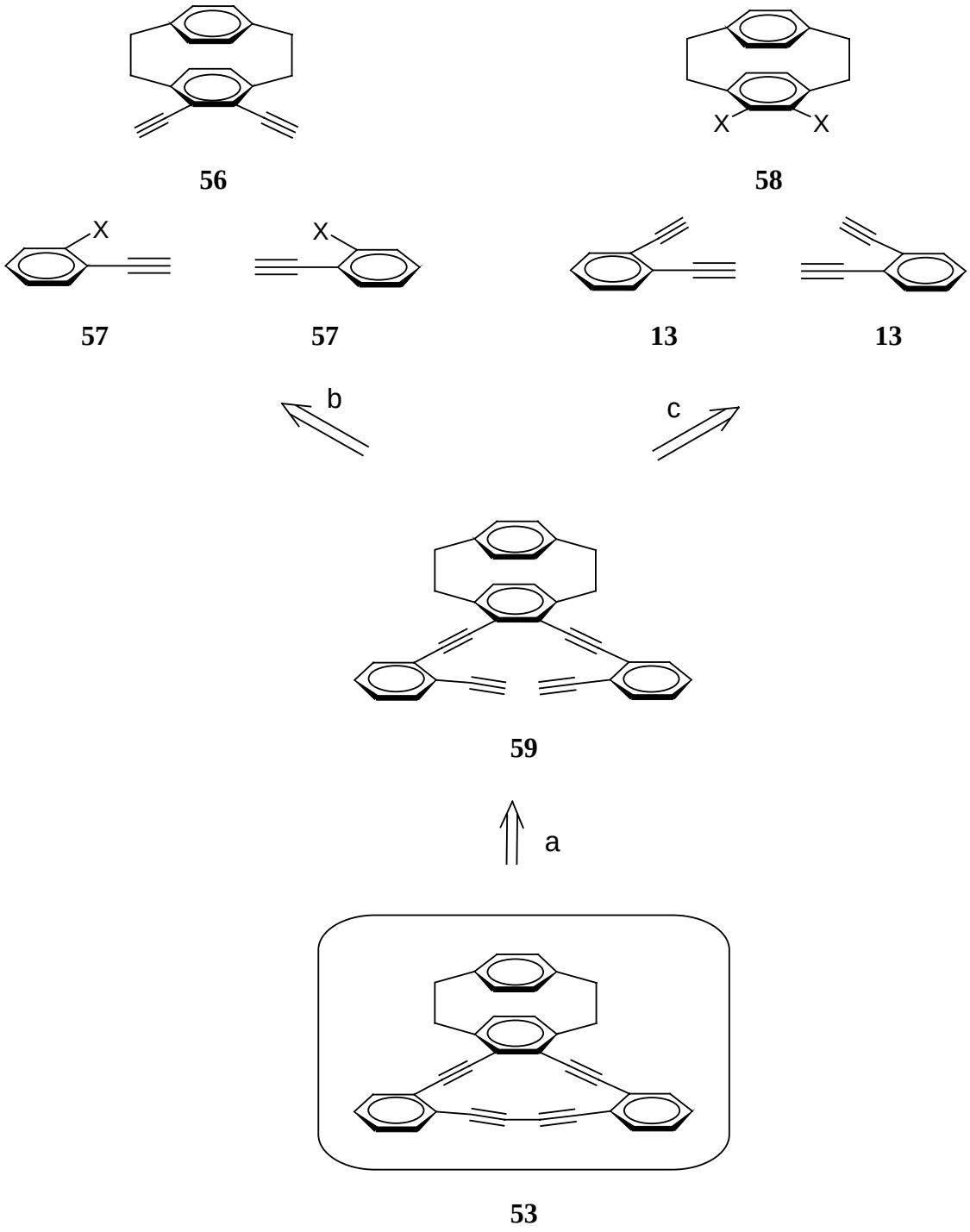

56 **58** **57** **57** **13** **13** **59** **53**

Scheme 14: Retrosynthesis of **53** by intramolecular cyclization.

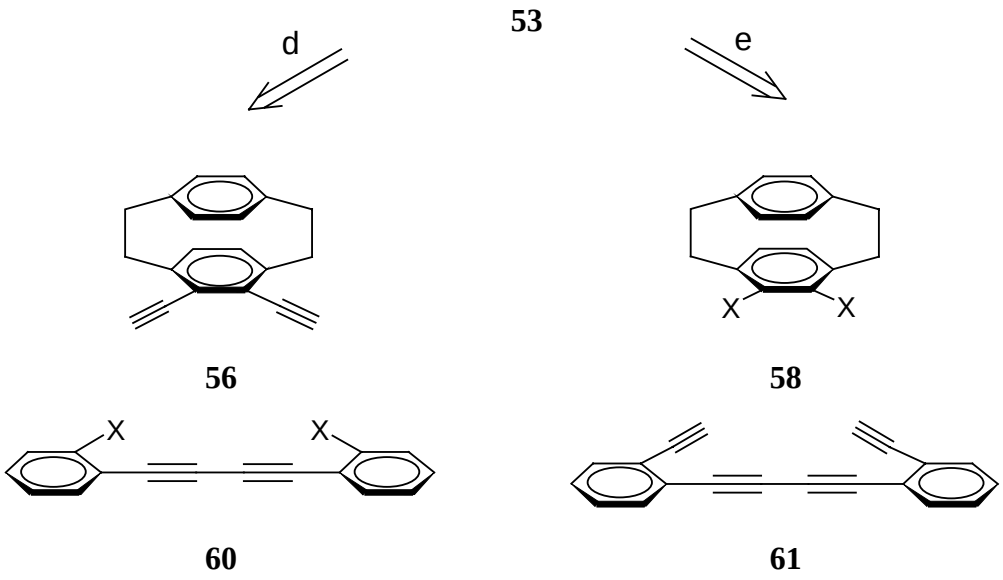

Scheme 15: ... and by intermolecular cyclization.

Step (a) can be split into two possible paths, the coupling of 4,5-diethynyl[2.2]paracyclophane (**56**) with a 2-ethynyl-halobenzene (**57**, cut b) or coupling of a 4,5-dihalo-[2.2]paracyclophane (**58**) with a 1,2-diethynylbenzene (**13**, cut c). The advantage of the intramolecular approach is that the formation of oligomeric compounds is minimized making purification much easier. The drawback is the increased number of steps needed to assemble the precursor for cyclization.

Regardless of the ultimately employed strategy, ethynyl[2.2]paracyclophanes are crucial synthetic intermediates and have hence to be prepared first.

3 4,5-Diethynyl[2.2]paracyclophane (56)

3.1 Synthesis

Several easily accessible precursors like arylhalides, -triflates or -aldehydes can be used for the synthesis of terminal arylacetylenes.

For the conversion of aldehydes, Wittig analogous reactions have usually been used. An example is the synthesis of 4-ethynyl[2.2]paracyclophane (**64**) first described by Hentschel (Scheme 16).[34]

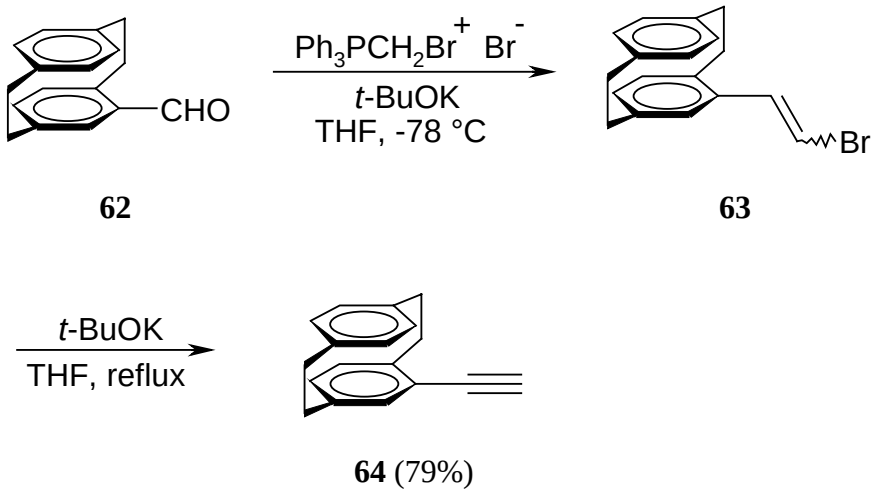

62 **63**

64 (79%)

Scheme 16: Synthesis of 4-ethynyl[2.2]paracyclophane (**64**) by Hentschel.[34]

The first step is a classical Wittig reaction of 4-formyl[2.2]paracyclophane (**62**) with bromomethyltriphenylphosphonium bromide to the vinylbromide **63**. Dehydrobromination then gave the terminal alkyne **64**.

Another Wittig type reaction is the Corey-Fuchs transformation of aldehydes with dibromomethylenetriphenylphosphane (*in situ* generated from triphenylphosphine and carbontetrabromide) to the dibromoolefin. Treatment with *n*-butyllithium or magnesium powder furnishes subsequently the corresponding terminal acetylene.[35]

Hillmer has used this method for the synthesis of the *pseudo-ortho* diethynyl[2.2]paracyclophane (**50**) from the *pseudo-ortho* dialdehyde **65** via the bis(dibromoolefin) **66** in 39% yield with magnesium powder and 78% yield with *n*-butyllithium for the elimination step (Scheme 17).[36]

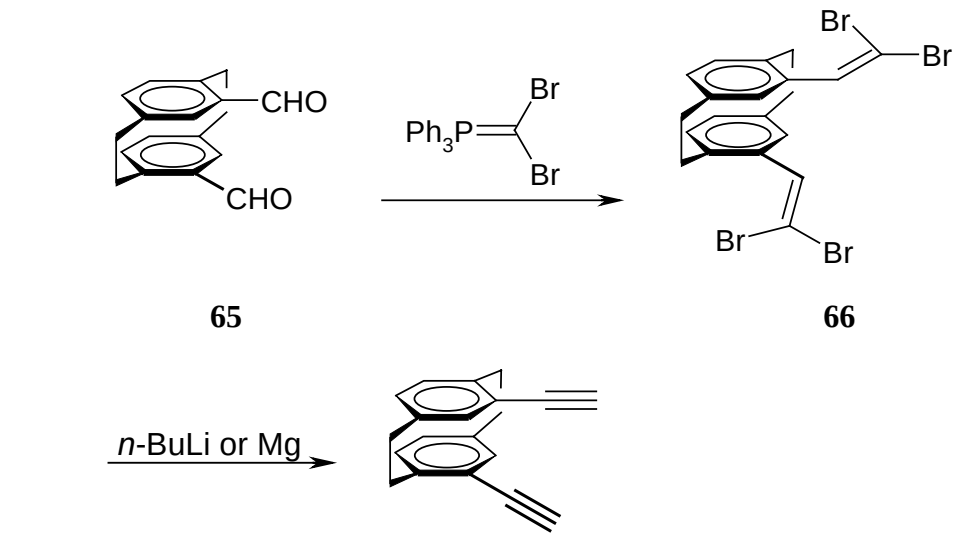

65 **66**

50 (78%, 39%)

Scheme 17: Synthesis of 4,15-diethynyl[2.2]paracyclophane (**50**) by Hillmer.[36]

Bestmann and coworkers have developed a general procedure to convert aldehydes to alkynes which uses dimethyl-1-diazo-2-oxopropylphosphonate (**67**).[37]

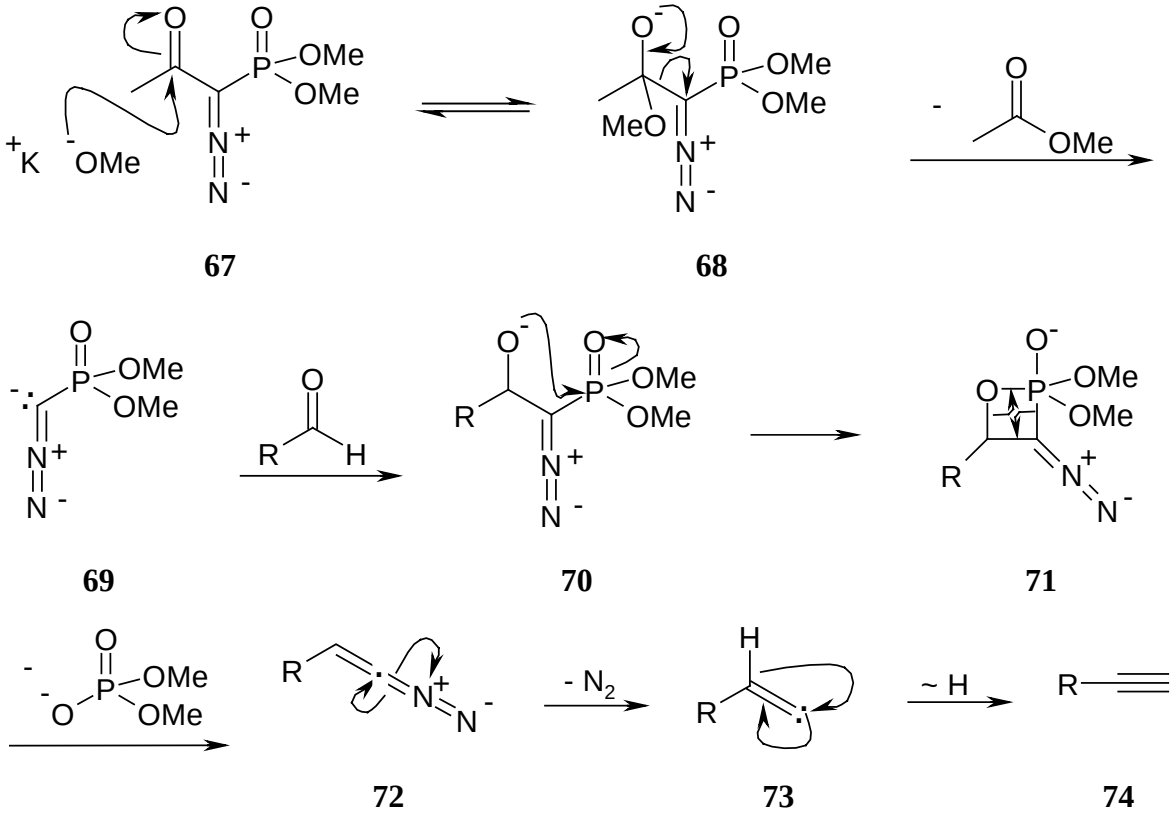

67 **68** **69** **70** **71** **72** **73** **74**

Scheme 18: Mechanism of the alkyne formation using the Bestmann reagent (**67**).

The first step is a nucleophilic attack of potassium methoxide to the carbonyl function of the so called Bestmann reagent **67**. In a retro Claisen reaction via the tetraedric intermediate **68**, the phosphonate anion **69** is formed. This reacts in a Wadsworth-

Emmons reaction with an aldehyde to give **70**. **70** cyclizes to the oxaphosphetane **71** which decomposes to **72**. Elimination of nitrogen forms the vinylcarbene **73**, which undergoes a [1,2]-hydrogen shift to form the terminal alkyne **74**.

Bestmann's method was used in paracyclophane chemistry by Bondarenko and Dix for the synthesis of the *pseudo-geminal* and *pseudo-ortho* diethynyl[2.2]paracyclophanes (**76**) and (**50**) from the corresponding aldehydes **75** and **65** respectively (Scheme 19).[38, 39]

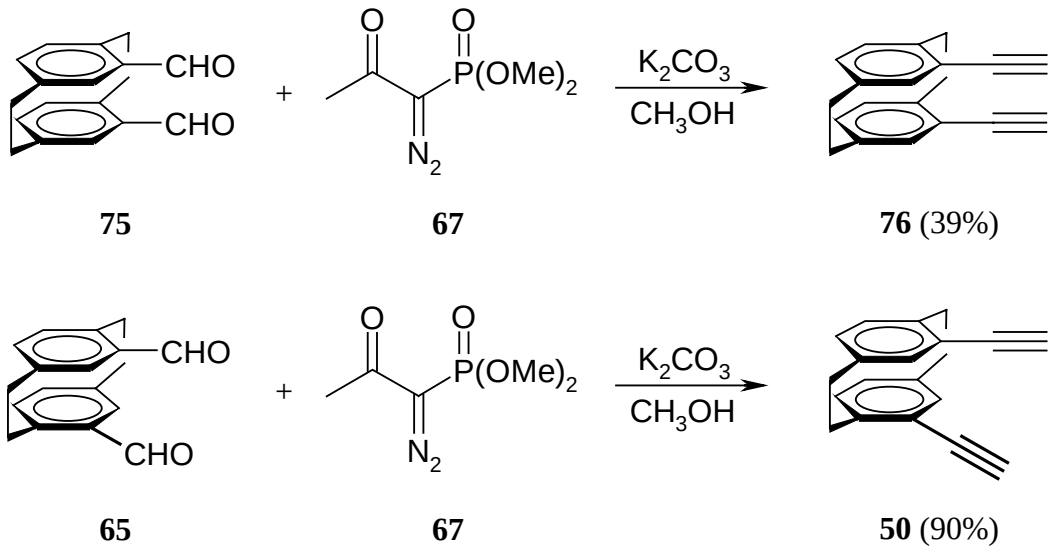

Scheme 19: Synthesis of diethynyl[2.2]paracyclophanes **76** and **50** by Bondarenko and Dix.[38, 39]

In the Sonogashira coupling reaction, widely used for the preparation of ethynyl-alkynes, in the first step (step 1a), a π-complex **78** between the *in situ* generated active Pd(0) species and the arene **77** is formed. By oxidative addition in step (2a), a Pd(II) complex with σ-bounded Pd **79** is formed. This reacts in a transmetallation reaction (step 3) with the copper acetylide **81**, formed in step (1b). Step (4) is a reductive elimination to an alkynylated arene **83** which decomposes in step (5) to give the ethynylbenzene **84** and regenerate the catalytic active Pd(0) species.

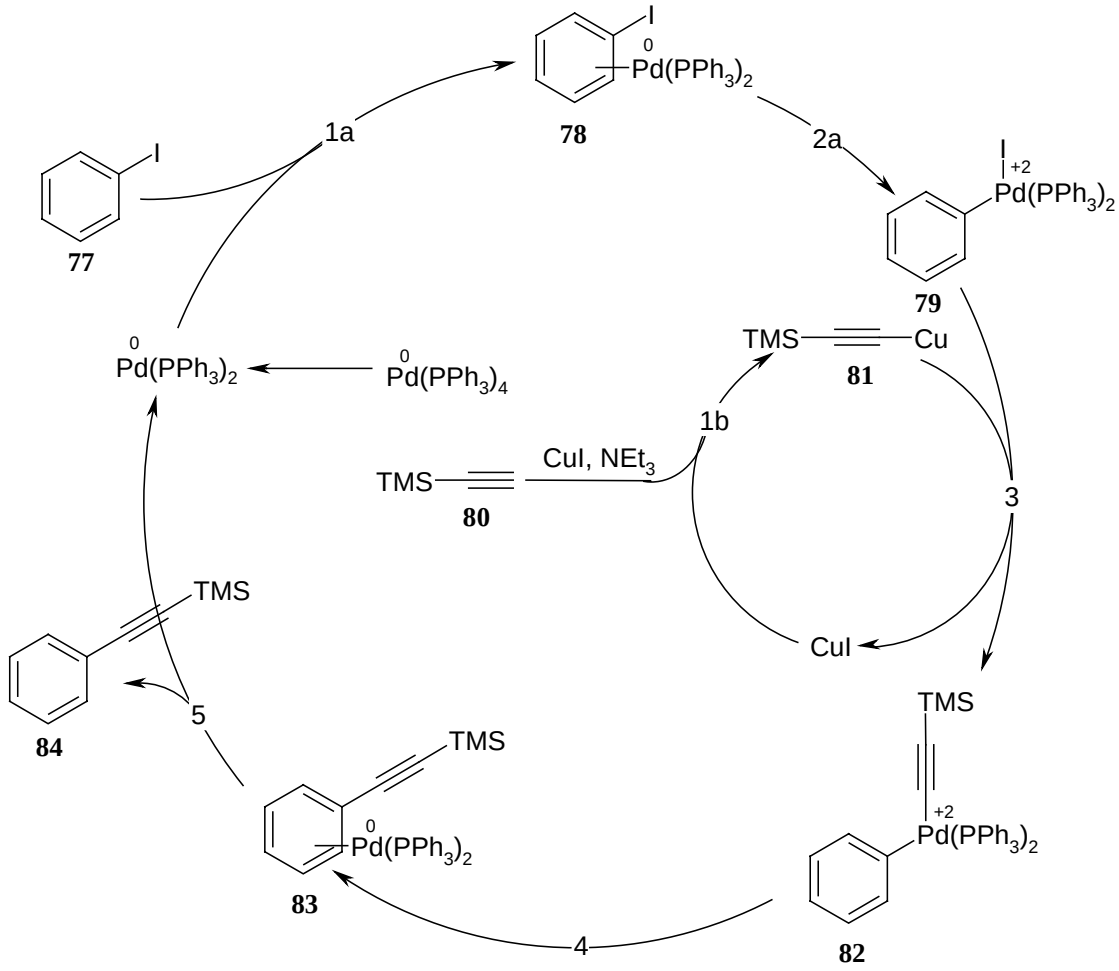

Scheme 20: Mechanism of the Sonogashira reaction.

The synthesis of 4,5-diethynyl[2.2]paracyclophane (**56**) using the previously described methods either needs a 4,5-dihalo[2.2]paracyclophane **58** or 4,5-diformyl[2.2]paracyclophane (**85**) as a precursor molecule (Scheme 21).

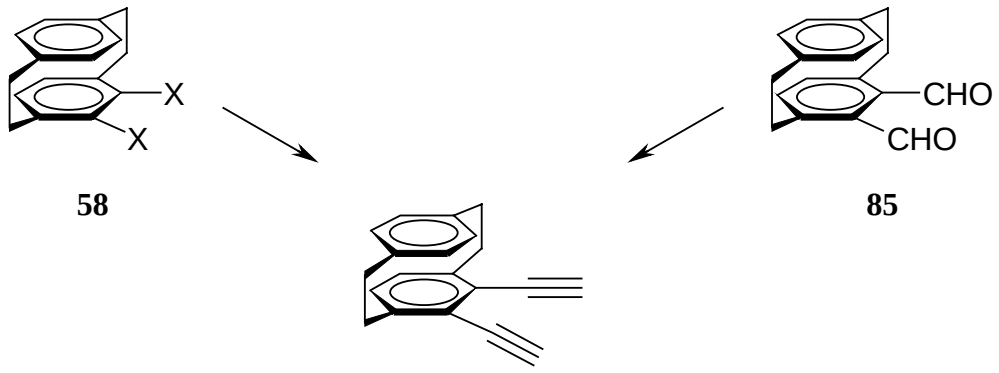

Scheme 21: Synthesis of 4,5-diethynyl[2.2]paracyclophane (**56**) using the dihalide (**58**) or the dialdehyde (**85**).

Several attempts to synthesize the required of 4,5-dibromo[2.2]paracyclophane (**58,** X=Br) have failed through. The bromination of [2.2]paracyclophane (**36**) under various conditions (Scheme 22 and Scheme 23) has been widely studied.

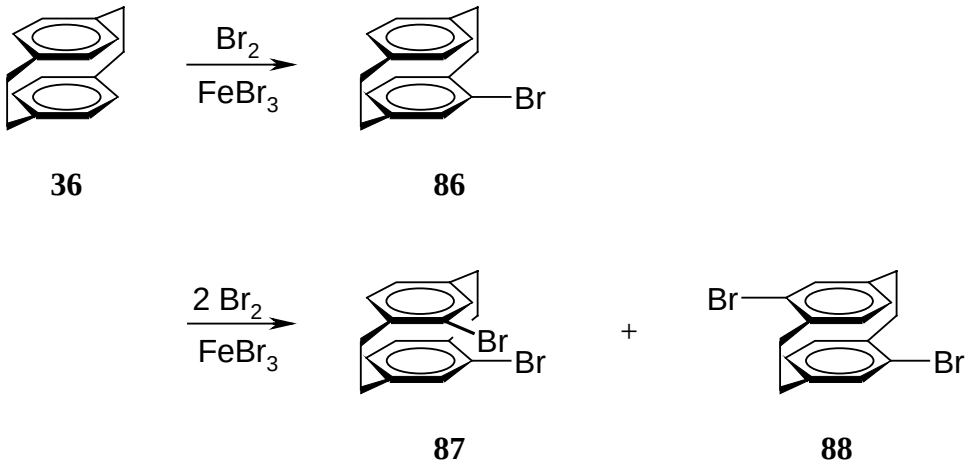

Scheme 22: Bromination of [2.2]paracyclophane (**36**) by Cram and coworkers.[40]

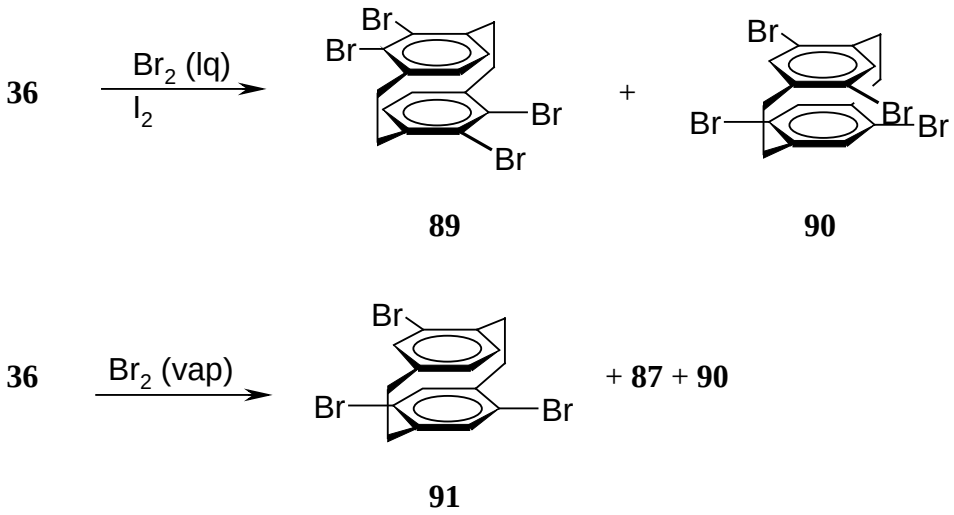

Scheme 23: Bromination of [2.2]paracyclophane (**36**) by König.[41]

The standard aromatic bromination **36** with bromine in the presence of a catalytic amount of $FeBr_3$ to 4-bromo[2.2]paracyclophane (**86**) was carried out in the late 1960s by Cram and coworkers.[40] When two equivalents of bromine were used, a mixture of the *pseudo-ortho* **87** and *pseudo-para* isomer **88** was obtained. König has reported the bromination **36** with liquid bromine and iodine as catalyst.[41] Under these conditions, two isomers, 4,5,12,13-tetrabromo[2.2]paracyclophane (**89**) and 4,7,13,16-tetrabromo-[2.2]paracyclophane (**90**) are obtained in 1:1 ratio (total yield: 91%). By treating **36** with bromine vapors, 4,7,13-tribromo[2.2]paracyclophane (**91**), and the previously described products **87** and **90** were isolated.[41]

The crossed dimerization of different substituted *para*-xylenes **92** and **93**, a standard method for the synthesis of [2.2]paracyclophane derivatives (see above) just gave the known homocoupled products **36** and **89** (Scheme 24).[42]

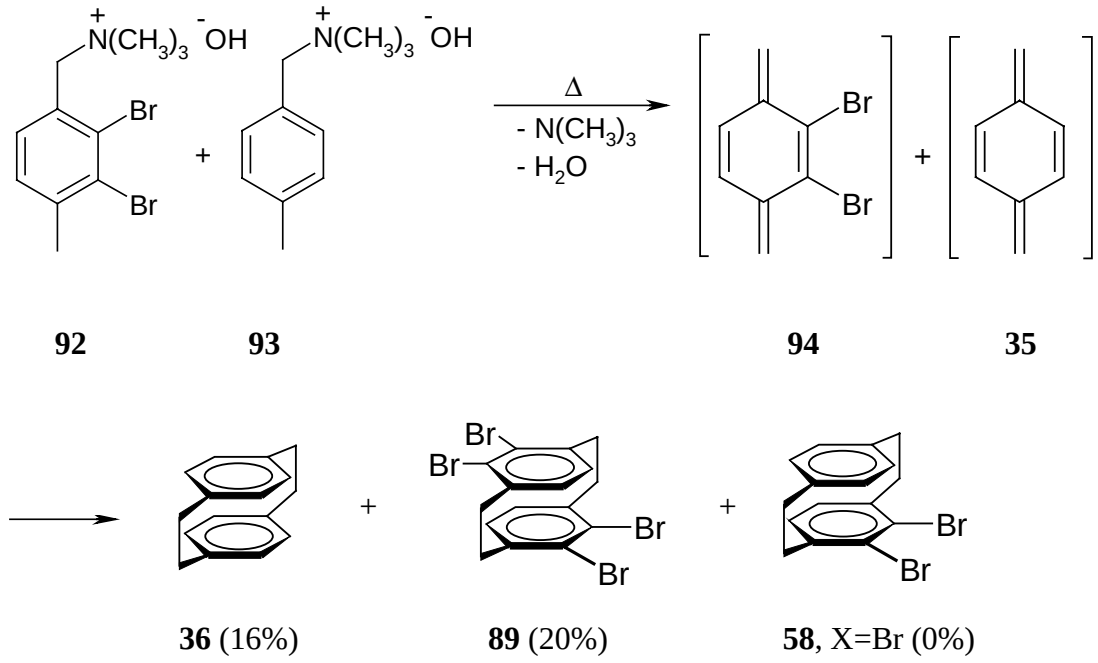

Scheme 24: Failed synthesis of 4,5-dibromo[2.2]paracyclophane by the Hofmann route.[42]

The finally successful synthesis of 4,5-diethynyl[2.2]paracyclophane (**56**) started from known 5-formyl-4-hydroxy[2.2]paracyclophane, FHPC (**97**)[43] which was synthesized in a 4'step reaction from [2.2]paracyclophane (**36**) (Scheme 25). Bromination of **36** with bromine in the presence of $FeBr_3$ as the catalyst in CH_2Cl_2/CCl_4 gave 4-bromo-[2.2]paracyclophane (**86**) in nearly quantitative yield.[44, 45] The conversion to the phenol **95** was carried out by metallation with *n*-butyllithium, reacting the anion with trimethylborate to the arylboronic ester and decomposing the ester with $NaOH/H_2O_2$.[46] The phenol **95** was reacted with diethylcarbamoyl chloride in toluene in the presence of 4-dimethylaminopyridine (DMAP), to give the carbamate **96** in nearly quantitative yield.[43] *Ortho*-lithiation with *sec*-butyllithium in the presence of TMEDA at -78 °C in THF and trapping the formed anion with DMF gave FHPC (**97**) in an overall yield of 47% after work-up.[43]

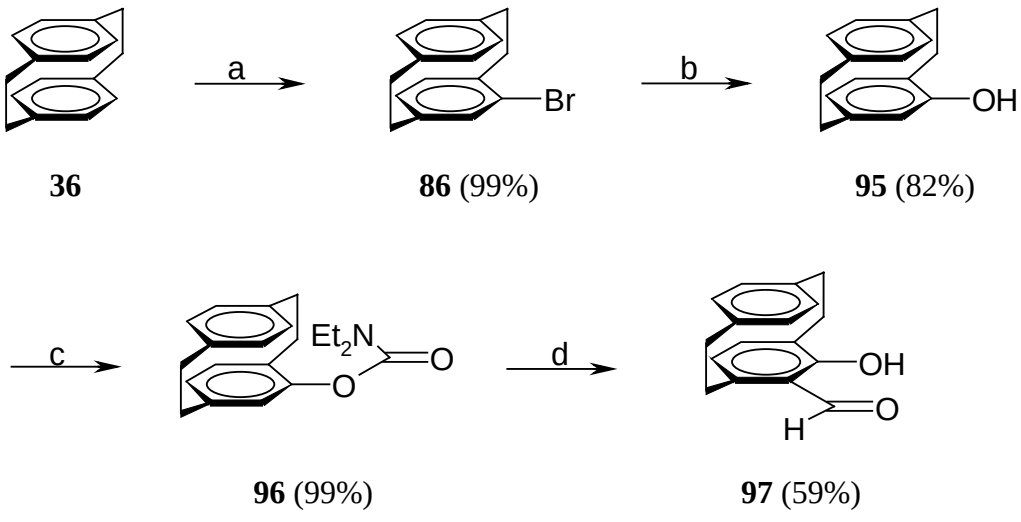

36 **86** (99%) **95** (82%)

96 (99%) **97** (59%)

(a) Fe, Br_2, CCl_4, CH_2Cl_2; (b) [i] *n*-BuLi, $B(OMe)_3$, [ii] NaOH (aq), H_2O_2, ether; (c) DMAP, diethylcarbamoyl chloride, toluene; (d) [i] *sec*-BuLi, TMEDA, [ii] DMF, HCl (aq), THF

Scheme 25: Synthesis of FHPC (**97**) by Hopf and coworkers.[43]

To convert **97** into **56** the following sequence was developed in this thesis (Scheme 26).

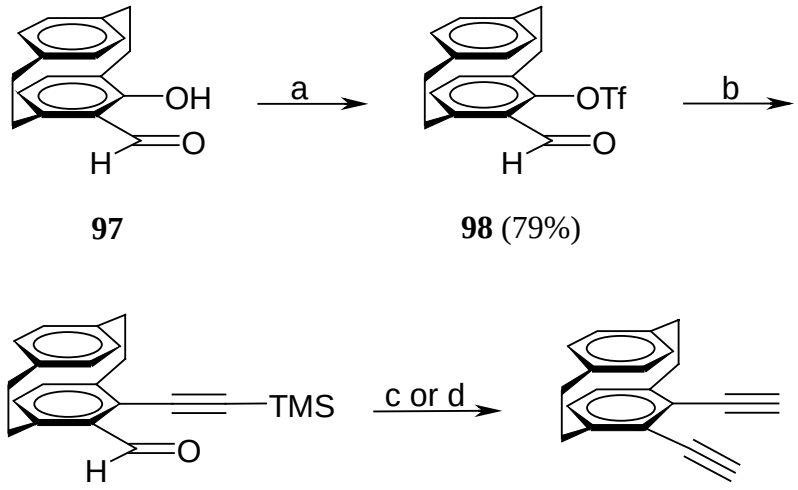

97 **98** (79%)

99 (79%) **56** (41%)

(a) $BnNTf_2$, Et_3N; (b) TMSA, $Pd(PPh_3)_4$, CuI, *i*-Pr_2NH, THF; (c) $CH_3C(O)C(N_2)P(O)(OMe)_2$, K_2CO_3, CH_3OH; (d) [i] $Ph_3PCH_2Br^+$ Br^-, *t*-BuOK, THF, -78°C, [ii] *t*-BuOK, THF, reflux

Scheme 26: Synthesis of 4,5-diethynyl[2.2]paracyclophane (**56**).

The hydroxyaldehyde **97** was first converted to the triflate **98** in 79% yield using *N*,*N*-bis(trifluoromethylsulfonyl)aniline in boiling triethylamine. Pd-catalyzed cross-

coupling of **98** with TMSA gave the monoyne **99** in 79% yield. Alkynylation of the monoyne **99** was carried out using Bestmann reagent **67**.[37] Under these reaction conditions, also desilylation of the previously introduced TMS-protected alkyne took place to furnish the diyne **56** in 41% yield. The novel [2.2]paracyclophane derivatives were characterized by the usual spectroscopic methods.

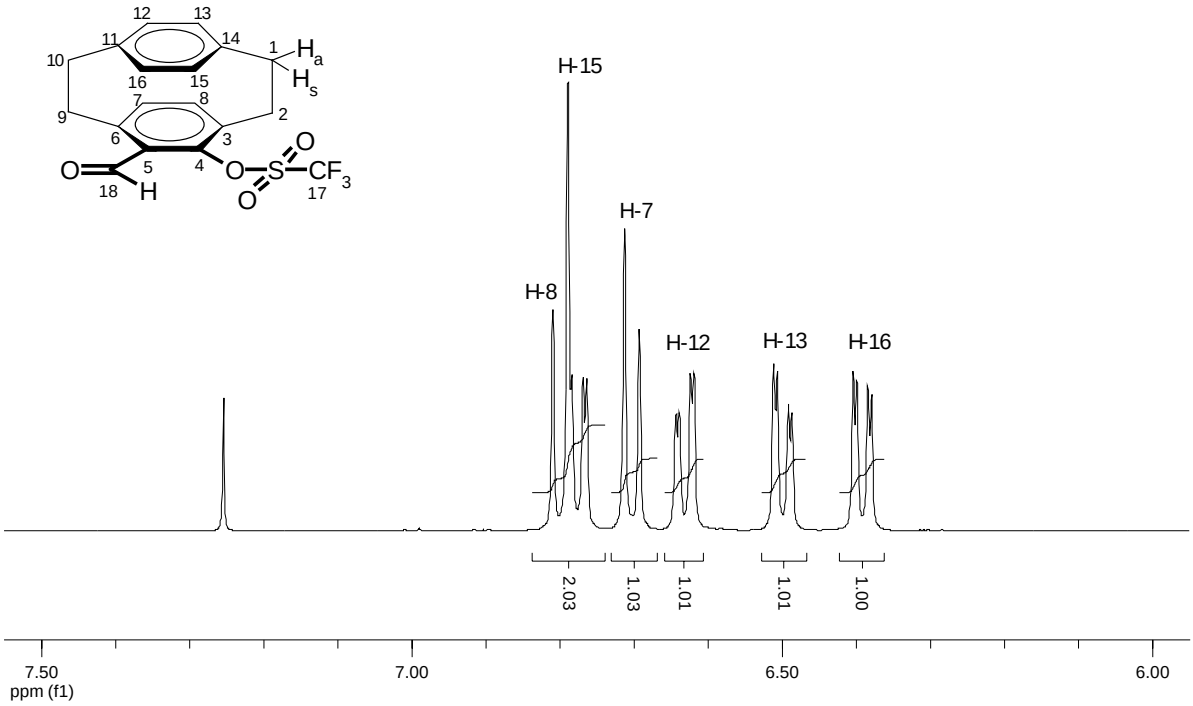

Figure 5: Aromatic region of the ^{1}H NMR of **98**.

The ^{1}H NMR spectrum of **98** shows two AGNX spectra for the bridge protons. The iterative analysis is summarized in Chapter 3.2. In the aromatic region (Figure 5), four doublets of doublets (dd) for the protons H-12 (δ = 6.64), H-13 (δ = 6.51), H-15 (δ = 6.78) and H-16 (δ = 6.40) in the unsubstituted ring and two doublets for the protons H-7 (δ = 6.71) and H-8 (δ = 6.81) in the substituted ring can be observed. The aldehyde proton gives a singlet at 10.10 ppm. The H,H-NOESY spectrum shows cross peaks between H-7 and H-12 and between H-8 and H-13.

The ^{13}C NMR spectrum was assigned by HSQC and HMBC spectra. It shows four signals in the region between δ = 31 and δ = 34 for the bridge carbon atoms C-1, C-2, C-9 and C-10. The triflate carbon atom gives a quartet with $^{1}J_{CF}$ = 321 Hz at δ = 117.0. For the carbonyl carbon atom, a signal at δ = 188.6 can be found.

The IR spectrum of **98** shows a strong band at 1691 cm^{-1} for the carbonyl function. The triflate group, gives strong bands at 1424, 1400, 1224 and 1141 cm^{-1}.

The mass spectrum is characterized by the molecular ion peak (*m/z* = 384) with 56% intensity, other typical peaks are at *m/z* = 251 (41%, cleavage of SO_2CF_3); *m/z* = 147 (59%) and *m/z* = 104 (100%) and can be explained by cleavage of the cyclophane bridges.

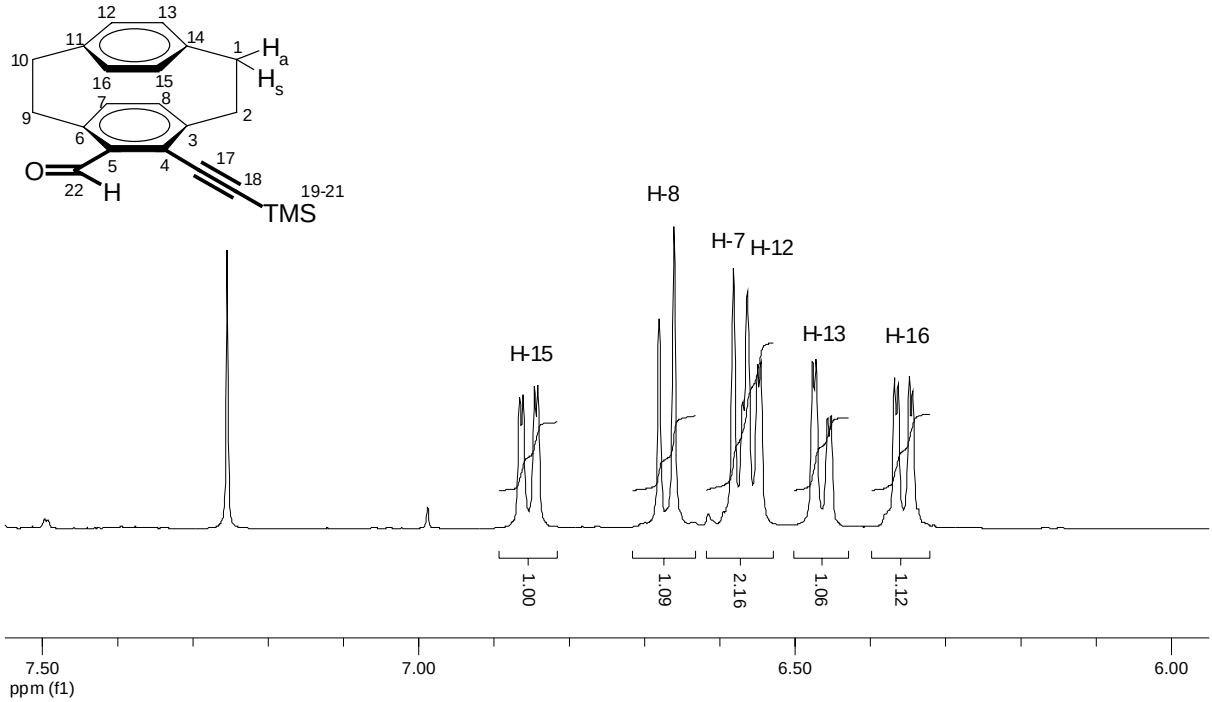

Figure 6: Aromaic region of the ^{1}H NMR of **99**.

For the bridge protons of **99**, two AMNX spectra were observed. The protons in *syn* position to the substituents give the X parts which can be described as doublets of doublets of doublets (ddd) at 3.65 and 4.14 ppm. The AMNX spectra were iteratively analyzed, the results -including, of course, the different coupling constants, are given in Chapter 3.2. The aromatic region of the ^{1}H NMR spectrum is shown in Figure 6. The protons in the unsubstituted ring give doublets of doublets at δ = 6.36 (H-16), 6.46 (H-13), 6.56 (H-12) and 6.85 (H-15). The protons of the substituted ring give doublets at δ = 6.57 (H-7) and 6.67 (H-8). For the aldehyde proton, a singlet at 10.35 ppm is found. When H-16 is irradiated, NOEs with the aldehyde proton, the proton in *ortho* position H-15 and the bridge proton at δ = 3.11 can be observed. Irradiation of H-13 gives NOEs with H-7 and H-8 and the bridge protons at δ = 2.90 and 3.07. When H-8 is irradiated, an additional NOE with the bridge proton at 2.90 is observed, indicating the *pseudo-ortho* orientation of H-8 and H-13.

The ^{13}C NMR spectrum shows a signal at δ = -0.1 for the trimethylsilyl protection group of the alkyne and four signals between 33 and 35 ppm for the bridge carbon

atoms. The alkyne function gives two signals at δ = 100.2 and δ = 107.3 and the aldehyde carbon atom a signal at δ = 194.1 ppm.

The IR spectrum of **99** shows a very intensive band at 1688 cm^{-1} which is caused by the carbonyl group of the aromatic aldehyde. The C≡C valence vibration causes a medium band at 2147 cm^{-1}.

Characteristic peaks in the mass spectrum are at *m/z* = 332 (100%) for the molecular ion, *m/z* = 228 (38%) and *m/z* = 104 (87%) for the cleavage of the cyclophane bridges; *m/z* = 73 indicates the presence of a trimethylsilyl group.

Because of the symmetry of **56**, only half of the signals are found in its NMR spectra. The ^{1}H NMR spectrum of the bridge protons shows an AGNX spectrum, in the form of doublets of doublets of doublets (ddd) at δ = 2.80, 2.96, 3.14 and 3.48. The alkyne protons give a singlet at δ = 3.46. In the aromatic region, multiplets at δ = 6.45 for the protons H-7, H-8, H-12, H-13 and between δ = 6.81 and δ = 6.82 for the protons H-15 and H-16 can be observed. The protons H-15 and H-16 in the *pseudo-geminal* position to the alkyne group are positioned in the anisotropic area of the alkyne function, they are hence deshielded. This causes the strong downfield shift of these protons.

The ^{13}C NMR spectrum displays two signals at δ = 33.9 and δ = 34.1 for the carbon atoms of the cyclophane bridge. The alkyne function gives two signals at δ = 82.0 and δ = 84.4, the cyclophane carbon atoms which are directly bond to the alkyne function cause a signal at δ = 127.1.

The IR spectrum shows strong bands at 3293 and 3275 cm^{-1} for the C-H vibration of the alkyne.

Due to the carbon richness of the molecule and an intensive molecular ion peak *m/z* = 256 (92%), the molecular ion peak of the ^{13}C substituted compound *m/z* = 257 can be observed with 20% intensity. Another intensive peak is at *m/z* = 255 which can be explained by loss of one hydrogen atom. Other characteristic peaks are at *m/z* = 152 (83%) and *m/z* = 104 (100%) for the two fragments of the bridge cleavage. The intense molecular ion peak and the intense peak for $[M^{+}\text{-H}]$ results in an inaccurate high resolution mass spectrum, since the $[M^{+}]$ peak overlaps with the $[^{12}C_{19}{}^{13}CH_{15}{}^{+}]$ signal. The $[M^{+}\text{-H}]$ signal gives a better high resolution mass spectrum.

A copper-free method for the cross coupling of the triflate **98** gave **99** in only 33% yield. As a side product, the indenonophane **100** was isolated in 6% yield.

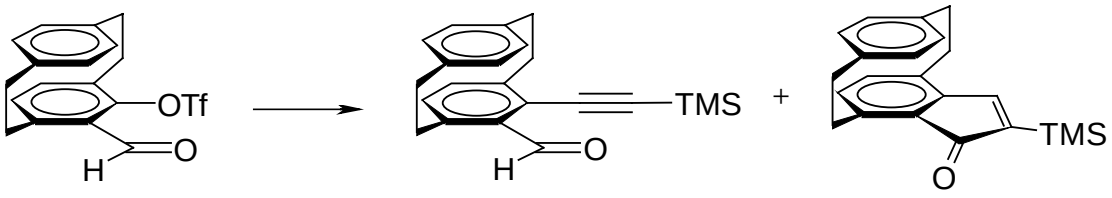

98 **99** (33%) **100** (6%)

TMSA, $Pd(PPh_3)_2Cl_2$, DMF, NEt_3, ampoule, 2d 130 °C

Scheme 27: Copper-free Pd catalyzed cross coupling of **98** with TMSA.

That the catalyst is involved in the formation process of **100** was seen by a control experiment. When a solution of **99** was heated in a sealed ampoule without the catalyst, no **100** was formed. In the presence of the catalyst, the formation of **100** was proven by GC-MS analysis.

The ^{13}C NMR spectrum of **100** shows a signal at $\delta = 203.1$. Since the ^{1}H NMR spectrum contains no signal for an aldehyde proton, a ketone must be present in the molecule. The ^{1}H NMR spectrum shows the existence of a trimethylsilyl group in the molecule, but in the ^{13}C NMR no signals in the region of acetylenic carbon atoms can be found. The bridge protons of the cyclophane absorb as an AMNX spectrum for one bridge and an ACDE spectrum for the other. The aromatic protons of the substituted ring form an AB multiplet which overlaps with the X part of an ABCX spectrum of the unsubstituted ring. Furthermore, a singlet at $\delta = 7.48$ can be found. In the HMBC spectrum, this singlet shows a cross peak with the carbon at 203.1 ppm.

The formation of the indenone can be explained by the following mechanism: in the first step, the active Pd species probably forms a π-complex **102** with the acetylene function possibly followed by insertion of the metal in the C-H-bond of the aldehyde function to give the intermediate **103**. Migration of PdH could lead to the indenone derivative **104** with σ-bounded Pd which could decompose to give the indenone **105** and regenerate the catalytically active Pd species.

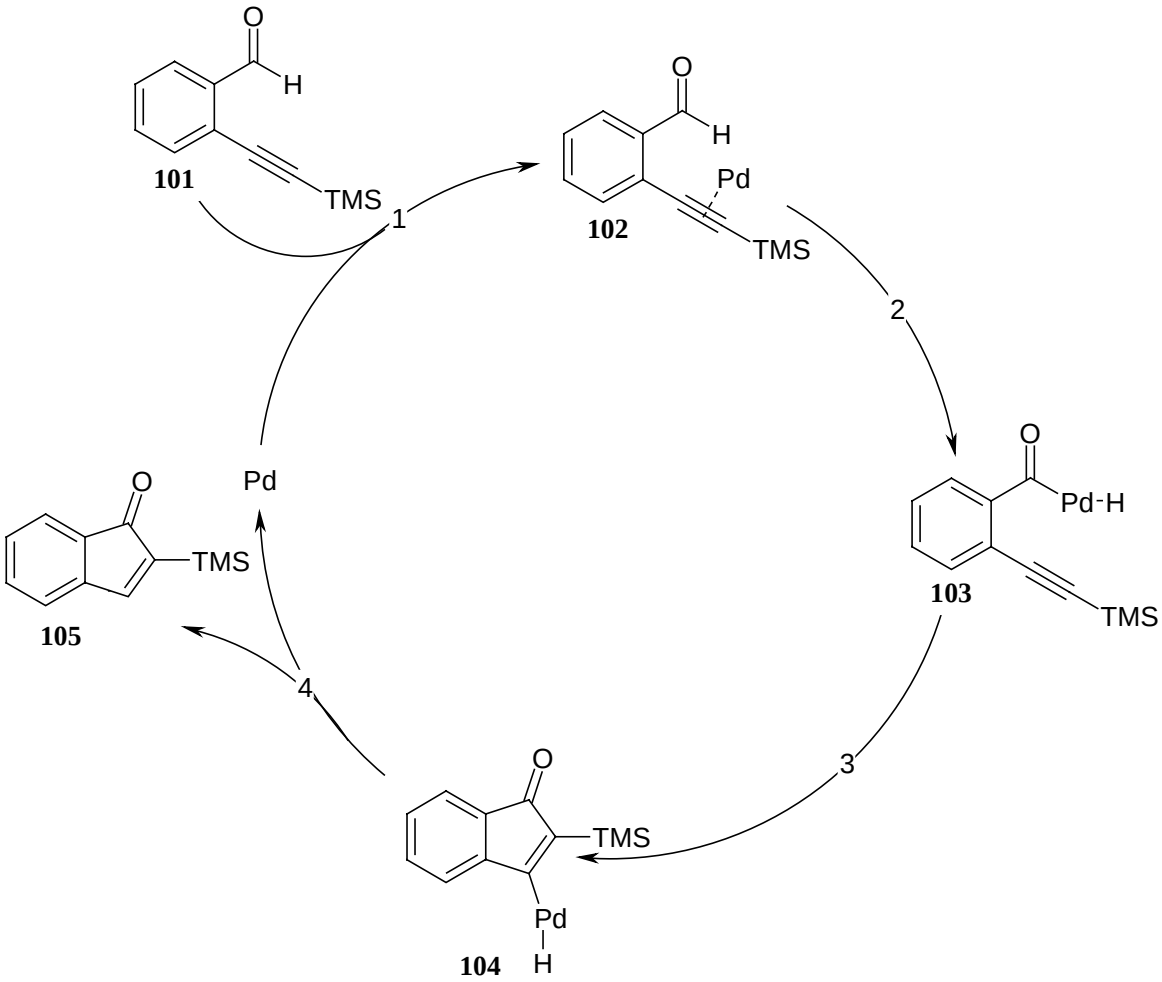

Scheme 28: Possible mechanism for the formation of the indenone **105**.

The Corey-Fuchs reaction of **99** provides access to the *ortho*-diyne derivative **107**, with one protected and one deprotected acetylene function.

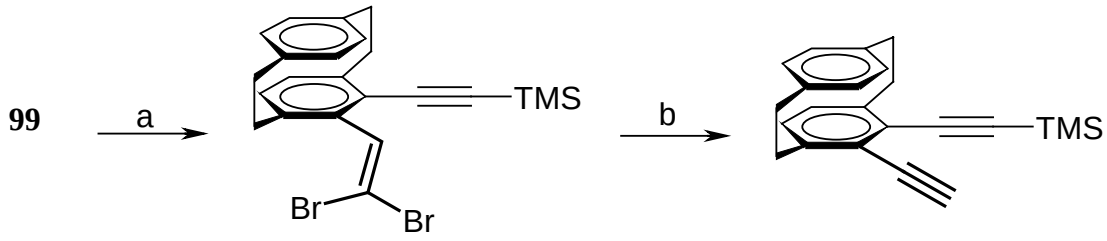

106 (25%) **107** (21%)

(a) Ph_3PCBr_2, CH_2Cl_2; (b) LDA, THF, -78 °C

Scheme 29: Synthesis of 5-ethynyl-4-(trimethylsilyl)ethynyl[2.2]paracyclophane (**107**) using the Corey-Fuchs reaction.

In the first step of the reaction sequence the ylide from triphenylphosphine, carbontetrabromide and zinc powder is generated in CH_2Cl_2. After 12 h at room temp., a purple suspension is formed to which the aldehyde **99** is added. The dibromoolefin **106**

was obtained in poor yield (25%) as a light yellow oil, the starting material was recovered in 70% yield. Treating a THF solution of **106** at -78 °C with freshly prepared LDA solution, the alkyne **107** was obtained in 21% yield. In this reaction, 75% of the starting material was recovered. It appears likely that this route to **56** could become preparatively useful if optimized.

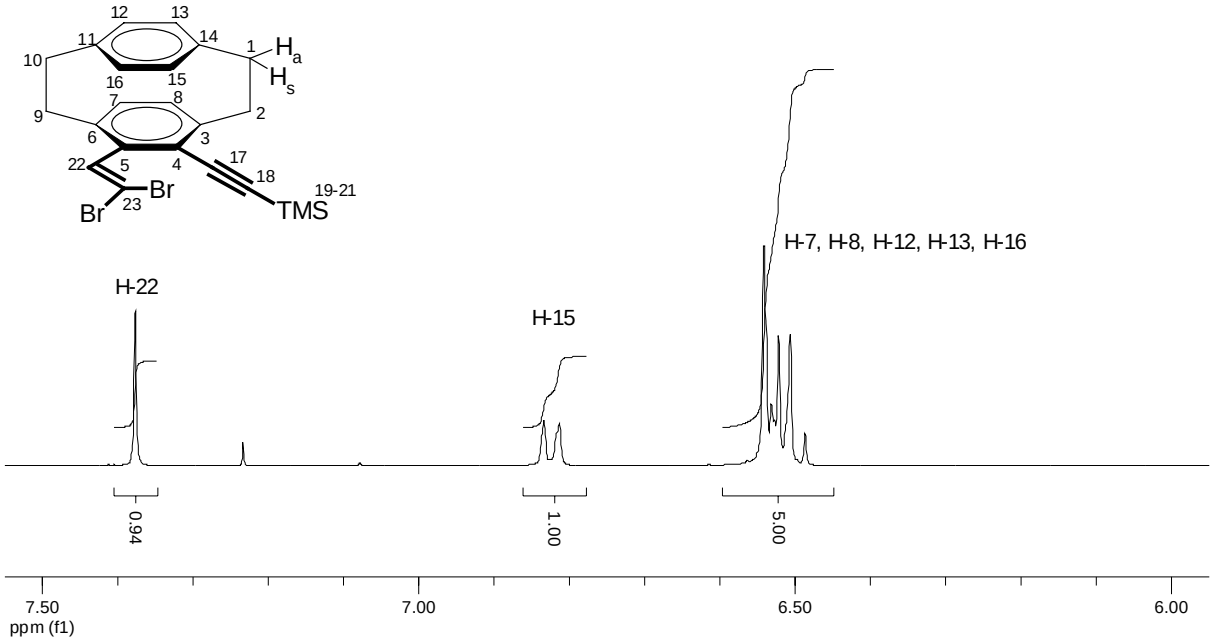

Figure 7: Aromatic region of the ^{1}H NMR spectrum of **106**.

The ^{1}H NMR spectrum of **106** shows a singlet at δ = 0.34 for the TMS protection group. The bridge protons of the cyclophane give four doublets of doublets of doublets (ddd) at δ = 2.81, 3.05, 3.14 and 3.52 for the protons of the bridge in *ortho* position to the alkyne function and a higher order spectrum for the bridge in *ortho* position to the dibromoolefin. The aromatic proton in *pseudo-geminal* position to the alkyne function gives a multiplet between δ = 6.81 and 6.83 which shows cross peaks in the NOESY spectrum with the olefinic proton and a proton of the bridge in *ortho* position to the alkyne function. The other aromatic protons give a multiplet between δ = 6.49 and 6.56. The olefinic proton provides a singlet at δ = 7.38.

The ^{13}C NMR spectrum displays a signal at δ = 0.1 for the TMS protection group. The carbon atoms of the bridges absorb between δ = 33.7 and δ = 34.7. The dibrominated olefinic carbon atom causes a signal at δ = 92.7, the other olefinic carbon atom gives a signal at δ = 137.4. Due to the complexity of the ^{1}H NMR spectrum, no complete assignment of all carbon atoms was possible.

The molecular ion peak in the mass spectrum shows the characteristic pattern of a dibrominated compound. Cleavage of the cyclophane bridges gives signals at *m/z* = 382/384/386 (isotope distribution: 1:2:1) for the substituted fragment and *m/z* = 104 for the unsubstituted fragment. The base peak (*m/z* = 303/305) shows the isotopic pattern of a monobrominated fragment (ratio 1:1), what can be explained by the loss of bromine from the substituted fragment. The peak at *m/z* = 73 indicates the presence of a trimethylsilyl group.

The ^{1}H NMR spectrum of the monoprotected diyne **107** shows a singlet at δ = 0.33 for the protection group. The unprotected alkyne gives a singlet at δ = 3.48. The ^{13}C NMR spectrum shows the complete set of signals. The trimethylsilyl protection group gives a signal at δ = 0.1. The alkyne carbon atoms absorb at δ = 82.2, 84.4, 102.4 and 103.7. The other signals are very similar to those observed for the diyne **56**.

As an alternative to the reaction sequence presented in Scheme 26, the following synthetic route was developed. *Ortho* lithiation of the carbamate **96** and trapping the formed anion with iodine gave the iodinated compound **108** in 81% yield. In contrast to the synthesis of FHPC (**97**), no cleavage of the carbamate function was observed. Pd catalyzed cross coupling of the iodide function with TMSA yielded 93% of the alkyne **109** from which the carbamate function was converted to the phenol in 87% yield using DIBAL-H. When lithium-aluminum hydride is used for reduction, cleavage of the trimethylsilyl group also takes place. Transformation of the phenol group into the triflate using *N*,*N*-bis(triflouromethylsulfonyl)aniline in the presence of K_2CO_3 as base gave 4-trifluoromethylsulfonyloxy-5-(trimethylsilyl)ethynyl[2.2]paracyclophane (**111**) in 76% yield.

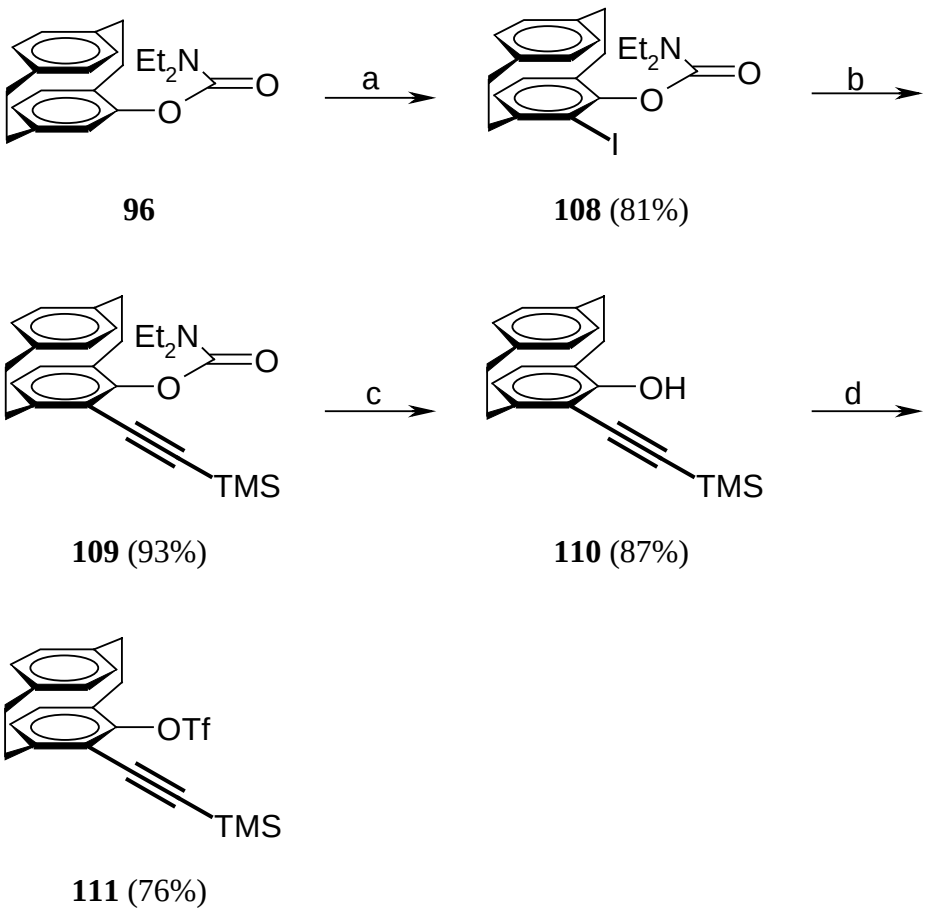

(a) [i] *sec*-BuLi, TMEDA, [ii] I_2, THF; (b) TMSA, $Pd(PPh_3)_4$, CuI, *i*-Pr_2NH, THF; (c) DIBAL-H, THF; (d) $BnNTf_2$, K_2CO_3, THF

Scheme 30: Attempted synthesis of **56** *via* the iodo compound **108**.

Unfortunately, the final conversion of the triflate to the alkyne function was not successful. Pd catalyzed cross coupling reactions under the conditions summarized in Table 1 gave back the starting material **111** almost quantitatively.

Table 1: Pd-catalyzed cross coupling reactions of the triflate **111**.

entry	catalyst	additive	solvents	acetylene	result
1	$Pd(PPh_3)_4$	CuI	*i*Pr_2NH, THF	$HC{\equiv}CSiMe_3$	**111** (98%)[a]
2	$Pd(PPh_3)_4$	LiCl	THF	(*n*$Bu)_3SnC{\equiv}CH$	**111** (93%)[a]
3	$(PPh_3)_2PdCl_2$	(*n*$Bu)_4NI$	DMF, NEt_3	$HC{\equiv}CSiMe_3$	**111** (100%)[b]

[a] isolated product

[b] GC analysis

The conditions used in entry 1 were sufficient to convert the triflate function in *ortho* position to an aldehyde group into the alkyne in 79 % yield; in case of an alkyne function in *ortho* position to the triflate, no reaction was observed.

Stille coupling with tributyl-tin-acetylene using $Pd(PPh_3)_4$ as catalyst and lithium chloride as additive was also not successful (entry 2).

Powell and Rychnovsky have converted *ortho* ditriflates to diynes, using the conditions presented in entry 3.[47] In case of the [2.2]paracyclophane derivative **111**, only starting material **111** was detected by GC analysis.

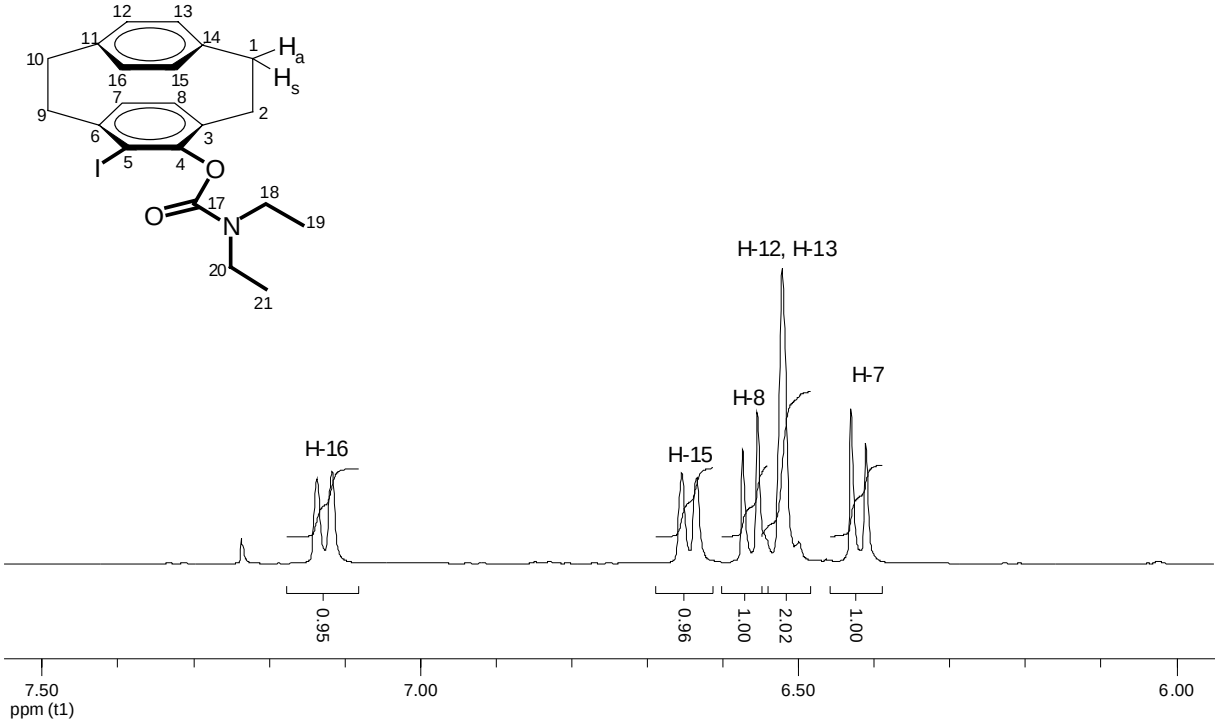

Figure 8: Aromatic region of the ^{1}H NMR of **108.**

The ^{1}H NMR spectrum of **108** shows triplets at δ = 1.20 and δ = 1.47 for the protons H-19 and H-21 of the carbamate group. The non equivalent protons H-20 give doublets of quartets at δ = 3.54 and δ = 3.78 with ^2J = 14.2 Hz. The aromatic proton H-7 causes a doublet at δ = 6.42, H-8 a doublet at δ = 6.58. The protons of the unsubstituted ring give a multiplet between δ = 6.50 and δ = 6.55 (H-12 and H-13). The multiplets for H-15 and H-16 at δ = 6.64 and δ = 7.13 can be described as pseudo doublets.

In the ^{13}C spectrum, C-5 gives a signal at δ = 103.5, C-4 is shifted to δ = 149.0. The carbonyl carbon of the carbamate group (C-17) is recorded at δ = 152.5.

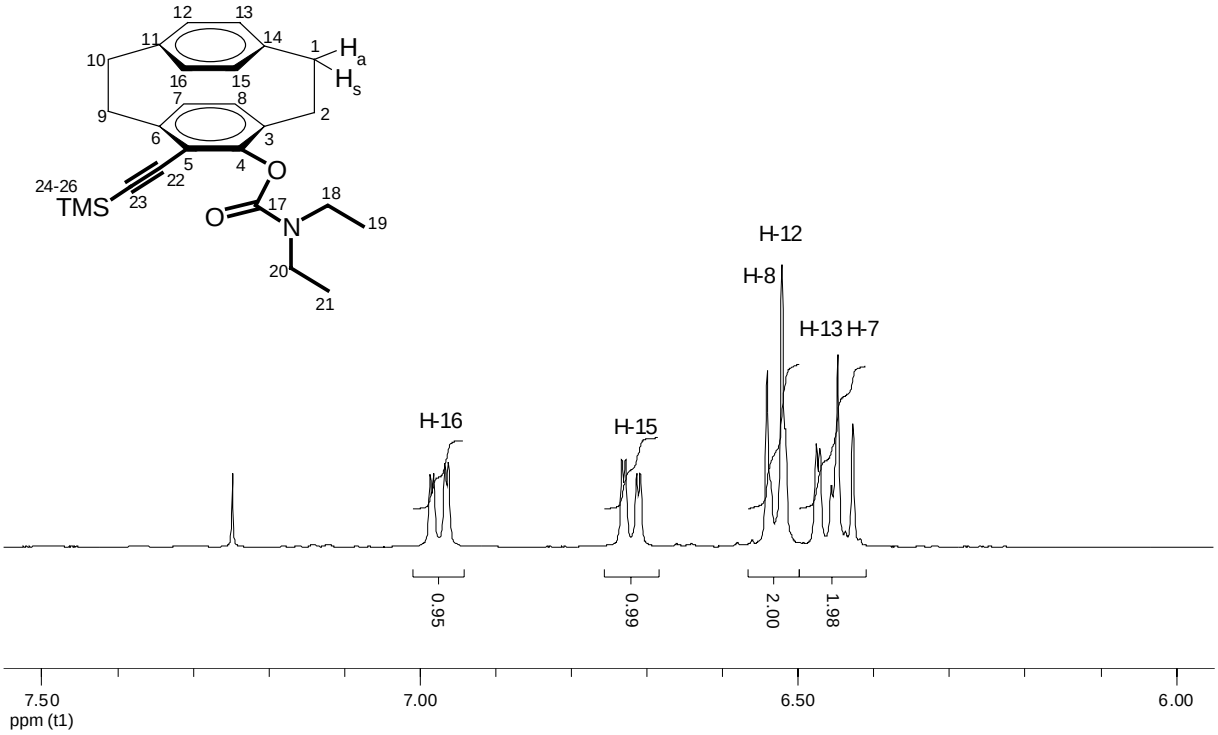

Figure 9: Aromatic region of the ^{1}H NMR spectrum of **109**.

The ^{1}H NMR spectrum of **109** shows a singlet for the TMS protection group of the alkyne at δ = 0.28. For the carbamate function, two triplets at δ = 1.20 (H-19) and δ = 1.47 (H-21) and a quartet at δ = 3.38 (H-18) are observed. The other two protons of the carbamate function (H-20) are not equivalent and give rise to two doublets of quartets at δ = 3.55 and δ = 3.69 with $^{2}J_{HH}$ = 14.2 Hz. The bridge proton H-2*a* gives a doublet of doublets of doublets at δ = 2.69, the proton H-9*a* gives a ddd-pattern at δ = 2.80. Proton H-9*s* shows a doublet of doublets of doublets at δ = 3.48 the other bridge protons give a multiplet between δ = 2.95 and 3.18. The doublets at δ = 6.44 and 6.53 are caused by the aromatic protons H-7 and H-8; the aromatic protons of the unsubstituted ring show a dd-splitting at δ = 6.46 (H-13), 6.53 (H-12), 6.71 (H-15) and 6.97 (H-16).

Characteristic signals in the ^{13}C NMR spectrum of **109** are at δ = 0.0 for the TMS protection group, δ = 101.1 and 102.4 for the alkyne function and δ = 150.7 for the carbonyl carbon atom of the carbamate function.

In the mass spectrum the molecular ion peak at *m*/*z* = 419 indicates that a nitrogen atom is present in the molecule. Other significant peaks are at *m/z* = 315 and *m/z* = 104 for the two fragments resulting by cleavage of the cyclophane bridges.

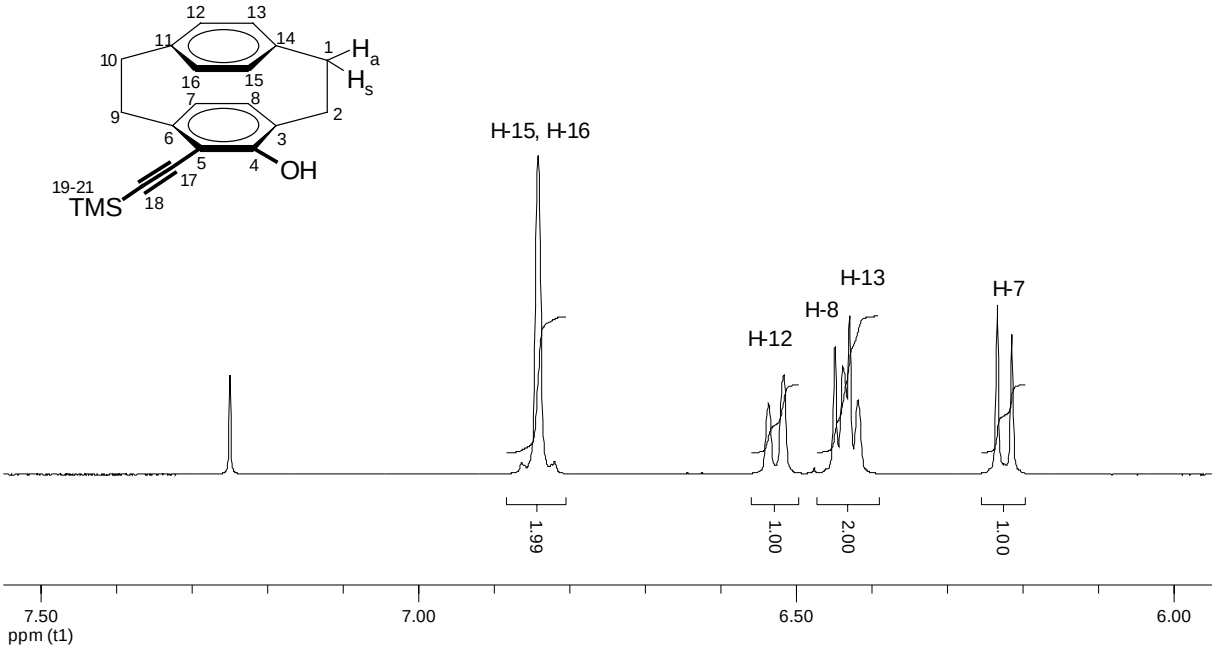

Figure 10: Aromatic region of the ^{1}H NMR spectrum of **110**.

Compound **110** shows a singlet at δ = 0.34 for the protection group of the alkyne in its proton spectrum. The bridge protons give doublets of doublets of doublets at δ = 2.59 (H-2*a*), 2.78 (H-9*a*), 3.39 (H-9*s*) and 3.41 (H-2*s*). The protons H-1*a*, H-1*s*, H-10*a* and H-10*s* give a multiplet between δ = 2.98 and 3.12. The phenol proton displays a singlet at δ = 5.62. The aromatic protons H-7 and H-8 give doublets at δ = 6.23 and δ = 6.44, the aromatic protons of the unsubstituted ring give pseudo doublets at δ = 6.43 (H-13) and 6.53 (H-12) and a multiplet between δ = 6.82 and 6.86 for H-15 and H-16.

Characteristic peaks in the ^{13}C NMR spectrum are at δ = 0.1 for the protection group of the alkyne, δ = 100.3 and 105.8 for the acetylenic carbon atoms and δ = 155.4 for the aromatic carbon atom bend to the phenol.

The mass spectrum of **110** shows the molecular ion peak at m/z = 320. The base peak of the spectrum is at *m/z* = 216, for the substituted fragment of the splitting of the cyclophane bridges. The other fragment at *m/z* = 104 can be observed with 15% intensity.

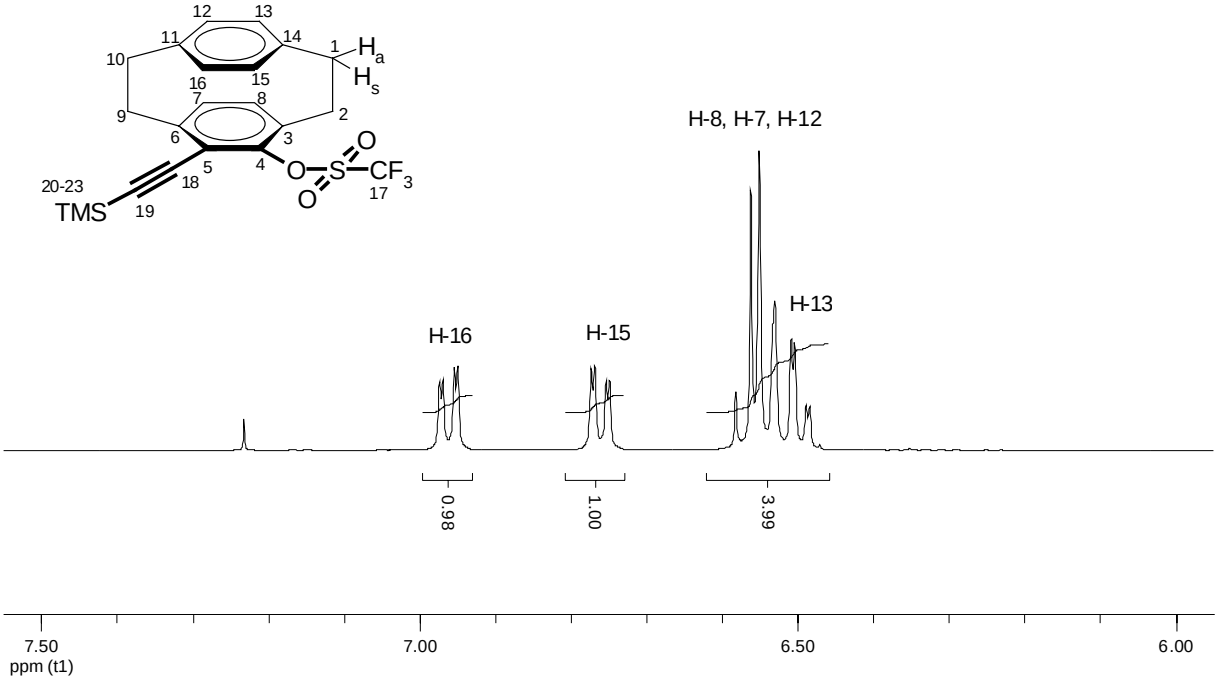

Figure 11: Aromatic region of the ^{1}H NMR spectrum of **111**.

The ^{1}H NMR spectrum of **111** shows a singlet at δ = 0.33 for the protection group of the alkyne function. The bridge protons H-2*a* and H-9*a* give doublets of doublets of doublets at δ = 2.81 and δ = 2.82; H-2*s* and H-9*s* give doublets of doublets of doublets at δ = 3.33 and 3.49. The other bridge protons absorb as a multiplet between δ = 2.99 and 3.21. For the aromatic protons, doublets of doublets at δ = 6.50 (H-13), δ = 6.76 (H-15) and δ = 6.96 (H-16) and a multiplet between δ = 6.53 and 6.58 (H-7, H-8 and H-12) are observed.

Characteristic peaks in the ^{13}C NMR spectrum are at δ = -0.3 for the protection group of the acetylene function. The acetylenic carbon atoms give signals at δ = 98.3 and δ = 106.3. The carbon atom of the triflate group gives a quartet with $^{1}J_{CF}$ = 321 Hz at δ = 118.7.

The mass spectrum of **111** shows the molecular ion peak (*m/z* = 452) with 57% intensity. Cleavage of the bridges gives signals at *m/z* = 348 (5%) and *m/z* = 104 (100%). The intensive peak at *m/z* = 319 (98%) can be explained by cleavage of the triflate function of the molecule. Full spectroscopic and analytical data are given in the experimental section.

3.2 NMR-Spectroscopy

Early X-ray studies have shown that [2.2]paracyclophane (**36**) posses a remarkable degree of flexibility in the solid state.[48] For studies in solution, NMR spectroscopy is a powerful method as shown already by Ernst in a study of the conformational equilibrium of monosubstituted [2.2]paracyclophanes, regarding the H,H coupling constants of the bridge protons.[49] In the case of monosubstituted [2.2]paracyclophanes (R^2 = H), nonbonding interactions between the proton H-2*s* and the substituent R^1 in structure **112a** cause a shift of the equilibrium towards **112b** (Scheme 31). In the case of 4,5-disubstituted [2.2]paracyclophanes, there is a competition between the interactions H-2*s*/R^1 and H-9*s*/R^2. When the two substituents are different, the equilibrium should be shifted to the side for which the sum of the two interactions is smaller.

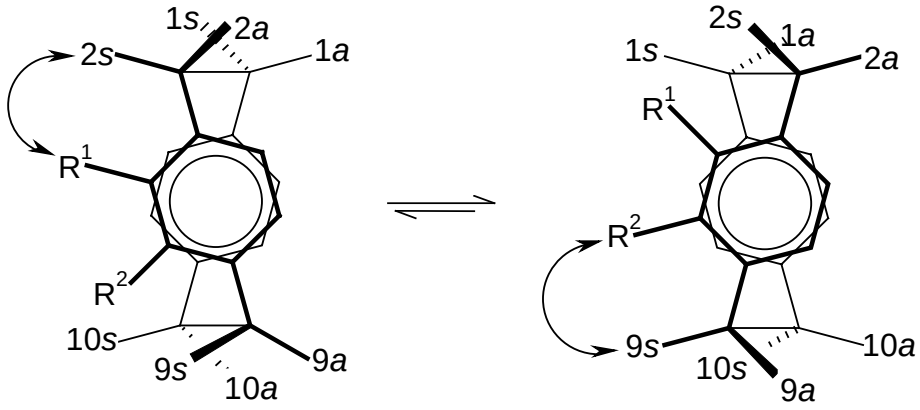

112a **112b**

Scheme 31: Conformational equilibrium between the conformations **112a** and **112b** with twisted benzene rings.

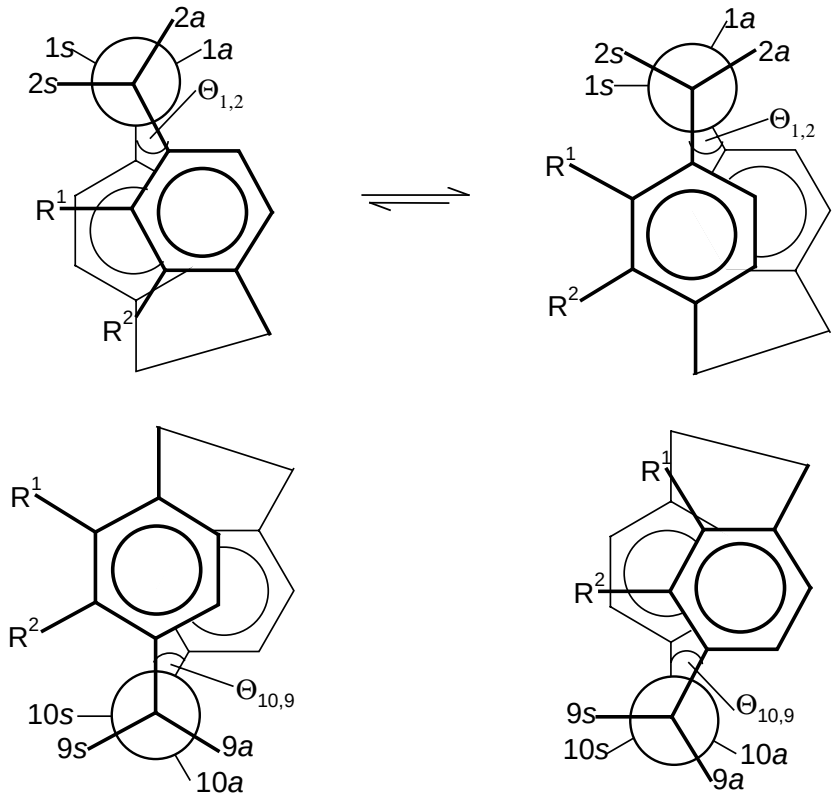

112a **112b**

Scheme 32: Newman projections of the conformational equilibrium of **112a** and **112b**.

As an alternative to the conformation with twisted benzene rings, a conformation with parallel-displaced benzene rings can be formulated.

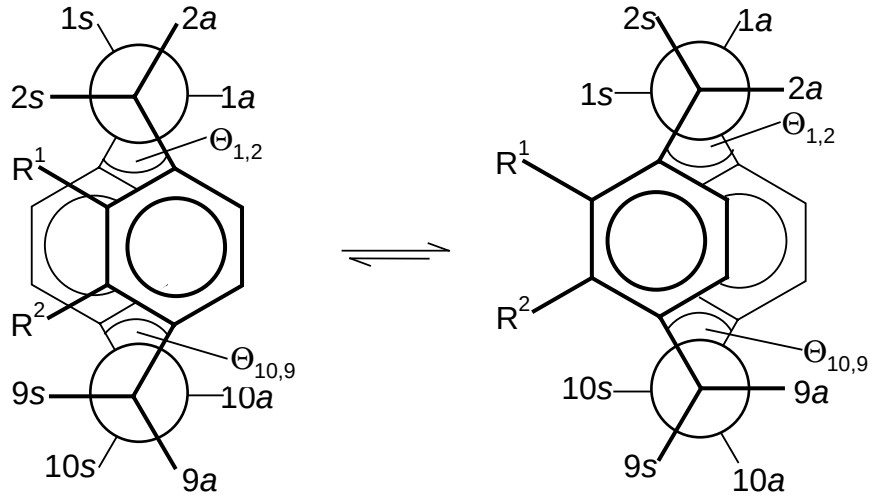

112c **112d**

Scheme 33: Conformational equilibrium between the conformations **112c** and **112d** with parallel-displaced benzene rings.

Karplus[50, 51] has shown that the coupling constant between vicinal protons depends on the torsion angle ϕ and can be described by the equation

$$^3J = A + B\cos\phi + C\cos 2\phi\,.$$

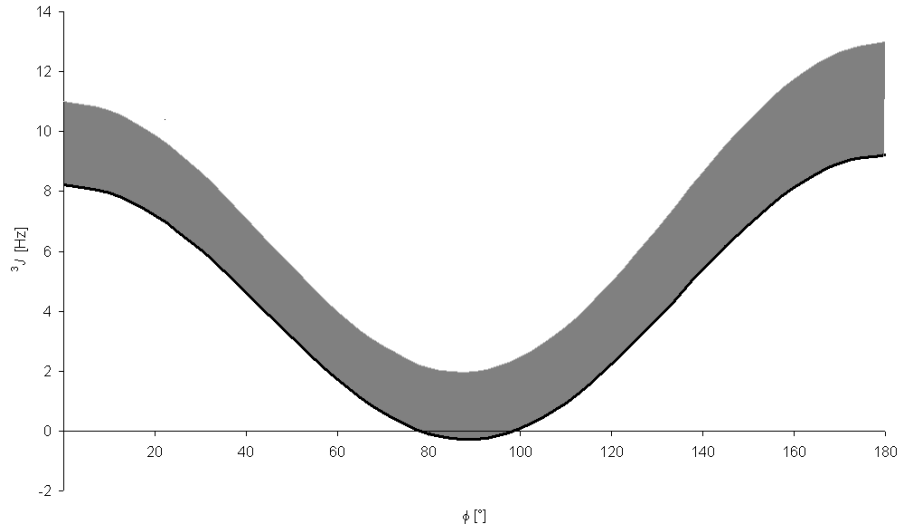

Figure 12: Karplus-Conroy-curve; black: theoretic values, gray: experimental observations.

Since the observed coupling constants are the average of the coupling constants of the conformers, a shift of the equilibrium from **112a** to **112b** will increase the 1*s*/2*a* and 10*a*/9*s* coupling and decrease the 1*a*/2*s* and 10*s*/9*a* coupling. In case of parallel-displaced benzene rings, a shift of the equilibrium from **112c** to **112d** will increase the 1*s*/2*a* and 10*s*/9*a* coupling and decrease the 1*a*/2*s* and 10*a*/9*s* coupling.

Table 2 shows the torsion angles ϕ between the C-H bonds in the conformational isomers **112a**, **112b**, **112c** and **112d** in relation to the torsion angle Θ of the bridge, Table 3 summarizes the H,H coupling constants of the bridge protons of the [2.2]paracyclophanes **98**, **99, 111** and **56**.

Table 2: Torsion angles ϕ between the C-H bonds in the conformational isomers.

	112a	**112b**	**112c**	**112d**
1*a*/2*a* (*cis*)	$\Theta_{1,2}$	$-\Theta_{1,2}$	$\Theta_{1,2}$	$-\Theta_{1,2}$
1*s*/2*s* (*cis*)	$\Theta_{1,2}$	$-\Theta_{1,2}$	$\Theta_{1,2}$	$-\Theta_{1,2}$
1*a*/2*s* (*trans*)	$\Theta_{1,2}$ + 120°	$-\Theta_{1,2}$ + 120°	$\Theta_{1,2}$ + 120°	$-\Theta_{1,2}$ + 120°
1*s*/2*a* (*trans*)	$\Theta_{1,2}$ - 120°	$-\Theta_{1,2}$ - 120°	$\Theta_{1,2}$ - 120°	$-\Theta_{1,2}$ - 120°
10*a*/9*a* (*cis*)	$\Theta_{10,9}$	$-\Theta_{10,9}$	$-\Theta_{10,9}$	$\Theta_{10,9}$
10*s*/9*s* (*cis*)	$\Theta_{10,9}$	$-\Theta_{10,9}$	$-\Theta_{10,9}$	$\Theta_{10,9}$
10*a*/9*s* (*trans*)	$\Theta_{10,9}$ - 120°	$-\Theta_{10,9}$ - 120°	$-\Theta_{10,9}$ - 120°	$\Theta_{10,9}$ - 120°
10*s*/9*a* (*trans*)	$\Theta_{10,9}$ + 120°	$-\Theta_{10,9}$ + 120°	$-\Theta_{10,9}$ + 120°	$\Theta_{10,9}$ + 120°

Table 3: ^{1}H,^{1}H coupling constants [Hz] in the bridges of **98**, **99, 111** and **56**.

		98	**99**	**111**	**56**
R (%)		0.45	0.98	3.76	0.49
J (1-H*a*, 1-H*s*)	*gem*	-13.43	-13.10	-13.36	-13.06
J (2-H*a*, 2-H*s*)	*gem*	-14.39	-13.29	-14.01	-13.20
J (9-H*a*, 9-H*s*)	*gem*	-13.23	-12.76	-13.40	-13.20
J (10-H*a*, 10-H*s*)	*gem*	-13.11	-12.96	-12.92	-13.06
J (1-H*a*, 2-H*a*)	*cis*	10.43	10.80	9.61	10.76
J (1-H*s*, 2-H*s*)	*cis*	10.21	10.64	10.31	10.60
J (9-H*a*, 10-H*a*)	*cis*	10.33	10.28	10.76	10.76
J (9-H*s*, 10-H*s*)	*cis*	10.29	10.30	10.55	10.60
J (1-H*a*, 2-H*s*)	*trans*	3.76	3.16	3.91	3.15
J (1-H*s*, 2-H*a*)	*trans*	4.83	4.60	3.85	4.73
J (9-H*a*, 10-H*s*)	*trans*	6.69	6.40	4.92	4.73
J (9-H*s*, 10-H*a*)	*trans*	1.46	1.69	2.57	3.15

For **98** and **99**, the *trans* coupling constants $^{3}J_{1a,2s}$ and $^{3}J_{9s,10a}$ are smaller than $^{3}J_{1s,2a}$ and $^{3}J_{9a,10s}$, indicating a structure with parallel displaced benzene rings with preference of conformation **112d**. For **111,** conformation **112a** with twisted benzene rings should be preferred ($^{3}J_{1s,2a}$ and $^{3}J_{9s,10a}$ are smaller than $^{3}J_{1a,2s}$ and $^{3}J_{9a,10s}$).

Molecular modeling studies for single molecules in the gas phase on B3LYP/6-31G(D) level have shown that the preferred conformation of **99** is not **112d** but **112a** with different torsion angles in the two bridges: 3.8° respectively 17.8°. The calculated torsion angles are summarized in Table 4, the structure is depicted in Figure 13. Comparison of this torsion angles mach with the theoretical values seen in Table 2 for **112a**.

Table 4: Calculated torsion angles [°] of **99**.

C(14)-C(1)-C(2)-C(3)	3.8	C(11)-C(10)-C(9)-C(6)	17.8
H(1*a*)-C(1)-C(2)-H(2*a*)	3.0	H(10*a*)-C(10)-C(9)-C(9*a*)	22.4
H(1*s*)-C(1)-C(2)-H(2*s*)	3.8	H(10*s*)-C(10)-C(9)-C(9*s*)	21.2
H(1*a*)-C(1)-C(2)-H(2*s*)	118.8	H(10*a*)-C(10)-C(9)-C(9*s*)	-94.3
H(1*s*)-C(1)-C(2)-H(2*a*)	-112	H(10*s*)-C(10)-C(9)-C(9*a*)	137.9

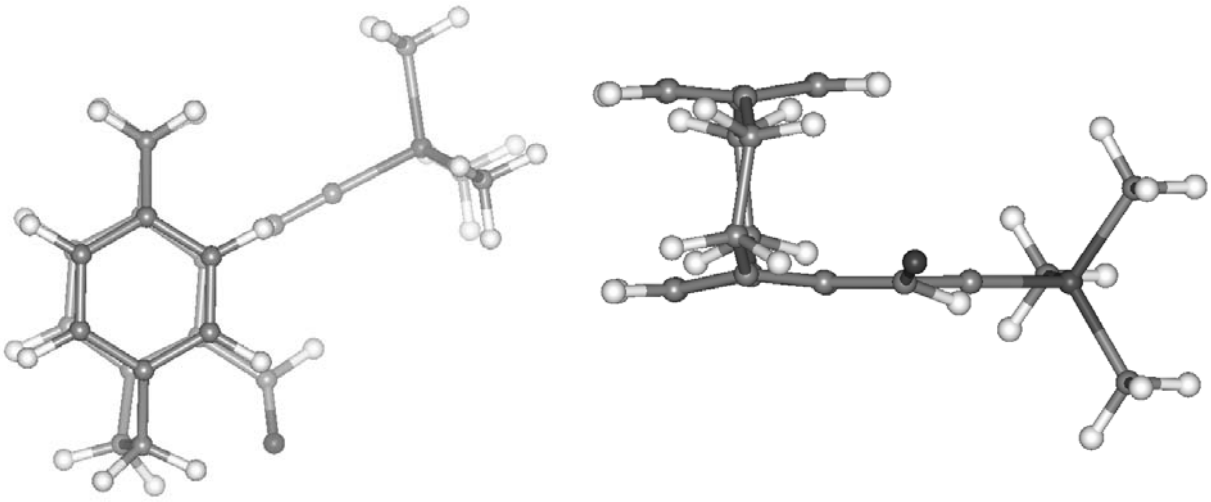

Figure 13: Calculated structure of **99**.

The calculations did not give an explanation why the measured coupling constant $^3J_{1s,2a}$ is higher than $^3J_{1a,2s}$ (what would indicate conformation **112d**). It was unfortunately not possible to calculate the torsion angles for the conformer **112b**, because the energy barrier between the two conformers is too low. Since the difference between the two experimental coupling constants $^3J_{1s,2a}$ and $^3J_{1a,2s}$ is only 1.44 Hz, a distortion of the torsion angles 1*a*/2*s* and 1*s*/2*a* in the less favored conformer **112b** from the geometry given in Table 2 could be an explanation why $^3J_{1s,2a}$ is higher than $^3J_{1a,2s.}$

For compound **98**, molecular modeling studies confirmed the postulated conformation **112d**. The calculated torsion angles are summarized in Table 5, the structure is displayed in Figure 14.

Table 5: Calculated torsion angles [°] of **98**.

C(14)-C(1)-C(2)-C(3)	10.8	C(11)-C(10)-C(9)-C(6)	13.7
H(1*a*)-C(1)-C(2)-H(2*a*)	-14.8	H(10*a*)-C(10)-C(9)-C(9*a*)	17.9
H(1*s*)-C(1)-C(2)-H(2*s*)	-15.1	H(10*s*)-C(10)-C(9)-C(9*s*)	16.6
H(1*a*)-C(1)-C(2)-H(2*s*)	99.8	H(10*a*)-C(10)-C(9)-C(9*s*)	-98.8
H(1*s*)-C(1)-C(2)-H(2*a*)	-129.7	H(10*s*)-C(10)-C(9)-C(9*a*)	132.2

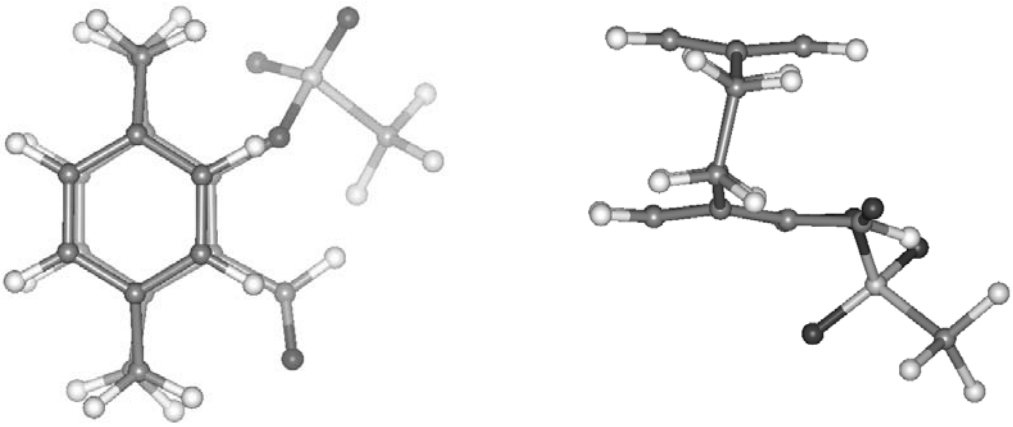

Figure 14: Calculated structure of **98**.

Nevertheless, there is no explanation for the differences between the coupling constants. Experimental $^3J_{1s,2a}$ and $^3J_{1a,2s}$ differ by only 1.07 Hz whereas $^3J_{10s,9a}$ and $^3J_{10a,9s}$ differ by 5.23 Hz. From the calculated torsion angles, the difference between $^3J_{1s,2a}$ and $^3J_{1a,2s}$ should be nearly the same as the difference between $^3J_{10s,9a}$ and $^3J_{10a,9s}$, since there is only a slight deviation in the torsion angles. The explanation could be an equilibrium with the less favored conformation **112a** in which the difference between $\Theta_{1,2}$ and $\Theta_{9,10}$ is larger. The calculation of this structure was not possible due to the too small energy barrier.

In case of equal substituents ($R^1 = R^2$) like in **56**, a shift of the equilibrium from **112a** to **112b** does not lead to a less hindered conformation since the decrease of interaction between H-2*s*/R^1 leads to an increased interaction between H-9*s*/R^2. In this case, the molecule should be present in a structure with parallel-displaced benzene rings with preference of conformation **112d**.

The postulated structure of **56** was confirmed by molecular modeling studies. **Figure 15** shows the B3LYP/6-31G(D) optimized structure of 4,5-diethynyl[2.2]paracyclophane (**56**). The calculated torsion angles are summarized in **Table 6**, showing a slight distortion from the ideal geometry. The torsion angles between the *cis* C-H bonds differ by 1.1 - 1.7° and the *trans* torsion angles by 3 - 5.9° from the values given in Table 2.

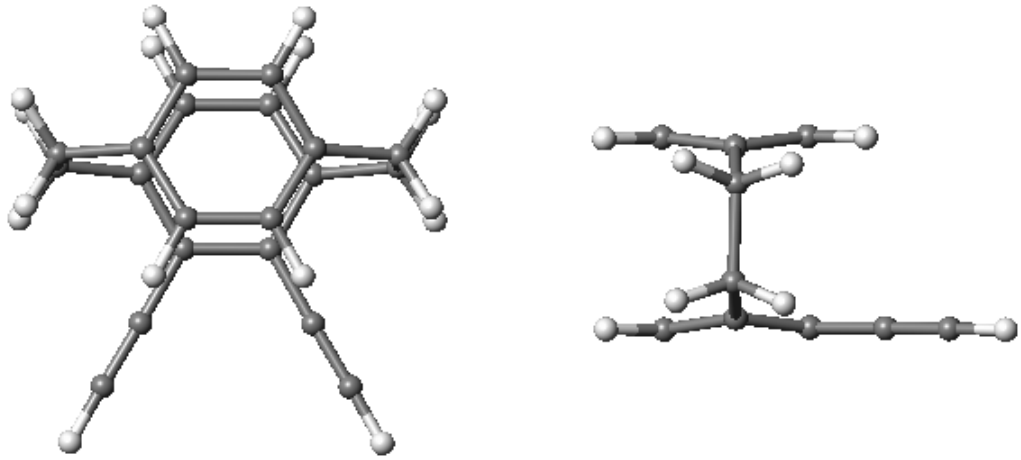

Figure 15: Calculated structure of **56**.

Table 6: Calculated torsion angles [°] of **56**.

C(14)-C(1)-C(2)-C(3)	-4.1	C(11)-C(10)-C(9)-C(6)	4.1
H(1*a*)-C(1)-C(2)-H(2*a*)	-5.8	H(10*a*)-C(10)-C(9)-C(9*a*)	5.8
H(1*s*)-C(1)-C(2)-H(2*s*)	-5.2	H(10*s*)-C(10)-C(9)-C(9*s*)	5.2
H(1*a*)-C(1)-C(2)-H(2*s*)	110.0	H(10*a*)-C(10)-C(9)-C(9*s*)	-110.0
H(1*s*)-C(1)-C(2)-H(2*a*)	-121.1	H(10*s*)-C(10)-C(9)-C(9*a*)	121.1

4 Synthesis of the iodobenzenes

Following the retrosynthetic analysis given in Chapter 2, 2-ethynyl-halobenzenes **57** are needed as coupling partners for the synthesis of [2.2]paracyclophane/dehydrobenzo-[14]annulenes. The synthesis of the substituted iodobenzenes **116**, **121** and **125** was described by Haley and coworkers for the TiPS protected derivatives.[52, 53, 54] Since the TMS protection group is easier to remove (K_2CO_3 rather than TBAF), it was chosen to protect the alkyne function of the 2-ethynyl-iodobenzenes.

Starting from commercially available 2-iodo-aniline (**113**), 2-(trimethylsilyl)ethynyl-iodobenzene (**116**) can be prepared in three steps in an overall yield of 69% (Scheme 34).

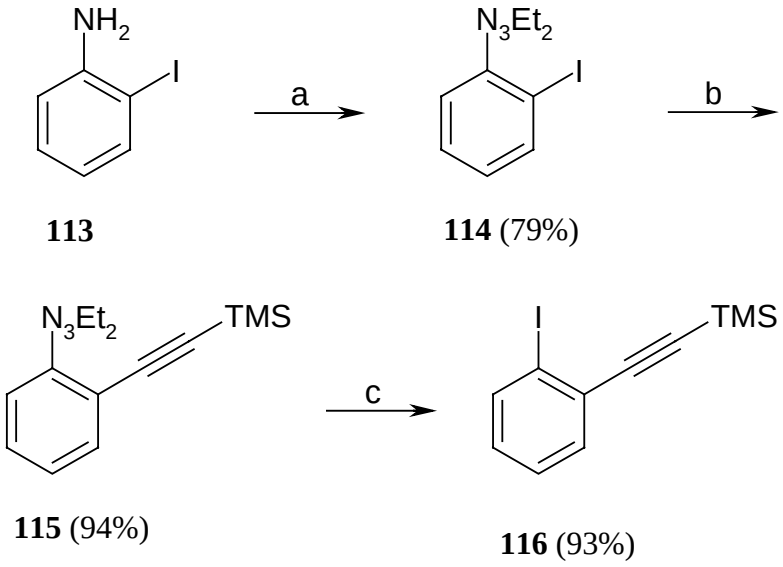

113 **114** (79%)

115 (94%) **116** (93%)

(a) [i] $NaNO_2$, HCl, H_2O, CH_3CN, THF, Et_2O; [ii] Et_2NH, K_2CO_3, H_2O, CH_3CN; (b) TMSA, $Pd(PPh_3)_4$, CuI, $^iPr_2NH$, THF; (c) CH_3I, 120 °C

Scheme 34: Synthesis of 2-(trimethylsilyl)ethynyl-iodobenzene (**116**).

Diazotization of **113** under standard conditions gave the diazonium salt which was reacted with diethylamine to the triazene **114**.[55] Pd catalyzed cross coupling with TMSA gave **115**. In the last step, the triazene was converted to the iodo compound **116** by heating **115** in CH_3I at 120 °C in a sealed ampoule.[55]

Substituents, usually in *para*-position to one of the alkyne groups can be used to increase the solubility of the later prepared annulenes. For this reason, 4-*tert*-butyl-2-[(trimethylsilyl)ethynyl]iodobenzene (**121**) was prepared using similar reactions (Scheme 35). The iodination of 4-*tert*-butyl-aniline (**117**) in the first step was performed

by reaction with benzyltrimethylammonia dichloroiodate.[56] The next steps follow the protocol, already given for the unsubstituted derivative.

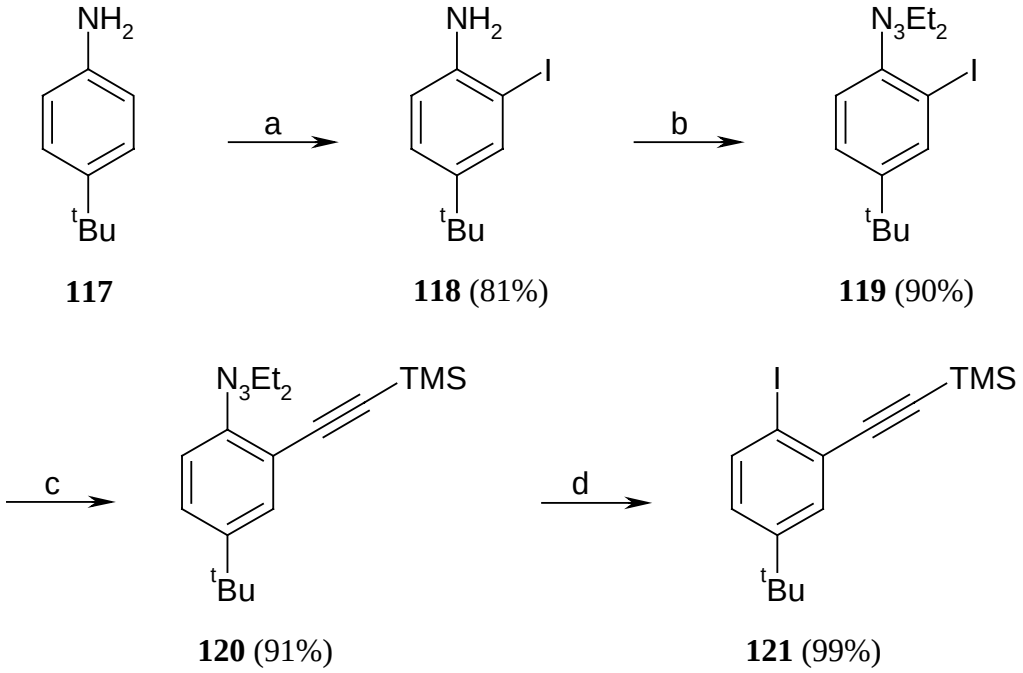

(a) $(BnNMe_3)^+ ICl_2^-$, $CaCO_3$, CH_2Cl_2, CH_3OH; (b) [i] $NaNO_2$, HCl, H_2O, CH_3CN, THF, Et_2O; [ii] Et_2NH, K_2CO_3, H_2O, CH_3CN; (c) TMSA, $Pd(PPh_3)_4$, CuI, $^iPr_2NH$, THF; (d) CH_3I, 120 °C

Scheme 35: Synthesis of 4-*tert*-butyl-2-[(trimethylsilyl)ethynyl]iodobenzene (**121**) by Haley and coworkers.

Scheme 36 summarizes the preparation of an annulene piece with an electron donating group. Alkylation of 3-iodo-aniline (**122**) with *n*-butylbromide in a THF/DMF mixture in the presence of $NaHCO_3$ generated *N*,*N*-dibutyl-3-iodo-aniline (**123**) in 78% yield. Pd catalyzed cross coupling with TMSA gave **124** which was iodinated to **125** using the mild reagent $(BnNMe_3)^+ ICl_2^-$.

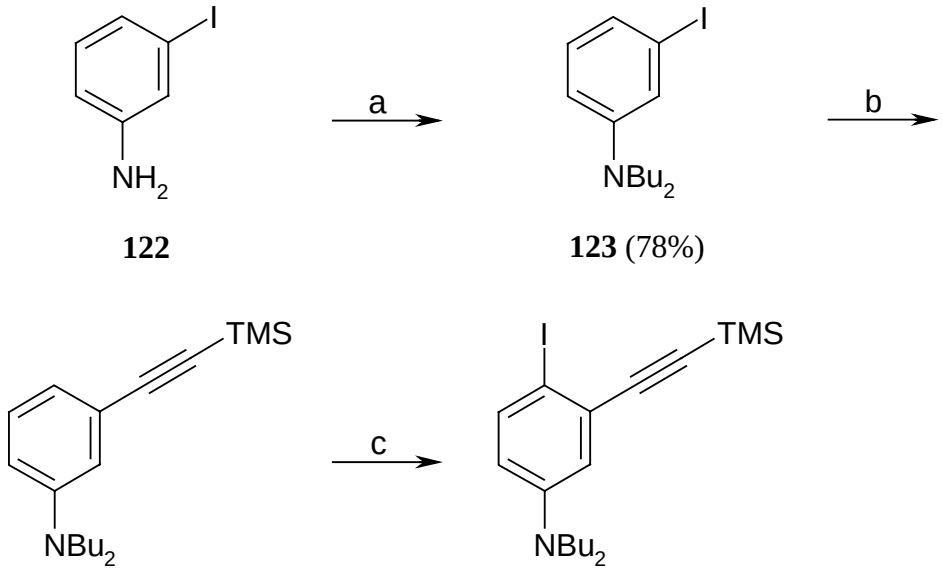

122 **123** (78%)

124 (93%) **125** (68%)

(a) BuBr, $NaHCO_3$, THF, DMF; (b) TMSA, $Pd(PPh_3)_4$, CuI, $^{i}Pr_2NH$, THF; (c) $(BnNMe_3)^+ ICl_2^-$, $CaCO_3$, CH_2Cl_2, CH_3OH

Scheme 36: Synthesis of *N*,*N*-dibutyl-4-iodo-3-[(trimethylsilyl)ethynyl]aniline (**125**).

5 [2.2]Paracyclophane/Dehydrobenzoannulene hybrids

As the first synthetic target in this group of hydrocarbons the achiral paracyclophane **53** was selected.

5.1 Synthesis

Sonogashira coupling of 4,5-diethynyl[2.2]paracyclophane (**56**) with 2-(trimethylsilyl)-ethynyl-iodobenzene (**116**)[52] gave the annulene precursor **126** in 58% yield. After its desilylation with potassium carbonate in methanol the free alkyne could be cyclized by heating with copper acetate in acetonitrile in an one pot reaction: the [2.2]paracyclophane/dehydrobenzoannulene hybrid **53** was obtained in nearly quantitative yield (97%, Scheme 37).

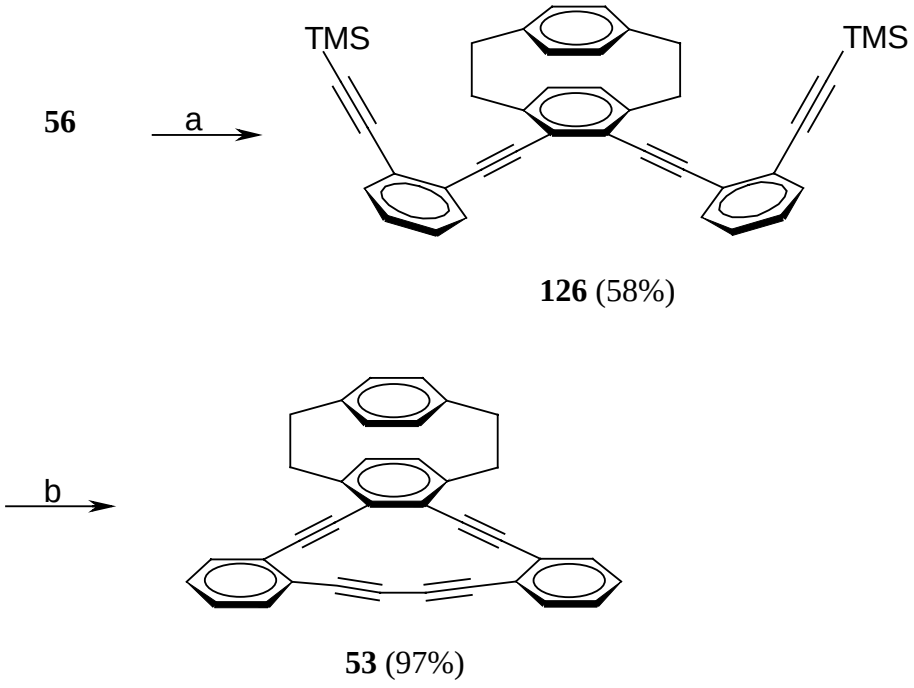

(a) 2-(trimethylsilylethynyl)iodobenzene (**116**), $Pd(PPh_3)_4$, CuI, NEt_3, THF; (b) K_2CO_3, $Cu(OAc)_2$, CH_3OH, CH_3CN

Scheme 37: Synthesis of the PC/DBA hybrid **53** by Pd-catalyzed cross coupling followed by cyclization.

Crystals of **126** suitable for X-ray crystallography were obtained by slow diffusion of pentane in CH_2Cl_2. For **53**, the solvent system benzene/CH_2Cl_2 was efficient to get single crystals which were analyzed by X-ray crystallography. These structures will be discussed below.

The NMR spectra of **126** show only half of the signals because of the symmetry of the cyclophane. In the ^{1}H NMR spectrum, the bridge protons appear as the usual ddd-pattern at 2.82, 3.01, 3.31 and 3.80 ppm. For the aromatic protons of the cyclophane, a multiplet at 6.48 ppm for H-12 and H-13, a singlet at 6.50 ppm for H-7 and H-8 and a multiplet at 6.95 ppm for the protons H-15 and H-16 can be found. The other aromatic protons give an AA'XX' spectrum with multiplets between 7.18 and 7.22 ppm (H-21 and H-22), 7.46 and 7.51 ppm (H-23) and between 7.52 and 7.57 ppm (H-20). These protons can be assigned because irradiation at H-15, H-16 results in an NOE with the protons H-20, H-20' (Figure 16).

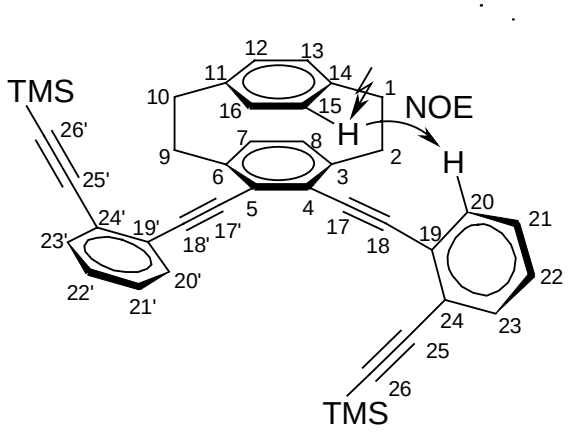

Figure 16: Assignment of the aryl-protons in the annulene precursor **126** by NOE experiments.

The ^{1}H NMR spectrum of the annulene **53** displays two sets of multiplets for the bridge protons; one between 3.05 and 3.23 ppm for the protons H-1*a*, H-1*s*, H-10*a*, H-10*s*, H-2*a* and H-9*a* and one between 3.94 and 4.00 for the protons H-2*s* and H-9*s*. The aromatic cyclophane protons give multiplets at 6.54 ppm (H-12 and H-13) and 6.65 ppm (H-15 and H-16). The protons H-7 and H-8 give a singlet at 6.76 ppm. For the aromatic protons of the annulene, four doublets of doublets of doublets at 7.45, 7.54, 7.65 and 7.93 ppm were are registered.

For spectral comparison, the non-benzo derivative **54** was prepared by palladium catalyzed cross coupling of 4,5-diethynyl[2.2]paracyclophane (**56**) with 1-chloro-4-trimethylsilylbuten-3-yne (**175**).[57] As solvent system, a 1:1 mixture of *n*-butylamine and THF was used. The final cyclization was carried out after *in situ* deprotection with K_2CO_3 by a Berscheid-Vögtle modification of the oxidative Eglinton coupling (use of acetonitrile rather than pyridine).

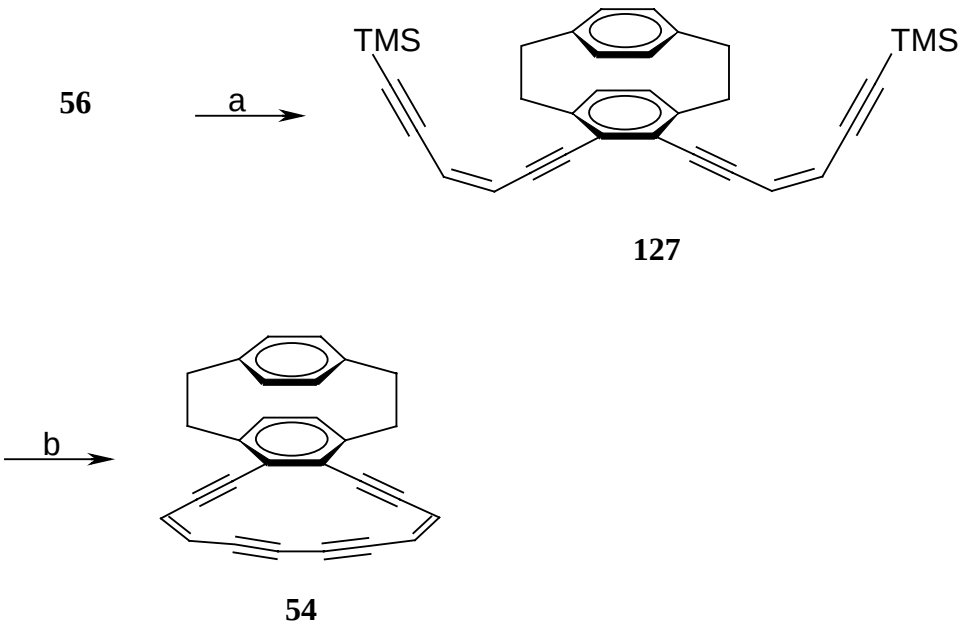

(a) 1-chloro-4-trimethylsilylbuten-3-yne (**175**), $Pd(PPh_3)_4$, CuI, $PrNH_2$, THF; (b) K_2CO_3, $Cu(OAc)_2$, CH_3OH, CH_3CN

Scheme 38: Synthesis of the [2.2]paracyclophane/dehydro[14]annulene **54**.

5.2 NMR Spectroscopy

NMR spectroscopy is one of the most powerful tools to investigate aromaticity. Both aromatic and anti-aromatic systems have the ability to sustain induced ring currents when they are placed in the magnetic field of an NMR spectrometer. In aromatic systems, the outer protons of the ring system are deshielded, the inner protons (if present) are shielded. Aromatic $(4n+2)\pi$-systems show a diamagnetic ring current, so they are called diatropic substances. In anti-aromatic $(4\ n)\pi$-systems, a paramagnetic ring current is present, so anti-aromatics are called paratropic substances. In this case, the outer protons are shielded and the inner protons are deshielded.[58]

By comparing the chemical shift range of the proximal and the distal protons (H_p and H_d) in an benzene ring of a DBA, it is possible to give a qualitative analysis of the nature of the ring currents in these systems.[59, 60] A diatropic ring current will cause a downfield shift of the H_p and H_d signals relative to a reference signal whereas a paratropic ring current will cause an upfield shift of the H_p and H_d signals. The strength of the induced ring current can be derived from the extent of the shift.

Figure 18 shows a comparison between the chemical shifts of the proximal and distal protons of the [14]annulenes, shown in Figure 17. The results are summarized in Table 7.

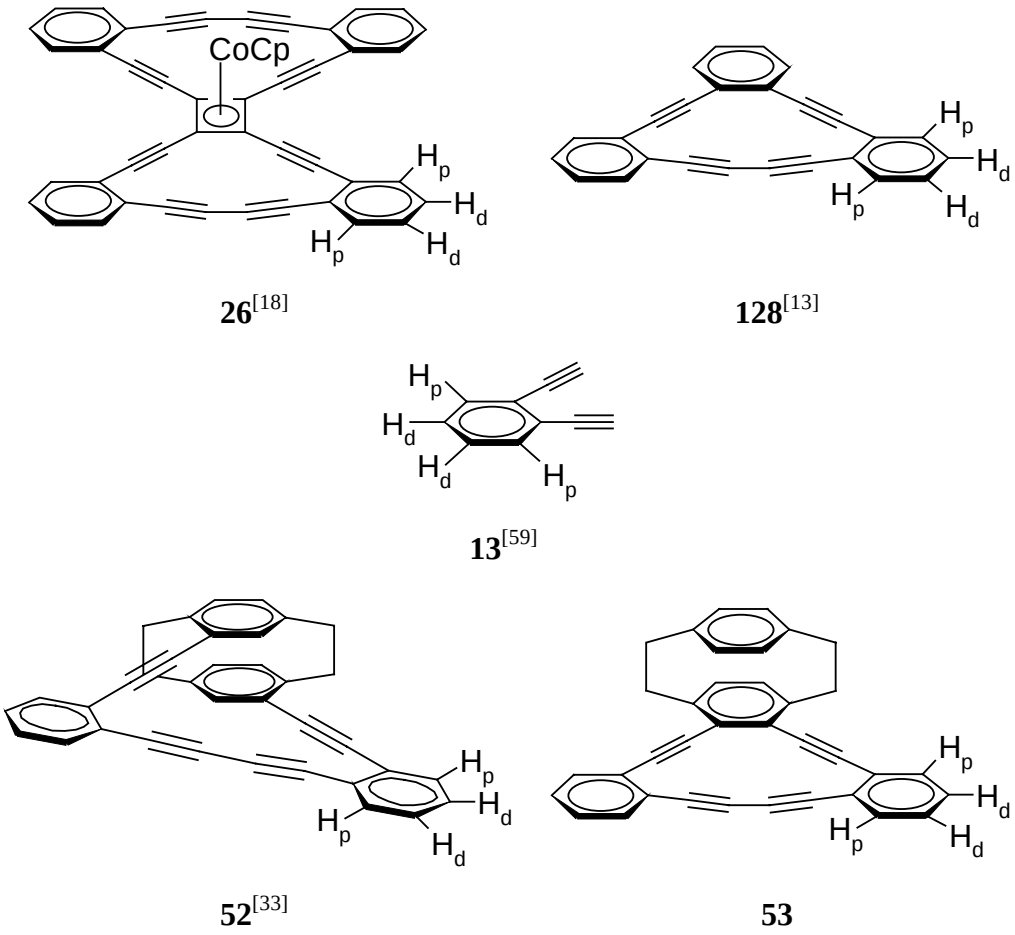

26[18] **128**[13]

13[59]

52[33] **53**

Figure 17: Different [14]annulenes with characteristic ring currents.

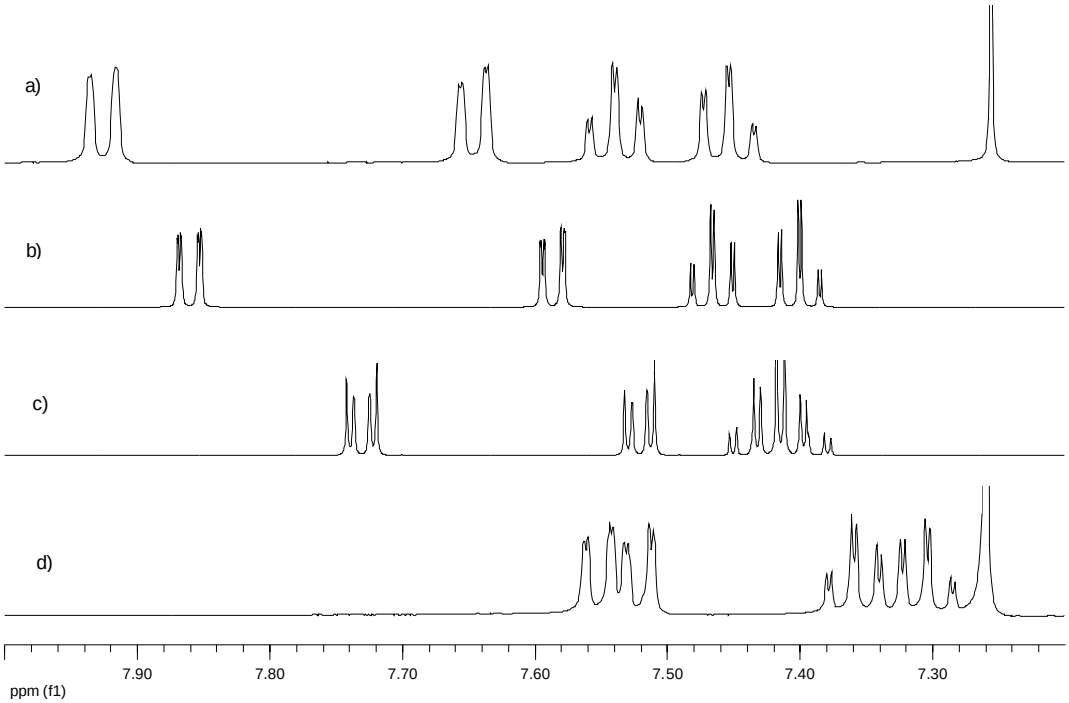

Figure 18: Aromatic region of the ^{1}H NMR spectra of the [14]annulenes summarized in Figure 17. a) **53**, b) **128**, c) **26**, d) **52**. The spectra b) and c) are simulated using the values published in the literature.

Table 7: Chemical shifts of proximal (H_p) and distal (H_d) protons relative to *o*-diethynylbenzene (**13**).

Compound	H_p [ppm]	deviation from **13**	H_d [ppm]	deviation from **13**
13	7.50		7.29	
52	7.55; 7.52	+0.05; +0.02	7.36; 7.30	+0.07; +0.01
26	7.73; 7.52	+0.23; +0.02	7.42[a]	+0.13
128	7.85; 7.58	+0.35; +0.08	7.46; 7.39	+0.17; +0.10
53	7.93; 7.65	+0.43; +0.15	7.54; 7.45	+0.25; +0.16

All systems show the expected downfield shift of the arene proton signals, indicating a diatropic ring current in the [14]annulene. The strength of the ring current is indicated by the downfield shift of the arene protons, demonstrating that the *pseudo-ortho* [2.2]paracyclophane derivative **52** possesses the weakest aromaticity in the [14]annulene ring. This is to be expected, because in this system, delocalization is only sustained by π-π-interactions between the cyclophane decks. The most pronounced aromatic [14]annulene is noted for the *ortho* [2.2]paracyclophane derivative **53**.

[a] The multiplicity of the two protons H_d is described in the literature as a quintet of doublets, in fact it has to be analyzed as two overlapping doublets of triplets.

In case of the [2.2]paracyclophane derivative **53**, protons H-15 and H-16 which lie above the dehydro[14]annulene ring, can be also used as a sensor for the ring current in the annulene. In the open compound **126**, H-15 and H-16 are in the deshielding region of the acetylene function. Upon ring closure, an aromatic system is formed, causing a shielding effect on the protons above or under the π-plane due to the now present ring current (Figure 19).

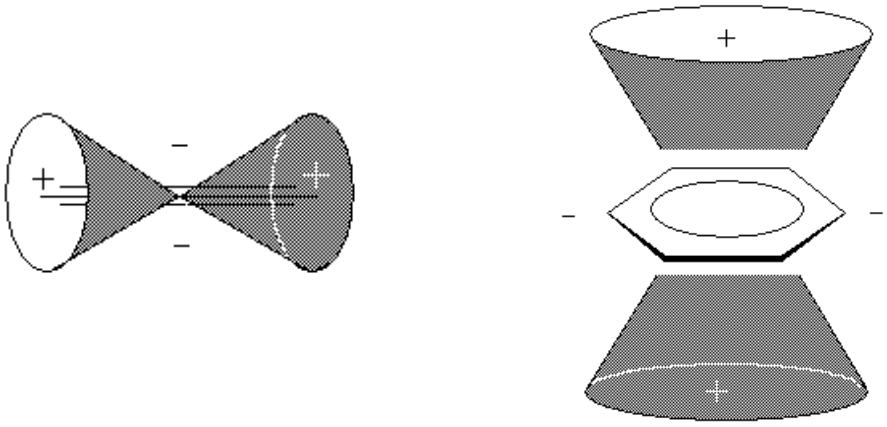

Figure 19: Shielding and deshielding cones of acetylenes and aromatic systems.

This effect is indicated by an upfield shift of the protons H-15 and H-16 after cyclization (Figure 20).

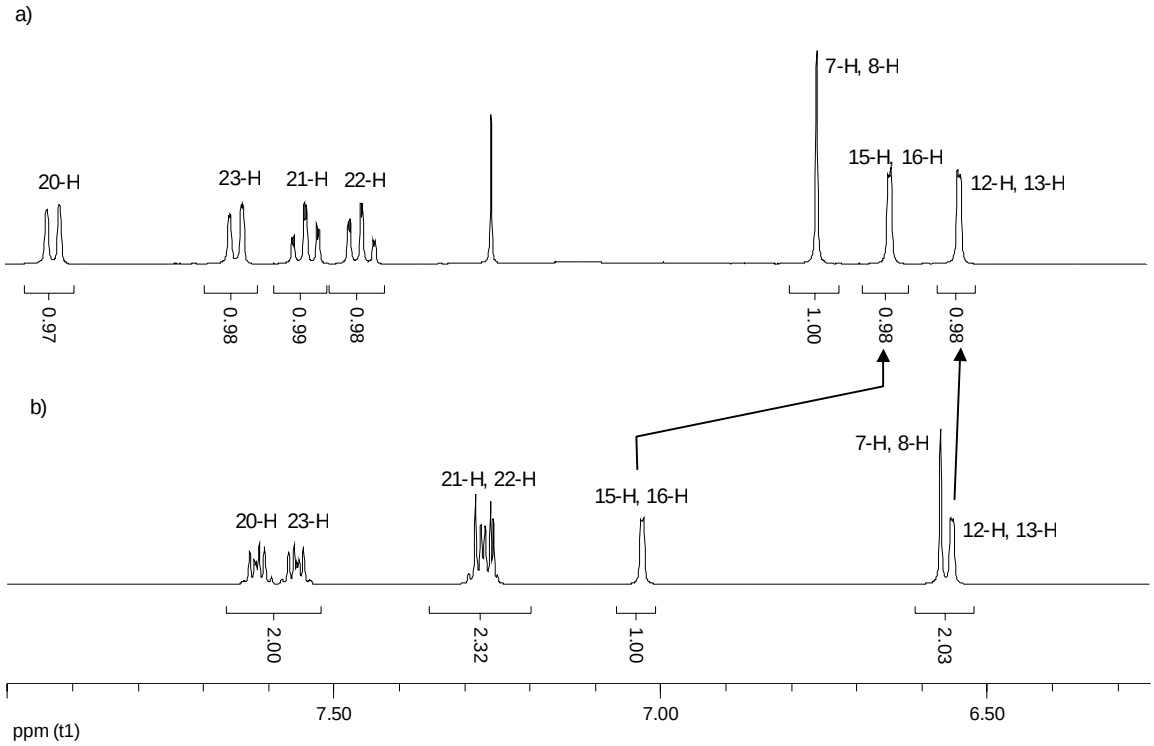

Figure 20: Aromatic region of the ^{1}H NMR spectra of a) dibenzo[2.2]paracyclophanotetradehydro[14]annulene (**53**) and b) its open precursor **126**.

The formation of the aromatic system has no effect to the protons H-12 and H-13 in *anti* position to the annulene, whereas the protons of the aromatic units fused to the [14]annulene are shifted downfield relative to the open precursor.

Another sensor for aromaticity are the vinylic protons located on dehydroannulenes.[17] Bunz has compared the aromaticity of ferrocene-, cyclobutadiene-(cyclopentadienylcobalt)- and benzene-fused dehydro[14]annulenes by regarding the differences in the chemical shifts and $^{3}J_{HH}$ coupling constants of the vinylic protons (H_a and H_b).[16] Because of the deshielding effect of the ring current in the [14]annulene, a downfield shift of the protons H_a and H_b upon ring closure should be observed. Attaching an aromatic system to the [14]annulene weakens the ring current; the strongest aromatic system fused to the [14]annulene core leads to the least aromatic [14]annulene, reflected by an upfield shift of the protons H_a and H_b relative to the systems with the less aromatic system fused to the [14]annulene.

To exclude local magnetic effects of the organometallic species, Bunz compared the downfield shift ($\Delta\delta$) of the vinylic protons upon ring closure. For the system with the smallest downfield shift the gain of aromaticity for the annulene formed would be the least. Table 8 shows the comparison of Bunz' annulenes, the already known PC/DBA hybrid and the PC/DBA hybrid synthesized in this work.

The *pseudo-ortho* [2.2]paracyclophane-dehydro[14]annulene (**130**) shows the smallest donwfield shift of the protons H_a and $H_{b,}$ followed by the organometallic dehydro[14]annulenes **24** and **132** which also have a smaller downfield shift than the benzo derivative **134**. Bunz concluded that benzene is less aromatic than cyclobutadiene(cyclopentadienylcobalt) or ferrocene. If one follows this argumentation, **130** should be even more aromatic than the latter two compounds. However, this is not the case. The weaker aromaticity of the [14]annulene in **130** can be explained by the necessity of π-π-interactions between the cyclophane decks to generate a delocalized π-system in the [14]annulene. These π-π interactions weaken the aromaticity of the [14]annulene. Bunz' result was confirmed by the results obtained for the [2.2]paracyclophane derivative **54**. Aromaticity is less pronounced in [2.2]paracyclophane than in benzene, a stronger aromatic dehydro[14]annulene should be observed. This can indeed be seen by a stronger downfield shift of the vinylic protons H_a and H_b in the [2.2]paracyclophane derivative **54**.

Table 8: Chemical shifts and $^{3}J_{HH}$ coupling of the alkene protons in open and cyclized octadehydro[14]annulenes.

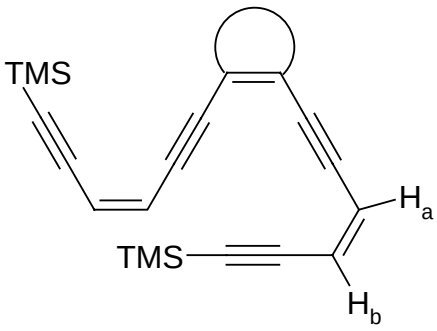

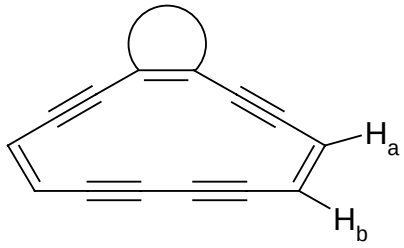

a **b**

compound		ref.	H_a [ppm]	H_b [ppm]	$^{3}J_{Ha,Hb}$ [Hz]	$\Delta\delta(H_a)$ [ppm]	$\Delta\delta(H_b)$ [ppm]
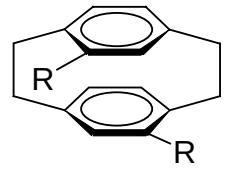	**a (129)**	[33]	6.17	5.94	11.0	0.21	-0.03
	b (130)		6.38	5.91	10.2		
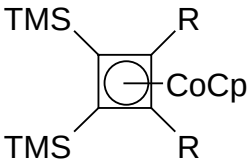	**a (23)**	[16]	5.84	5.80	11.2	0.68	0.38
	b (24)		6.52	6.18	10.0		
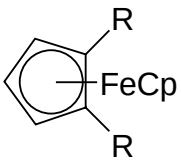	**a (131)**	[16]	5.98	5.81	11.0	0.77	0.40
	b (132)		6.75	6.21	10.2		
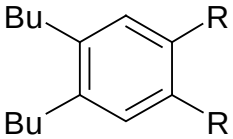	**a (133)**	[16]	6.15	5.85	11.0	1.18	0.78
	b (134)		7.33	6.63	10.0		
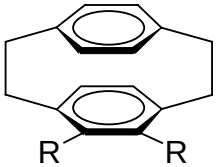	**a (127)**		6.17	5.92	11.0	1.37	0.82
	b (54)		7.54	6.74	9.9		

5.3 UV/Vis-Spectroscopy

The absorption of ultraviolet or visible light by a molecule causes the excitation of an electron from an initially occupied orbital with lower energy to a previously unoccupied orbital with higher energy.[61] Usual transitions are from binding σ- or π-orbitals or nonbinding n-orbitals (lone electron pairs) to antibinding σ^*- or π^*-orbitals ($\sigma\rightarrow\sigma^*$, $\pi\rightarrow\pi^*$, $n\rightarrow\pi^*$ or $n\rightarrow\sigma^*$ transitions).[62] Delocalization of the π-electrons results a lower energy of the π*-orbital and give it a less antibinding character causing a bathochromic shift of the absorption maxima.

Figure 21 shows the electronic absorption spectrum of the PC/DBAs **53**, **52**[33], the dehydrobenzo[14]annulene **128**[13, 33] and the acyclic model compound **135**[33].

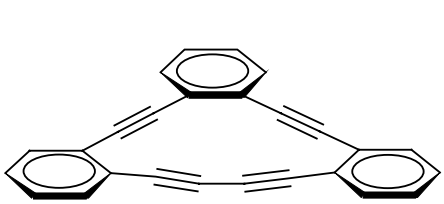

128

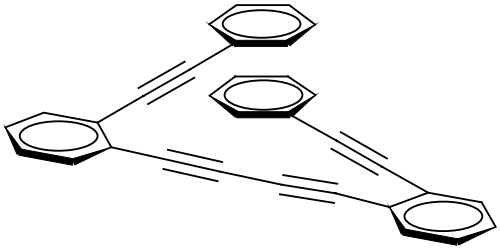

135

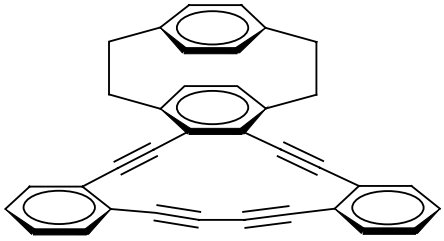

53

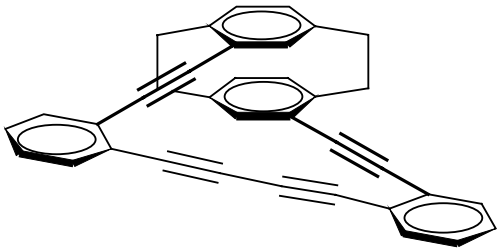

52

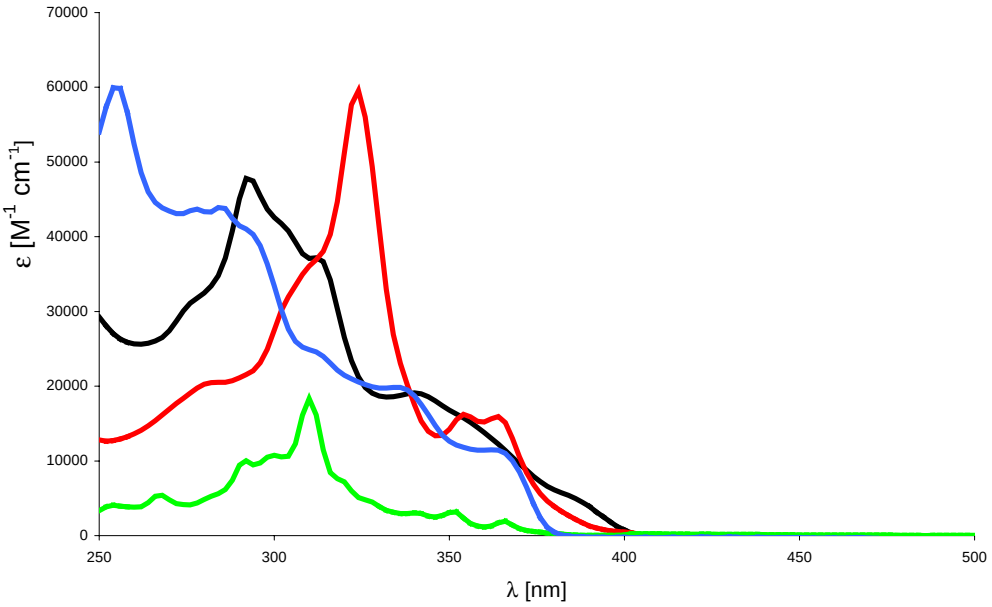

Figure 21: Electronic absorption spectra of PC/DBA **53** (red), PC/DBA **52**[33] (black), annulene **128**[13, 33] (green) and open analogue **135**[33] (blue).

Comparison of PC/DBA **52** with dehydrobenzo[14]annulene **128** shows a small bathochromic shift for **128** indicating slightly stronger delocalization in **128**. Since the acyclic hydrocarbon **135** has the same chromophore as **52** just without the bridging ethano units, the comparison between these two compounds should give an answer about the transannular interactions in the [2.2]paracyclophane unit. The expected bathochromic shift for PC/DBA **52** can definitely be found in the electronic absorption spectrum indicating transannular delocalization by through space interactions in the cyclophane.

PC/DBA **53** shows the strongest bathochromic shift of these four compounds, indicating the strongest ring current in the [14]annulene. This finding agrees with the results from the proton NMR spectra of **53** and **128** (see above).

5.4 X-Ray structure analysis

X-Ray structure analysis provides bonding parameters (bond length, angles, intramolecular distances etc). From the packing diagram intermolecular structure parameters can be obtained.

Figure 22 shows the molecular structure of the "open" hydrocarbon **126** in the crystal. Some selected bond lengths and angles are given in Table 9.

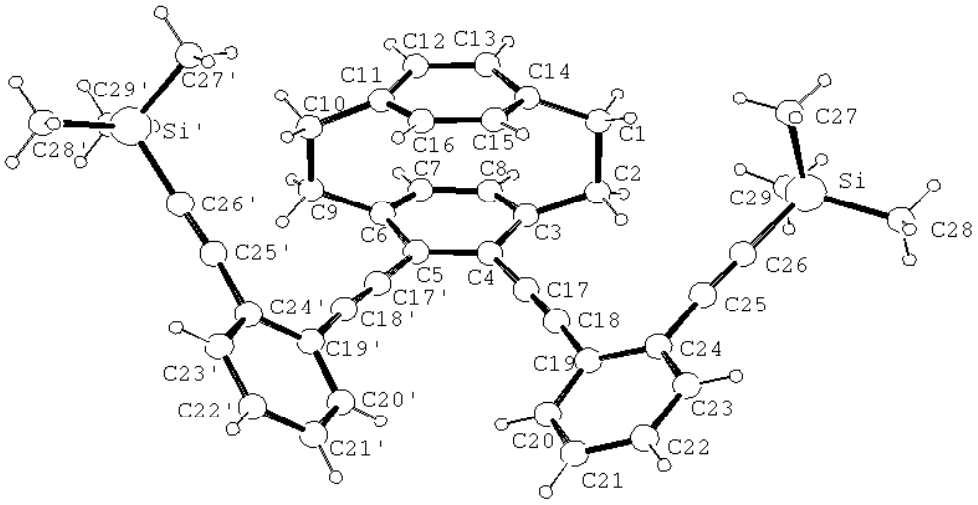

Figure 22: X-ray structure of **126** in the crystal.

Table 9: Selected bond lengths [Å] and angles [°] of **126**.

C(17)-C(18)	1.1970(19)	C(17')-C(18')	1.202(2)
C(25)-C(26)	1.204(2)	C(25')-C(26')	1.209(2)
C(4)-C(17)	1.4337(19)	C(5)-C(17')	1.4348(19)
C(18)-C(19)	1.4373(19)	C(18')-C(19')	1.4390(19)
C(24)-C(25)	1.4374(19)	C(24')-C(25')	1.434(2)
C(26)-Si	1.8452(15)	C(26')-Si'	1.8440(15)
C(3)-C(4)-C(17)	120.76(12)	C(6)-C(5)-C(17')	120.38(12)
C(5)-C(4)-C(17)	119.13(13)	C(4)-C(5)-C(17')	119.30(12)
C(20)-C(19)-C(18)	119.23(12)	C(20')-C(19')-C(18')	119.23(12)
C(24)-C(19)-C(18)	121.71(12)	C(24')-C(19')-C(18')	121.86(13)
C(19)-C(24)-C(25)	121.74(12)	C(19')-C(24')-C(25')	122.54(13)
C(23)-C(24)-C(25)	119.30(12)	C(23')-C(24')-C(25')	118.69(13)
C(4)-C(17)-C(18)	178.80(15)	C(5)-C(17')-C(18')	177.70(15)
C(17)-C(18)-C(19)	174.41(14)	C(17')-C(18')-C(19')	173.65(14)
C(24)-C(25)-C(26)	176.24(14)	C(24')-C(25')-C(26')	174.24(16)
C(25)-C(26)-Si	176.99(14)	C(25')-C(26')-Si'	174.09(15)

The [2.2]paracyclophane unit of **126** shows the typical geometry, bond lengths and -angles for this class of hydrocarbons. Comparing to standard bond length (C*sp*≡C*sp*: 118 pm[63]), the carbon-carbon triple bonds C(25)-C(26) and C(25')-C(26') are elongated

about 2.3 to 2.8 pm, due to the silyl protection group; the carbon-silicon single bonds C(26)-Si and C(26')-Si' agree with the standard bond length (C*sp*-Si: 184 pm[63]). The bonds C(17)-C(18) and C(17')-C(18') show the typical bond length of 119 pm for ar-C*sp*≡C*sp*-ar triple bonds. Regarding the bond angles, the alkyne units C(4)-C(17)-C(18)-C(19) and C(5)-C(17')-C(18')-C(19') deviate from linearity on the order of 1.2 to 6.4°, the alkyne units C(24)-C(25)-C(26)-Si and C(24')-C(25')-C(26')-Si' deviate between of 3.0 and 5.9°.

The structures of the cyclized molecule **53** are shown in Figure 23 and Figure 24. The asymmetric unit contains two inequivalent molecules of the annulene, three half benzene and one half CH_2Cl_2 molecule. Some selected bond lengths are given in Table 10, selected angles are given in Table 11.

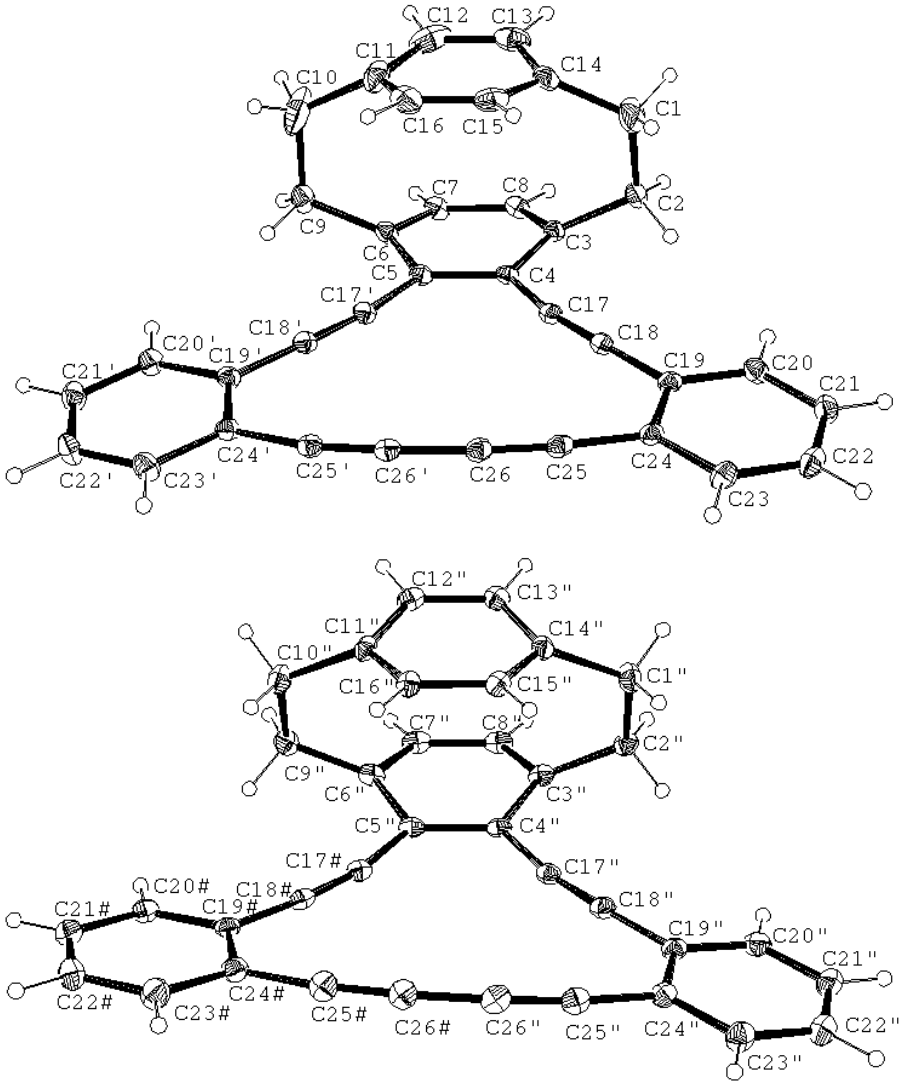

Figure 23: X-ray structure of the two inequivalent molecules of **53**, ellipsoids are drawn with 30% probability.

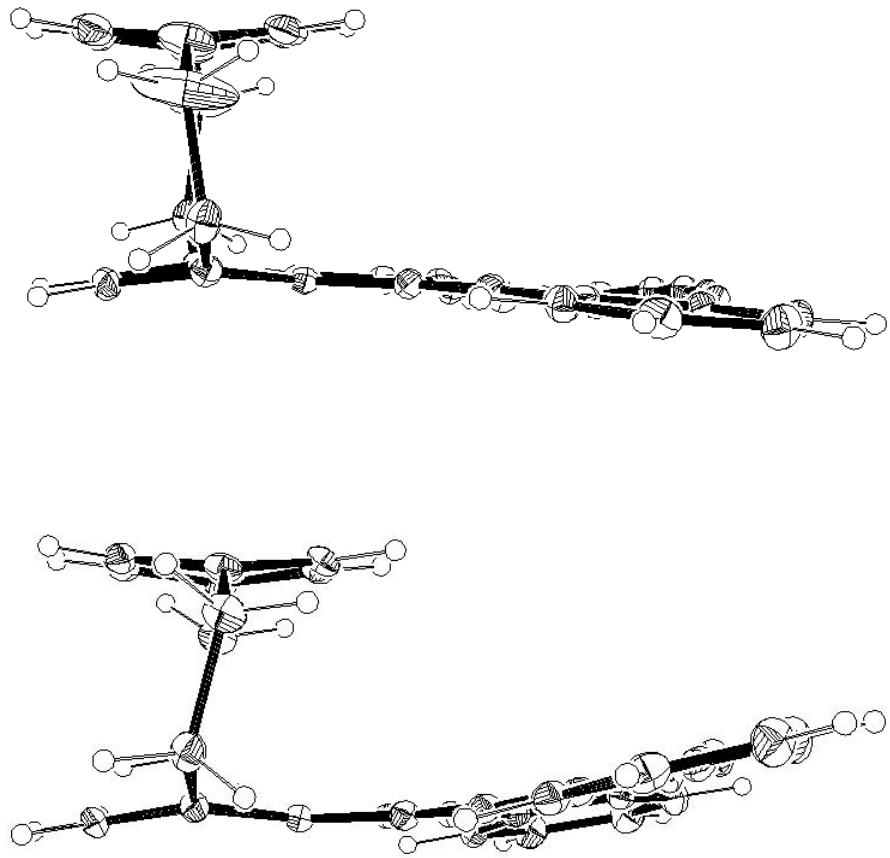

Figure 24: Side view of the two inequivalent molecules of **53**.

Table 10: Selected bond lengths [Å] of **53**.

C(17)-C(18)	1.206(3)	C(17')-C(18')	1.210(4)
C(25)-C(26)	1.206(4)	C(25')-C(26')	1.207(3)
C(4)-C(17)	1.434(3)	C(5)-C(17')	1.433(4)
C(18)-C(19)	1.439(3)	C(18')-C(19')	1.429(4)
C(24)-C(25)	1.424(4)	C(24')-C(25')	1.421(3)
C(26)-C(26')	1.365(4)		

Table 11: Selected bond angles [°] of **53**.

C(14)-C(1)-C(2)	114.3(2)	C(14")-C(1")-C(2")	112.7(2)
C(3)-C(2)-C(1)	112.3(2)	C(3")-C(2")-C(1")	112.9(2)
C(6)-C(5)-C(17')	117.0(2)	C(6")-C(5")-C(17#)	116.1(2)
C(4)-C(5)-C(17')	123.2(2)	C(4")-C(5")-C(17#)	124.1(2)
C(5)-C(6)-C(9)	122.5(2)	C(5")-C(6")-C(9")	121.6(2)
C(6)-C(9)-C(10)	113.4(2)	C(6")-C(9")-C(10")	113.3(2)
C(11)-C(10)-C(9)	115.0(3)	C(11")-C(10")-C(9")	112.0(2)
C(15)-C(14)-C(1)	118.8(3)	C(15")-C(14")-C(1")	120.7(2)
C(13)-C(14)-C(1)	123.1(3)	C(13")-C(14")-C(1")	120.9(2)
C(15)-C(16)-C(11)	120.6(3)	C(11")-C(16")-C(15")	120.7(2)

Table 12: Selected torsion angles [°] of **53**.

C(14)-C(1)-C(2)-C(3)	-15.4(5)	C(14")-C(1")-C(2")-C(3")	-11.5(3)
C(1)-C(2)-C(3)-C(8)	92.2(3)	C(1")-C(2")-C(3")-C(8")	98.4(3)
C(1)-C(2)-C(3)-C(4)	-74.6(4)	C(1")-C(2")-C(3")-C(4")	-69.0(3)
C(6)-C(9)-C(10)-C(11)	-6.6(6)	C(6")-C(9")-C(10")-C(11")	15.1(3)
C(7)-C(6)-C(9)-C(10)	-76.8(4)	C(7")-C(6")-C(9")-C(10")	-101.2(3)
C(5)-C(6)-C(9)-C(10)	89.9(4)	C(5")-C(6")-C(9")-C(10")	65.8(3)
C(9)-C(10)-C(11)-C(12)	90.6(5)	C(9")-C(10")-C(11")-C(12")	67.7(3)
C(9)-C(10)-C(11)-C(16)	-73.8(5)	C(9")-C(10")-C(11")-C(16")	-97.8(3)

The two inequivalent molecules of **53** represent the two possible conformations (twisted- and parallel displaced benzene rings) of the [2.2]paracyclophane core.

In the conformer with twisted benzene rings, the bond angles C(14)-C(1)-C(2) and C(11)-C(10)-C(9) are increased by 1.6 and 3.0° relative to the conformer with parallel displaced benzene rings whereas the bond angles C(3)-C(2)-C(1) and C(6)-C(9)-C(10) show practically no difference between the conformations. The bond angle C(15)-C(14)-C(1) is slightly diminished to 118.8° and the angle C(13)-C(14)-C(1) is enlarged to 123.1° in the conformer with twisted benzene rings. In the other conformer, these bond angles differ slightly from the typical 120° angle (0.7 - 0.9°). The most significant differences between the two conformers are the torsion angles of the bridges (see Table 12). For example the difference of the torsion angles between the bridges C(14)-C(1)-

C(2)-C(3) and C(6)-C(9)-C(10)-C(11) is 8.8° in the conformer with twisted benzene rings, and 26.6° in the conformer with parallel displaced benzene rings.

As seen in the side view (Figure 24), the conformer with twisted benzene rings exhibits just a slightly bowl-shaped topology of the [14]annulene unit. The conformer with parallel displaced benzene rings displays a curved structure in the [14]annulene. A prominent feature of the [14]annulene core of both conformers of **53** is the inward bending of the monoyne units C(4)-C(17)-C(18)-C(19) and C(5)-C(17')-C(18')-C(19') by 4.5 - 11.8°, whereas the diyne unit C(24)-C(25)-C(26)-C(26')-C(25')-C(24') bends outwards by 8.1 - 11.9°. Similar values were observed by Vollhardt and coworkers for all benzo derivative **128**, showing an inward bend of the monoyne units by 3.9 - 11.5° and an outward bend of the diyne unit by 8.6 - 11.2°.[13]

5.5 Molecular modeling studies

Since the alkyne units in the [14]annulene diverge from the typical linear geometry, some ring strain must be present in the [14]annulene unit. Surprisingly, the yield of cyclization to the strained molecule is nearly quantitative (97%), what arose the question of ring strain in the [14]annulene unit. The ring strain in the [14]annulene **53** was calculated by density functional theory.[64] Because molecular modeling calculations gave information about single molecules in the gas phase, the first step was a geometry optimization of the X-ray data using B3LYP/6-31G(d) method. In the next step, the optimized molecule was "cut" in two pieces, the monoyne part and the diyne part (Figure 25). Relaxation of the strained pieces gave a free energy of -5.1 kcal/mol for thy diyne fragment and -1.4 kcal/mol for the monoyne unit. Because the annulene contains two monoyne units, this energy has to be multiplied with two, to give a ring strain of 7.9 kcal/mol (33.08 kJ/mol) for the [14]annulene (Figure 26).

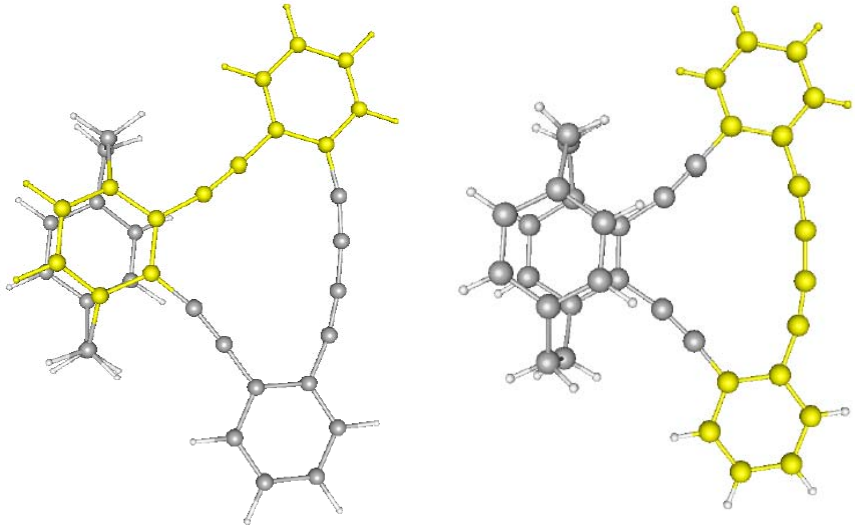

Figure 25: Monoyne and diyne part of **53**.

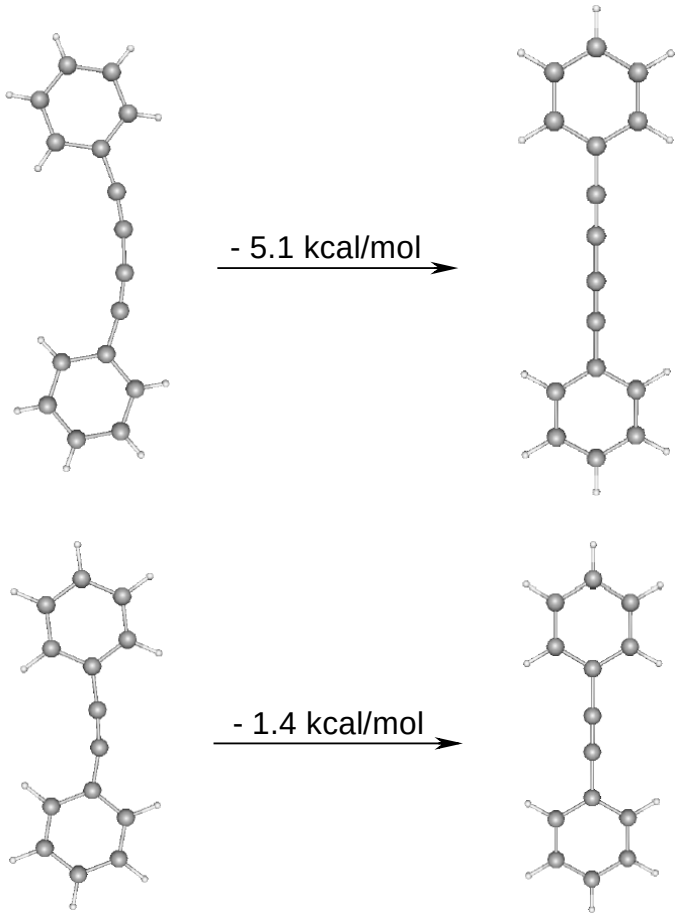

Figure 26: Free energy by relaxation of the strained annulene pieces.

6 [2.2]Paracyclophane derivatives containing smaller (anti)aromatic units

6.1 Synthesis of [2.2]paracyclophane derivatives of biphenylenes

In 1982, Vollhardt and co-workers discovered a new biphenylene synthesis.[65] The reaction can be described as a [2+2+2]cycloaddition of bis(trimethylsilyl)acetylene (**136**, BTMSA) to *o*-diethynylbenzene (**13**) catalyzed by η^5-cyclopentadienylcobalt dicarbonyl (**137**, $CpCo(CO)_2$). Because of the steric bulk of the TMS group, self-trimerization of **136** does not occur; in fact, it can be used as solvent for the reaction.

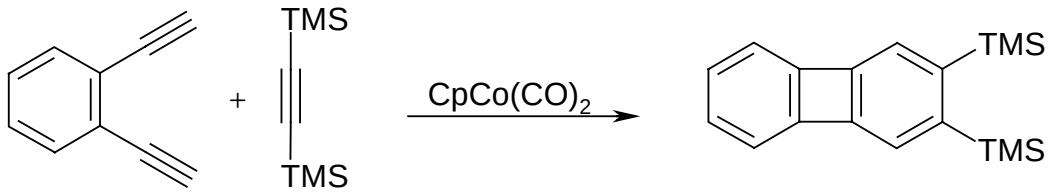

13 **136** **137** **138**

Scheme 39: Biphenylene synthesis by Vollhardt and co-workers.[65]

The mechanism of transition metal catalyzed cyclotrimerization of acetylene to benzene can be described as follow[66]: stepwise ligand exchange of the carbonyl ligands leads to the bis alkyne complex **139** from which by oxidative coupling and association of a third alkyne molecule, the metalocyclopentadiene **140** is formed. Alkyne insertion provides the metalocycloheptatriene **141**. Bercaw and Bergman have suggested an Diels-Alder reaction to **142** as an alternative to **141**.[67] The final step is a reductive elimination of the arene.

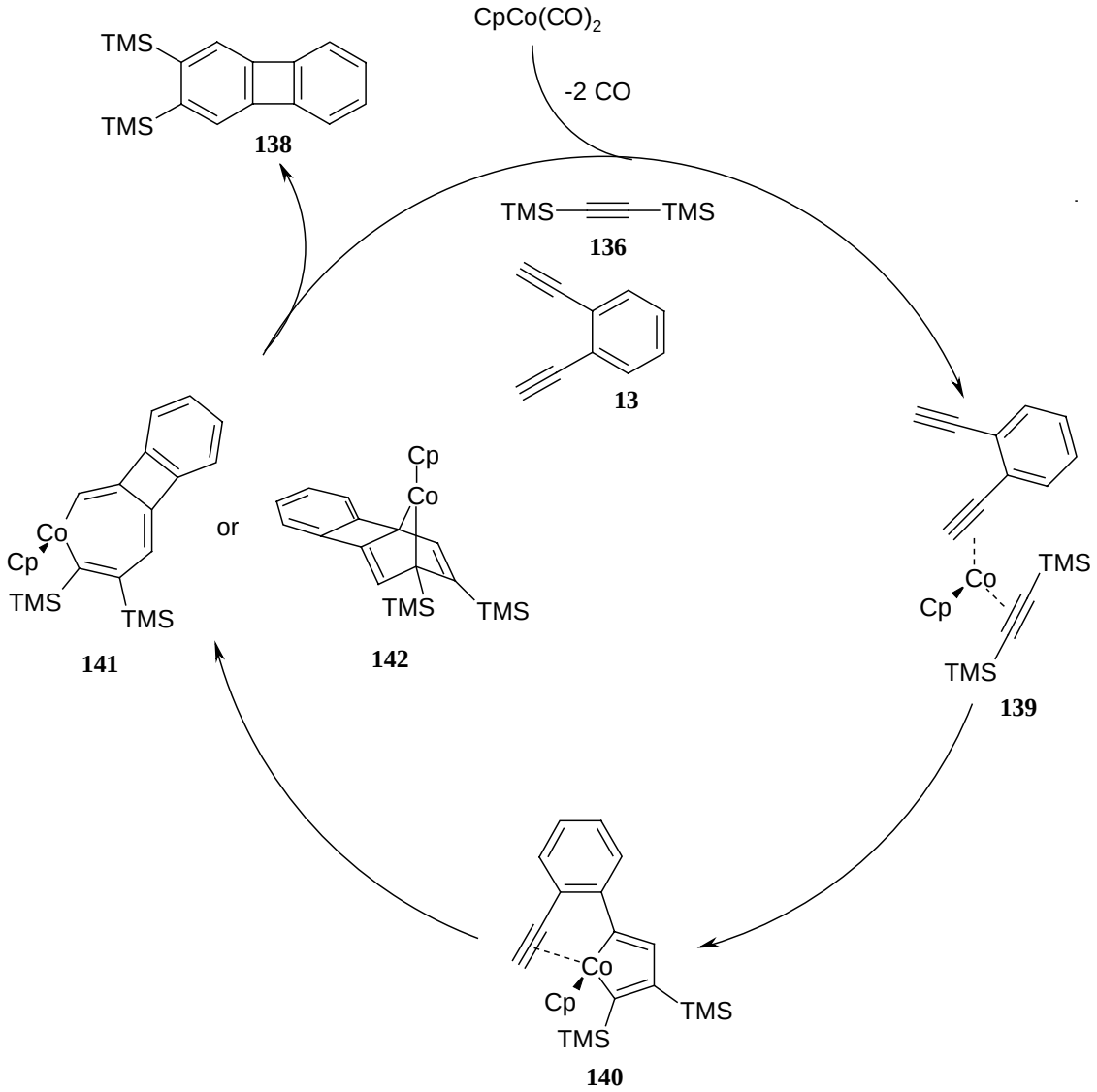

Scheme 40: Mechanism of the [2+2+2]cycloaddition.[66, 67]

Since phenylenes can be regarded as an alternation of aromatic (benzene) and antiaromatic (cyclobutadiene) units, phenylenes can have aromatic, antiaromatic or nonaromatic character. In case of higher oligomers **143**, the molecules are formally antiaromatic (n = 0, 2, 4, ...) or aromatic (n = 1, 3, 5, ...).

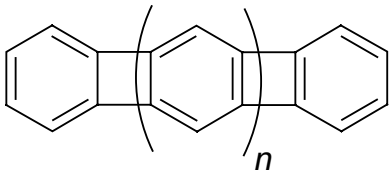

143

It was shown that even terphenylene (**143**, n = 1), an 18 π-electron species, does not react like an [18]annulene. The center ring shows unusual high reactivity; hydration occurs even faster than in normal unstrained olefins.[68]

Because [2.2]paracyclophane can be used as a probe for aromatic annulenes (see Chapter 5), it is reasonable to synthesize [2.2]paracyclophane/biphenylene hybrids. This was done by addition of BTMSA to *o*-diethynyl[2.2]paracyclophane (**56**) to give the [2.2]paracyclophane-biphenylene derivative (**144**) in 59% yield (Scheme 41).

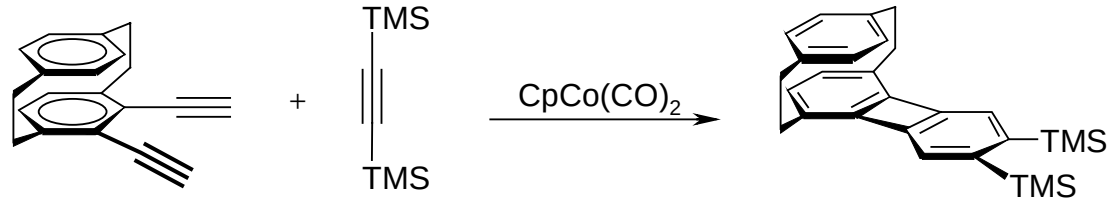

56 **136** **137** **144** (59%)

Scheme 41: Cyclotrimerization of **56** with BTMSA.

The ^{1}H NMR spectrum of **144** shows a singlet at δ = 0.38 for the trimethylsilyl protection groups. The bridge protons of the cyclophane give an ABCD spectrum, the iterative analysis of which is summarized in Chapter 6.3. The aromatic region of the ^{1}H NMR spectrum is displayed in Figure 27. The protons H-7 and H-8 give a singlet at δ = 5.81, upfield shifted relative to **56** ($\Delta\delta$ = -0.64) and [2.2]paracyclophane ($\Delta\delta$ = -0.67). The protons in *pseudo geminal* position to the substituents H-15 and H-16 give a multiplet at δ = 6.56 upfield shifted relative to **56** ($\Delta\delta$ = -0.25). Since the acetylene function as well as antiaromatic systems have deshielding effects on the protons above or below, no information about the antiaromaticity of the biphenylene can be obtained from this upfield shift. A comparison of the NMR shifts with the formally aromatic terphenylene derivative could give information about the nature of the biphenylene derivative.

The protons H-12 and H-13 give a multiplet at δ = 6.80 and the protons H-28 and H-21 show a singlet at δ = 6.95.

Characteristic signals in the ^{13}C spectrum of **144** are δ = 149.0 (C-17, C-22) and δ = 153.0 (C-4, C-5) for the cyclobutadiene ring of the biphenylene.

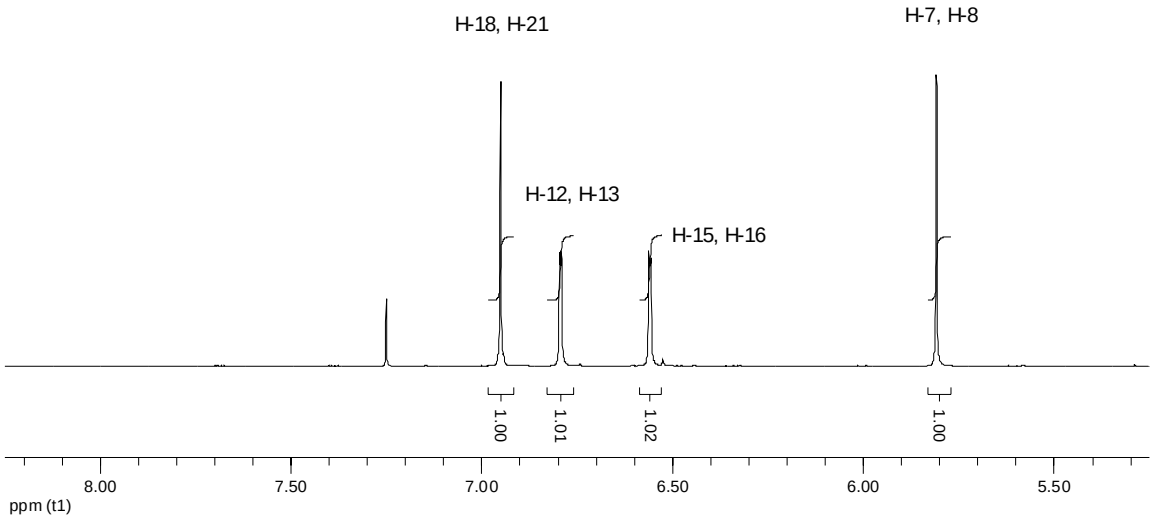

Figure 27: Aromatic region of the ^{1}H NMR spectrum of **144**.

Single crystals suitable for X-ray structure analysis were obtained by slow diffusion of methanol in a $CDCl_3$ solution of **144**. The compound crystallizes in the monoclinic crystal system with the space group $P2_1/c$. Figure 28 shows the molecular structure in the crystal.

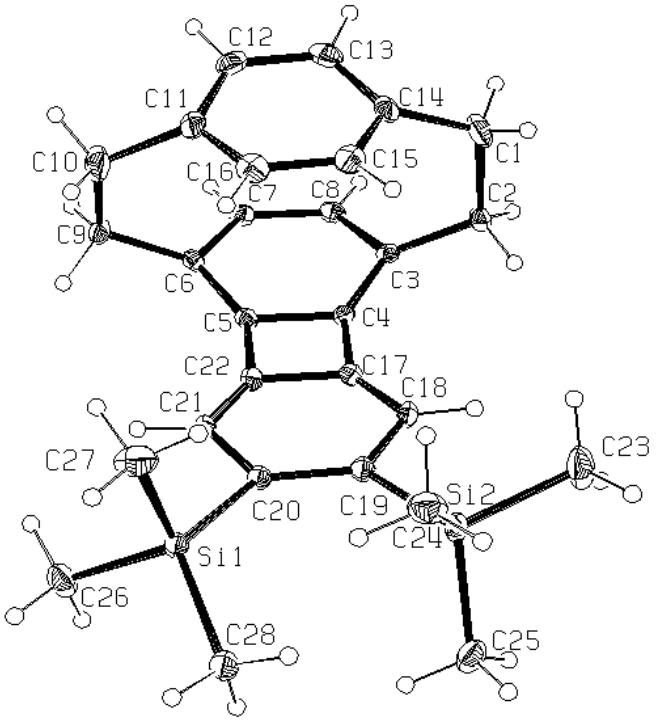

Figure 28: X-ray structure of **144**. Ellipsoids are drawn with 30% probability.

Figure 29 shows a view from below and a view from the side of the molecule; some selected bond lengths and angles are given in Table 13.

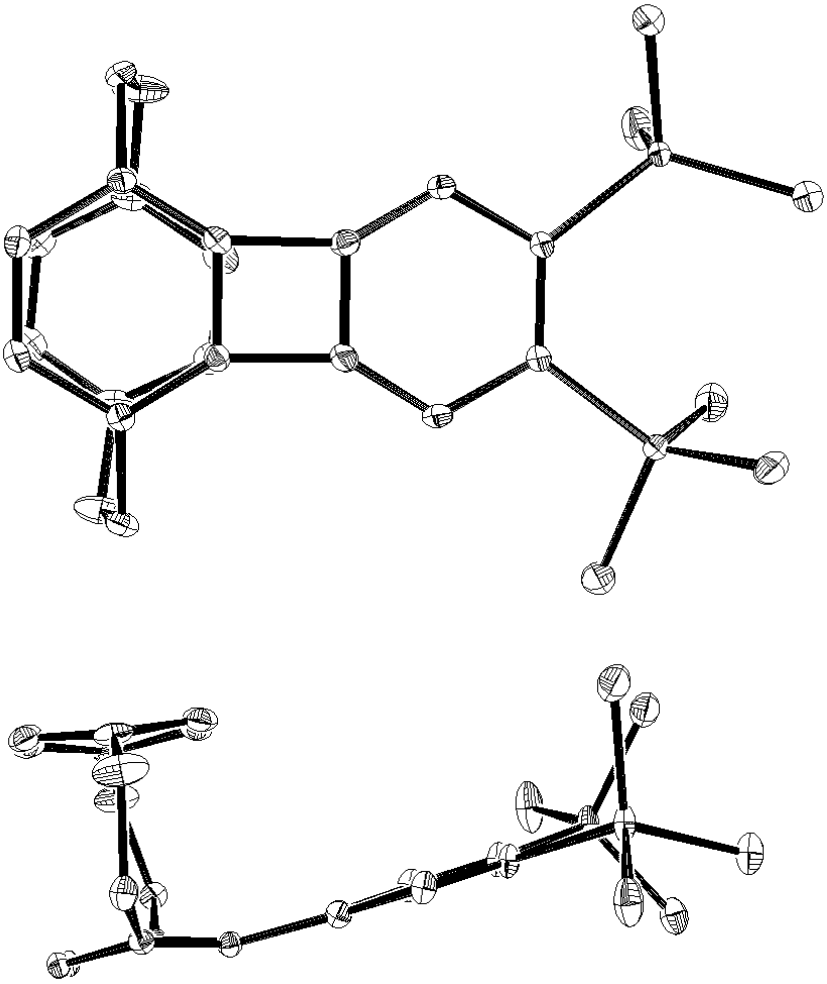

Figure 29: Structure of **144** in the crystal: views from below (top) and the side (bottom). Hydrogen atoms are omitted for clarity.

Table 13: Selected bond lengths [Å] and angles [°] of **144**.

C(4)-C(5)	1.438(6)	C(17)-C(22)	1.421(7)
C(4)-C(17)	1.511(6)	C(5)-C(22)	1.523(6)
C(4)-C(5)-C(22)	89.2(4)	C(17)-C(22)-C(5)	90.4(4)
C(5)-C(4)-C(17)	90.2(4)	C(22)-C(17)-C(4)	90.3(4)

The bonds C(4)-C(17) (1.438 Å) and C(5)-C(22) (1.523 Å) connecting the benzene and the [2.2]paracyclophane unit are longer than the sp^2-sp^2 bond between the two benzene rings in biphenyl (1.489 ± 0.007 Å)[69], they are rather close to a normal sp^3-sp^3 single bond (1.533 ± 0.002 Å).[70] The structural parameters are in good agreement with corresponding values for biphenylene[71] except the longer bond C(19)-C(20) (1.425 ±

0.007 Å in **144**, 1.385 ± 0.004 Å in biphenylene). This can be explained by the bulky TMS groups in *ortho* position to each other. In TMS-protected terphenylenes, this bond is also elongated to 1.425 Å.[72] The side view shows clearly a bent conformation of the biphenylene unit making the whole molecule resemble a "loafer". The four membered ring lies nearly in the same plane with the benzoic system, the interplanar angle is just 2.7°. The interplanar angle between C(3)-C(4)-C(5)-C(6) and the four membered ring C(4)-C(5)-C(17)-C(22) is 17.8°. The plane C(6)-C(7)-C(8)-C(3) is nearly parallel to the cyclobutadiene unit.

Derivative **144** is the first representative of a novel class of cyclophanes. Clearly, more biphenylenes have to be synthesized and their structural and chemical properties be studied.

6.2 Bergman cyclization of 4,5-diethynyl[2.2]paracyclophane (56)

In 1972, Bergman reported the formation of 1,4-dehydrobenzene (**146**) as an intermediate in the thermal isomerization of *cis*-3-hexene-1,5-diyne (**145**). In the presence of CCl_4, *p*-dichlorobenzene (**147**) was formed. Hydrogen donors (usually 1,4-cyclohexadiene) in the reaction mixture lead to the formation of benzene (**148**) and when methanol was present, benzyl alcohol (**149**) was produced (Scheme 42).[73, 74]

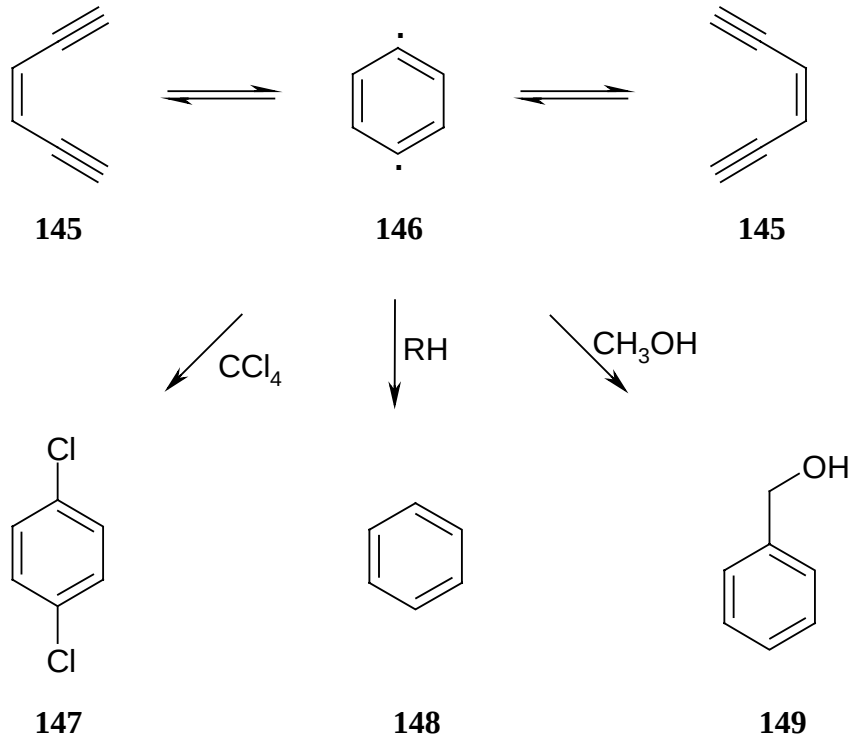

Scheme 42: Bergman cyclization of *cis*-3-hexene-1,5-diyne (**145**).

Benzo[2.2]paracyclophane (**153**), was first synthesized by Cram and coworkers in 1963[75] by a multistep procedure beginning with [2.2]paracyclophane (**36**). Succinoylation with succinic anhydride in the presence of $AlCl_3$ gave the keto acid **150** from which the keto function was reduced using zinc/hydrochloric acid. Ring closure with anhydrous hydrogen fluoride gave the ketone **151**. Reduction of the keto function gave 4,5-tetramethylene[2.2]paracyclophane (**152**) what was finally aromatized using chloranil (Scheme 43).

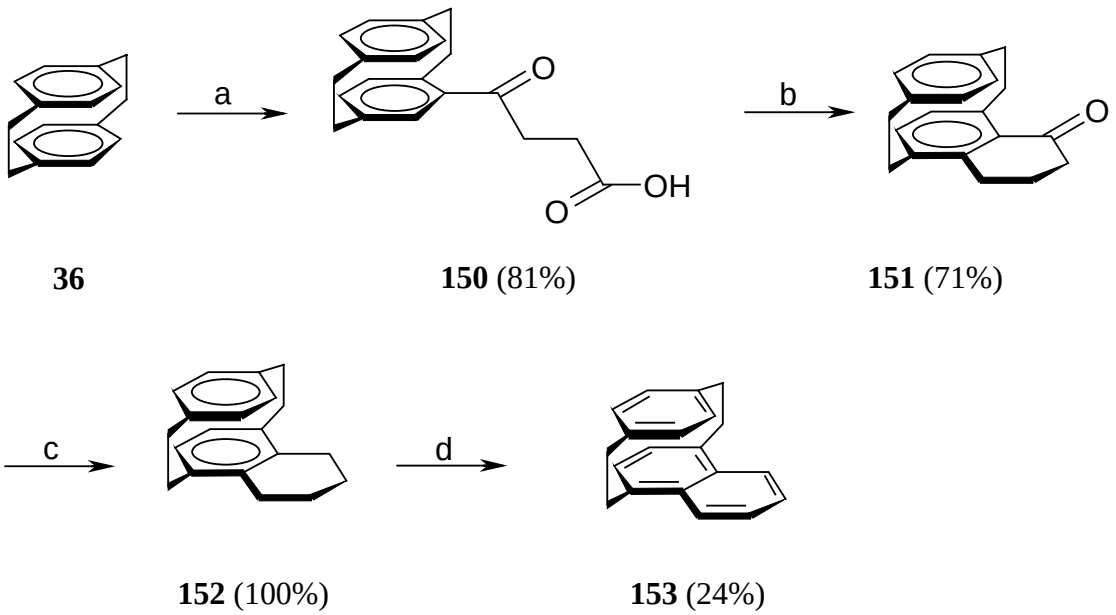

36 **150** (81%) **151** (71%)

152 (100%) **153** (24%)

(a) succinic anhydride, $AlCl_3$; (b) [i] Zn, HCl; [ii] HF; (c) Zn, HCl; (d) chloranil

Scheme 43: Synthesis of benzo[2.2]paracyclophane (153) by Cram and coworkers.[75]

The hydrocarbon can also be obtained by heating 4,5-diethynyl[2.2]paracyclophane (**56**) in chlorobenzene in the presence of 1,4-cyclohexadiene in an sealed ampoule at 190 °C. Under these conditions, **153** was formed in 90% yield (Scheme 44). This is the first time that Bergman cyclization has been applied to cyclophane chemistry. It seems save to predict that it also could develop to a very useful preparative method in this area of hydrocarbon chemistry.

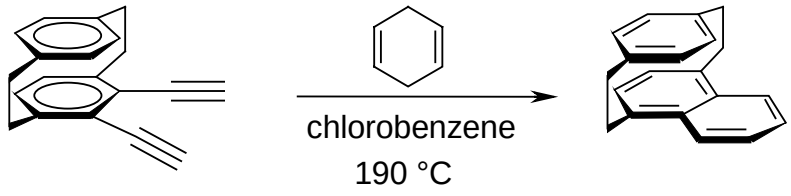

56 **153** (89%)

Scheme 44: Synthesis of benzo[2.2]paracyclophane (**153**) using the Bergman cyclization.

The ^{1}H NMR spectrum of **153** shows an AMNX spectrum for the bridge protons, the iterative analysis is summarized in Chapter 6.3. For the cyclophane unit, two AA'XX' multiplets at δ = 5.58 (H-15, H-16) and δ = 6.44 (H-12, H-13) for the protons of the unsubstituted cyclophane ring and a singlet at δ = 6.73 for the protons H-7 and H-8 are observed. The protons of the benzene unit give an AA'XX' spectrum with multiplets at 7.38 ppm for the distal protons and at δ = 7.68 for the proximal protons.

The ^{13}C NMR spectrum shows signals at δ = 124.8 and δ = 125.3 for C-18, C-19 and C-17, C-20. The carbon atoms C-4 and C-5 absorb at δ = 135.3.

The mass spectrum is characterized by the molecular ion peak at *m*/*z* = 258 with 30% intensity and the peaks obtained by cleavage of the cyclophane bridges (*m*/*z* = 154, 100%; *m*/*z* = 104, 22%).

6.3 Flexibility of 144 and 153 by NMR spectroscopy

In Chapter 3.2, NMR spectroscopy was used to study the flexibility of substituted [2.2]paracyclophanes in solution. It was shown, that substituted [2.2]paracyclophanes can exist in four different conformations, two with twisted benzene rings (Scheme 45:), and two with parallel displaced benzene rings (Scheme 46:).

In case of the twisted conformation, there is an equilibrium between the two conformers **112a** and **112b**. The equilibrium is shifted to that side with the least interactions between the substituent and the *syn* hydrogen at the bridge in *ortho* position to the substituent. In case of two equivalent substituents in *ortho* position to each other, a shift of the equilibrium to a smaller interaction between the substituent and proton H-2*s* leads to an increased interaction between the substituent in *ortho* position and the proton H-9*s* meaning that no conformer is favored. Expressed differently, the two conformers are enantiomorphic and, hence, are of the same energy.

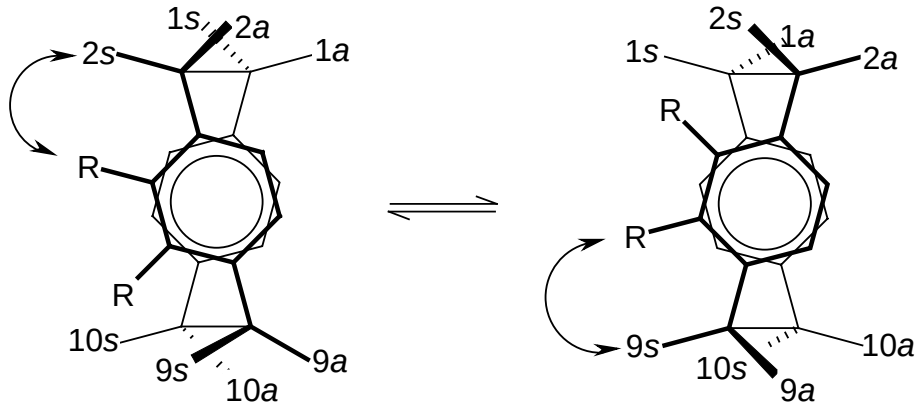

112a **112b**

Scheme 45: Conformational equilibrium between the conformations with twisted benzene rings **112a** and **112b**.

In case of the conformation with parallel displaced benzene rings, there is an equilibrium between the conformers **112c** and **112d**.

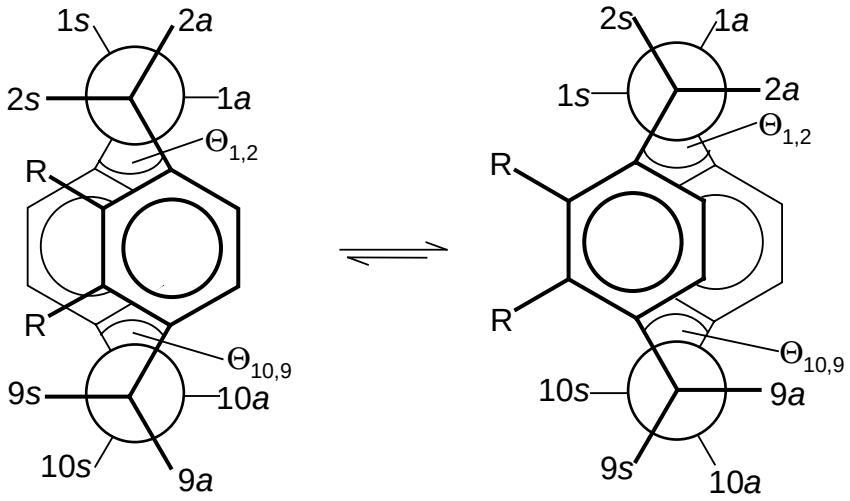

112c **112d**

Scheme 46: Conformational equilibrium between the conformations with parallel displaced benzene rings **112c** and **112d**.

The torsion angles between the C-H bonds of the four conformers are summarized in Table 14.

Table 14: Torsion angles ϕ between the C-H bonds in the conformational isomers.

	112a	**112b**	**112c**	**112d**
1*a*/2*a* (*cis*)	$\Theta_{1,2}$	$-\Theta_{1,2}$	$\Theta_{1,2}$	$-\Theta_{1,2}$
1*s*/2*s* (*cis*)	$\Theta_{1,2}$	$-\Theta_{1,2}$	$\Theta_{1,2}$	$-\Theta_{1,2}$
1*a*/2*s* (*trans*)	$\Theta_{1,2} + 120°$	$-\Theta_{1,2} + 120°$	$\Theta_{1,2} + 120°$	$-\Theta_{1,2} + 120°$
1*s*/2*a* (*trans*)	$\Theta_{1,2} - 120°$	$-\Theta_{1,2} - 120°$	$\Theta_{1,2} - 120°$	$-\Theta_{1,2} - 120°$
10*a*/9*a* (*cis*)	$\Theta_{10,9}$	$-\Theta_{10,9}$	$-\Theta_{10,9}$	$\Theta_{10,9}$
10*s*/9*s* (*cis*)	$\Theta_{10,9}$	$-\Theta_{10,9}$	$-\Theta_{10,9}$	$\Theta_{10,9}$
10*a*/9*s* (*trans*)	$\Theta_{10,9} - 120°$	$-\Theta_{10,9} - 120°$	$-\Theta_{10,9} - 120°$	$\Theta_{10,9} - 120°$
10*s*/9*a* (*trans*)	$\Theta_{10,9} + 120°$	$-\Theta_{10,9} + 120°$	$-\Theta_{10,9} + 120°$	$\Theta_{10,9} + 120°$

As explained in Chapter 3.2, the extent of the equilibrium can be recognized from the change of the vicinal *trans* coupling constants. Table 15 summarizes the coupling constants of the bridge protons of **144** and **153**. In case of a twisted conformation, all *trans* coupling constants should have similar values whereas in case of a conformation with parallel displaced benzene rings, the *trans* coupling constants are different and depend on the equilibrium.

Table 15: ^{1}H,^{1}H coupling constants [Hz] in the bridges of [2.2]paracyclophane derivatives.

		144	**153**
R (%)		0.22	rms 0.022 Hz
J (1-H*a*, 1-H*s*) = *J* (10-H*a*, 10-H*s*)	*gem*	-13.3	-13.2
J (2-H*a*, 2-H*s*) = *J* (9-H*a*, 9-H*s*)	*gem*	-13.5	-13.6
J (1-H*a*, 2-H*a*) = *J* (10-H*a*, 9-H*a*)	*cis*	10.2	10.7
J (1-H*s*, 2-H*s*) = *J* (10-H*s*, 9-H*s*)	*cis*	10.3	10.2
J (1-H*a*, 2-H*s*) = *J* (10-H*a*, 9-H*s*)	*trans*	4.8	2.0
J (1-H*s*, 2-H*a*) = *J* (10-H*s*, 9-H*a*)	*trans*	4.1	6.2

This leads to the conclusion, that **153** should exist in conformations with parallel displaced benzene rings whereas the situation is less clear for **144**. Molecular modeling studies of benzo[2.2]paracyclophane (**153**) have confirmed the expected conformation (Figure 30).

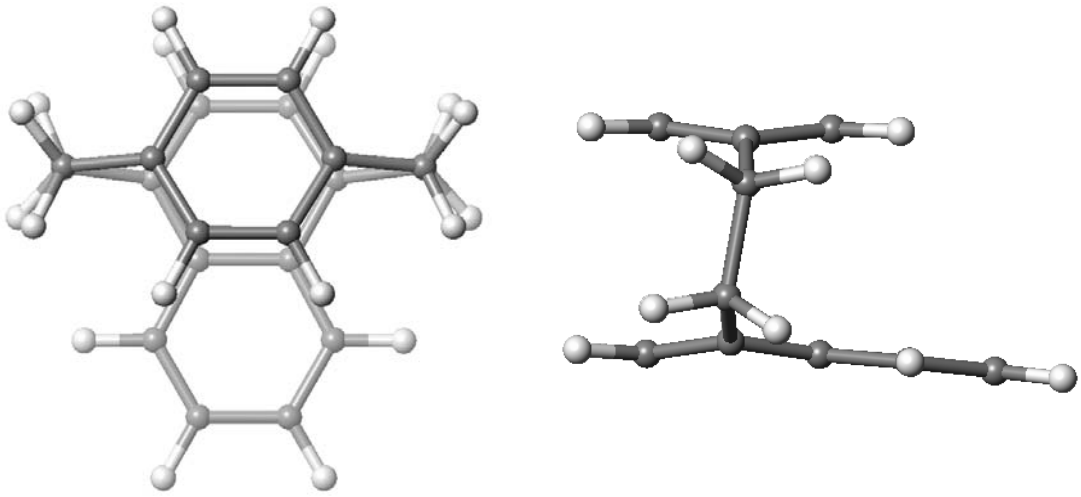

Figure 30: Calculated structure of **153**.

Table 16 summarizes the calculated torsion angles of **153** showing a distortion from the ideal eclipsed geometry. The torsion angles H(1*a*)-C(1)-C(2)-H(2*a*) and H(1*s*)-C(1)-C(2)-H(2*s*) are diminished by 3.4 to 4.1° relative to -Θ; H(1*a*)-C(1)-C(2)-H(2*s*) is diminished by 8.8° relative to 120°-Θ, whereas H(1*s*)-C(1)-C(2)-H(2*a*) is enlarged by 1.3° relative to -120°-Θ. For the other bridge, the torsion angles H(10*a*)-C(10)-C(9)-C(9*a*) and H(10*s*)-C(10)-C(9)-C(9*s*) are enlarged by 3.4 to 4.1° relative to Θ. The torsion angle H(10*a*)-C(10)-C(9)-C(9*s*) is enlarged by 8.8° relative to Θ-120° whereas H(10*s*)-C(10)-C(9)-C(9*a*) is diminished by 1.3° relative to Θ+120°.

Table 16: Calculated torsion angles [°] of **153**.

C(14)-C(1)-C(2)-C(3)	-11.7	C(11)-C(10)-C(9)-C(6)	11.7
H(1*a*)-C(1)-C(2)-H(2*a*)	-15.1	H(10*a*)-C(10)-C(9)-C(9*a*)	15.1
H(1*s*)-C(1)-C(2)-H(2*s*)	-15.8	H(10*s*)-C(10)-C(9)-C(9*s*)	15.8
H(1*a*)-C(1)-C(2)-H(2*s*)	99.5	H(10*a*)-C(10)-C(9)-C(9*s*)	-99.5
H(1*s*)-C(1)-C(2)-H(2*a*)	-130.4	H(10*s*)-C(10)-C(9)-C(9*a*)	130.4

In contrast, X-ray structure analysis has shown that the biphenylene derivative **144** exist in a conformation with twisted benzene rings (see above). To avoid crystal packing effects, the gas phase structure was calculated and resulted in the same conformation. The calculated torsion angles are summarized in Table 17.

Table 17: Calculated torsion angles [°] of **144**.

C(14)-C(1)-C(2)-C(3)	12.9	C(11)-C(10)-C(9)-C(6)	10.4
H(1*a*)-C(1)-C(2)-H(2*a*)	14.8	H(10*a*)-C(10)-C(9)-C(9*a*)	12.4
H(1*s*)-C(1)-C(2)-H(2*s*)	15.0	H(10*s*)-C(10)-C(9)-C(9*s*)	12.3
H(1*a*)-C(1)-C(2)-H(2*s*)	130.0	H(10*a*)-C(10)-C(9)-C(9*s*)	-102.7
H(1*s*)-C(1)-C(2)-H(2*a*)	-100.1	H(10*s*)-C(10)-C(9)-C(9*a*)	127.4

The values given in the table show a distortion from the ideal geometry. The torsion angles of the bridges C(14)-C(1)-C(2)-C(3) and C(11)-C(10)-C(9)-C(6) differ by 2.5° giving a mean value of $\overline{\Theta}$=11.7°. The torsion angle H(1*a*)-C(1)-C(2)-H(2*s*) is diminished by 1.7° relative to $\overline{\Theta}$+120°, H(1*s*)-C(1)-C(2)-H(2*a*) is enlarged by 8.3° relative to $\overline{\Theta}$-120°. In the other bridge, H(10*a*)-C(10)-C(9)-C(9*s*) is enlarged by 5.7° relative to $\overline{\Theta}$-120° whereas H(10*s*)-C(10)-C(9)-C(9*a*) is diminished by 4.3° relative to $\overline{\Theta}$+120°.

Due to symmetry, the torsion angles H(1*a*)-C(1)-C(2)-H(2*s*) and H(10*a*)-C(10)-C(9)-C(9*s*) have an influence on the equivalent coupling constants $^3J_{1a,2s}$ and $^3J_{10a,9s}$, whereas the torsion angles H(1*s*)-C(1)-C(2)-H(2*a*) and H(10*s*)-C(10)-C(9)-C(9*a*) influence the coupling constants $^3J_{1s,2a}$ and $^3J_{10s,9a}$ as described by the Karplus function (see Chapter 3.2). The average of the absolute values of the torsion angles H(1*a*)-C(1)-C(2)-H(2*s*) and H(10*a*)-C(10)-C(9)-C(9*s*) is larger by 2.6° than the average of the absolute values of the torsion angles H(1*s*)-C(1)-C(2)-H(2*a*) and H(10*s*)-C(10)-C(9)-C(9*a*). This difference can cause the difference in the *trans* coupling constants in **144**.

7 Propeller type PC/DBAs

7.1 Introduction

The physical properties of DBAs can be controlled by a variety of factors like planarity or non-planarity, double or triple bonds or the introduction of donor and/or acceptor groups. Also the aromaticity of the fused aromatic system has a strong influence on the properties of the DBA.

In 2000, Fallis reported the synthesis of "Novel Acetylenic Cyclophanes with Helical Chirality" like **29** using Pd- and Cu-mediated cross coupling reactions.[20] X-ray studies gave an inter-ring distance of 3.57 Å, which is beyond the typical 3.09 Å found in most [2.2]paracyclophanes. To learn more about the transannular interactions in [2.2]paracyclophane/dehydrobenzoannulenes, [2.2]paracyclophane derivatives **157** and **158** and the unbridged derivatives **154** and **155** were synthesized and compared. The aim of this project was to answer the question to what extent the spectroscopic properties change by fixing the helical structure and shortening the inter ring distance between the *para*-substituted units.

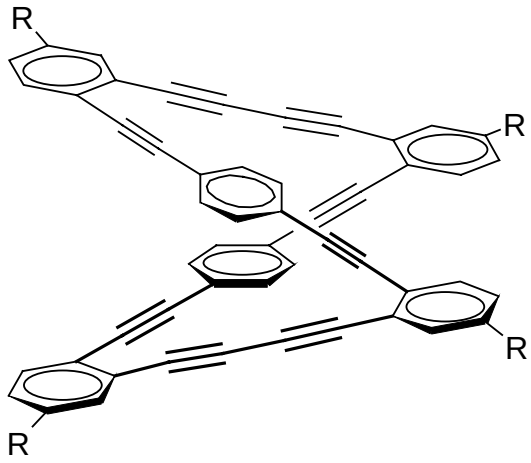

R	
H	**29**
tert-Bu	**154**
Bu_2N	**155**

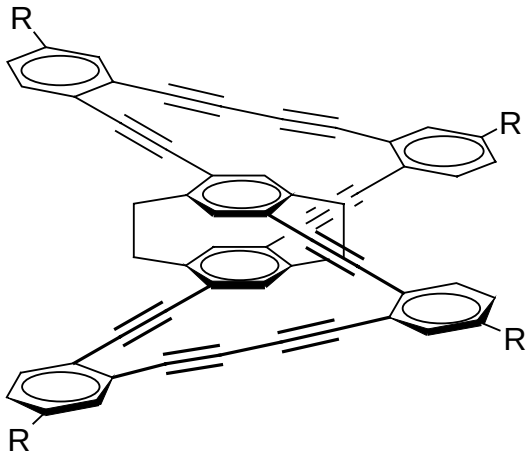

R	
H	**156**
tert-Bu	**157**
Bu_2N	**158**

Figure 31: Propeller type annulenes.

7.2 Synthesis

To increase the solubility, *tert*-butyl and dibutylamino substituted macrocycles were designed. The syntheses of the non-ethanobridged cyclophanes were carried out in a slightly different way than reported by Fallis for **29**.

In the first step a Pd-catalyzed cross coupling reactions of iodobenzene **121**[53] or **125**[54] with 1,4-diethynylbenzene (**177**)[76] were employed (Scheme 47). The products **159** and **160** were obtained in 56% and 39% yield, respectively. Deprotection with K_2CO_3 in methanol under standard conditions gave the diacetylenes **161** and **162** in more than 90% yield. The final dimerization was accomplished by using $Cu(OAc)_2$ in a 3:1 mixture of pyridine:ether under high dilution conditions, to yield the propeller type annulenes in 8 to 15% yield.

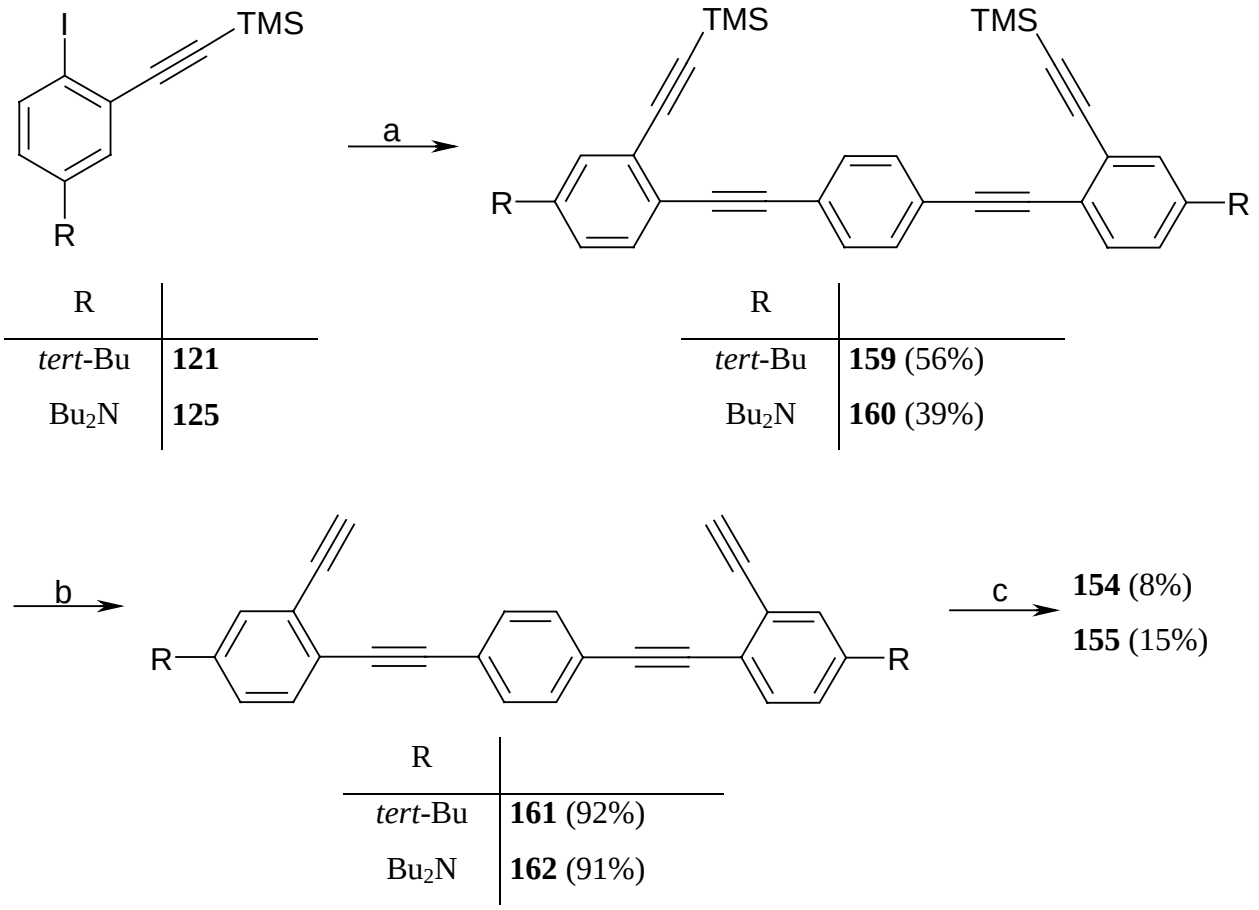

R	
tert-Bu	**121**
Bu_2N	**125**

R	
tert-Bu	**159** (56%)
Bu_2N	**160** (39%)

R	
tert-Bu	**161** (92%)
Bu_2N	**162** (91%)

(a) 1,4-diethynylbenzene (**177**), $Pd(PPh_3)_4$, CuI, $^iPr_2NH$, THF; (b) K_2CO_3, CH_3OH, CH_2Cl_2; (c) $Cu(OAc)_2$, pyridine:ether 3:1

Scheme 47: Syntheses of the propeller type annulenes **154** and **155**.

One reason for the low yields in the last step is decomposition of the target compounds during purification by column chromatography on silica.

The ^{1}H NMR spectrum of the propeller type molecules **154** and **155** show two doublets (H-6', H-6", H-6'", H-6"" and H-3', H-3", H-3'", H-3"") and one doublet of doublets (H-5', H-5", H-5'", H-5"") for the edge benzene rings and a singlet for the *para*-substituted benzene ring (H-2, H-3, H-5, H-6, H-8, H-9, H-11, H-12). This can be explained either by a staggered confirmation in solution (in case of an eclipsed conformation, an AA'XX' spectrum for H-2, H-3, H-5, H-6, H-8, H-9, H-11 and H-12 should be observed) or by dynamic effects. In case of fast rotation of the *para*-substituted benzene rings or fast racemization, a singlet is also to be expected. Figure 32 shows the aromatic region of the ^{1}H NMR spectrum of derivative **154**.

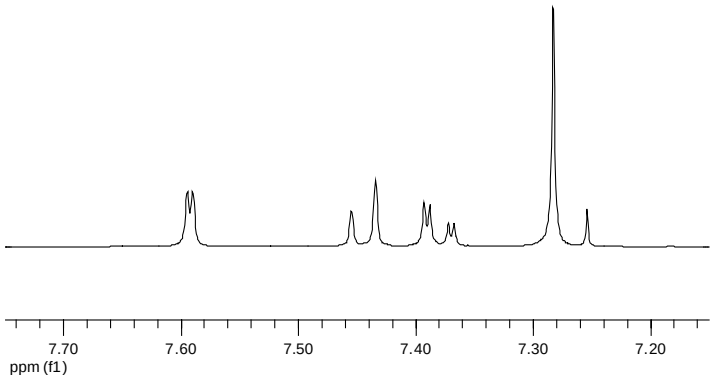

Figure 32: Aromatic region of the ^{1}H NMR spectrum of **154**.

To determine the molecular mass, matrix-assisted laser desorption ionization time-of-flight (MALDI-TOF) mass spectrometry was used.[77] The MALDI-TOF spectrum of the *tert*-butyl substituted propeller type molecule shows a signal at *m/z* = 872, the spectrum is reproduced in Figure 33. In the MALDI-TOF spectrum of **162** (Figure 34) the molecular ion peak appears at *m/z* = 1158. The peak of the dimer (*m/z* = 2315) presumably is an artifact.

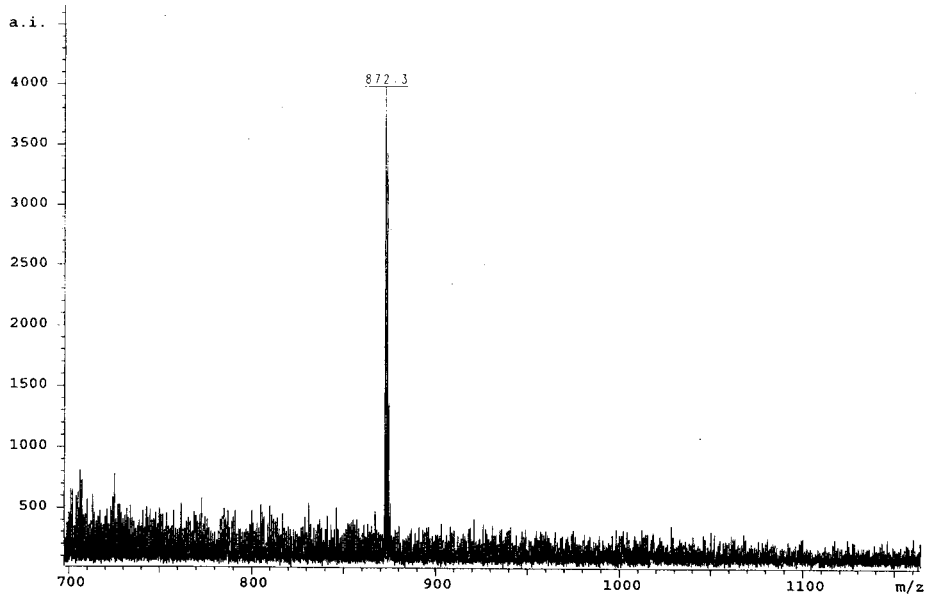

Figure 33: MALDI-TOF spectrum of the propeller type molecule **154**.

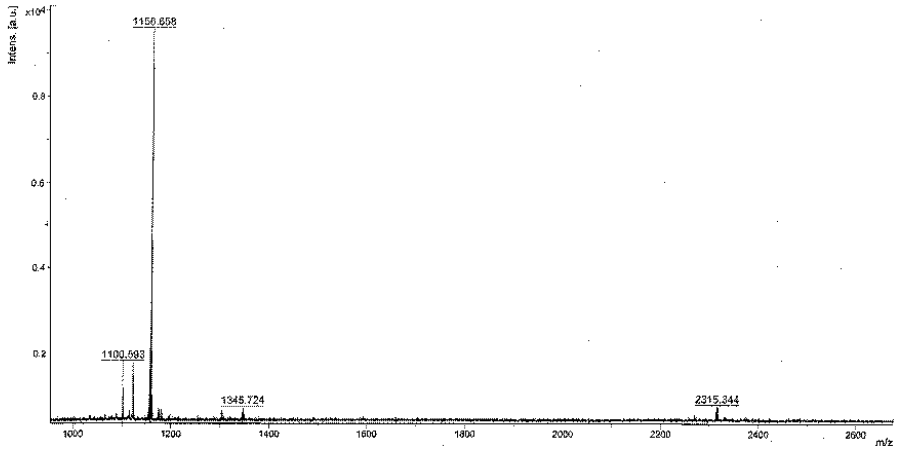

Figure 34: MALDI-TOF spectrum of **162**.

The synthesis of the [2.2]paracyclophane derivatives **157** and **158** started from known 4,7,13,16-tetrabromo[2.2]paracyclophane (**90**) which can be obtained in 40% yield by bromination of [2.2]paracyclophane (**36**) with bromine in the presence of a catalytic amount of iodine.[41] Sonogashira coupling of **90** with TMSA gave 4,7,13,16-tetrakis-(trimethylsilylethynyl)[2.2]paracyclophane (**163**) in 45% yield which was desilylated in nearly quantitative yield using K_2CO_3 in methanol to give 4,7,13,16-tetraethynyl[2.2]paracyclophane (**164**) (Scheme 48).

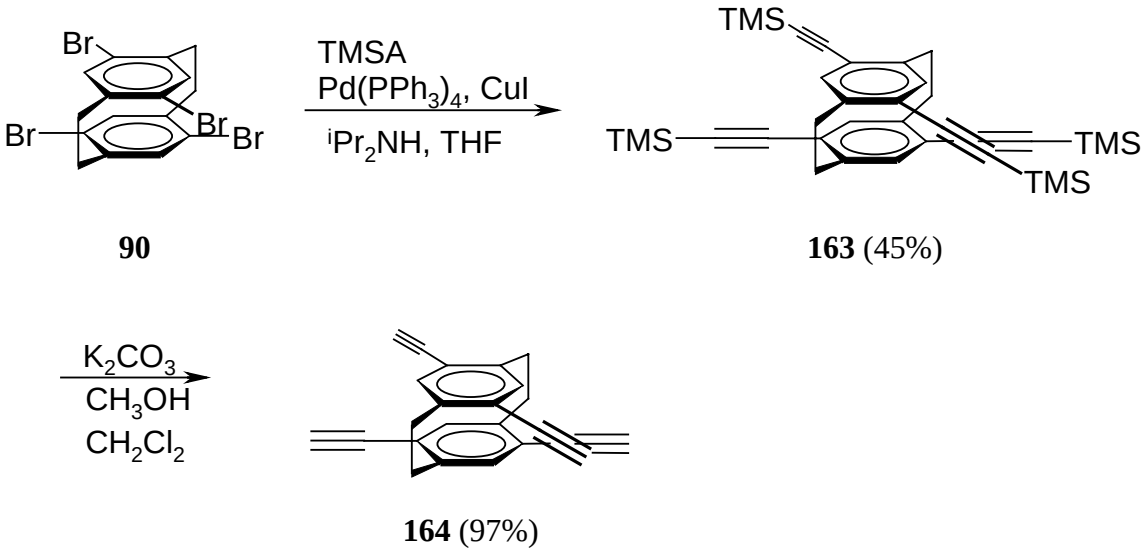

Scheme 48: Synthesis of 4,7,13,16-tetraethynyl[2.2]paracyclophane (**164**).

As side products in the Sonogashira coupling, 4-bromo-7,13,16-tris(trimethylsilyl-ethynyl)[2.2]paracyclophane (**165**) and 4,7-dibromo-13,16-bis(trimethylsilylethynyl)-[2.2]paracyclophane (**166**) were formed (Figure 35). The other two dibromo-bis(trimethylsilylethynyl)[2.2]paracyclophane isomers could not been isolated. The constitution of **166** was proven by mass spectrometry. The EI mass spectrum shows the molecular peak at *m/z* = 556/558/560 with the isotopic pattern of a dibrominated substance (1:2:1). The base peak in the spectrum (*m/z* = 296), does not display the isotopic pattern of a brominated fragment; instead, it contains the two TMS protected acetylene functions. This fragment is generated by splitting the [2.2]paracyclophane molecule at the bridges in two parts. The dibrominated fragment (*m/z* = 260/262/264) cannot be found in the mass spectrum.

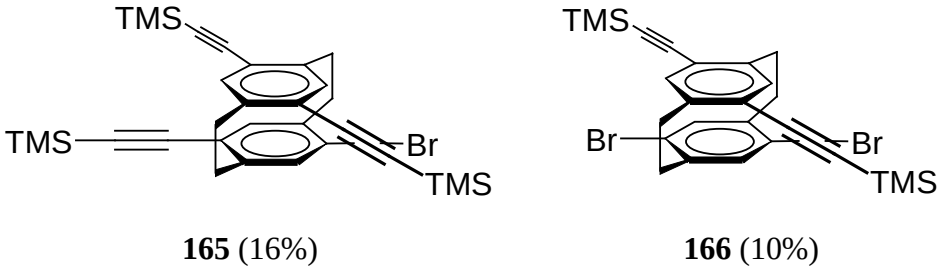

Figure 35: Side products in the Sonogashira coupling of 4,7,13,16-tetrabromo[2.2]paracyclophane.

Pd catalyzed cross coupling of **164** with the iodobenzenes **121**[53] and **125**[54] gave the propeller precursors **167** and **168**. These were finally desilylated and cyclized in an one pot sequence to yield the propeller type [2.2]paracyclophane/dehydrobenzoannulenes **157** and **158** (Scheme 49).

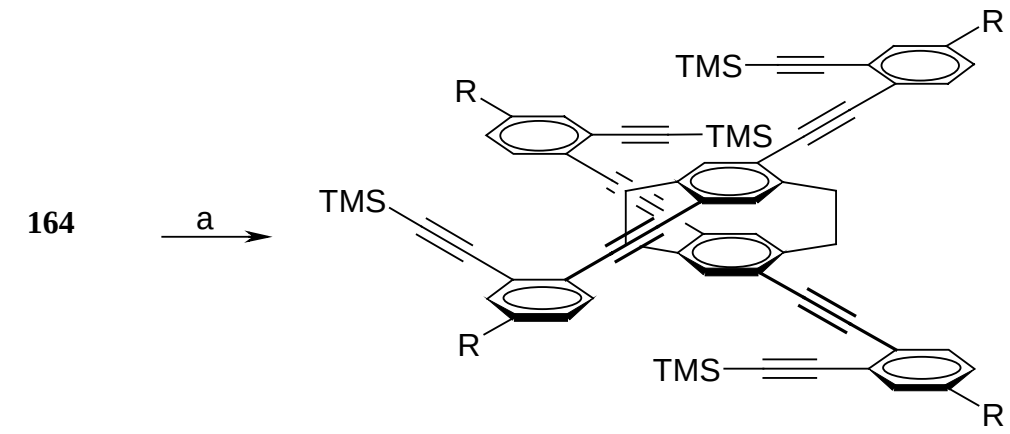

R	
tert-Bu	**167** (15%)
NBu_2	**168** (39%)

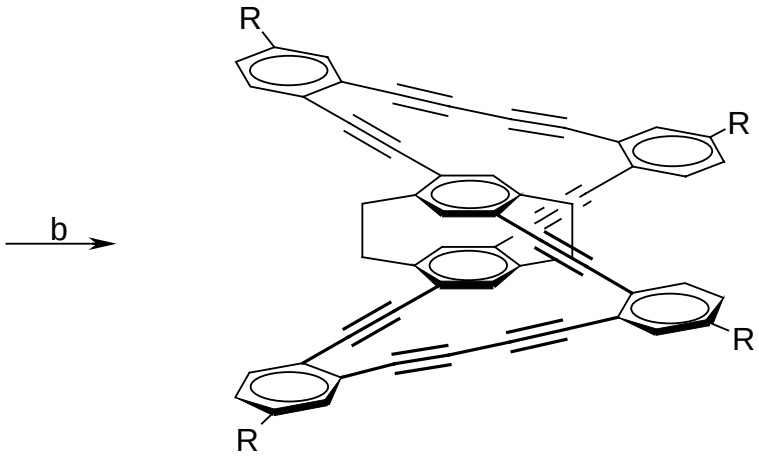

R	
tert-Bu	**157** (40%)
NBu_2	**158** (66%)

(a) **121** or **125**, $Pd(PPh_3)_4$, CuI, $^{i}Pr_2NH$, THF; (b) K_2CO_3, $Cu(OAc)_2$, CH_3OH, CH_3CN

Scheme 49: Synthesis of the propeller type [2.2]paracyclophane/dehydrobenzoannulenes.

The ^1H NMR spectra of **157** and **158** show AA'XX' spectra for the bridge protons of the cyclophanes H-1, H-2, H-9 and H-10. The *tert*-butyl substituted derivative **157** gives in the aromatic region a singlet at $\delta = 7.18$ for the cyclophane protons H-5, H-8, H-12 and H-15, a doublet of doublets at $\delta = 7.40$ for H-5', H-5", H-5"' and H-5"', a doublet at $\delta =$

7.48 for H-6', H-6", H-6'" and H-6"" and a doublet at δ = 7.55 for H-3', H-3", H-3'", H-3"".

For the *N*,*N*-dibutylamino derivative **158** the aromatic protons absorb as a doublet of doublets for H-5', H-5", H-5'" and H-5"" at δ = 6.61, a doublet at δ = 6.72 for H-3', H-3", H-3'" and H-3"" a singlet at δ = 7.14 for the cyclophane protons H-5, H-8, H-12 and H-15 and a doublet at δ = 7.35 for H-6', H-6", H-6'" and H-6"".

In the MALDI-TOF spectra of **157** and **158** the molecular ion peaks are clearly visible. Other fragments can be explained by decomposition of the material, since the UV absorption maxima of these molecules lie in the region of the laser light which is used for ionization (λ = 337 nm).

7.3 X-Ray structure analysis

By slow diffusion of methanol in a CH_2Cl_2 solution of **154**, single crystals suitable for X-ray structure analysis were obtained. Figure 37 and Figure 37 show the structure of **154** in the crystal.

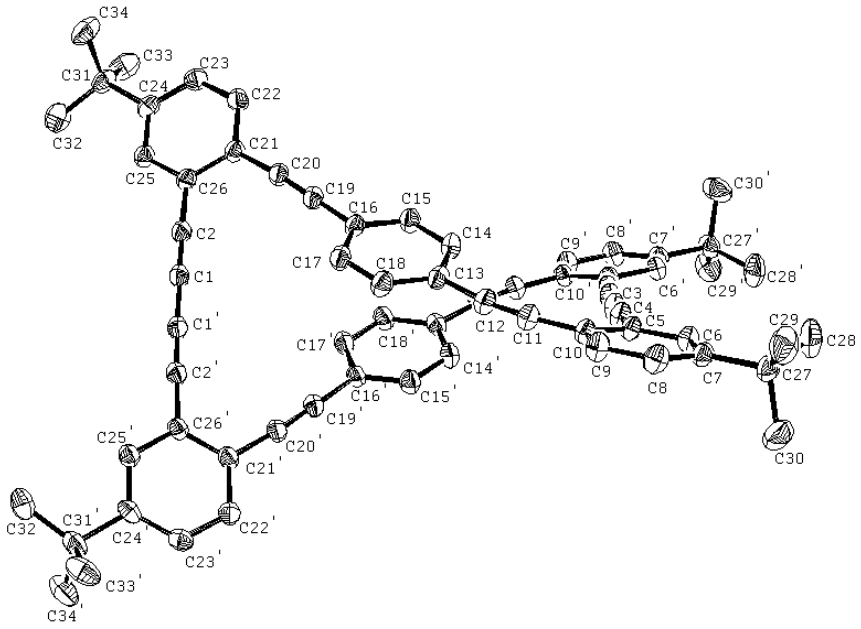

Figure 36: X-ray crystal structure of the acetylenic cyclophane **154** (side view) showing the propeller type structure. Ellipsoids are drawn with 50% probability.

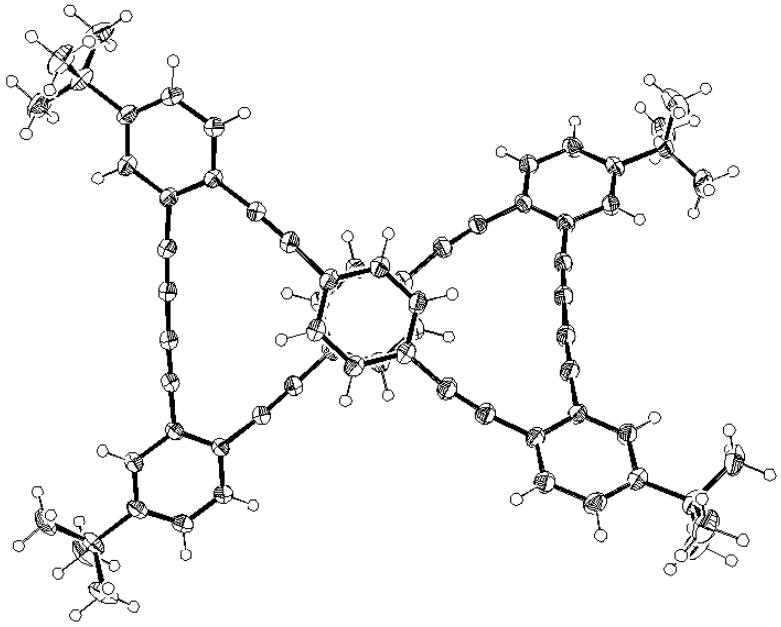

Figure 37: X-ray crystal structure of the acetylenic cyclophane **154** (top view) showing the propeller type structure. Ellipsoids are drawn with 50% probability.

The propeller type molecule **154** crystallizes in the monoclinic crystal system in space group C2/c with half a molecule in the asymmetric unit.

The two *para* substituted benzene rings are in a staggered configuration with a dehedral angle of 30° and an inter ring distance of 3.79 Å.

The alkyne units C16-C19-C20-C21 and C10-C11-C12-C13 bend outwards (2.1 - 7.76° and 7.76 - 7.91°). The diyne unit C26-C2-C1-C1'-C2'-C26' is almost linear (0.73 - 2.9°) whereas the diyne unit C5-C4-C3-C3'-C4'-C5' bends slightly inwards (2.33 - 3.31°).

Selected bond lengths are given in Table 18, selected bond angles in Table 19.

Table 18: Selected bond lengths [Å] of **154**.

C(1)-C(2)	1.2009(17)	C(10)-C(11)	1.4333(16)
C(1)-C(1')	1.374(2)	C(11)-C(12)	1.1978(16)
C(2)-C(26)	1.4276(17)	C(12)-C(13)	1.4385(16)
C(3)-C(4)	1.2044(17)	C(16)-C(19)	1.4333(16)
C(3)-C(3')	1.370(2)	C(19)-C(20)	1.1974(16)
C(4)-C(5)	1.4257(17)	C(20)-C(21)	1.4328(16)

Table 19: Selected bond angles [°] of **154**.

C(2)-C(1)-C(1')	179.27(9)	C(12)-C(11)-C(10)	172.09(13)
C(1)-C(2)-C(26)	177.10(13)	C(11)-C(12)-C(13)	172.24(13)
C(4)-C(3)-C(3')	177.67(9)	C(19)-C(20)-C(21)	175.24(13)
C(3)-C(4)-C(5)	176.69(13)	C(20)-C(19)-C(16)	177.90(14)

Single crystals of 4,7,13,16-tetraethynyl[2.2]paracyclophane (**164**) were obtained by slow evaporation of the solvent from a CH_2Cl_2 solution. **164** crystallizes in the orthorhombic crystal system in the space group $Pca2_1$. Figure 38 shows the structure of **164** in the crystal, selected bond lengths and angles are given in Table 20.

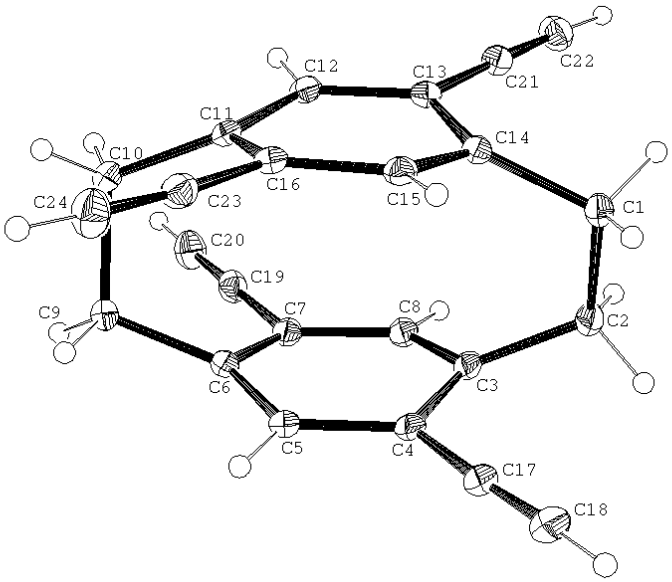

Figure 38: X-ray crystal structure of 4,7,13,16-tetraethynyl[2.2]paracyclophane (**164**), ellipsoids are drawn with 30% probability.

Table 20: Selected bond lengths [Å] and angles [°] of **164**.

C(4)-C(17)	1.436(2)	C(17)-C(18)	1.194(2)
C(7)-C(19)	1.439(2)	C(19)-C(20)	1.188(2)
C(13)-C(21)	1.438(2)	C(21)-C(22)	1.189(2)
C(16)-C(23)	1.440(2)	C(23)-C(24)	1.192(2)
C(4)-C(17)-C(18)	176.57(18)	C(13)-C(21)-C(22)	177.34(17)
C(7)-C(19)-C(20)	179.01(19)	C(16)-C(23)-C(24)	175.15(17)

The [2.2]paracyclophane unit shows the typical geometry, bond lengths and -angels for this class of hydrocarbons. The bond lengths of the alkyne units agree with the standard bond lengths[63] (C*sp*≡C*sp*: 118 pm, C*ar*-C*sp*: 143 pm) for the bond angles, only marginal deviation from linearity on the order of 1.0 to 4.8° is observed.

7.4 UV/Vis spectroscopy

Figure 39 shows a comparison of the electronic absorption spectra of the *tert*-butyl substituted propeller type molecules **161**, **157** and their precursors **159** and **167**; a comparison between the dibutylamino substituted molecules **160**, **155**, **168** and **158** is shown in Figure 40.

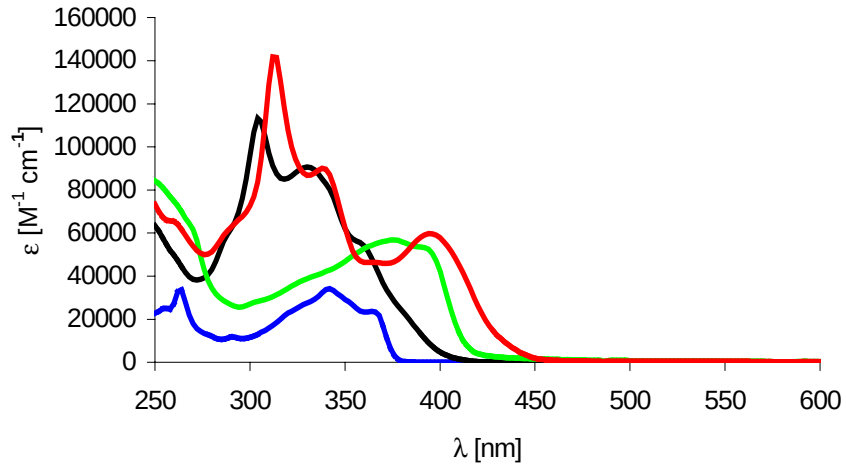

Figure 39: Electronic absorption spectra of the propeller type molecules **154** (black) **157** (red) and their open precursors **159** (blue) and **167** (green).

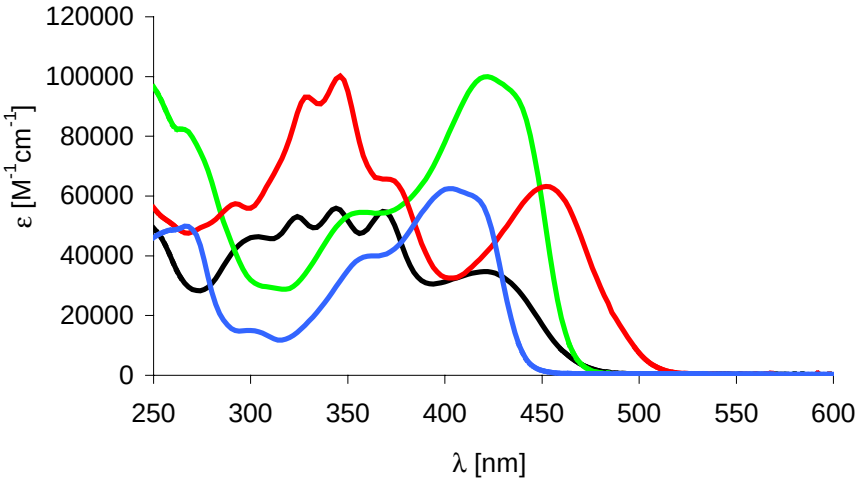

Figure 40: Electronic absorption spectra of the propeller type molecules **155** (black) **158** (red) and their open precursors **160** (blue) and **168** (green).

The UV spectra show a stronger bathochromic shift of the [2.2]paracyclophane derivatives **157** and **158** relative to their open precursors **167** and **168**. The unbridged annulenes **154** and **155** show nearly no bathochromic shift relative to **159** and **160**. This indicates global transannular delocalization in the [2.2]paracyclophane derivatives **157** and **158**, whereas the non-ethanobridged derivatives **154** and **155** do not display delocalization in the annulene ring.

7.5 Molecular modeling studies

Delocalization is a phenomenon that can only be explained by quantum theory. Principally this explanation rests on VB- or MO-theory. Valence bond theory describes delocalization by drawing mesomeric structures; MO theory explains delocalization by linear combination of atomic orbitals to a set of molecular orbitals extending over the whole molecule. Herges has developed a method to visualize delocalized electrons using the anisotropy of the induced current density (ACID).[78] The current density is a vector field, which can be calculated by regarding the current induced by an external magnetic field at each point in space. The drawbacks are:

a) vector fields are difficult to visualize because a vector is assigned to each point in space, so this method is limited to planar systems.
b) the current density is a function of the overall electron density. Because the largest currents are induced close to the nuclei (where the electron density is the highest), these local currents are much larger than interatomic currents; this can obscure delocalization effects.
c) current density maps in terms of delocalization are only interpretable in case of cyclic conjugation (aromaticity and antiaromaticity)

To overcome this problems, the delocalization should be represented by a scalar field, which can be plotted on an isosurface. Such a parameter is the anisotropy of the induced current density, which can be calculated from the current density tensor. This can be computed using the continuous set of gauge transformation method implemented in the Gaussian program.

Figure 41 shows the ACID plots of the propeller type molecules **29** and **156**. In case of the [2.2]paracyclophane derivative **156** (bottom), transannular delocalization through the alkyne units can be observed, whereas in the unbridged system **29** (top) no delocalization is present. It can also be seen that in case of the [2.2]paracyclophane

system, π-π-interactions in the cyclophane are weaker than the delocalization through the alkyne units.

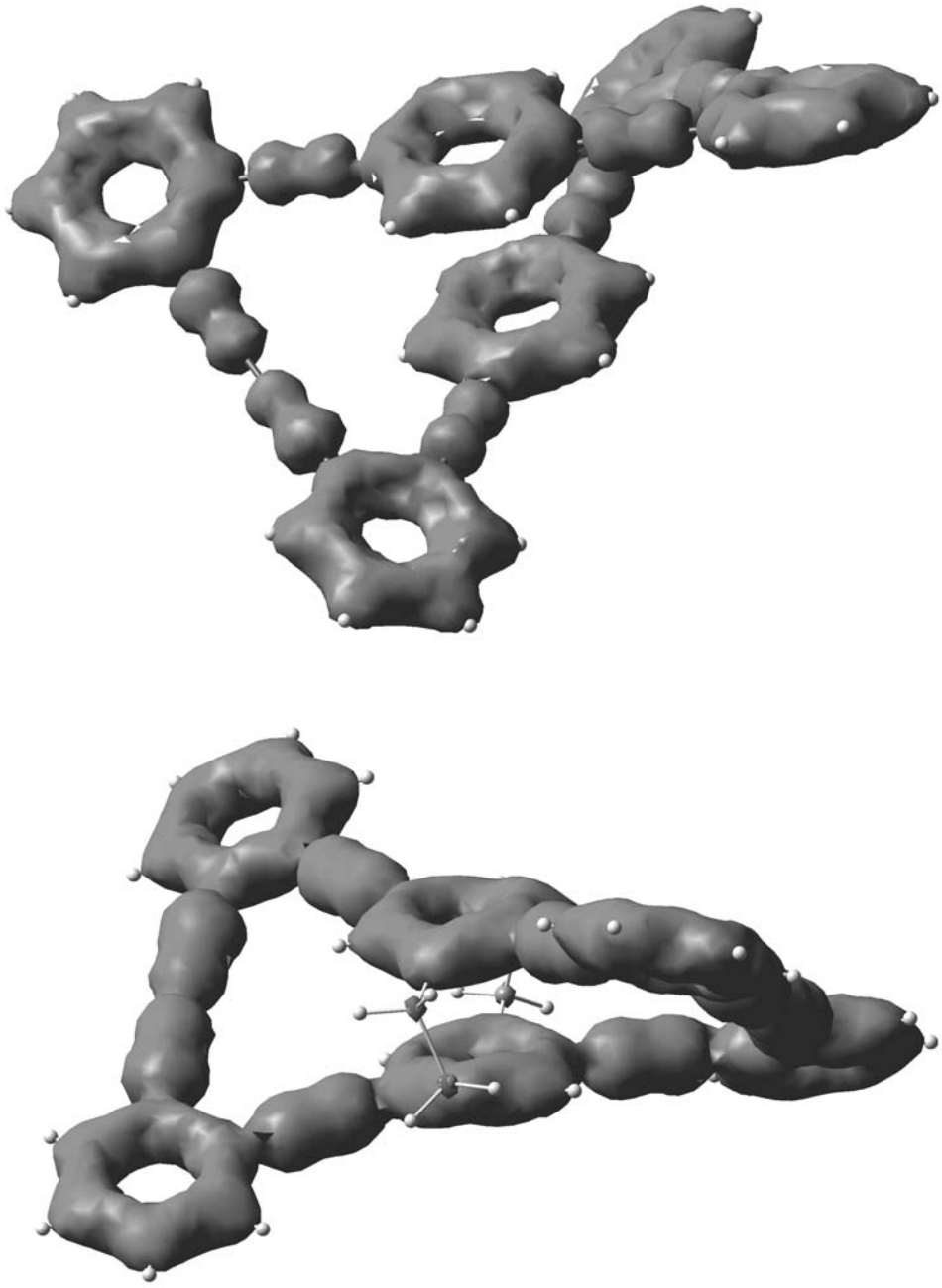

Figure 41: ACID plots of the propeller type molecules **29** and **156** (isosurface value: 0.04).

8 Chirality of [2.2]paracyclophane derivatives

8.1 Introduction

Since most of the cyclophanes synthesized in this work are chiral, some aspects of chirality should be mentioned in this chapter. In principle, there are four classes of chirality: central-, axial-, planar- and helical chirality. Among molecules with planar chirality, the cyclophanes and the metallocenes are the most important. The chirality of cyclophanes was discovered in the 1940s by Lüttringhaus and Gralheer in ansa compounds **169**.[79]

The first resolved compound was **169** with n = 10 and X = Br. The two bulky substituents prevent the benzene ring from rotation. With X = H, the product becomes nonresolvable. In case of a shorter bridge (n = 8 but with X = H), **169** can be resolved and racemizes extremely slowly.

Substituted [m.n]paracyclophanes **170** in which the benzene rings cannot swivel are also chiral. For example, the carboxylic acid derived from [3.4]paracyclophane has been resolved and racemized when heated above its melting point, whereas resolution of the acid derived from [4.4]paracyclophane was unsuccessful.[80]

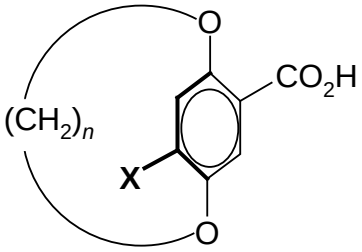

169

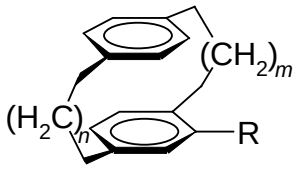

170

8.2 Nomenclature and absolute configuration

In 1951, Cahn and Ingold introduced a nomenclature system to denote the configurations of enantiomers and diastereomers.[81] In this classical paper, only central chirality was covered. This system was extended in 1956 and improved in 1966 by Cahn, Ingold and Prelog to include axial-, planar- and helical chirality. [82, 83]

To find the descriptor for planar chiral molecules, one views the chiral plane from the out-of-plane atom (pilot atom, P) closest to the plane. The pilot atom should be chosen from that side of the plane preferred by the standard subrules. If the neighboring three

atoms (a, b and c) describe a clockwise move on the chiral plane, the configuration is p*R*, in case of a counterclockwise move, the descriptor is p*S* (the prefix p is used to signal planar chirality; it is sometimes omitted).

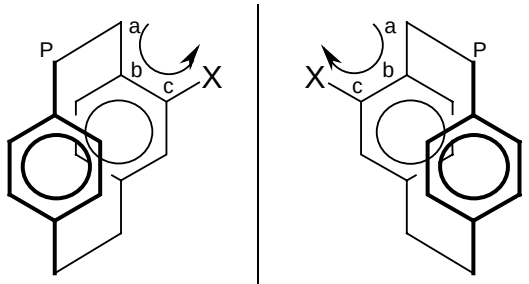

(p*S*)-enantiomer (p*R*)-enantiomer

Figure 42: Absolute configuration of a monosubstituted [2.2]paracyclophane.

In case of higher substituted [2.2]paracyclophanes, the atom closest to the atom of higher precedence according to the sequence rules is chosen as the pilot atom.

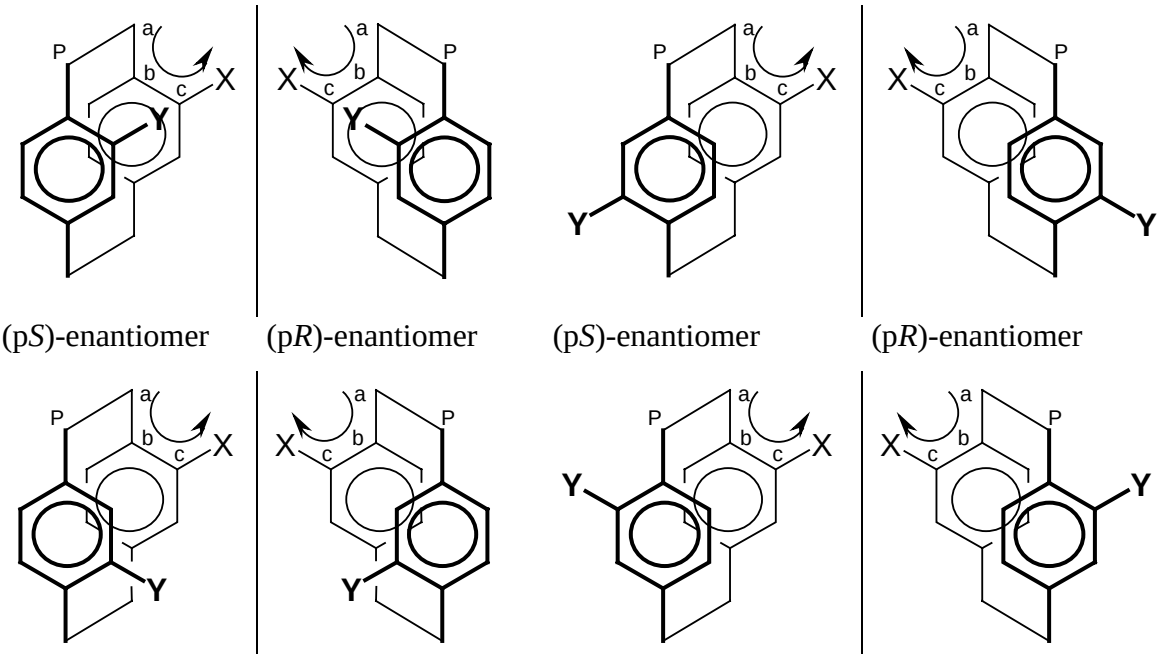

(p*S*)-enantiomer (p*R*)-enantiomer (p*S*)-enantiomer (p*R*)-enantiomer

(p*S*)-enantiomer (p*R*)-enantiomer (p*S*)-enantiomer (p*R*)-enantiomer

Figure 43: Absolute configuration in disubstituted [2.2]paracyclophanes (priority: X > Y).

With two different substituents, *ortho* disubstituted [2.2]paracyclophanes are also chiral.

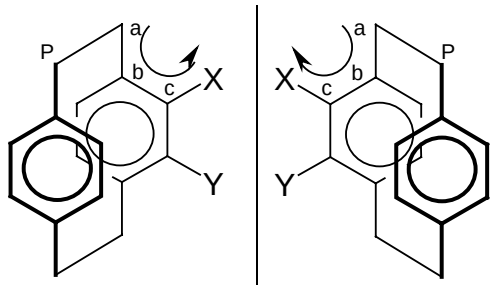

(p*S*)-enantiomer (p*R*)-enantiomer

Figure 44: Absolute configuration of *ortho* disubstituted [2.2]paracyclophanes (priority: X >Y).

When the two substituents are equal (X = Y), the C_2 symmetric *pseudo-ortho*- and the *pseudo-meta*-isomers are chiral, whereas the *ortho*, *pseudo-geminal*- and *pseudo-para*-isomers are achiral because of S_2 symmetry.

In case of tetrasubstituted [2.2]paracyclophanes (all substituents being equal), the crossed derivatives are chiral whereas the anti isomers are achiral due to S_2 symmetry.

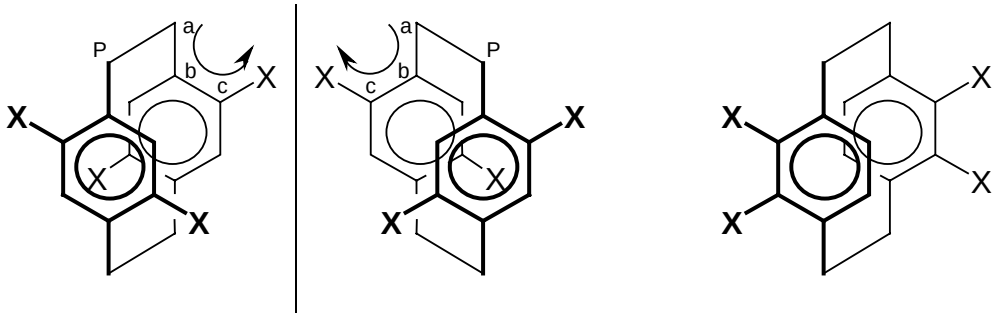

(p*S*)-enantiomer (p*R*)-enantiomer anti isomer (achiral)

Figure 45: A selection of tetrasubstituted [2.2]paracyclophanes.

8.3 Results and Discussion

In cooperation with the group of Okamoto, the two enantiomers of the crossed tetraalkyne **164** were separated by HPLC using an cellulose tris(3,5-dimethylphenyl carbamate) OD-column with *n*-hexane/2-propanol (90/10) as the solvent system.

The first eluted enantiomer is the (-)enantiomer; it has an optical rotation of $[\alpha]_D^{25}$ = -63. The (+)enantiomer has an optical rotation of $[\alpha]_D^{25}$ = +73. Due to the small amount of material, the two α values differ slightly from each other.[84]

Regarding the *ortho*-disubstituted [2.2]paracyclophanes, Schulz was able to obtain optically pure (*S*)-5-formyl-4-hydroxy[2.2]paracyclophane (*S*)-**97** (ee > 99%) by a chemoenzymatic procedure starting from racemic 4-acetoxy[2.2]paracyclophane (**171**,

Scheme 50).[85, 86] Hydrolysis of racemic **171** by the lipase *candida rugosa* gave (*R*)-4-hydroxy[2.2]paracyclophane (**95**) in 51% yield and 90% ee. Enantiomerically pure (*S*)-**171** remained in 44% yield (ee > 99.9%). After separation, (*S*)-**171** was hydrolyzed with KOH in methanol to give (*S*)-**95** in 95% yield. The final steps towards FHPC (**97**) follow the procedure given by Hopf and Barret.[43] The phenols **95** were converted to the carbamates **96** without racemization. Finally, the carbamates were *ortho* lithiated, and the formed anions trapped with DMF. Upon acidic workup, cleavage of the carbamate function to the phenol occurs to give FHPC **97**.

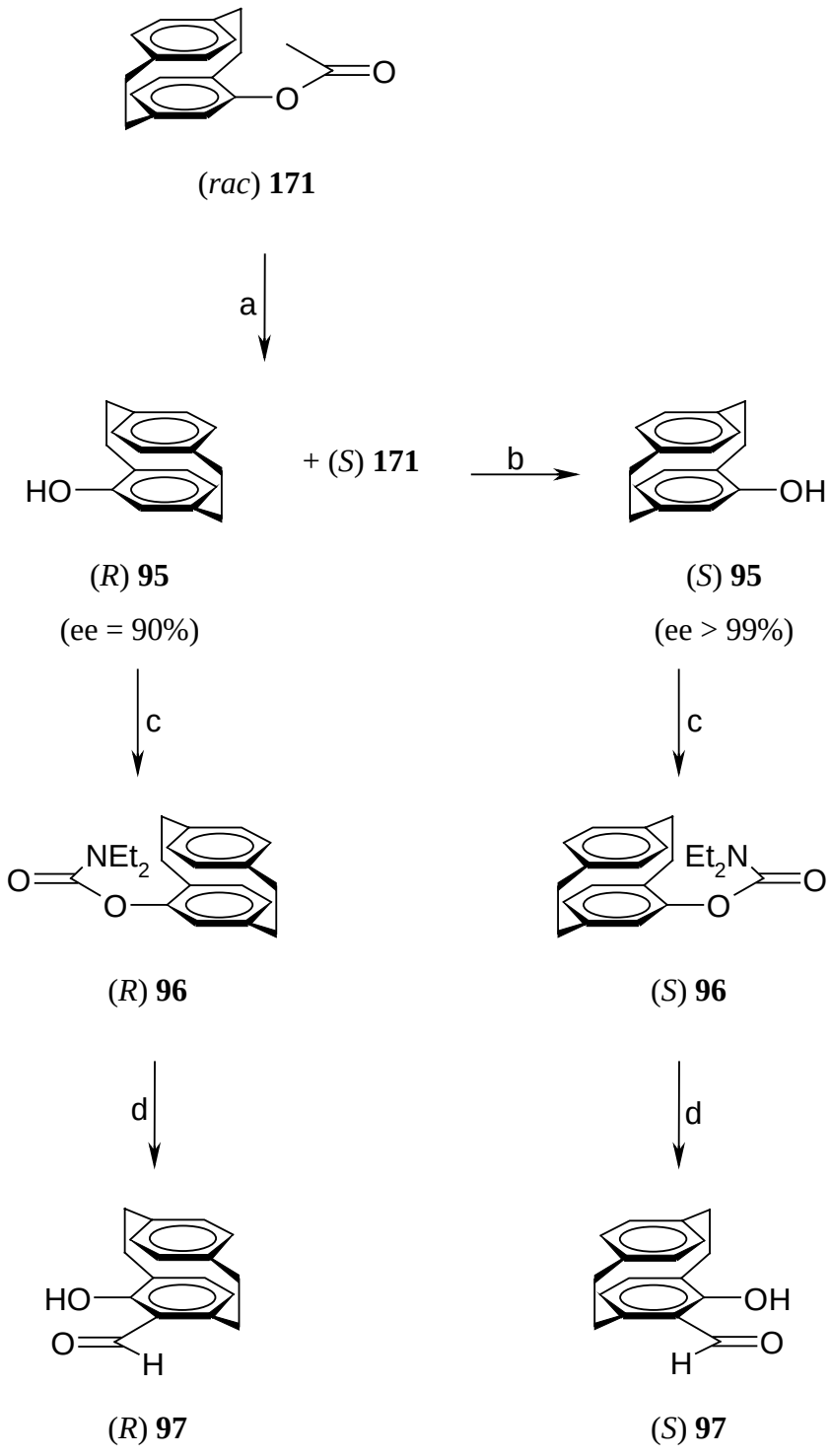

(a) lipase *candida rugosa*; (b) KOH, CH_3OH; (c) $Et_2NC(O)Cl$, DMAP, toluene; (d) [i] TMEDA, *sec*-BuLi, THF [ii] DMF

Scheme 50: Chemoenzymatic synthesis of 5-formyl-4-hydroxy[2.2]paracyclophane (**97**) by Schulz.

rac-FHPC (**97**) was used as an intermediate in the synthesis of *rac*-5-ethynyl-4-(trimethylsilyl)ethynyl[2.2]paracyclophane (**107**) by the Corey-Fuchs reaction as described in Section 3.1. Using optically pure **97**, it should be possible to synthesize

chiral [2.2]paracyclophane/dehydrobenzoannulenes in optical pure form *via* the route proposed in Scheme 51.

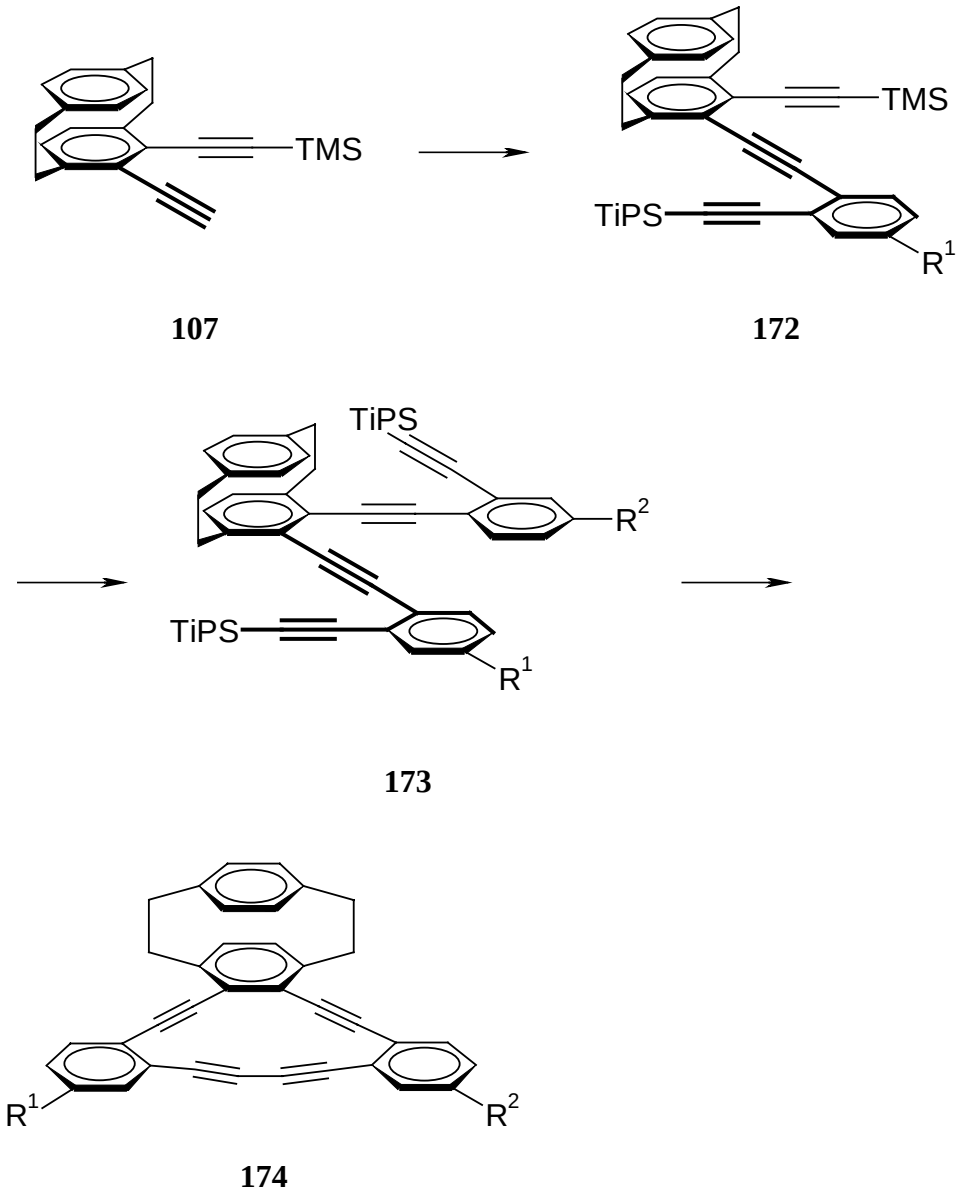

107 **172** **173** **174**

Scheme 51: Possible synthesis of optically active [2.2]paracyclophane/dehydrobenzo[14]annulenes.

9 Summary

The aim of this study was the synthesis and study of carbon rich systems incorporating the [2.2]paracyclophane unit as a building block. The first chapter gives a short historical background of annulene and cyclophane chemistry.

In the first project the synthesis of the [2.2]paracyclophane/dehydrobenzo[14]annulene **53** is described. The retrosynthetic analysis discussed in the second chapter shows, that it should be possible to synthesize **53** from 4,5-diethynyl[2.2]paracyclophane (**56**) and an *ortho*-ethynyl-halobenzene (**57**).

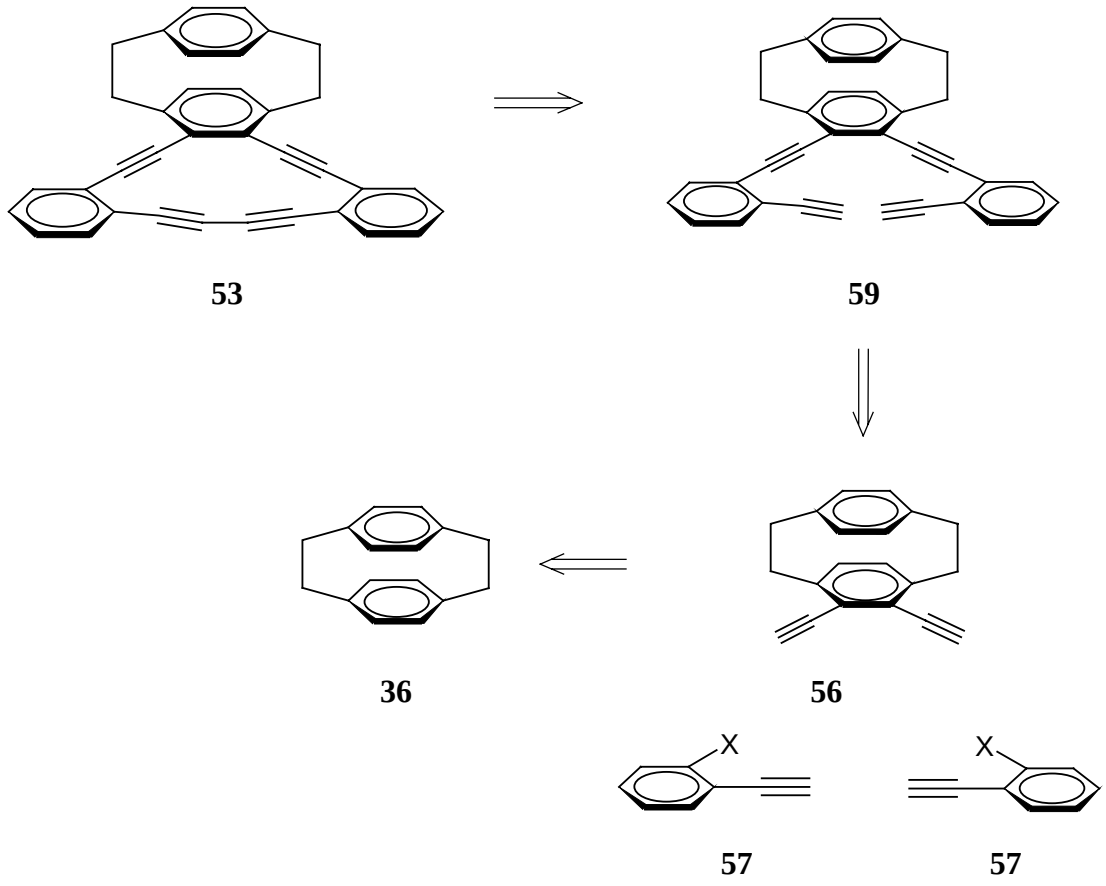

53 **59** **36** **56** **57** **57**

Scheme 52: Retrosynthetic analysis of **53**.

The synthesis of **56** is described in the third chapter. Following the protocol given by Hopf and Barrett,[43] 5-formyl-4-hydroxy[2.2]paracyclophane (FHPC, **97**) was synthesized from commercially available [2.2]paracyclophane (**36**). The phenol function of **97** was converted to the triflate which was reacted in a Pd catalyzed cross-coupling reaction to the *ortho* formyl-alkyne **99**. For the final conversion of the aldehyde group, different methods like the Corey-Fuchs reaction or the Bestman alkynylation protocol can be used.

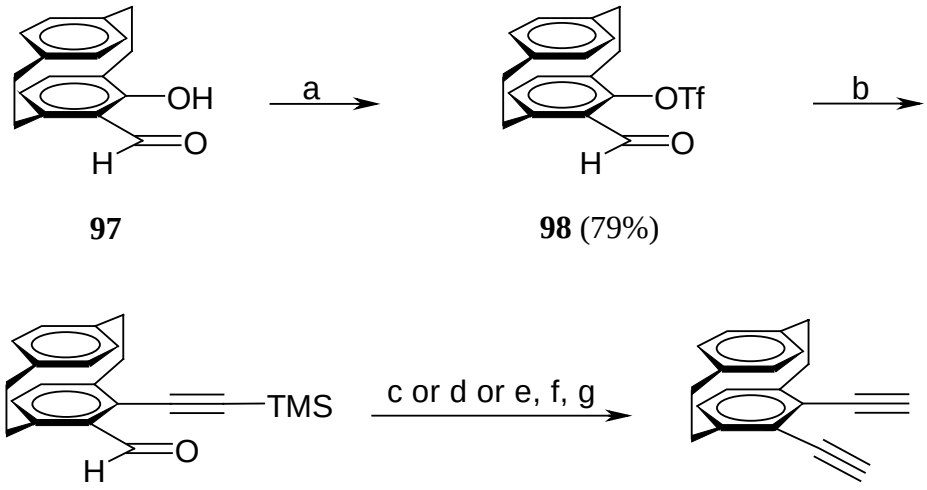

(a) $BnNTf_2$, Et_3N; (b) TMSA, $Pd(PPh_3)_4$, CuI, *i*-Pr_2NH, THF; (c) $CH_3C(O)C(N_2)P(O)(OMe)_2$, K_2CO_3, CH_3OH; (d) [i] $Ph_3PCH_2Br^+$ Br^-, *t*-BuOK, THF, -78°C, [ii] *t*-BuOK, THF, reflux; (e) Ph_3PCBr_2, CH_2Cl_2; (f) LDA, THF, -78 °C; (g) K_2CO_3, CH_3OH

Scheme 53: Synthesis of **56** from FHPC (**97**).

Different *ortho* ethynyl-iodobenzenes **116**, **121** and **125** were needed for the synthesis of the macrocyclic systems. Their synthesis, following a procedure developed by Haley and coworkers,[52, 53, 54] is summarized in the fourth chapter.

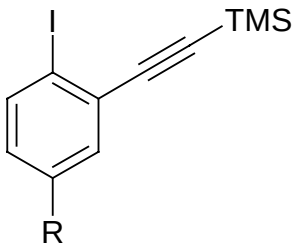

R	
H	**116**
t-Bu	**121**
NBu_2	**125**

The bulky substituents in **121** and **125** were needed to increase the solubility of the macrocyclic systems.

The synthesis of the [2.2]paracyclophane/dehydrobenzoannulene **53**, performed by Pd catalyzed cross-coupling of **56** with 2-(trimethylsilyl)ethynyl-iodobenzene (**116**)

followed by *in situ* deprotection and dimerization, is discussed in chapter five. Electronic absorption spectroscopy as well as NMR spectroscopy has shown, that delocalization through the alkyne units is present in **53**. Comparison with the known *pseudo-ortho* derivative **52**, the all benzo derivative **128** and Bunz derivatives containing organometal complexes **26** has shown, that the strongest ring current is present in **53**.

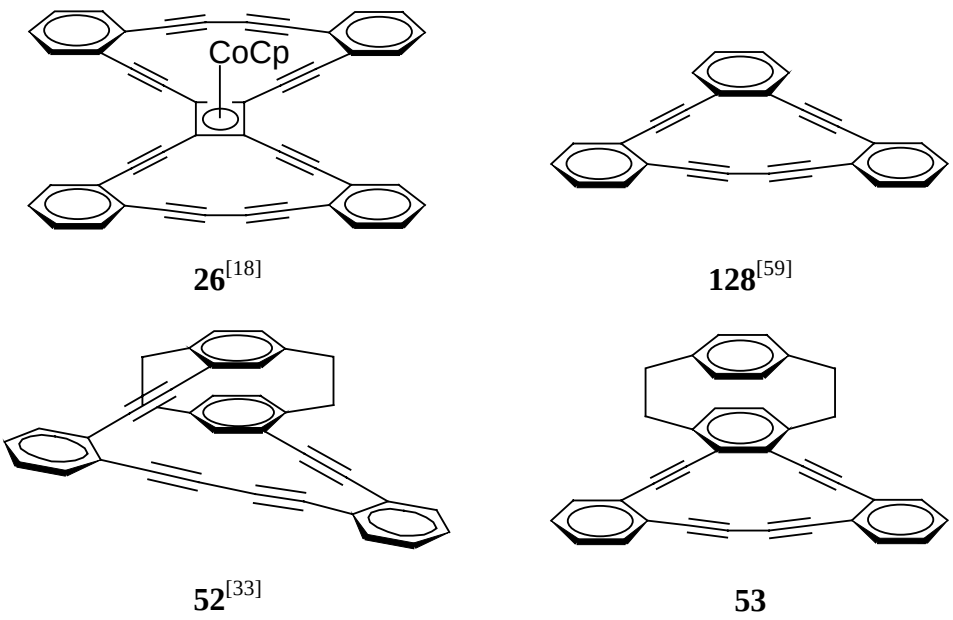

26[18] **128**[59]

52[33] **53**

Figure 46: Different [14]annulenes.

In the sixth section, the synthesis of a biphenylene derivative of [2.2]paracyclophane **144** by [2+2+2]cycloaddition of BTMSA (**136**) to 4,5-diethynyl[2.2]paracyclophane (**56**) and the Bergman cyclization of **56** to benzo[2.2]paracyclophane (**153**) is discussed.

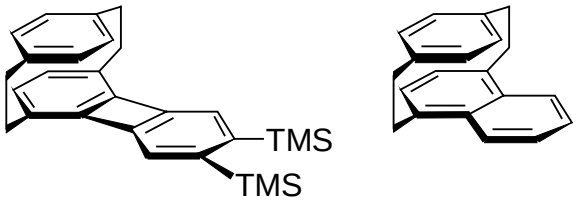

144 **153**

Figure 47: [2.2]Paracyclophane derivatives described in Chapter 6.

The second project which is described in the seventh chapter deals with the synthesis and properties of propeller type molecules. The properties of the [2.2]paracyclophane containing systems **157** (R = *t*-Bu) and **158** (R = NBu_2) were compared with the unbridged systems **154** and **155**. It was shown by electron absorption spectroscopy, that

in **157** and **158** stronger delocalization is present than in the unbridged systems **154** and **155**. ACID calculations have confirmed this observations.

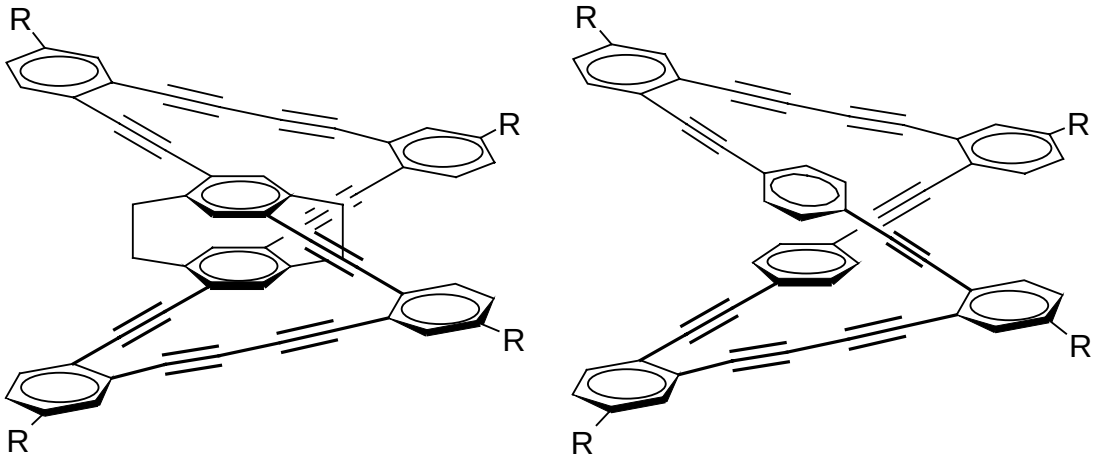

R	
tert-Bu	**157**
Bu_2N	**158**

R	
tert-Bu	**154**
Bu_2N	**155**

Figure 48: Propeller type molecules, synthesized in this thesis.

The eighth chapter gives a view on further work to be done in this field. Since the precursor of **56** is chiral and was already prepared in enantiomerically pure form, the synthesis of chiral [2.2]paracyclophane/dehydrobenzoannulenes is at hand.

10 Experimental

10.1 Instrumentation and general experimental considerations

Thin Layer Chromatrography: Macherey-Nagel & Co (Düren) "Polygram Sil G/UV_{254}" silica gel plates were used for analytical thin layer chromatography.

Preparative Thin Layer Chromatography: Preparative thin layer chromatography was performed with 20x20 cm Merck silica gel 60 plates 2mm with $F_{254+366}$ indicator.

Column Chromatography: Column chromatography was performed on Merck (Darmstadt) silica gel 60 (70-230 mesh).

Melting Points: Melting points were determined on a Meltemp II apparatus from Labaratory Devices. The melting points are uncorrected.

Sublimation: For sublimation a temperature gradient sublimer from Esoteric Chemicals was employed.

NMR Spectroscopy: ^{1}H and ^{13}C NMR spectra were recorded using a Bruker AC-200 (^{1}H NMR 200.1 MHz; ^{13}C NMR 50.3 MHz) or a Bruker DRX-400 (^{1}H NMR 400.1 MHz; ^{13}C NMR 100.6 MHz) spectrometer. Deuteriochloroform ($CDCl_3$) was usually used as the NMR solvent. Chemical shifts are reported in ppm downfield from internal tetramethylsilane as reference. Spin multiplicities are indicated by the following symbols: s (singlet), d (doublet), t (triplet), q (quartet), qui (quintet), six (sixtet), m (multiplet).

IR Spectroscopy: IR Spectra were recorded on a Nicolet DX320 FT-IR spectrometer as KBr pallets or on a Bruker Tensor 27 spectrometer using the ATR-Diamond technique.

UV/Vis Spectroscopy: UV/Vis spectra were obtained using a Hewlett-Packard 8452 A diode array or a Varian Cary 100 Bio spectrometer.

Mass Spectrometry: MS spectra were recorded on a Finnigan MAT95 mass spectrometer using electron ionization (EI, 70 eV). GC/MS spectra were recorded on a Jeol GCMate spectrometer. MALDI-TOF spectra were recorded by Dr. Manfred Nimtz (Gesellschaft für Biotechnologische Forschung, GBF) on a Bruker MALDI-TOF mass spectrometer.

Elemental Analysis: Analysis were carried out at the Institut für Pharmazeutische Chemie, and the Institut für Anorganische und Analytische Chemie, TU Braunschweig.

X-ray Structure Analysis

For X-ray structure analysis, a Bruker SMART 1000 CCD diffractometer was used.

10.2 General experimental procedures

General procedure A:

A solution of the iodoarene in THF and diisopropylamine was deoxygenated by bubbling argon through it. The reaction mixture was cooled in an ice bath and $Pd(PPh_3)_4$, CuI and TMSA were added. After stirring for 24 h, the solvents were evaporated and the residue purified by column chromatography.

General procedure B:

A solution of the iodoarene in THF and diisopropylamine was deoxygenated by bubbling argon through it. To this solution, $Pd(PPh_3)_4$ and CuI were added. A deoxygenated solution of the terminal acetylene in THF was added with a syringe pump at 60 °C. After 24 h, the reaction mixture was concentrated *in vacuo* and purified by column chromatography.

General procedure C:

In an Schlenk tube with screw cap, a solution of the bromoarene in THF and diisopropylamine was deoxygenated by bubbling argon through it. $Pd(PPh_3)_4$, CuI and TMSA were added and the reaction mixture was heated to 60 °C in the closed Schlenk tube. The solvents were evaporated and the residue purified by column chromatography.

General procedure D:

The protected alkyne was dissolved in methanol and dichloromethane. To this solution, K_2CO_3 was added. The reaction mixture was stirred for 12 to 24 h at room temp, diluted with dichloromethane and washed with aqueous NH_4Cl solution. The aqueous phase was reextracted with dichloromethane and the combined organic phases were dried with Na_2SO_4.

General procedure E:

To a solution of the TMS-protected alkyne in methanol/acetonitrile, K_2CO_3 and $Cu(OAc)_2 \cdot H_2O$ were added. The mixture was heated to reflux for 24 h, diluted with dichloromethane and washed with brine. The organic phase was dried with Na_2SO_4 and the solvent removed *in vacuo*.

General procedure F:

A solution of the terminal acetylene in pyridine/ether was added with a syringe pump to a solution of $Cu(OAc)_2 \cdot H_2O$ in pyridine/ether at room temp. Upon completion, the mixture was diluted with ether and washed with water. The solvents were removed *in vacuo*, the residue dissolved in dichloromethane and dried with Na_2SO_4.

10.3 Experimental procedures

Exp. 1: Dimethyl-1-diazo-2-oxopropylphosphonate (67)

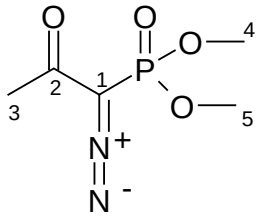

67

2.5 g (62.5 mmol) of NaH (60% in mineral oil) was suspended in 25 mL of abs. THF and 150 mL of abs. toluene. The suspension was cooled to 0 °C and 8.29 g (50 mmol) of dimethyl-2-oxo-propylphosphonate in 50 mL of toluene was added dropwise. After 1.5 h, 10.35 g (52.5 mmol) of $TosN_3$ in 25 mL of toluene was added dropwise and after 10 min, the cooling bath was removed. After stirring overnight, the reaction was filtered under nitrogen through a pad of Celite and washed with 150 mL of toluene. The solvent was removed at room temp. and the product purified by column chromatography with ether (R_f = 0.2) to yield 7.52 g (39 mmol, 78%; 83% [37]) of **67** as a light yellow oil.

^{1}H NMR ($CDCl_3$): δ = 2.28 (s, 3 H, 3-H), 3.86 (d, $^3J_{H,P}$ = 12.0 Hz, 6 H, 4-H, 5-H)

^{13}C NMR ($CDCl_3$): δ = 27.2 (q, C-3), 53.7 (dq, $^2J_{C,P}$ = 5.5 Hz, C-4, C-5), 63.5 (d, $^1J_{C,P}$ = 220.5 Hz, C-1), 189.9 (d, $^2J_{C,P}$ = 13.0 Hz, C-2)

IR (ATR): $\tilde{\nu}$ = 3500 cm^{-1} (br w), 2960 (w), 2122 (s), 1657 (s), 1458 (w), 1365 (m), 1267 (vs), 1181 (m), 1021 (vs), 971 (m), 836 (m), 804 (m), 784 (m), 648 (w), 580 (m), 551 (m)

MS (GC-MS): *m/z* (%) = 192 (3) [M^+], 164 (100) [M^+-N_2], 136 (39), 135 (86), 133 (48), 110 (70), 109 (93), 106 (70), 95 (46), 93 (51), 79 (95)

Exp. 2: (Z)-1-Chloro-4-trimethylsilylbuten-3-yne (175)

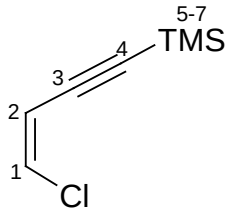

175

In a Schlenk tube with screw cap, 3.877 g (40 mmol) of (Z)-1,2-dichloroethene was added to a deoxygenated mixture of 4 mL (40 mmol) of *n*-butylamine and 25 mL of benzene. To this solution, 231 mg (0.2 mmol) of $Pd(PPh_3)_4$ and 2.8 mL (20 mmol) of TMSA were added. The mixture was cooled with a water bath and after 10 min, 381 mg (2 mmol) of CuI was added. After stirring for 20 h at room temp., the mixture was hydrolyzed with NH_4Cl solution, extracted with ether and washed with brine. The organic phase was dried with Na_2SO_4, and the solvent was evaporated. Purification by column chromatography on silica gel using pentane (R_f = 0.3) gave 2.32 g (14.6 mmol, 73% ; 76%[57]) of **175** as a colorless oil.

^{1}H NMR ($CDCl_3$): δ = 0.22 (s, 9 H, Si(C**H**$_3$)$_3$), 5.88 (d, ^3J = 7.6 Hz, 1 H, 2-H), 6.39 (d, ^3J = 7.6 Hz, 1 H, 1-H)

^{13}C NMR ($CDCl_3$): δ = -0.3 (q, Si(**C**H$_3$)$_3$), 98.2 (s, C-3), 103.7 (s, C-4), 112.1 (d, C-2), 129.2 (d, C-1)

IR (ATR): $\tilde{\nu}$ = 2962 cm^{-1} (m), 2158 (w), 1251 (m), 1041 (m), 1009 (m), 844 (vs), 792 (m), 760 (m), 724 (m)

MS (GC-MS): *m/z* (%) = 158/160 (27/10) [M^+], 143/145 (100/74) [M^+-CH_3], 117/119 (57/21)

10.3.1 Synthesis of the substituted iodobenzenes

Exp. 3: *N*,*N*-Diethyl-*N*'-(2-iodophenyl)triazene (114)

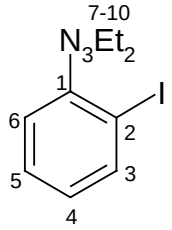

114

4.63 g (21.1 mmol) of 2-iodoaniline (**113**) was dissolved in a solution of 79 mL of diethyl ether, 68 mL of THF and 12 mL of acetonitrile. 46 mL of 4.5 M HCl (207 mmol) was added and the reaction mixture was cooled to –5 °C. 5.35 g (78 mmol) of $NaNO_2$ in 16 mL of acetonitrile and 23 mL of water was added dropwise, and the reaction was stirred for 1.5 h at -5 to 0 °C. The mixture was poured into a chilled solution of 15.76 g (114 mmol) of K_2CO_3 and 12 mL (114 mmol) of Et_2NH in 150 mL of acetonitrile and 75 mL of water. After stirring for 1.5 h, the mixture was extracted twice with ether. The combined ether layers were washed twice with brine, dried with Na_2SO_4, filtered and concentrated by rotary evaporation. Purification by column chromatography on silica gel with 5% dichloromethane in pentane (R_f = 0.16) gave 4.9 g (16.16 mmol, 79%) of **114** as an orange oil. Since the yield and the spectroscopic data are not given in the literature[52], the spectroscopic data are listed here.

^{1}H NMR ($CDCl_3$): δ = 1.27 (t, ^3J = 7.2 Hz, 6 H), 3.73 (q, ^3J = 7.2 Hz, 4 H), 6.79 (ddd, ^3J = 7.9 Hz, ^3J = 7.0 Hz, ^4J = 1.7 Hz, 1 H), 7.24 (ddd, ^3J = 8.0 Hz, ^3J = 7.0 Hz, ^4J = 1.4 Hz, 1 H), 7.35 (dd, ^3J = 8.0 Hz, ^4J = 1.7 Hz, 1 H), 7.81 (dd, ^3J = 7.9 Hz, ^4J = 1.4 Hz, 1 H)

^{13}C NMR ($CDCl_3$): δ = 11.1 (br q), 14.3 (br q), 42.0 (br t), 49.1 (br t), 96.5 (s), 117.4 (d), 126.2 (d), 128.3 (d), 138.8 (d), 150.2 (s)

IR (ATR): $\tilde{\nu}$ = 3057 cm^{-1} (w), 2972 (m), 2931 (m), 2870 (w), 1577 (w), 1592 (w), 1454 (s), 1431 (m), 1397 (s), 1326 (vs), 1260 (s), 1246 (s), 1231 (s), 1196 (s), 1097 (s), 1072 (m), 1011 (s), 939 (m), 749 (vs), 712 (m), 662 (m), 627 (m), 580 (m)

MS (GC-MS): *m/z* (%) = 303 (25) [M^+], 231 (47), 203 (100), 76 (30)

Exp. 4: *N*,*N*-Diethyl-*N*'-[2-(trimethylsilylethynyl)phenyl]triazene (115)

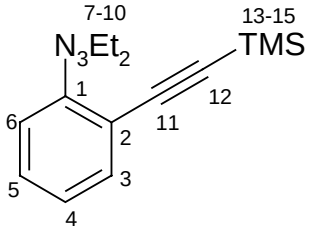

115

3.64 g (12 mmol) of **114** in 40 mL of THF and 40 mL of diisopropylamine was subjected to general procedure C using 139 mg (0.12 mmol) of $Pd(PPh_3)_4$, 46 mg (0.24 mmol) of CuI and 2.55 mL (18 mmol) of TMSA. Purification by column chromatography on silica gel with 50% dichloromethane in pentane (R_f = 0.5) gave 3.07 g (11.2 mmol, 94%) of **115** as a yellow oil. Since the spectroscopic data of **115** are incomplete in the literature[52] they are listed here.

^{1}H NMR ($CDCl_3$): δ = 0.24 (s, 9 H, $Si(C\mathbf{H}_3)_3$), 1.31 (t, ^3J = 7.2 Hz, 6 H), 3.79 (q, ^3J = 7.2 Hz, 4 H), 6.99-7.06 (m "ddd", 1 H), 7.19-7.28 (m "ddd", 1 H), 7.36-7.40 (m "ddd", 1 H), 7.44-7.49 (m "ddd", 1 H)

^{13}C NMR ($CDCl_3$): δ = 0.0 (q, $Si(\mathbf{C}H_3)_3$), 11.0 (br q), 14.0 (br q), 41.6 (br t), 48.8 (br t), 97.6 (s), 103.5 (s), 116.6 (d), 117.9 (s), 124.4 (d), 128.9 (d), 133.1 (d), 152.7 (s)

IR (ATR): $\tilde{\nu}$ = 3067 cm^{-1} (w), 2963 (m), 2934 (m), 2898 (w), 2872 (w), 2154 (m), 1470 (m), 1443 (m), 1406 (m), 1378 (m), 1328 (s), 1271 (m), 1154 (w), 1114 (m), 1088 (s), 1038 (w), 998 (w), 947 (w), 860 (vs), 835 (vs), 753 (vs), 698 (m), 651 (m), 603 (m), 588 (m), 549 (w)

MS (GC-MS): *m/z* (%) = 273 (6) [M^+], 201 (15), 173 (65), 145 (100), 79 (15), 70 (77)

Exp. 5: 2-[(Trimethylsilyl)ethynyl]iodobenzene (116)

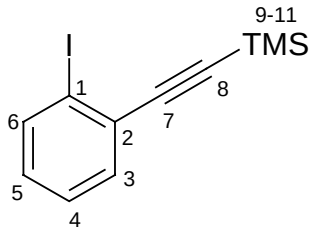

116

2.97 g (10.9 mmol) of **115** was heated in 6 mL of freshly distilled methyliodide in a pressure tube with teflon screw cap to 120 °C for 24 h. The reaction mixture was cooled to room temp. and the solvent was evaporated. Column chromatography on silica gel with 5% dichloromethane in pentane (R_f = 0.54) gave 3.03 g (10.1 mmol, 93%; >95%[52]) of **116** as a light yellow oil. Since the spectroscopic data of **116** are incomplete in the literature[52] they are given here.

^{1}H NMR ($CDCl_3$): δ = 0.3 (s, 9 H, Si(C**H**$_3$)$_3$), 6.99 (dt, ^3J = 7.7 Hz, ^4J = 1.7 Hz, 1 H, 5-H), 7.28 (dt, ^3J = 7.7 Hz, ^4J = 1.2 Hz, 1 H, 4-H), 7.48 (dd, ^3J = 7.7 Hz, ^4J = 1.7 Hz, 1 H, 3-H), 7.74 (dd, ^3J = 7.7 Hz, ^4J = 1.2 Hz, 1 H, 6-H)

^{13}C NMR ($CDCl_3$): δ = -0.2 (q), 98,7 (s), 101.3 (s), 106.5 (s), 127.6 (d), 129.5 (d), 129.6 (s), 132.6 (d), 138.6 (d)

IR (ATR): $\tilde{\nu}$ = 3062 cm^{-1} (w), 2958 (m), 2897 (w), 2161 (m), 1578 (w), 1554 (w), 1459 (m), 1429 (m), 1249 (m), 1429 (m), 1042 (m), 1016 (m), 860 (vs), 840 (vs), 753 (vs), 706 (m), 658 (m), 639 (m)

MS (GC-MS): *m/z* (%) = 300 (37) [M$^+$], 285 (100), 173 (6), 143 (21), 79 (7)

Exp. 6: 4-*tert*-Butyl-2-iodoaniline (118)

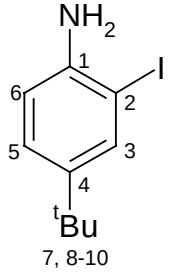

118

10.0 g (68 mmol) of 4-*tert*-butylaniline **(117)** was dissolved in 1 L of dichloromethane and 500 mL of methanol. To this mixture was added 24.35 g (70 mmol) of $(BnMe_3N)^+ ICl_2^-$ and 13.4 g (134 mmol) of $CaCO_3$. The suspension was stirred at room temp. for 3 h. The reaction mixture was filtered through a pad of Celite and concentrated *in vacuo* to approximately 1/3 of its volume. The residual mixture was washed with a 5% $NaHSO_3$ solution, a saturated $NaHCO_3$ solution, water and brine. The organic layer was dried with Na_2SO_4, filtered and concentrated to give an orange oil. Purification by column chromatography on silica gel with 5% EtOAc in hexane (R_f = 0.21) furnished 15.2 g (55 mmol, 81%; 90%[53]) of **118** as a viscous red oil.

^{1}H NMR ($CDCl_3$): δ = 1.21 (s, 9 H, $C(CH_3)_3$), 3.88 (s, 2 H, NH_2), 6.58 (d, ^3J = 8.4 Hz, 1 H, 6-H), 7.10 (dd, ^3J = 8.4 Hz, ^4J = 2.2 Hz, 1 H, 5-H), 7.59 (d, ^4J = 2.2 Hz, 1 H, 3-H)

^{13}C NMR ($CDCl_3$): δ = 31.3 (q, $C(CH_3)_3$), 33.5 (s, $C(CH_3)_3$), 84.5 (s, C-2), 114.4 (d, C-6), 126.2 (d, C-5), 135.3 (d, C-3), 142.8 (s, C-4), 144.1 (s, C-1)

IR (ATR): $\tilde{\nu}$ = 3457 cm^{-1} (m), 3368 (m), 3201 (w), 3073 (w), 3020 (w), 2961 (vs), 2905 (m), 2867 (m), 1615 (vs), 1498 (vs), 1478 (m), 1465 (m), 1395 (m), 1298 (m), 1258 (s), 1202(m), 1162 (m), 1118 (m), 1027 (m), 879 (m), 816 (s)

MS (GC-MS): *m/z* (%) = 275 (37) [M^+], 260 (100), 133 (14)

Exp. 7: *N*,*N*-Diethyl-*N*'-(4-*tert*-butyl-2-iodophenyl)triazene (119)

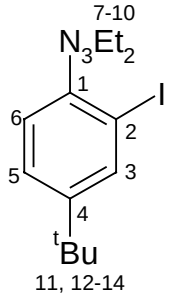

119

15.179 g (55 mmol) of **118** was dissolved in a solution of 190 mL of diethyl ether, 164 mL of THF and 27 mL of acetonitrile. 110 mL of 4.5 M HCl (495 mmol) was added and the reaction mixture was cooled to –5 °C. 12.95 g (187 mmol) of $NaNO_2$ in 38 mL of acetonitrile and 56 mL of water was added dropwise and the mixture was stirred for 1.5 h at –5 to 0 °C. The mixture was poured into a chilled solution of 38.14 g (275 mmol) of K_2CO_3 and 29 mL (276 mmol) of Et_2NH in 365 mL of acetonitrile and 182 mL of water. After stirring for 1.5 h, the mixture was extracted twice with ether. The combined ether layers were washed twice with brine, dried with Na_2SO_4, filtered and concentrated by rotary evaporation. Purification by column chromatography on silica gel with 5% EtOAc in hexane (R_f = 0.35) gave 17.8 g (0.49 mmol, 90%; 93% [53]) of **119** as an orange oil.

^{1}H NMR ($CDCl_3$): δ = 1.29 (s, 9 H, C(C**H**$_3$)$_3$), 1.30 (t, ^3J = 7.2 Hz, 6 H, N(CH$_2$C**H**$_3$)$_2$), 3.77 (q, ^3J = 7.2 Hz, 4 H, N(C**H**$_2$CH$_3$)$_2$), 7.26 (d, ^3J = 8.4 Hz, 1 H, 6-H), 7.30 (dd, ^3J = 8.4 Hz, ^4J = 2.0 Hz, 1 H, 5-H), 7.82 (d, ^4J = 2.0 Hz, 1 H, 3-H)

^{13}C NMR ($CDCl_3$): δ = 11.2, 14.3 (br q), 31.3 (q), 34.3 (s), 41.9, 49.0 (br t), 96.6 (s), 116.9 (d), 125.9 (d), 135.8 (d), 148.1 (s), 149.8 (s)

IR (ATR): $\tilde{\nu}$ = 2963 cm^{-1} (s), 2933 (m), 2903 (m), 2870 (m), 1589 (w), 1541 (w), 1462 (vs), 1432 (s), 1414 (s), 1380 (vs), 1331 (vs), 1282 (m), 1256 (vs), 1236 (s), 1207 (m), 1104 (s), 1077 (m), 1032 (m), 880 (w), 847 (w), 827 (m), 768 (w), 730 (w), 717 (w)

MS (GC-MS): *m/z* (%) = 359 (18) [M^+], 287 (24) [M^+-$C_4H_{10}N$], 259 (100), 72 (18) [$C_4H_{10}N^+$]

Exp. 8: *N*,*N*-Diethyl-*N*'-[4-*tert*-butyl-2-(trimethylsilylethynyl)phenyl]triazene (120)

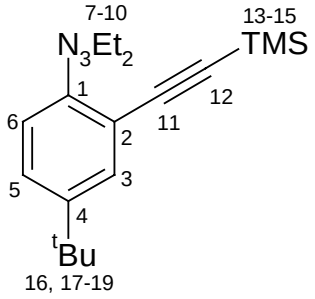

120

1.44 g (4 mmol) of **119** in 40 mL of THF and 40 mL of diisopropylamine was subjected to general procedure C using 46 mg (0.04 mmol) of $Pd(PPh_3)_4$, 15 mg (0.08 mmol) of CuI and 0.85 mL (6 mmol) of TMSA. Purification by column chromatography on silica gel with 20% dichloromethane in pentane (R_f = 0.3) gave 1.21 g (3.6 mmol, 91%) of **120** as light yellow solid (m.p. 38 °C).

^{1}H NMR ($CDCl_3$): δ = 0.25 (s, 9 H, $Si(C\mathbf{H}_3)_3$), 1.29 (s, 9 H, $C(C\mathbf{H}_3)_3$), 1.32 (t, ^3J = 7.1 Hz, 6 H, $N(CH_2C\mathbf{H}_3)_2$), 3.77 (q, ^3J = 7.1 Hz, 4 H, $N(C\mathbf{H}_2CH_3)_2$), 7.27 (dd, ^3J = 8.9 Hz, ^4J = 2.4 Hz, 1 H, 6-H), 7.30 (d, ^3J = 8.9 Hz, 1 H, 5-H), 7.50 (d, ^4J = 2.4 Hz, 1 H, 3-H)

^{13}C NMR ($CDCl_3$): δ = 0.1 (q), 11.2, 14.3 (br q), 31.3 (q), 34.3 (s), 41.9, 49.0 (br t), 97.0 (s), 104.2 (s), 116.4 (d), 117.3 (s), 126.5 (d), 129.9 (d), 147.5 (s), 150.5 (s)

IR (ATR): $\tilde{\nu}$ = 2969 cm^{-1} (m), 2961 (m), 2902 (w), 2868 (w), 2156 (m), 1485 (w), 1465 (m), 1450 (m), 1431 (w), 1416 (w), 1385 (m), 1331 (m), 1248 (m), 1204 (m), 1109 (m), 1090 (m), 927 (m), 885 (w), 831 (vs), 756 (s), 698 (m), 652 (m), 640 (m), 624 (m), 584 (m)

MS (EI): *m/z* (%) = 329 (11) [M^+], 230 (26), 229 (100) [M^+-$C_4H_{10}N_3$], 215 (41), 214 (20), 190 (25), 173 (24), 145 (37), 70 (76), 57 (74) [*t*-Bu^+]

$C_{19}H_{31}N_3Si$ (329.56) calcd. C 69.25, H 9.48, N 12.75, Si 8.52; found C 69.42, H 9.59, N 12.88

Exp. 9: 4-*tert*-Butyl-2-[(trimethylsilyl)ethynyl]iodobenzene (121)

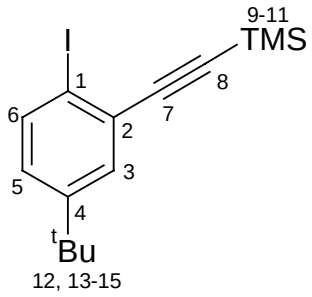

121

In a pressure tube with teflon screw cap, a solution of 3.58 g (10.8 mmol) of **120** in 19 mL of freshly distilled methyliodide was heated for 24 h at 120 °C. The reaction mixture was cooled to room temp. and the solvent was removed. Column chromatography on silica gel with 20% dichloromethane in pentane (R_f = 0.74) gave 3.81 g (10.7 mmol, 99%) of **121** as a light yellow oil.

^{1}H NMR ($CDCl_3$): δ = 0.29 (s, 9 H, Si(C**H**$_3$)$_3$), 1.28 (s, 9 H, C(C**H**$_3$)$_3$), 7.02 (dd, ^3J = 8.4 Hz, ^4J = 2.5 Hz, 1 H, 5-H), 7.49 (d, ^4J = 2.5 Hz, 1 H, 3-H), 7.73 (d, ^3J = 8.4 Hz, 1 H, 6-H)

^{13}C NMR ($CDCl_3$): δ = -0.1 (q), 31.0 (q), 34.5 (s), 97.5 (s), 97.9 (s), 107.1 (s), 127.3 (d), 129.1 (s), 130.0 (d), 138.3 (d), 151.1 (s)

IR (ATR): $\tilde{\nu}$ = 2960 cm^{-1} (m), 2901 (w), 2867 (w), 2160 (m), 1459 (m), 1382 (m), 1248 (m), 1113 (m), 1014 (m), 919 (m), 838 (vs), 817 (s), 757 (s), 706 (m), 647 (m), 634 (m)

MS (GC-MS): *m/z* (%) = 356 (54) [M$^+$], 341 (100), 229 (4) [M$^+$-I], 199 (16), 149 (22)

$C_{15}H_{21}ISi$ (356.29) calcd. C 50.56, H 5.94, I 35.61, Si 7.88; found C 50.58, H 5.92

Exp. 10: *N*,*N*-Dibutyl-3-iodoaniline (123)

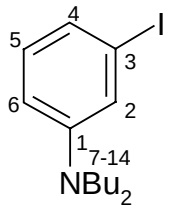

123

A mixture of 1.97 g (9.0 mmol) of 3-iodoaniline (**122**), 2.27 g (27 mmol) of $NaHCO_3$ and 12.3 g (90 mmol) of 1-bromobutane in 50 mL of THF and 10 mL of DMF was stirred at reflux for 7 d. The cooled reaction mixture was washed with water (3 x 50 mL) and extracted with 50 mL of diethyl ether. The organic layer was dried with Na_2SO_4 and concentrated. Column chromatography on silica gel with 10% dichloromethane in pentane gave 2.33 g (7.0 mmol, 78%; 94%[54]) of **123** as a light yellow oil.

^{1}H NMR ($CDCl_3$): δ = 0.94 (t, ^3J = 7.4 Hz, 6 H, $NCH_2CH_2CH_2C\mathbf{H}_3$), 1.33 (six, ^3J = 7.4 Hz, 4 H, $NCH_2CH_2C\mathbf{H}_2CH_3$), 1.49-1.57 (m, 4 H, $NCH_2C\mathbf{H}_2CH_2CH_3$), 3.18-3.22 (m, 4 H, $NC\mathbf{H}_2CH_2CH_2CH_3$), 6.55-6.57 (m, 1 H, 6-H), 6.84-6.93 (m, 3 H, 2-H, 4-H, 5-H)

^{13}C NMR ($CDCl_3$): δ = 13.9 (q), 20.3 (t), 29.2 (t), 50.6 (t), 95.8 (s), 110.8 (d), 120.3 (d), 123.9 (d), 130.4 (d), 149.3 (s)

IR (ATR): $\tilde{\nu}$ = 2956 cm^{-1} (m), 2930 (m), 2871 (m), 1585 (vs), 1547 (w), 1490 (m), 1367 (w), 1219 (w), 1180 (w), 977 (w), 755 (w)

MS (GC-MS): *m/z* (%) = 331 (31) [M^+], 289 (11), 288 (100), 256 (54), 231 (23)

Exp. 11: *N*,*N*-Dibutyl-3-[(trimethylsilyl)ethynyl]aniline (124)

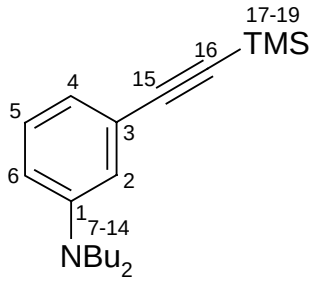

124

1.69 g (5 mmol) of **123** in 40 mL of THF and 40 mL of diisopropylamine was subjected to general procedure C using 58 mg (0.05 mmol) of $Pd(PPh_3)_4$, 19 mg (0.1 mmol) of CuI and 1.1 mL (7.5 mmol) of TMSA. Column chromatography on silica gel with 5% dichloromethane in pentane (R_f = 0.15) gave 1.4 g (4.6 mmol, 93%) of **124** as a light yellow oil.

^{1}H NMR (CDCl$_3$): δ = 0.29 (s, 9 H, Si(C**H**$_3$)$_3$), 0.99 (t, ^3J = 7.4 Hz, 6 H, NCH$_2$CH$_2$CH$_2$C**H**$_3$), 1.38 (six, ^3J = 7.4 Hz, 4 H, NCH$_2$CH$_2$C**H**$_2$CH$_3$), 1.54-1.61 (m, 4 H, NCH$_2$C**H**$_2$CH$_2$CH$_3$), 3.25-3.28 (m, 4 H, NC**H**$_2$CH$_2$CH$_2$CH$_3$), 6.62-6.64 (m, 1 H, 6-H), 6.75-6.78 (m, 2 H, 2-H, 4-H), 7.13 (t, ^3J = 7.9 Hz, 1 H, 5-H)

^{13}C NMR (CDCl$_3$): δ = 0.0 (q), 14.0 (q), 20.3 (t), 29.3 (t), 50.6 (t), 92.3 (s), 106.5 (s), 112.4 (d), 114.9 (d), 119.1 (d), 123.5 (s), 128.9 (d), 147.9 (s)

IR (ATR): $\tilde{\nu}$ = 2957 cm^{-1} (m), 2930 (m), 2898 (w), 2871 (m), 2155 (m), 1592 (m), 1566 (m), 1493 (m), 1463 (m), 1367 (m), 1288 (w), 1248 (m), 1189 (m), 1145 (m), 1108 (w), 1025 (w), 937 (w), 889 (m), 839 (vs), 761 (m), 687 (m), 647 (m)

MS (GC-MS): *m/z* (%) = 301 (22) [M$^+$], 259 (18), 258 (100), 216 (43), 202 (16), 186 (19)

Exp. 12: *N*,*N*-Dibutyl-4-iodo-3-[(trimethylsilyl)ethynyl]aniline (125)

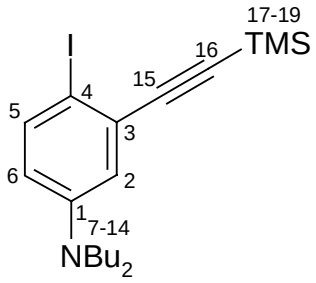

125

2.81 g (9.3 mmol) of **124** was treated with 3.24 g (9.3 mmol) of $(BnNMe_3)^+$ ICl_2^- and 1.33 g (13.3 mmol) of $CaCO_3$ in 170 mL of dichloromethane and 30 mL of methanol. The reaction mixture was stirred for 2 h and filtered. The filtrate was washed with 200 mL of 5% $NaHSO_3$ solution which was subsequently extracted with ether. The combined organic layers were dried with Na_2SO_4 and concentrated *in vacuo*. Chromatography on silica gel with pentane (R_f = 0.27) gave 2.70 g (6.3 mmol, 68%) of **125** as a light yellow oil.

^{1}H NMR ($CDCl_3$): δ = 0.28 (s, 9 H, $Si(C\mathbf{H}_3)_3$), 0.94 (t, ^3J = 7.4 Hz, 6 H, $NCH_2CH_2CH_2C\mathbf{H}_3$), 1.33 (six, ^3J = 7.4 Hz, 4 H, $NCH_2CH_2C\mathbf{H}_2CH_3$), 1.48-1.56 (m, 4 H, $NCH_2C\mathbf{H}_2CH_2CH_3$), 3.18-3.22 (m, 4 H, $NC\mathbf{H}_2CH_2CH_2CH_3$), 6.32 (dd, ^3J = 8.9 Hz, ^4J = 3.1 Hz, 1 H, 6-H), 6.75 (d, ^4J = 3.1 Hz, 1 H, 2-H), 7.51 (d, ^3J = 8.9 Hz, 1 H, 5-H)

^{13}C NMR ($CDCl_3$): δ = 0.0 (q), 14.0 (q), 20.3 (t), 29.2 (t), 50.6 (t), 82.5 (s), 96.8 (s), 107.6 (s), 114.3 (d), 116.0 (d), 129.4 (s), 138.7 (d), 147.8 (s)

IR (ATR): $\tilde{\nu}$ = 2958 cm^{-1} (s), 2927 (s), 2871 (m), 2857 (m), 2361 (s), 1583 (s), 1482 (m), 1464 (m), 1369 (m), 1249 (m), 1028 (m), 949 (s), 844 (vs), 620 (m), 586 (vs)

MS (GC-MS): *m/z* (%) = 427 (45) [M^+], 385 (20), 383 (100), 341 (49), 184 (42), 163 (54), 73 (18)

10.3.2 Synthesis of 4,5-diethynyl[2.2]paracyclophane

Exp. 13: 4-Bromo[2.2]paracyclophane (86)

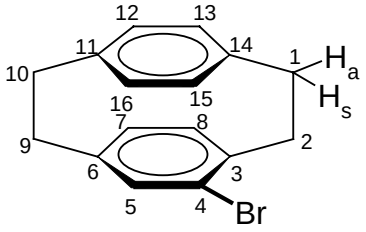

86

A 500 mL three-necked flask was equipped with reflux-condenser, dropping funnel and mechanical stirrer and wrapped with aluminum foil to exclude daylight. 8 mL of a solution of 1.8 mL (36.0 mmol) of Br_2 in 60 mL of abs. CCl_4 was added to 39 mg (0.7 mmol) of iron powder. The suspension was stirred for 40 min at room temp., diluted with 160 mL of anhydrous dichloromethane, and 7.25 g (34.8 mmol) of [2.2]paracyclophane (**36**) was added. After 1 h, the remaining solution of Br_2 in CCl_4 was added dropwise. The mixture was stirred for 5 h, washed with $NaHSO_3$ solution and the aqueous phase was extracted with dichloromethane. The organic phase was dried with Na_2SO_4. Evaporation of the solvent gave 9.87 g (24.4 mmol, 99%; 99%[45]) of **86** as a colorless solid (m.p. 133 °C; 134 °C[45]). Since the spectroscopic data are incomplete in the literature they are listed here.

^{1}H NMR ($CDCl_3$): δ = 2.81 (ddd, $^2J_{2a,2s}$ = 13.4 Hz, $^3J_{2a,1a}$ = 10.7 Hz, $^3J_{2a,2s}$ = 6.0 Hz, 1 H, 2-H*a*), 2.85-2.92 (m, 1 H, 9-H*s*), 2.97-3.12 (m, 4 H, 1-H, 9-H, 10-H), 3.19 (ddd, $^2J_{1s,1a}$ = 13.0 Hz, $^3J_{1s,2s}$ = 10.3 Hz, $^3J_{1s,2a}$ = 6.0 Hz, 1 H, 1-H*s*), 3.45 (ddd, $^2J_{2s,2a}$ = 13.4 Hz, $^3J_{2s,1s}$ = 10.3 Hz, $^3J_{2s,1a}$ = 2.2 Hz, 1 H, 2-H*s*), 6.42-6.47 (m, 3 H, 8-H, 13-H, 16-H), 6.49-6.51 (m, 2 H, 5-H, 7-H), 6.55 (dd, $^4J_{12,16}$ = 1.9 Hz, $^3J_{12,13}$ = 7.8 Hz, 1 H, 12-H), 7.16 (dd, $^4J_{15,13}$ = 1.9 Hz, $^3J_{15,16}$ = 7.8 Hz, 1 H, 15-H)

^{13}C NMR ($CDCl_3$): δ = 33.5 (t, C-1), 43.8 (t, C-9), 35.5 (t, C-10), 35.8 (t, C-2), 127.0 (s, C-4), 128.7 (d, C-15), 131.5 (d, C-7), 132.3 (d, C-16), 133 (d, C-12), 133.3 (d, C-13), 135.0 (d, C-8), 137.3 (d, C-5), 139.1 (s, C-11), 139.1 (s, C-3), 139.3 (s, C-14), 141.6 (s, C-6)

IR (KBr): $\tilde{\nu}$ = 3061 cm^{-1} (w), 3030 (w), 2985 (w), 2953 (m), 2926 (vs), 2888 (m), 2851 (s), 1893 (w), 1586 (m), 1542 (m), 1498 (s), 1477 (m), 1446 (m), 1431 (m), 1391 (s),

1321 (w), 1238 (w), 1204 (w), 1187 (m), 1163 (w), 1156 (w), 1124 (w), 1092 (w), 1037 (s), 942 (m), 906 (s), 841 (vs), 805 (m), 793 (m), 720 (s), 710 (vs), 691 (w), 669 (m), 641 (vs), 577 (m), 551 (vs), 474 (m)

UV (CH_3OH): λ_{max} (lg ε) = 206 nm (4.31), 226 (4.13), 228 (4.12), 254 (3.52), 290 (2.79)

MS (EI): *m/z* (%) = 286/288 (18/18) [M^+], 182/184 (12/12), 104 (100), 77 (12)

Exp. 14: 4-Hydroxy[2.2]paracyclophane (95)

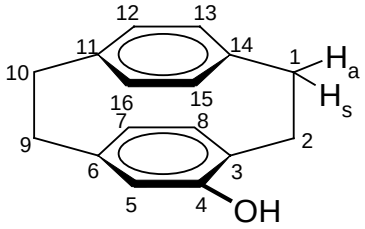

95

A solution of 3.85 g (13.4 mmol) of 4-bromo[2.2]paracyclophane (**86**) in 175 mL of anhydrous ether was cooled to 0 °C. 16.8 mL (26.8 mmol) of *n*-BuLi (1.6 M solution in hexane) was added with a syringe. The solution was stirred at room temp. for 45 min, cooled again to 0 °C and 3.0 mL (26.8 mmol) of trimethyl borate was added. After stirring for 1 h at room temp., 6.8 mL (3.4 mmol) of a 0.5 M aqueous NaOH solution and 6.7 mL of 30% H_2O_2 were added. The reaction mixture was diluted with ether, washed with water and dried with Na_2SO_4. Column chromatography on silica gel with dichloromethane gave 441 mg (2.1 mmol, 16%) of [2.2]paracyclophane (**36**, R_f = 0.95) in the first fraction and 2.50 g (11.0 mmol, 82%; 74%[46]) of 4-hydroxy[2.2]paracyclophane (**95**, R_f = 0.29) as a colorless solid (m.p. 227 °C; 225 °C[46]) in the second fraction.

^{1}H NMR ($CDCl_3$): δ = 2.60-3.35 (m, 8 H, 1-H, 2-H, 9-H, 10-H), 5.50 (d, $^4J_{5,7}$ = 1.5 Hz, 1 H, 5-H), 6.25 (dd, $^4J_{7,5}$ = 1.6 Hz, $^3J_{7,8}$ = 7.7 Hz, 1 H, 7-H), 6.37 (d, $^3J_{8,7}$ = 7.7 Hz, 1 H, 8-H), 6.38 (dd, $^4J_{12,16}$ = 1.9 Hz, $^3J_{12,13}$ = 7.8 Hz, 1 H, 12-H), 6.43 (dd, $^4J_{13,15}$ = 1.9 Hz, $^3J_{13,12}$ = 7.8 Hz, 1 H, 13-H), 6.54 (dd, $^4J_{16,12}$ = 1.9 Hz, $^3J_{16,15}$ = 7.8 Hz, 1 H, 16-H), 6.98 (dd, $^4J_{15,13}$ = 1.9 Hz, $^3J_{15,16}$ = 7.8 Hz, 1 H, 15-H)

^{13}C NMR ($CDCl_3$): δ = 30.5 (t, C-2), 33.3, 34.3, 34.8 (t, C-1, C-9, C-10), 122.0, 124.5, 124.9, 127.4, 1331.3, 132.2, 133.0 (d, C-5, C-6, C-7, C-8, C-12, C-13, C-15, C-16), 134.9, 138.3, 139.1, 141.4 (s, C-3, C-6, C-11, C-14), 153.1 (s, C-4)

IR (KBr): $\tilde{\nu}$ = 3600 - 3200 cm^{-1} (br), 3064 (w), 3031 (m), 3010 (m), 2987 (m), 2951 (m), 2925 (vs), 2890 (m), 2870 (m), 2851 (s), 1600 (m), 1565 (s), 1499 (m), 1436 (m), 1417 (vs), 1330 (m), 1321 (m), 1262 (m), 1216 (s), 1179 (m), 1162 (s), 1142 (vs), 1103 (m), 1087 (vs), 977 (m), 933 (m), 894 (m), 872 (m), 796 (m), 717 (vs), 658 (m), 590 (m), 561 (m), 515 (s), 495 (m), 465 (m)

UV (CH_3OH): λ_{max} (lg ε) = 206 nm (4.30), 226 (4.15), 228 (4.13), 256 (3.35), 292 (2.90), 312 (2.86)

MS (EI): *m/z* (%) = 224 (52) [M^+], 209 (6), 120 (100), 105 (13), 104 (41), 103 (11), 92 (17), 91 (25), 84 (6), 78 (11), 77 (7)

Exp. 15: *O*-(4-[2.2]paracyclophanyl) diethylcarbamate (96)

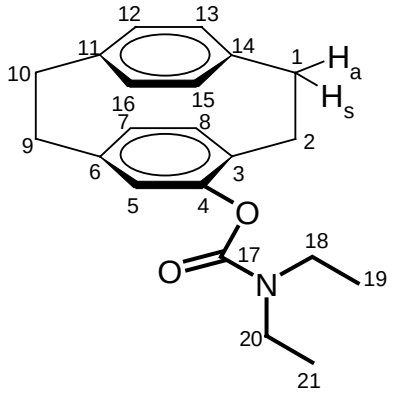

96

To a solution of 3.6 g (15.9 mmol) of 4-hydroxy[2.2]paracyclophane (**95**) in 240 mL of dry toluene, 3.9 g (31.8 mmol) of 4-(dimethylamino)pyridine (DMAP) and 4.3 g (31.8 mmol) of diethylcarbamoyl chloride were added under nitrogen. The mixture was heated to reflux for 12 h and then cooled to room temp. 250 mL of water was added and the reaction mixture was extracted several times with dichloromethane. The combined organic phases were dried with Na_2SO_4 and the solvents were removed *in vacuo*. Purification by column chromatography on silica gel with dichloromethane (R_f = 0.4) yielded 5.12 g (15.8 mmol, 99%; 97%[43]) of **96** as a colorless oil which slowly crystallized (m.p. 152 °C; 152 °C[43]).

^{1}H NMR ($CDCl_3$): δ = 1.18-1.21 (m, 3 H, 21-H), 1.40-1.43 (m, 3 H, 19-H), 2.67-3.25 (m, 8 H, 1-H, 2-H, 9-H, 10-H), 3.37-3.39 (m, 2 H, 20-H), 3.59-3.61 (m, 2 H, 18-H), 6.03 (d, $^{4}J_{5,7}$ = 1.7 Hz, 1 H, 5-H), 6.22-6.48 (m, 4 H, 7-H, 8-H, 13-H, 16-H), 6.54 (dd, $^{3}J_{12,13}$ = 7.8 Hz, $^{4}J_{12,16}$ = 1.9 Hz, 1 H, 12-H), 6.84 (dd, $^{3}J_{15,16}$ = 7.8 Hz, $^{4}J_{15,13}$ = 1.9 Hz, 1 H, 15-H)

^{13}C NMR ($CDCl_3$): δ = 13.4 (q, C-21), 14.5 (q, C-19), 31.6, 34.5, 34.8, 35.3 (t, C-1, C-2, C-9, C-10), 41.9 (t, C-20), 42.1 (t, C-18), 128.5 (d), 129.3 (d, C-15), 129.5 (d), 131.0 (d), 132.1 (d), 133.0 (d, C-12), 133.4 (d), 135.1 (d), 139.2 (s), 139.4 (s), 141.3 (s, C-6), 149.5 (s, C-4), 153.6 (s, C-17)

IR (KBr): $\tilde{\nu}$ = 2986 cm^{-1} (w), 2954 (w), 2927 (m), 2891 (w), 2852 (w), 1713 (vs), 1500 (w), 1471 (m), 1459 (m), 1435 (w), 1423 (m), 1379 (m), 1365 (w), 1271 (m), 1239 (s), 1224 (m), 1161 (s), 1156 (s), 1139 (m), 1107 (w), 1099 (m), 1090 (m), 985 (w), 981 (w), 796 (w), 754 (w), 716 (m), 653 (w)

UV (CH_3OH): λ_{max} (lg ε) = 204 nm (4.29), 224 (4.28), 250 (3.45), 286 (2.77), 296 (2.66)

MS (EI): *m/z* (%) = 323 (78) [M^+], 219 (11), 104 (11) [$C_8H_8^+$], 100 (100) [$CON(Et)_2^+$], 72 (28)

Exp. 16: 5-Formyl-4-hydroxy[2.2]paracyclophane (FHPC) (97)

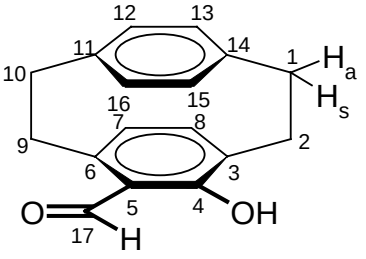

97

A solution of 6.47 g (20.0 mmol) of *O*-(4-[2.2]paracyclophanyl) diethylcarbamate (**96**) in 500 mL of anhydrous THF was cooled to –78 °C. 3.6 mL (24.0 mmol) of freshly distilled TMEDA was added followed by 18.5 mL (24.0 mmol) of *sec*-BuLi (1.3 M solution in pentane). The reaction mixture was stirred at –78 °C for 1 h and 4.6 mL (60.0 mmol) of dry dimethylformamide was added. The product mixture was set aside at room temp. overnight, hydrolyzed with 200 mL of 10% HCl and extracted with

dichloromethane. The organic phases were dried with Na_2SO_4. Column chromatography on silica gel with dichloromethane (R_f = 0.63) gave 2.96 g (12.0 mmol, 59%; 64%[43]) of **97** as a yellow solid (m.p. 193 °C; 193 °C [43]). The fully assigned NMR spectroscopic data follow:

^{1}H NMR ($CDCl_3$): δ = 2.58 (ddd, $^2J_{2s,2a}$ = 13.3 Hz, $^3J_{2s,1s}$ = 10.6 Hz, $^3J_{2s,1a}$ = 5.2 Hz, 1 H, 2-H*s*), 2.82 (ddd, $^2J_{10s,10a}$ = 13.2 Hz, $^3J_{10s,9s}$ = 10.5 Hz, $^3J_{10s,9a}$ = 6.4 Hz, 1 H, 10-H*s*), 2.94 (ddd, $^2J_{9a,9s}$ = 13.8 Hz, $^3J_{9a,10a}$ = 10.4 Hz, $^3J_{9a,10s}$ = 6.4 Hz, 1 H, 9-H*a*), 3.03 (ddd, $^2J_{1s,1a}$ = 13.1 Hz, $^3J_{1s,2s}$ = 10.6 Hz, $^3J_{1s,2a}$ = 2.9 Hz, 1 H, 1-H*s*), 3.15 (ddd, $^2J_{1a,1s}$ = 13.1 Hz, $^3J_{1a,2a}$ = 10.2 Hz, $^3J_{1a,2s}$ = 5.2 Hz, 1 H, 1-H*a*), 3.27-3.33 (m, 1 H, 10-H*a*), 3.44 (ddd, $^2J_{2a,2s}$ = 13.3 Hz, $^3J_{2a,1a}$ = 10.2 Hz, $^3J_{2a,1s}$ = 2.9 Hz, 1 H, 2-H*a*), 3.53 (ddd, $^2J_{9s,9a}$ = 13.8 Hz, $^3J_{9s,10s}$ = 10.5 Hz, $^3J_{9s,10a}$ = 1.6 Hz, 1 H, 9-H*s*), 6.26 (dd, $^3J_{12,13}$ = 7.9 Hz, $^4J_{12,16}$ = 2.2 Hz, 1 H, 12-H), 6.28 (d, $^3J_{7,8}$ = 7.7 Hz, 1 H, 7-H), 6.40 (dd, $^3J_{13,12}$ = 7.9 Hz, $^4J_{13,15}$ = 1.9 Hz, 1 H, 13-H), 6.63 (dd, $^3J_{16,15}$ = 7.8 Hz, $^4J_{16,12}$ = 2.2 Hz, 1 H, 16-H), 6.63 (d, $^3J_{8,7}$ = 7.7 Hz, 1 H, 8-H), 6.91 (dd, $^3J_{15,16}$ = 7.8 Hz, $^4J_{15,13}$ = 1.9 Hz, 1 H, 15-H), 9.78 (s, 1 H, OH), 11.94 (s, 1 H, C(O)H)

^{13}C NMR ($CDCl_3$): δ = 29.3, 33.8, 33.7, 35.7 (t, C-1, C-2, C-9, C-10), 121.8 (s), 125.6 (s), 127.1 (d), 128.3 (s), 132.1 (d), 132.3 (d), 133.7 (d), 137.5 (s), 140.2 (s), 142.0 (d), 145.5 (s), 162.1 (s), 193.4 (s, C=O)

IR (KBr): $\tilde{\nu}$ = 3028 cm^{-1} (w), 3010 (w), 2962 (m), 2952 (m), 2928 (m), 2893 (m), 2877 (m), 2854 (m), 2778 (w), 2773 (m), 1627 (vs), 1606 (s), 1594 (s), 1570 (m), 1533 (m), 1500 (m), 1432 (m), 1417 (vs), 1399 (s), 1341 (m), 1315 (s), 1281 (vs), 1222 (s), 1155 (m), 1100 (m), 1022 (m), 1002 (m), 969 (m), 942 (m), 874 (m), 800 (m), 767 (s), 721 (s), 704 (m), 687 (m), 664 (m), 602 (m), 587 (m), 549 (m), 528 (m), 514 (m), 481 (m), 460 (m)

UV (CH_3OH): λ_{max} (lg ε) = 210 nm (4.35), 212 (4.35), 246 (3.95), 252 (3.87), 290 (3.50), 300 (3.61), 326 (3.32), 386 (3.25)

MS (EI): *m/z* (%) = 252 (56) [M^+], 148 (19), 147 (23), 120 (17), 104 (100), 91 (19), 78 (12)

Exp. 17: 5-Formyl-4-trifluoromethylsulfonyloxy[2.2]paracyclophane (98)

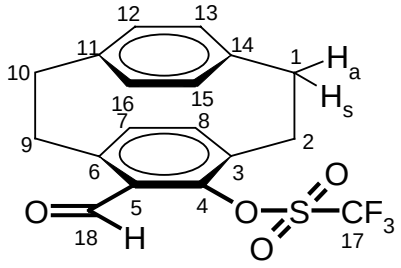

98

A solution of 1.77 g (7.0 mmol) of FHPC (**97**) and 2.50 g (7.0 mmol) of *N*,*N*-bis(trifluoromethylsulfonyl)aniline in 50 mL of dry triethylamine was heated to reflux for 24 h. The solvent was removed *in vacuo* and the residue purified by column chromatography on silica gel with 50% dichloromethane in pentane (R_f = 0.32) yielding 2.12 g (5.5 mmol, 79%) of **98** as a colorless solid (m.p. 72 °C). An analytically pure sample was obtained by sublimation (85 °C, 10^{-2} mbar).

^{1}H NMR ($CDCl_3$): δ = 2.89 (AGNX, $^{2}J_{9a,9s}$ = -13.2 Hz, $^{3}J_{9a,10a}$ = 10.3 Hz, $^{3}J_{9a,10s}$ = 6.7 Hz, 1 H, 9-H*a*), 2.93 (AGNX, $^{2}J_{2a,2s}$ = -14.4 Hz, $^{3}J_{2a,1a}$ = 10.4 Hz, $^{3}J_{2a,1s}$ = 4.8 Hz, 1 H, 2-H*a*), 3.06 (AGNX, $^{2}J_{10s,10a}$ = -13.1 Hz, $^{3}J_{10s,9s}$ = 10.3 Hz, $^{3}J_{10s,9a}$= 6.7 Hz, 1 H, 10-H*s*), 3.09 (AGNX, $^{2}J_{1a,1s}$ = -13.4 Hz, $^{3}J_{1a,2a}$ = 10.4 Hz, $^{3}J_{1a,2s}$ = 3.8 Hz, 1 H, 1-H*a*), 3.21 (AGNX, $^{2}J_{1s,1a}$ = -13.4 Hz, $^{3}J_{1s,2s}$ = 10.2 Hz, $^{3}J_{1s,2a}$ = 4.8 Hz, 1 H, 1-H*s*), 3.26 (AGNX, $^{2}J_{10s,10a}$ = -13.1 Hz, $^{3}J_{10s,9s}$ = 10.3 Hz, $^{3}J_{10s,9a}$ = 1.5 Hz, 1 H, 10-H*s*), 3.46 (AGNX, $^{2}J_{2s,2a}$ = -14.4 Hz, $^{3}J_{2s,1s}$ = 10.2 Hz, $^{3}J_{2s,1a}$ = 3.8 Hz, 1 H, 2-H*s*), 4.05 (AGNX, $^{2}J_{9s,9a}$ = -13.2 Hz, $^{3}J_{9s,10s}$ = 10.3 Hz, $^{3}J_{9s,10a}$ = 6.7 Hz, 1 H, 9-H*s*), 6.40 (dd, $^{3}J_{16,15}$ = 7.9 Hz, $^{4}J_{16,12}$ = 1.9 Hz, 1 H, 16-H), 6.51 (dd, $^{3}J_{13,12}$ = 7.9 Hz, $^{4}J_{13,15}$ = 1.9 Hz, 1 H, 13-H), 6.64 (dd, $^{3}J_{12,13}$ = 7.9 Hz, $^{4}J_{12,16}$ = 1.9 Hz, 1 H, 12-H), 6.71 (d, $^{3}J_{7,8}$ = 8.0 Hz, 1 H, 7-H), 6.78 (dd, $^{3}J_{15,16}$ = 7.9 Hz, $^{4}J_{15,13}$ = 1.9 Hz, 1 H, 15-H), 6.81 (d, $^{4}J_{8,7}$ = 8.0 Hz, 1 H, 8-H), 10.10 (s, 1 H, C(O)H)

^{13}C NMR ($CDCl_3$): δ = 31.2 (t, C-2), 33.9, 33.9, 34.1 (t, C-1, C-9, C-10), 118.6 (q, $^{1}J_{CF}$ = 321 Hz, CF_3), 129.3 (d, C-15), 129.6 (s, C-5), 131.4 (d, C-16), 132.9 (d, C-12), 133.8 (d, C-13), 133.8 (s, C-3), 135.7 (d, C-7), 139.2 (s, C-14), 139.5 (s, C-11), 140.2 (d, C-8), 145.9 (s, C-6), 148.4 (s, C-4), 188.6 (d, CO)

^{19}F NMR ($CDCl_3$): δ = -73.59 (s, CF_3)

IR (KBr): $\tilde{\nu}$ = 3072 cm^{-1} (w), 3049 (w), 3017 (w), 2978 (w), 2956 (m), 2933 (m), 2909 (w), 2860 (w), 2798 (w), 1691 (vs), 1596 (m), 1542 (m), 1502 (w), 1474 (m), 1452 (w), 1424 (s), 1399 (s), 1223 (vs), 1208 (vs), 1180 (m), 1141 (vs), 1100 (m), 1004 (m), 947 (m), 909 (s), 883 (s), 844 (m), 830 (m), 810 (m), 801 (m), 786 (m), 762 (m), 745 (w), 719 (m), 659 (m), 639 (m), 622 (m), 604 (m), 585 (m), 513 (m)

UV (CH_3OH): λ_{max} (lg ε) = 208 nm (4.52), 292 (3.50), 220 (4.34), 234 (3.98), 248 (3.85), 260 (3.50), 276 (3.34), 310 (3.33)

MS (EI): *m/z* (%) = 384 (56) [M^+], 251 (41) [M^+ - SO_2CF_3], 233 (13) [251 - H_2O], 160 (14), 147 (59) [$C_9H_7O_2^+$], 104 (100) [$C_8H_8^+$], 91 (13) [$C_7H_7^+$], 78 (13) [$C_6H_6^+$]

$C_{18}H_{15}F_3O_4S$ (384.4) calcd. C 56.25, H 3.93, F 14.83, S 8.34; found C 56.08, H 3.78, S 8.49

Exp. 18: 5-Formyl-4-(trimethylsilyl)ethynyl[2.2]paracyclophane (99)

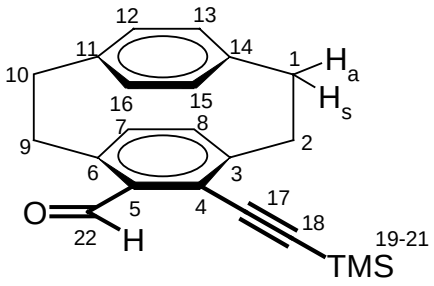

99

Method A:

In an ampoule, a solution of 384 mg (1 mmol) of **98**, 0.7 mL (5 mmol) of TMSA and 20 mg (0.02 mmol) of triphenylphosphinepalladium(II)-chloride in 2.5 mL of triethylamine and 7.5 mL of DMF was degassed by several freeze-pump-thaw cycles. The ampoule was sealed under vacuum and heated for 2 d at 130 °C. The solvents were removed under reduced pressure and the residue purified by column chromatography on silica gel using 50% dichloromethane in pentane to give 20 mg (0.06 mmol, 6%) of 2-trimethylsilyl-[2,2](4,7)indenonoparacyclophane (**100**) (R_f = 0.32) as a yellow solid and 110 mg (0.33 mmol, 33%) (R_f = 0.30) of **99**.

Method B:

384 mg (1 mmol) of **98** was subjected to general procedure C at 80 °C for 36 h using 0.56 mL (4 mmol) of TMSA, 116 mg (0.1 mmol) of $Pd(PPh_3)_4$, 19 mg (0.1 mmol) of

CuI, 10 mL of diisopropylamine and 10 mL of THF. Column chromatography on silica gel with 20% dichloromethane in pentane (R_f = 0.12) gave 262 mg (0.79 mmol, 79%) of **99** as a colorless solid (m.p. 81 °C).

5-Formyl-4-(trimethylsilyl)ethynyl[2.2]paracyclophane (99):

^{1}H NMR ($CDCl_3$): δ = 0.34 (s, 9 H, Si(C**H**$_3$)$_3$), 2.81 (AMNX, $^2J_{9a,9s}$ = -12.8 Hz, $^3J_{9a,10a}$ = 10.3 Hz, $^3J_{9a,10s}$ = 6.4 Hz, 1 H, 9-H*a*), 2.90 (AMNX, $^2J_{2a,2s}$ = -13.3 Hz, $^3J_{2a,1a}$ = 10.8 Hz, $^3J_{2a,1s}$ = 4.6 Hz, 1 H, 2-H*a*), 3.07 (AMNX, $^2J_{1a,1s}$ = -13.1 Hz, $^3J_{1a,2a}$ = 10.8 Hz, $^3J_{1a,2s}$ = 3.2 Hz, 1 H, 1-H*a*), 3.11 (AMNX, $^2J_{10s,10a}$ = -13.0 Hz, $^3J_{10s,9s}$ = 10.3 Hz, $^3J_{10s,9a}$ = 6.4 Hz, 1 H, 10-H*s*), 3.17 (AMNX, $^2J_{10a,10s}$ = -13.0 Hz, $^3J_{10a,9a}$ = 10.3 Hz, $^3J_{10a,9s}$ = 1.7 Hz, 1 H, 10-H*a*), 3.22 (AMNX, $^2J_{1s,1a}$ = -13.1 Hz, $^3J_{1s,2s}$ = 10.6 Hz, $^3J_{1s,2a}$ = 4.6 Hz, 1 H, 1-H*s*), 3.65 (AMNX, $^2J_{2s,2a}$ = -13.3 Hz, $^3J_{2s,1s}$ = 10.6 Hz, $^3J_{2s,1a}$ = 3.2 Hz, 1 H, 2-H*s*), 4.14 (AMNX, $^2J_{9s,9a}$ = -12.8 Hz, $^3J_{9s,10s}$ = 10.3 Hz, $^3J_{9s,10a}$ = 1.7 Hz, 1 H, 9-H*s*), 6.36 (dd, $^3J_{16,15}$ = 7.8 Hz, $^4J_{16,12}$ = 1.9 Hz, 1 H, 16-H), 6.46 (dd, $^3J_{13,12}$ = 7.9 Hz, $^4J_{13,15}$ = 1.9 Hz, 1 H, 13-H), 6.56 (dd, $^3J_{12,13}$ = 7.9 Hz, $^4J_{12,16}$ = 1.9 Hz, 1 H, 12-H), 6.57 (d, $^3J_{7,8}$ = 7.8 Hz, 1 H, 7-H), 6.67 (d, $^3J_{8,7}$ = 7.8 Hz, 1 H, 8-H), 6.85 (dd, $^3J_{15,16}$ = 7.8 Hz, $^4J_{15,13}$ = 1.9 Hz, 1 H, 15-H), 10.35 (s, 1 H, C(O)**H**)

^{13}C NMR ($CDCl_3$): δ = -0.1 (q, Si(**C**H$_3$)$_3$), 33.6 (t, C-2), 33.7 (t, C-1), 34.0 (t, C-10), 34.5 (t, C-9), 100.2 (s, **C**≡C-Si), 107.3 (s, C≡**C**-Si), 129.3 (d, C-15), 129.7 (s, C-4), 131.4 (d, C-16), 132.6 (d, C-12), 133.5 (d, C-13), 135.4 (d, C-7), 136.6 (s, C-5), 137.5 (d, C-8), 139.1 (s, C-14), 139.9 (s, C-11), 142.6 (s, C-6), 144.3 (s, C-3), 194.1 (d, C=O)

IR (KBr): $\tilde{\nu}$ = 3067 cm^{-1} (w), 3036 (m), 3010 (m), 2959 (m), 2930 (s), 2891 (m), 2854 (m), 2817 (m), 2795 (w), 2790 (w), 2779 (w), 2756 (m), 2147 (m), 1688 (vs), 1656 (m), 1649 (m), 1566 (m),1549 (m), 1500 (m), 1461 (m), 1448 (m), 1436 (m), 1411 (m), 1386 (m), 1249 (s), 1214 (m), 1029 (m), 942 (m), 908 (m), 871 (s), 846 (vs), 800 (m), 760 (s), 743 (m), 718 (m), 699 (m), 656 (m), 589 (m), 515 (m)

UV (CH_3OH): λ_{max} (lg ε) = 212 nm (4.42), 260 (4.18), 368 (3.29), 218 (4.29), 230 (4.14), 252 (4.12), 256 (4.18), 268 (4.04), 278 (3.89)

MS (EI): *m/z* (%) = 332 (100) [M^+], 317 (10), 228 (38) [M^+-C_8H_8], 227 (68) [M^+-C_8H_8-H], 213 (28), 198 (14), 104 (87) [$C_8H_8^+$], 78 (12), 73 (35) [$SiMe_3^+$]

$C_{22}H_{24}OSi$ (332.52) calcd. C 79.47, H 7.27; found C 79.20, H 7.19

2-Trimethylsilyl-[2.2](4,7)indenonoparacyclophane (100):

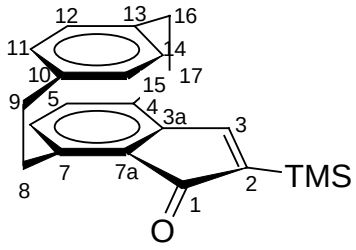

100

^{1}H NMR ($CDCl_3$): δ = 0.3 (s, Si(C**H**$_3$)$_3$), 2.68 (ddd, $^{2}J_{8a,8s}$ = 12.8 Hz, $^{3}J_{8a,9a}$ = 9.8 Hz, $^{3}J_{8a,9s}$ = 2.7 Hz ,1 H, 8-H*a*), 2.87 (ddd, $^{2}J_{17a,17s}$ = 13.2 Hz, $^{3}J_{17a,16a}$ = 10.4 Hz, $^{3}J_{17a,16s}$ = 4.3 Hz, 1 H, 17-H*a*), 2.97-3.13 (m, 4 H, 9-H*s*, 9-H*a*, 16-H*s*, 16-H*a*), 3.19 (ddd, $^{2}J_{17s,17a}$ = 13.2 Hz, $^{3}J_{17s,16s}$ = 10.0 Hz, $^{3}J_{17s,16a}$ = 3.3 Hz, 1 H, 17-H*s*), 3.99 (ddd, $^{2}J_{8s,8a}$ = 12.8 Hz, $^{3}J_{8s,9s}$ = 9.2 Hz, $^{3}J_{8s,9a}$ = 3.8 Hz, 1 H, 8-H*s*), 6.33 (AB, $^{3}J_{6,5}$ = 8.1 Hz, 1 H, 6-H), 6.34 (dd, $^{3}J_{15,14}$ = 7.7 Hz, $^{4}J_{15,11}$ = 1.9 Hz,1 H, 15-H), 6.36 (AB, $^{3}J_{5,6}$ = 8.1 Hz, 1 H, 5-H), 6.56 (dd, $^{3}J_{12,11}$ = 7.8 Hz, $^{4}J_{12,14}$ = 1.9 Hz, 1 H, 12-H), 6.60 (dd, $^{3}J_{14,15}$ = 7.7 Hz, $^{4}J_{14,12}$ = 1.9 Hz, 1 H, 14-H), 6.64 (dd, $^{3}J_{11,12}$ = 7.8 Hz, $^{4}J_{11,15}$ = 1.9 Hz, 1 H, 11-H)

^{13}C NMR ($CDCl_3$): δ = -1.4 (q, Si(**C**H$_3$)$_3$), 30.7 (t, C-8), 31.1 (t, C-17), 34.1 (t, C-9), 35.2 (t, C-16), 129.2 (d, C-15), 129.4 (d, C-14), 132.7 (s, C-7a), 133.1 (d, C-11), 133.6 (d, C-12), 134.7 (s, C-4), 136.2 (d, C-6), 138.4 (d, C-5), 138.9 (d, C-13), 139.3 (s, C-2), 139.8 (s, C-10), 141.0 (s, C-7), 146.5 (s, C-3a), 155.2 (d, C-3), 203.1 (s, C-1)

IR (ATR): $\tilde{\nu}$ = 3034 (w), 3009 (w), 2952 (m), 2929 (m), 2897 (m), 2855 (m), 1682 (s), 1571 (m), 1537 (m), 1468 (m), 1453 (m), 1436 (m), 1410 (m), 1248 (m), 1211 (m), 1182 (m), 1159 (m), 1100 (m), 1080 (m), 941 (m), 838 (vs), 795 (m), 758 (m), 717 (m), 700 (m), 645 (m), 623 (m), 579 (m)

UV (CH_2Cl_2): λ_{max} (lg ε) = 229 nm (4.11), 267 (4.10), 345 (3.01), 417 (3.05)

MS (EI): *m/z* (%) = 332 (92) [M^+], 317 (10), 229 (23), 228 (100) [M^+-C_8H_8], 227 (15) [M^+-C_8H_8-H], 213 (56), 185 (28), 104 (46) [$C_8H_8^+$]

HR MS ($C_{22}H_{24}OSi$) calcd. 332.1596; found 332.1591 ± 1.35 ppm (Δ_{rel} = .1.5 ppm)

Exp. 19: 4,5-Diethynyl[2.2]paracyclophane (56)

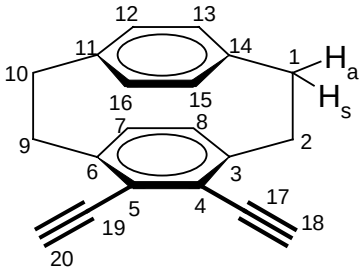

56

Method A:

To a solution of 166 mg (0.5 mmol) of **99** in 5 mL of dry methanol, 173 mg (0.9 mmol) of dimethyl-1-diazo-2-oxopropylphosphonate (**67**) and 295 mg (1.25 mmol) of Cs_2CO_3 were added at 0 °C. After 30 min, the cooling bath was removed and the reaction mixture was stirred at room temp for 16 h. Dichloromethane was added and the mixture was washed with brine. The organic phase was dried with Na_2SO_4 and the solvent evaporated. Column chromatography on silica gel with 50% dichloromethane in pentane (R_f = 0.67) gave 52 mg (0.2 mmol, 41%) of 4,5-diethynyl[2.2]paracyclophane **56** as a colorless solid (m.p. 98 °C).

Method B:

240 mg (0.55 mmol) of bromomethyltriphenylphosphonium bromide was dissolved in 7 mL of anhydrous THF and the solution cooled to -78 °C. 146 mg (1.3 mmol) of potassium-*tert*-butoxide was added. After dropwise addition of a solution of 166 mg (0.5 mmol) of **99** in 13 mL of anhydrous THF, the cooling bath was removed and the mixture was stirred for 90 min at room temp. 112 mg (1 mmol) of potassium-*tert*-butoxide was added, the mixture was heated to reflux for 3 h and stirred overnight at room temp. The reaction mixture was hydrolyzed and extracted with dichloromethane. The organic layers were dried with Na_2SO_4 and the solvents were evaporated *in vacuo*. Column chromatography on silica gel with 50% dichloromethane in pentane (R_f = 0.67) gave 56 mg (0.22 mmol, 40%) of **56**.

^{1}H NMR ($CDCl_3$): δ = 2.80 (AGNX, $^2J_{2a,2s}$ = -13.2 Hz, $^3J_{2a,1a}$ = 10.8 Hz, $^3J_{2a,1s}$ = 4.7 Hz, 2 H, 2-H*a*, 9-H*a*), 2.96 (AGNX, $^2J_{1a,1s}$ = -13.1 Hz, $^3J_{1a,2a}$ = 10.8 Hz, $^3J_{1a,2s}$ = 3.2 Hz, 2 H, 1-H*a*, 10-H*a*), 3.14 (AGNX, $^2J_{1s,1a}$ = -13.1 Hz, $^3J_{1s,2s}$= 10.6 Hz, $^3J_{1s,2a}$ = 4.7 Hz, 2 H, 1-H*s*, 10-H*s*), 3.46 (s, 2 H, C≡C**H**), 3.48 (AGNX, $^2J_{2s,2a}$ = -13.2 Hz, $^3J_{2s,1s}$ = 10.6 Hz,

$^3J_{2s,1a}$ = 3.2 Hz, 2 H, 2-H*s*, 9-H*s*), 6.45 (m, 4 H, 7-H, 8-H, 12-H, 13-H), 6.81-6.82 (m, 2 H, 15-H, 16-H)

^{13}C NMR ($CDCl_3$): δ = 33.9 (t, C-1, C-10), 34.1 (t, C-2, C-9), 82.0 (s, **C**≡C-H), 84.4 (d, C≡**C**-H), 127.1 (s, C-4, C-5), 129.6 (d, C-15, C-16), 132.9 (d, C-12, C-13), 133.4 (d, C-7, C-8), 139.2 (s, C-11, C-14), 143.5 (s, C-3, C-6)

IR (KBr): $\tilde{\nu}$ = 3293 cm^{-1} (vs), 3275 (vs), 3049 (w), 3031 (w), 3010 (w), 2964 (m), 2935 (s), 2889 (m), 2853 (m), 1500 (s), 1458 (m), 1449 (m), 1411 (s), 1261 (m), 1255 (m), 1249 (m), 1243 (m), 1237 (m), 1230 (m), 1224 (m), 1220 (m), 1214 (m), 1208 (m), 1099 (m), 943 (m), 909 (m), 891 (m), 867 (m), 795 (m), 749 (m), 721 (s), 684 (s), 669 (s), 637 (vs), 618 (vs); 607 (s), 584 (s), 518 (s)

UV (CH_3OH): λ_{max} (lg ε) = 216 nm (4.71), 246 (4.10), 220 (4.31), 228 (4.15), 242 (4.07), 258 (3.84), 266 (3.74), 288 (3.49), 348 (2.82)

MS (EI): *m/z* (%) = 257 (20) [$^{12}C_{19}H_{16}{}^{13}C^+$], 256 (92) [$M^+$], 255 (28) [$M^+$-H], 241 (26) [$M^+$-$CH_3$], 152 (83) [$M^+$-$C_8H_8$], 151 (38) [$M^+$-$C_8H_8$-H], 104 (100) [$C_8H_8{}^+$]

HR MS ($C_{20}H_{15}$) calcd. 255.1174 [M^+-H]; found 255.1173 ± 2.2 ppm (Δ_{rel} = 0.39 ppm)

Exp. 20: 5-(2,2-Dibromo-1-ethenyl)-4-(trimethylsilyl)ethynyl[2.2]paracyclophane (106)

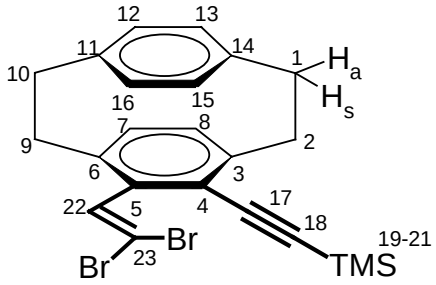

106

A mixture of 663 mg (2 mmol) of CBr_4, 525 mg (2 mmol) of PPh_3 and 131 mg (2 mmol) of zinc powder was stirred in 20 mL of abs. dichloromethane overnight under argon. To the purple suspension was added 166 mg (0.5 mmol) of **99** and the mixture was stirred for 2 d at room temp and subsequently heated for 3 d to reflux. The mixture was filtered through a plug of silica gel eluting with dichloromethane. Purification by

column chromatography using pentane gave 60 mg (0.12 mmol, 25%) of **106** (R_f = 0.1) as light yellow oil and 116 mg (0.35 mmol, 70%) of starting material.

^{1}H NMR ($CDCl_3$): δ = 0.34 (s, 9 H, Si(C**H**$_3$)$_3$), 2.81 (ddd, $^2J_{2a,2s}$ = 13.0, $^3J_{2a,1a}$ = 10.4 Hz, $^3J_{2a,1s}$ = 5.5 Hz, 1 H, 2-H*a*), 2.87-2.93 (m, 1 H, 9-H*a*), 2.96-3.03 (m, 2 H, 10-H*s*, 10-H*a*), 3.05 (ddd, $^2J_{1a,1s}$ = 13.0 Hz, $^3J_{1a,2a}$ = 10.4 Hz, $^3J_{1a,2s}$ = 2.9 Hz, 1-H*a*), 3.14 (ddd, $^2J_{1s,1a}$ = 13.0 Hz, $^3J_{1s,2s}$ = 10.2 Hz, $^3J_{1s,2a}$ = 5.5 Hz, 1 H, 1-H*s*), 3.19-3.26 (m, 1 H, 9-H*s*), 3.52 (ddd, $^2J_{2s,2a}$ = 13.0 Hz, $^3J_{2s,1s}$ = 10.2 Hz, $^3J_{2s,1a}$ = 2.9 Hz, 1 H, 2-H*s*), 6.49-6.56 (m, 5 H, 7-H, 8-H, 12-H, 13-H, 16-H), 6.81-6.83 (m, 1 H, 15-H), 7.38 (s, 1 H, C(**H**)=CBr_2)

^{13}C NMR ($CDCl_3$): δ = 0.1 (q, Si(**C**H$_3$)$_3$), 33.7 (t, C-1), 34.0 (t, C-9), 34.1 (t, C-2), 34.7 (t, C-10), 92.7 (s, C(H)=**C**Br_2), 103.2 (s, **C**≡C-TMS), 104.1 (s, C≡**C**-TMS), 124.2 (s, C-4), 128.9 (d, C-15), 129.0, 133.0, 133.0, 133.4, 134.3 (d, C-7, C-8, C-12, C-13, C-16), 137.4 (d, **C**(H)=CBr_2), 138.6 (s, C-6), 139.0, 139.3, 139.4, 142.7 (s, C-3, C-5, C-11, C-14)

IR (ATR): $\tilde{\nu}$ = 3009 (m), 2957 (m), 2854 (m), 2145 (m), 1727 (w), 1599 (w), 1500 (w), 1456 (w), 1409 (w), 1249 (m), 1026 (w), 922 (w), 841 (vs), 759 (m), 744 (m), 719 (w), 659 (w), 626 (w), 595 (w)

UV (CH_2Cl_2): λ_{max} (lg ε) = 228 nm (4.25), 253 (4.15)

MS (EI): *m/z* (%) = 486/488/490 (18/41/21) [M^+], 382/384/386 (4/7/4) [M^+-C_8H_8], 303/305 (96/100) [M^+-C_8H_8-Br], 224 (74) [M^+-C_8H_8-2 Br], 165 (77), 104 (59) [$C_8H_8^+$], 73 (91) [$SiMe_3^+$]

HR MS ($C_{23}H_{24}Br_2Si$) calcd. 486.0014; found 486.0035 ± 0.7 ppm (Δ_{rel} = 4.3 ppm)

Exp. 21: 5-Ethynyl-4-(trimethylsilyl)ethynyl[2.2]paracyclophane (107)

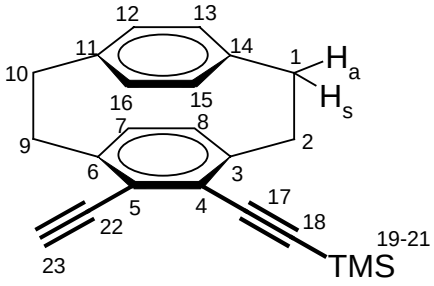

107

To a solution of 78 mg (0.16 mmol) of **106** in 4 mL of anhydrous THF cooled to -78 °C was added a freshly prepared LDA solution [0.09 mL (0.64 mmol) of *i*-Pr_2NH, 0.4 mL (0.64 mmol) of *n*-BuLi (1.6 M solution in hexane), 1.5 mL of THF]. After 15 min, the reaction was quenched with sat. NH_4Cl solution and the mixture was warmed to room temp. The mixture was diluted with ether, washed with water and the organic phase was dried with Na_2SO_4. Purification by column chromatography on silica gel with 20% dichloromethane in pentane gave 59 mg (0.12 mmol, 75%) of starting material (R_f = 0.22) and 11 mg (0.033 mmol, 21%) of **107** (R_f = 0.20).

^{1}H NMR ($CDCl_3$): δ = 0.33 (s, 9 H, Si(C**H**$_3$)$_3$), 2.78-2.88 (m, 2 H, 2-H*a*, 9-H*a*), 2.98-3.07 (m, 2 H, 1-H*a*, 10-H*a*), 3.15-3.24 (m, 2 H, 1-H*s*, 10-H*s*), 3.48 (s, 1 H, C≡C-**H**), 3.51-3.58 (m, 2 H, 2-H*s*, 10-H*s*), 6.50 (AB, $^3J_{7,8}$ = 8.3 Hz, 2 H, 7-H, 8-H), 6.50-6.51 (m, 2 H, 12-H, 13-H), 6.87-6.89 (m, 2 H, 15-H, 16-H)

^{13}C NMR ($CDCl_3$): δ = 0.1 (q, Si(**C**H$_3$)$_3$), 33.8, 33.9, 34.1, 34.4 (t, C-1, C-2, C-9, C-10), 82.2 (s, **C**≡C-H), 84.4 (d, C≡**C**-H), 102.4 (s, C≡C-TMS), 103.7 (s, C≡C-TMS), 127.0, 128.4 (s, C-4, C-5), 129.4, 129.5 (d, C-15, C-16), 132.9, 132.9, 133.0, 133.3 (d, C-7, C-8, C-11, C-12), 139.2, 139.2 (s, C-11, C-14), 143.1, 143.2 (s, C-3, C-6)

IR (ATR): $\tilde{\nu}$ = 3262 (m), 3035 (w), 3008 (m), 2956 (m), 2927 (m), 2894 (m), 2149 (m), 1499 (w), 1460 (w), 1405 (m), 1249 (m), 1015 (m), 916 (m), 839 (vs), 795 (m), 719 (m), 695 (m), 674 (m), 642 (m), 614 (m), 582 (m)

UV (CH_2Cl_2): λ_{max} (lg ε) = 228 nm (4.29), 252 (4.26), 290 (3.81), 353 (3.09)

MS (EI): *m/z* (%) = 328/329 (100/28) [M^+], 313 (9), 255 (15) [M^+-$SiMe_3$], 241 (12), 224 (78) [M^+-C_8H_8], 209 (41), 165 (25), 104 (31) [$C_8H_8^+$], 73 (28) [$SiMe_3^+$]

HR MS ($C_{23}H_{24}Si$) calcd. 328.16473; found 328.1618

Exp. 22: 4-Diethylcarbamoyl-5-iodo[2.2]paracyclophane (108)

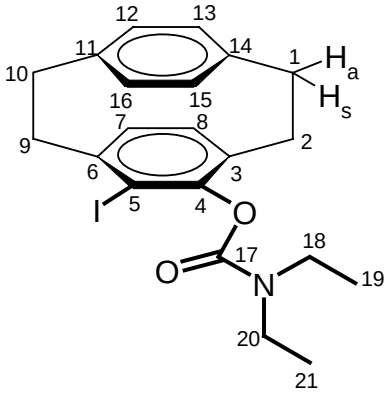

108

A solution of 809 mg (2.5 mmol) of **96** in 60 mL abs. of THF was cooled to -78 °C. To this solution, 0.45 mL (3 mmol) of freshly destilled TMEDA and 2.3 mL (3 mmol) of *sec*-BuLi (1.3 M solution in pentane) were added. After 1 h, a solution of 1.9 g (7.5 mmol) of iodine in 10 mL of THF was added. The cooling bath was removed and the reaction stirred overnight at room temp. The mixture was hydrolyzed with 100 mL of 10% HCl, washed with $NaHSO_3$ solution and extracted with dichloromethane. The organic phase was dried with Na_2SO_4. Column chromatography on silica gel with dichloromethane (R_f = 0.24) gave 912 mg (2.0 mmol, 81%) of **108** as a colorless solid (m.p. 117 °C).

^{1}H NMR ($CDCl_3$): δ = 1.20 (t, $^3J_{19,18}$ = 7.1 Hz, 3 H, 19-H), 1.47 (t, $^3J_{21,20}$ = 7.1 Hz, 3 H, 21-H), 2.76-2.83 (m, 1 H, 2-H), 2.94-3.18 (m, 6 H, 1-H*a*, 1-H*s*, 2-H, 9-H, 10-H*a*, 10-H*s*), 3.30-3.44 (m, 3 H, 9-H, 18-H, 18-H), 3.54 (dq, $^2J_{20,20}$ = 14.2 Hz, $^3J_{20,21}$ = 7.1 Hz, 1 H, 20-H), 3.78 (dq, $^2J_{20,20}$ = 14.2 Hz, $^3J_{20,21}$ = 7.1 Hz, 1 H, 20-H), 6.42 (d, $^3J_{7,8}$ = 7.8 Hz, 1 H, 7-H), 6.50-6.55 (m, 2 H, 12-H, 13-H), 6.56 (d, $^3J_{8,7}$ = 7.8 Hz, 1 H, 8-H), 6.64 (m "d", *J* = 7.8 Hz, 1 H, 15-H), 7.13 (m "d", *J* = 7.8 Hz, 1 H, 16-H)

^{13}C NMR ($CDCl_3$): δ = 13.4 (q, C-19), 14.7 (q, C-21), 31.7 (t, C-2), 33.0 (t, C-10), 34.5 (t, C-1), 39.1 (t, C-9), 42.1 (t, C-18), 42.3 (t, C-20), 103.5 (s, C-5), 128.5 (d, C-16), 128.8 (d, C-15), 130.5 (d, C-7), 132.8 (s, C-3), 132.9 (d, C-13), 133.2 (d, C-12), 134.3 (d, C-8), 138.6 (s, C-11), 139.1 (s, C-14), 145.2 (s, C-6), 149.0 (s, C-4), 152.5 (s, C-17)

IR (ATR): $\tilde{\nu}$ = 2973 cm^{-1} (m), 2930 (m), 2891 (w), 2853 (w), 1714 (vs), 1584 (w), 1500 (w), 1460 (m), 1419 (m), 1386 (m), 1314 (m), 1274 (m), 1237 (s), 1218 (m), 1149

(vs), 1110 (m), 1091 (m), 1047 (w), 997 (w), 981 (w), 956 (m), 922 (w), 889 (w), 845 (w), 796 (m), 748 (m), 717 (m), 665 (m), 637 (m), 580 (m)

UV (CH_3OH): λ_{max} (lg ε) = 217 (4.24), 247 (3.67)

MS (EI): *m/z* (%) = 450 (10), 449 (46) [M^+], 345 (6), 218 (5), 100 (100)

$C_{21}H_{24}NO_2I$ (449.34) calcd. C 56.13, H 5.38, N 3.12, I 28.24, O 7.12; found C 56.40, H 5.46, N 3.08

Exp. 23: 4-Diethylcarbamoyl-5-(trimethylsilyl)ethynyl [2.2]paracyclophane (109)

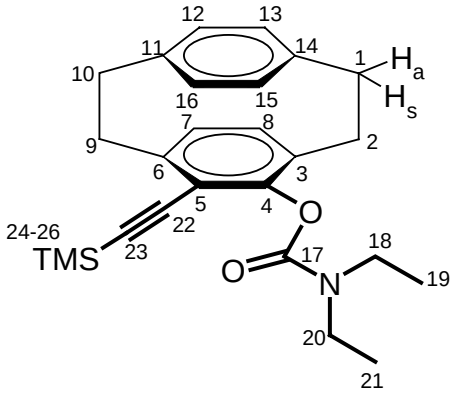

109

337 mg (0.75 mmol) of **108** was subjected to general procedure A using 0.16 mL (1.13 mmol) of TMSA, 9 mg (0.008 mmol) of $Pd(PPh_3)_4$, 2 mg (0.008 mmol) of CuI, 7.5 mL of diisopropylamine and 7.5 mL of THF. Column chromatography on silica gel with dichloromethane (Rf = 0.22) gave 293 mg (0.7 mmol, 93%) of **109** as a colorless solid (m.p. 128 - 131 °C).

^{1}H NMR ($CDCl_3$): δ = 0.28 (s, 9 H, Si(C**H**$_3$)$_3$), 1.20 (t, $^3J_{19,18}$ = 7.0 Hz, 3 H, 19-H), 1.47 (t, $^3J_{21,20}$ = 7.1 Hz, 3 H, 21-H), 2.69 (ddd, $^2J_{2a,2s}$ = 13.3 Hz, $^3J_{2a,1a}$ = 10.3 Hz, $^3J_{2a,1s}$ = 5.2 Hz, 1 H, 2-H*a*), 2.80 (ddd, $^2J_{9a,9s}$ = 13.0 Hz, $^3J_{9a,10a}$ = 10.5 Hz, $^3J_{9a,10s}$ = 5.0 Hz, 1 H, 9-H*a*), 2.95-3.18 (m, 5 H, 1-H*a*, 1-H*s*, 10-H*a*, 10-H*s*, 2-H*s*), 3.38 (q, $^3J_{18,19}$ = 7.0 Hz, 2 H, 18-H), 3.48 (ddd, $^2J_{9s,9a}$ = 13.0 Hz, $^3J_{9s,10s}$ = 10.3 Hz, $^3J_{9s,10a}$ = 2.8 Hz, 1 H, 9-H*s*), 3.55 (dq, $^2J_{20,20}$ = 14.2 Hz, $^3J_{20,21}$ = 7.0 Hz, 1 H, 20-H), 3.69 (dq, $^2J_{20,20}$ = 14.2 Hz, $^3J_{20,21}$ = 7.1 Hz, 1 H, 20-H), 6.44 (d, $^3J_{7,8}$ = 7.9 Hz, 1 H, 7-H), 6.46 (dd, $^3J_{13,12}$ = 7.9 Hz, $^4J_{13,15}$ = 1.8 Hz, 1 H, 13-H), 6.53 (dd, $^3J_{12,13}$ = 7.9 Hz, $^4J_{12,16}$ = 1.8 Hz, 1 H, 12-H), 6.53 (d, $^3J_{8,7}$ = 7.9 Hz, 1 H, 8-H), 6.71 (dd, $^3J_{15,16}$ = 7.8 Hz, $^4J_{15,13}$ = 1.8 Hz, 1 H, 15-H), 6.97 (dd, $^3J_{16,15}$ = 7.8 Hz, $^4J_{16,12}$ = 1.8 Hz, 1 H, 16-H)

^{13}C NMR ($CDCl_3$): δ = 0.0 (q, Si(**C**H_3)$_3$), 13.6 (q, C-19), 14.7 (q, C-21), 31.0 (t, C-2), 33.6 (t, C-10), 33.8 (t, C-9), 34.4 (t, C-1), 42.2 (t, C-20), 42.5 (t, C-18), 101.1 (s, **C**≡C-TMS), 102.4 (s, C≡**C**-TMS), 120.8 (s, C-5), 129.0 (d, C-15, C-16), 130.1 (d, C-7), 132.2 (s, C-6), 132.8 (d, C-13), 133.3 (d, C-12), 134.5 (d, C-8), 138.9 (s, C-4), 139.3 (s, C-14), 145.1 (s, C-3), 150.7 (s, C-4), 153.1 (s, C-17)

IR (ATR): $\tilde{\nu}$ = 2960 cm^{-1} (m), 2936 (m), 2895 (m), 2852 (m), 2145 (m), 1708 (s), 1593 (m), 1501 (m), 1467 (m), 1404 (s); 1378 (m), 1316 (m), 1247 (s), 1207 (s), 1158 (s), 1092 (m), 1056 (m), 1018 (m), 963 (m), 940 (m), 919 (m), 837 (vs), 751 (s), 720 (s), 697 (m), 663 (m), 640 (m), 555 (m)

UV (CH_3OH): λ_{max} (lg ε) = 281 nm (3.92), 317 (2.83)

MS (EI): *m/z* (%) = 419 (61) [M^+], 315 (19) [M^+-C_8H_8], 104 (9) [$C_8H_8^+$], 100 (100), 72 (33) [$SiMe_3^+$-H]

$C_{26}H_{33}NO_2Si$ (419.64) calcd. C 74.42, H 7.93, N 3.34, O 7.63, Si 6.69; found C 74.35, H 7.93, N 3.30

Exp. 24: 4-Hydroxy-5-(trimethylsilyl)ethynyl[2.2]paracyclophane (110)

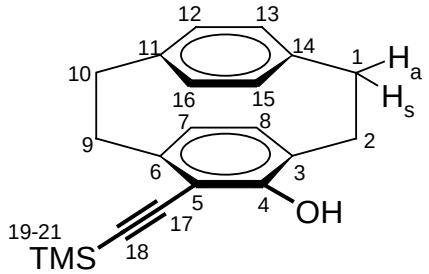

110

To a solution of 210 mg (0.5 mmol) of **109** in 0.5 mL of abs. THF, 1.5 mL (1.5 mmol) of DIBAL-H solution (1.0 M in pentane) was added. The reaction was stirred at room temp. and the progress was monitored by TLC (R_f dichloromethane = 0.9). After 4 h, the mixture was diluted with ether, acidified with 2 M HCl and washed with K-Na-tartrate solution. The aqueous phase was extracted with ether and the combined organic phases were dried with Na_2SO_4. The solvents were evaporated under reduced pressure and the residue purified by column chromatography on silica gel using 20% dichloromethane in pentane (R_f = 0.27) to yield 140 mg (0.44 mmol, 87%) of **110** as a colorless solid (m.p. 83 °C).

^{1}H NMR ($CDCl_3$): δ = 0.34 (s, 9 H, Si(C**H**$_3$)$_3$), 2.59 (ddd, $^{2}J_{2a,2s}$ = 13.2 Hz, $^{3}J_{2a,1a}$ = 10.3 Hz, $^{3}J_{2a,1s}$ = 5.7 Hz, 1 H, 2-H*a*), 2.78 (ddd, $^{2}J_{9a,9s}$ = 12.9 Hz, $^{3}J_{9a,10a}$ = 10.2 Hz, $^{3}J_{9a,10s}$ = 5.1 Hz, 1 H, 9-H*a*), 2.98-3.12 (m, 4 H, 1-H*a*, 1-H*s*, 10-H*a*, 10-H*s*), 3.39 (ddd, $^{2}J_{9s,9a}$ = 12.9 Hz, $^{3}J_{9s,10s}$ = 9.8 Hz, $^{3}J_{9s,10a}$ = 3.4 Hz, 1 H, 9-H*s*), 3.41 (ddd, $^{2}J_{2s,2a}$ = 13.2 Hz, $^{3}J_{2s,1s}$ = 9.9 Hz, $^{3}J_{2s,1a}$ = 3.1 Hz, 1 H, 2-H*s*), 5.62 (s, 1 H, OH), 6.23 (d, $^{3}J_{7,8}$ = 7.8 Hz, 1 H, 7-H), 6.43 (m "d", *J* = 7.9 Hz, 1 H, 13-H), 6.44 (d, $^{3}J_{8,7}$ = 7.8 Hz, 1 H, 8-H), 6.53 (m "d", *J* = 7.9 Hz,1 H, 12-H), 6.82-6.86 (m, 2 H, 15-H, 16-H)

^{13}C NMR ($CDCl_3$): δ = 0.1 (q, Si(**C**H$_3$)$_3$), 30.5 (t, C-2), 33.8 (t, t, C-9, C-10), 33.9 (t, C-1), 100.3 (s, **C**≡C-TMS), 105.8 (s, C≡**C**-TMS), 113.1 (s, C-5), 125.0 (d, C-7), 125.5 (s, C-3), 127.3 (d, C-15), 128.5 (d, C-16), 132.8 (d, C-13), 133.0 (d, C-12), 135.6 (d, C-8), 138.1 (s, C-11), 139.8 (s, C-14), 144.0 (s, C-6), 155.4 (s, C-4)

IR (ATR): $\tilde{\nu}$ = 3501 cm^{-1} (m), 2957 (m), 2927 (m), 2891 (m), 2850 (m), 2136 (m), 1879 (w), 1594 (w), 1562 (w), 1499 (w), 1480 (w), 1417 (s), 1321 (m), 1295 (m), 1245 (s), 1211 (m), 1199 (m), 1148 (m), 1026 (m), 989 (m), 930 (m), 836 (vs), 795 (s), 755 (s), 698 (s), 665 (s), 624 (m), 584 (m), 555 (m)

UV (CH_3OH): λ_{max} (lg ε) = 281nm (3.90), 337 (3.35)

MS (EI): *m/z* (%) = 320 (68) [M^+], 216 (100) [M^+-C_8H_8], 201 (44), 188 (20), 173 (26), 104 (15) [$C_8H_8^+$], 73 (26) [$SiMe_3^+$]

$C_{21}H_{24}OSi$ (320.50) calcd. C 78.70, H 7.55, O 4.99, Si 8.76; found C 78.57, H 7.77

Exp. 25: 4-Trifluoromethylsulfonyloxy-5-(trimethylsilyl)ethynyl[2.2]paracyclophane (111)

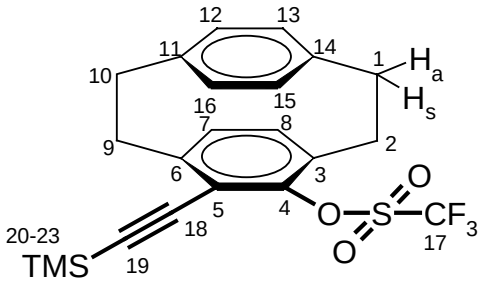

111

A solution of 641 mg (2 mmol) of **110**, 715 mg (2 mmol) of *N*,*N*-bis(trifluoromethylsulfonyl)aniline and 829 mg (6 mmol) of K_2CO_3 in 40 mL of abs. THF was heated to reflux for 40 h. The mixture was diluted with dichloromethane and filtered through a pad of silica gel. The solvents were removed and the residue purified by column chromatography on silica gel using 20% dichloromethane as eluent (R_f = 0.32), to yield 691 mg (1.53 mmol, 76%) of **111** as a colorless solid (m.p. 121 °C).

^{1}H NMR ($CDCl_3$): δ = 0.33 (s, 9 H, Si(C**H**$_3$)$_3$), 2.81 (ddd, $^2J_{2,2}$ = 13.8 Hz, $^3J_{2,1}$ = 10.3 Hz, $^3J_{2,1}$ = 5.2 Hz, 1 H, 2-H), 2.82 (ddd, $^2J_{9,9}$ = 13.3 Hz, $^3J_{9,10}$ = 10.5 Hz, $^3J_{9,10}$ = 5.1 Hz, 1 H, 9-H), 2.99-3.21 (m, 4 H, 1-H, 1-H, 10-H, 10-H), 3.33 (ddd, $^2J_{2,2}$ = 13.8 Hz, $^3J_{2,1}$ = 10.0 Hz, $^3J_{2,1}$ = 3.6 Hz, 1 H, 2-H), 3.49 (ddd, $^2J_{9,9}$ = 13.3 Hz, $^3J_{9,10}$ = 10.3 Hz, $^3J_{9,10}$ = 2.8 Hz, 1 H, 9-H), 6.50 (dd, $^3J_{13,12}$ = 7.9 Hz, $^4J_{13,15}$ = 1.8 Hz, 1 H, 13-H), 6.53-6.58 (m, 3 H, 12-H, 7-H, 8-H), 6.76 (dd, $^3J_{15,16}$ = 7.9 Hz, $^4J_{15,13}$ = 1.8 Hz, 1 H, 15-H), 6.96 (dd, $^3J_{16,15}$ = 7.9 Hz, $^4J_{16,12}$ = 1.8 Hz, 1 H, 16-H)

^{13}C NMR ($CDCl_3$): δ = -0.3 (q, Si(**C**H$_3$)$_3$), 31.4 (t, C-2), 33.5 (t, C-10), 33.8 (t, C-9), 34.0 (t, C-1), 98.3 (s, **C**≡C-TMS), 106.3 (s, C≡**C**-TMS), 118.7 (q, $^1J_{CF}$ = 321 Hz, CF_3), 121.1 (s, C-5), 129.2 (d, C-16), 129.2 (d, C-15), 132.8 (s, d, d, C-3, C-7, C-13), 133.1 (d, C-12), 135.2 (d, C-8), 138.9 (s, C-11), 139.1 (s, C-14), 146.7 (s, C-6), 148.3 (s, C-4)

IR (ATR): $\tilde{\nu}$ = 2966 cm^{-1} (m), 2934 (m), 2899 (w), 2858 (w), 2160 (m), 1597 (w), 1501 (w), 1414 (vs), 1323 (w), 1247 (m), 1202 (vs), 1129 (vs), 1014 (s), 930 (s), 875 (s), 838 (vs), 792 (vs), 757 (vs), 713 (s), 661 (m), 616 (vs), 593 (vs), 580 (vs), 545 (m)

UV (CH_3OH): λ_{max} (lg ε) = 281 nm (3.91), 326 (2.87), 353 (1.55)

MS (EI): *m/z* (%) = 452 (57) [M^+], 348 (5) [M^+-C_8H_8], 319 (98) [M^+-SO_2CF_3], 104 (100) [$C_8H_8^+$], 73 (20) [$SiMe^+$]

$C_{22}H_{23}F_3O_3SSi$ (452.52) calcd. C 58.39, H 5.12, S 7.08, F 12.59, O 10.61, Si 6.21; found C 58.61, H 5.26

Exp. 26: Pd-catalyzed cross coupling reactions of 111

Method A:

498 mg (1.1 mmol) of **111** was subjected to general procedure C at 80 °C for 36 h using 0.62 mL (4.4 mmol) of TMSA, 127 mg (0.11 mmol) of $Pd(PPh_3)_4$, 21 mg (0.11 mmol) of CuI. 11 mL of diisopropylamine and 11 mL of THF. After column chromatography on silica gel with 20% dichloromethane in pentane (R_f = 0.31), 490 mg (1.08 mmol, 98%) starting material **111** was recovered.

Method B:

A mixture of 113 mg (0.25 mmol) of **111**, 32 mg (0.75 mmol) of LiCl, 158 mg (0.5 mmol) of tributylstannylacetylene and 15 mg (0.013 mmol) $Pd(PPh_3)_4$ in 10 mL of THF was heated under argon for 3 d. After evaporation of the solvent under reduced pressure and purification of the residue by column chromatography on silica gel with 20% dichloromethane in pentane (R_f = 0.31) 105 mg (0.23 mmol, 93%) of starting material **111** was recovered.

Method C:

A solution of 113 mg (0.25 mmol) of **111** in 1 mL of DMF and 0.5 mL of triethylamine was deoxygenated by passing a stream of argon through it. To this solution, 18 mg (0.03 mmol) of $Pd(PPh_3)_2Cl_2$, 277 mg (0.75 mmol) of *n*-Bu_4NI, 16 mg (0.08 mmol) of CuI and 0.07 mL (0.5 mmol) of TMSA were added. The mixture was heated to 70° in a sealed ampoule for 2 d. The reaction mixture was diluted with dichloromethane and filtered through a pad of silica gel. By GC-MS analysis only the starting material was detected.

Exp. 27: Benzo[2.2]paracyclophane (153)

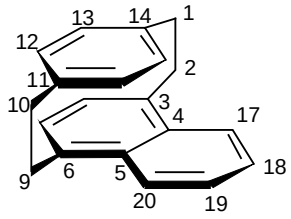

153

26 mg (0.1 mmol) of **56** and 160 mg (2 mmol) of 1,4-cyclohexadiene were dissolved in 15 mL of chlorobenzene. The solution was heated in a sealed ampoule for 16 h at 190 °C. After cooling to room temp., the solvent was evaporated and the residue purified by column chromatography on silica gel using 50% dichloromethane in pentane (R_f = 0.67) to yield 23 mg (0.089 mmol, 89%) of benzo[2.2]paracyclophane (**153**) as a colorless solid (m.p. 112 °C; lit.[78] 114-115 °C). Since the spectroscopic data of **153** are incomplete in the literature[78] they are given here.

^{1}H NMR ($CDCl_3$): δ = 2.88 (AMNX, $^2J_{1s,1a}$ = -13.2 Hz, $^3J_{1s,2s}$ = 10.2 Hz, $^3J_{1s,\ 2a}$ = 6.2 Hz, 2 H, 1-H*s*, 10-H*s*), 3.05 (AMNX, $^2J_{2a,2s}$ = -13.6 Hz, $^3J_{2a,1a}$ = 10.7 Hz, $^3J_{2a,1s}$ = 6.2 Hz, 2 H, 2-H*a*, 9-H*a*), 3.09 (AMNX, $^2J_{1a,1s}$ = -13.2 Hz, $^3J_{1a,2a}$ = 10.7 Hz, $^3J_{1a,\ 2s}$ = 2.0 Hz, 2 H, 1-H*a*, 10-H*a*), 3.78 (AMNX, $^2J_{2s,2a}$ = -13.6 Hz, $^3J_{2s,1s}$ = 10.2 Hz, $^3J_{2s,1a}$ = 2.0 Hz, 2 H, 2-H*s*, 9-H*s*), 5.58 (m, 2 H, 15-H, 16-H), 6.44 (m, 2 H, 12-H, 13-H), 6.73 (s, 2 H, 7-H, 8-H), 7.38 (AA'XX', J_{AX} = 8.3 Hz, $J_{XX'}$ = 6.8 Hz, $J_{AX'}$ = 1.2 Hz, 2 H, 18-H, 19-H), 7.68 (AA'XX', J_{AX} = 8.3 Hz, $J_{AX'}$ = 1.2 Hz, $J_{AA'}$ = 0.7 Hz, 2 H, 17-H, 20-H)

^{13}C NMR ($CDCl_3$): δ = 32.9 (t, C-2, C-9), 34.4 (t, C-1, C-10), 124.8 (d, C-18, C-19), 125.3 (d, C-17, C-20), 127.8 (d, C-15, C-16), 130.7 (d, C-7, C-8), 132.2 (d, C-12, C-13), 135.3 (d, C-4, C-5), 136.6(s, C-3, C-6), 137.9 (s, C-11, C-14)

IR (ATR): $\tilde{\nu}$ = 3062 cm^{-1} (w), 3012 (w), 2926 (m), 2852 (m), 1674 (w), 1578 (w), 1499 (w), 756 (vs), 715 (s), 641 (m), 616 (m), 580 (s)

UV (CH_2Cl_2): λ_{max} (lg ε) = 229 nm (4.24), 265 (4.02), 290 (3.56)

MS (EI): *m/z* (%) = 258 (30) [M^+], 154 (100) [$C_{12}H_{10}^+$], 104 (22) [$C_8H_8^+$]

Exp. 28: 8,9-Bis(trimethylsilyl)[2.2](1,4)biphenylenoparacyclophane (144)

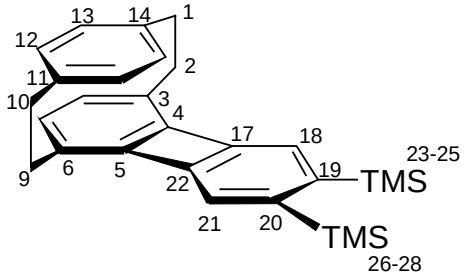

144

A solution of 55 mg (0.21 mmol) of **56** and 2 µL (0.016 mmol) of $CpCo(CO)_2$ in 1 mL of BTMSA and 1.5 mL of *p*-xylene was added with a syringe pump to 2.5 mL of boiling BTMSA over a period of 8 h. During the reaction, the flask was irradiated with a 1000 W halogen lamp. Heating and irradiation was continued for 1 h. The solvents were removed under reduced pressure and the residue purified by column chromatography on silica gel using pentane as eluent (R_f = 0.1) to yield 53 mg (0.12 mmol, 59%) of 8,9-bis-(trimethylsilyl)[2.2](1,4)biphenylenoparacyclophane (**144**) as a yellow solid (m.p. 187 - 189 °C).

^{1}H NMR ($CDCl_3$): δ = 0.38 (s, 18 H, Si(C**H**$_3$)$_3$), 2.68 (ABCD, $^2J_{1s,1a}$ = -13.3 Hz, $^3J_{1s,2s}$ = 10.3 Hz, $^3J_{1s,2a}$ = 4.1 Hz, 2 H, 1-H*s*, 10-H*s*), 2.86 (ABCD, $^2J_{1a,1s}$ = -13.3 Hz, $^3J_{1a,2a}$ = 10.2 Hz, $^3J_{1a,2s}$ = 4.8 Hz, 2 H, 1-H*a*, 10-H*a*), 2.97 (ABCD, $^2J_{2s,2a}$ = -13.5 Hz, $^3J_{2s,1s}$ = 10.3 Hz, $^3J_{2s,1a}$ = 4.8 Hz, 2 H, 2-H*s*, 9-H*s*), 3.08 (ABCD, $^2J_{2a,2s}$ = -13.5 Hz, $^3J_{2a,1a}$ = 10.2 Hz, $^3J_{2a,1s}$ = 4.1 Hz, 2 H, 2-H*a*, 9-H*a*), 5.81 (s, 2 H, 7-H, 8-H), 6.56 (m, 2 H, 15-H, 16-H), 6.80 (m, 2 H, 12-H, 13-H), 6.95 (s, 2 H, 18-H, 21-H)

^{13}C NMR ($CDCl_3$): δ = 2.3 (q, Si(**C**H$_3$)$_3$), 31.6 (t, C-2, C-9), 34.7 (t, C-1, C-10), 122.9 (d, C-18, C-21), 129.0 (d, C-15, C-16), 131.6 (s, C-3, C-6), 133.0 (d, C-12, C-13), 134.4 (d, C-7, C-8), 139.5 (s, C-11, C-14), 147.2 (s, C-19, C-20), 149.0 (s, C-17, C-22), 153.0 (s, C-4, C-5)

IR (ATR): $\tilde{\nu}$ = 3032 cm^{-1} (w), 2948 (m), 2926 (m), 2893 (m), 2851 (m), 1450 (w), 1433 (m), 1409 (m), 1316 (w), 1247 (s), 1122 (w), 1082 (w), 1044 (s), 963 (m), 914 (w), 830 (vs), 752 (vs), 714 (s), 687 (s), 645 (s), 565 (s), 544 (s)

UV (CH_2Cl_2): λ_{max} (lg ε) = 228 nm (4.04), 281 (4.37), 368 (3.11), 386 (3.11)

MS (EI): *m/z* (%) = 426/427/428 (100/38/14) [M^+], 322/323/324 (80/26/14) [M^+-C_8H_8], 219 (14), 195 (13), 167 (15), 149 (28), 73 (74) [$SiMe_3^+$]

HR MS ($C_{28}H_{34}Si_2$): calcd. 426.2199; found 426.2192 ± 1.4 ppm (Δ_{rel} = 1.6 ppm)

10.3.3 Synthesis of the annulenes with 4,5-diethynyl[2.2]paracyclophane (56) as a building block

Exp. 29: 4,5-Bis(2'-(trimethylsilylethynyl)phenylethynyl)[2.2]paracyclophane (126)

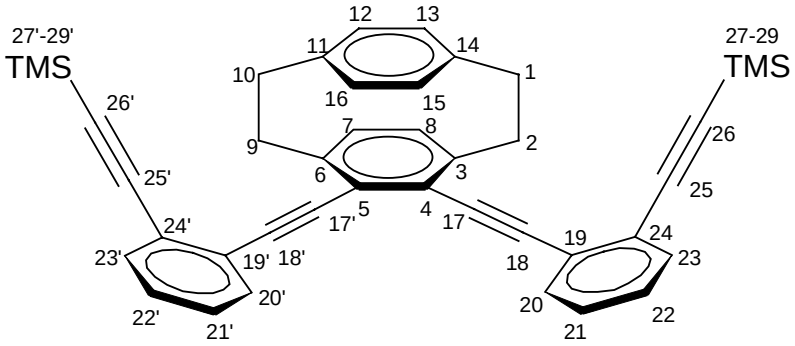

126

A solution of 150 mg (0.5 mmol) of 2-trimethylsilylethynyl-iodobenzene (**116**) in 10 mL of triethylamine was deoxygenated by bubbling N_2 for 15 min through it. To this solution, 30 mg (0.026 mmol) of $Pd(PPh_3)_4$ and 14 mg (0.076 mmol) of CuI were added. The mixture was heated to 40 °C and a deoxygenated solution of 51 mg (0.2 mmol) of 4,5-diethynyl[2.2]paracyclophane (**56**) in 1 mL of THF was added over a period of 4 h using a syringe pump. After stirring for 18 h at 40 °C, the solvents were removed *in vacuo*. Purification by column chromatography on silica gel with 10% dichloromethane in hexane (R_f = 0.07) gave 69 mg (0.11 mmol, 58%) of **126** as a colorless solid (m.p. 146 °C). Slow diffusion of hexanes in a dichloromethane solution gave single crystals suitable for X-ray structure analysis.

^{1}H NMR ($CDCl_3$): δ = 0.25 (s, 18 H, Si(C**H**$_3$)$_3$), 2.89 (ddd, $^2J_{2a,2s}$ = 12.9 Hz, $^3J_{2a,1a}$ = 10.7 Hz, $^3J_{2a,1s}$ = 4.7 Hz, 2 H, 2-H*a*, 9-H*a*), 3.08 (ddd, $^2J_{1a,1s}$ = 13.0 Hz, $^3J_{1a,2a}$ = 10.7 Hz, $^3J_{1a,2s}$ = 2.6 Hz, 2 H, 1-H*a*, 10-H*a*), 3.38 (ddd, $^2J_{1s,1a}$ = 13.0 Hz, $^3J_{1s,2s}$= 10.6 Hz, $^3J_{1s,2a}$ = 4.7 Hz, 2 H, 1-H*s*, 10-H*s*), 3.87 (ddd, $^2J_{2s,2a}$ = 12.9 Hz, $^3J_{2s,1s}$ = 10.6 Hz, $^3J_{2s,1a}$ = 2.6 Hz, 2 H, 2-H*s*, 9-H*s*), 6.55-6.56 (m, 2 H, 12-H, 13-H), 6.57 (s, 2 H, 7-H, 8-H), 7.02-

7.03 (m, 2 H, 15-H, 16-H), 7.24-7.29 (m, 4 H, 21-H, 22-H, 21'-H, 22'-H), 7.53-7.58 (m, 2 H, 23-H, 23'-H), 7.59-7.63 (m, 2 H, 20-H, 20'-H)

^{13}C NMR ($CDCl_3$): δ = -0.02 (q, Si(**C**H_3)$_3$), 34.1 (t, C-1, C-10), 34.6 (t, C-2, C-9), 92.6 (s, C-17, C-17'), 95.8 (s, C-18, C-18'), 98.3 (s, C-26, C-26'), 104.0 (s, C-25, C-25'), 125.0 (s, C-24, C-24'), 126.2 (s, C-19, C-19'), 127.7 (d, C-22, C-22'), 128.1 (s, C-4, C-5), 128.2 (d, C-21, C-21'), 129.9 (d, C-15, C-16), 132.7 (d, C-20, C-20'), 132.9 (d, C-12, C-13), 133.1 (d, C-7, C-8), 133.2 (d, C-23, C-23'), 139.3 (s, C-11, C-14), 143.0 (s, C-3, C-6)

IR (KBr): $\tilde{\nu}$ = 3059 cm^{-1} (w), 2958 (m), 2929 (m), 2898 (m), 2855 (w), 2191 (w), 2151 (m), 1483 (m), 1458 (m), 1436 (m), 1413 (m), 1262 (m), 1251 (s), 1211 (m), 1159 (m), 1094 (m), 1039 (m), 1025 (m), 1021 (m), 862 (vs), 844 (vs), 797 (m), 764 (vs), 728 (m), 713 (m), 698 (m), 675 (m), 644 (m), 611 (m), 521 (m)

UV (CH_2Cl_2): λ_{max} (lg ε) = 263 nm (4.50), 306 (4.06), 351 (4.31)

MS (EI): *m/z* (%) = 600 (3) [M^+], 527 (7) [M^+-$SiMe_3$], 453 (16) [M^+-2 $SiMe_3$-H], 73 (100) [$SiMe_3^+$]

HR MS ($C_{42}H_{40}Si_2$): calcd. 600.2669; found 600.2657 ± 1 ppm (Δ_{rel} = 2 ppm)

Exp. 30: 1,2:9,10-Dibenzo-5,6-[2.2]paracyclophano-3,7,11,13-tetradehydro-[14]annulene (53)

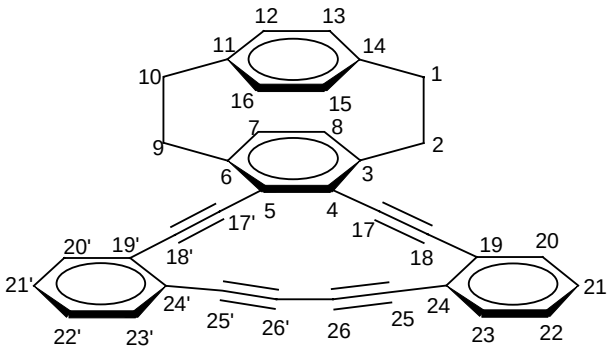

53

38 mg (0.06 mmol) of **126** in 100 mL of methanol and 100 mL of acetonitrile was subjected to general procedure E using 42 mg (0.3 mmol) of K_2CO_3 and 250 mg (1.26 mmol) of $Cu(OAc)_2$•H_2O. Purification by preparative thick layer chromatography with 10% dichloromethane in hexanes (R_f = 0.17) gave 32 mg (0.058 mmol, 97%) of **53** as a

colorless solid (m.p. 225 °C). Slow diffusion of benzene in a dichloromethane solution gave single crystals suitable for X-ray structural analysis.

^{1}H NMR ($CDCl_3$): δ = 3.05-3.23 (m, 6 H, 1-H, 2-H*a*, 9-H*a*, 10-H), 3.94-4.00 (m, 2 H, 2-H*s*, 9-H*s*), 6.54 (m, 2 H, 12-H, 13-H), 6.65 (m, 2 H, 15-H, 16-H), 6.76 (s, 2 H, 7-H, 8-H), 7.45 (ddd, $^{3}J_{22,21}$ = 8.9 Hz, $^{3}J_{22,23}$ = 7.7 Hz, $^{4}J_{22,20}$ = 1.2 Hz, 2 H, 22-H, 22'-H), 7.54 (ddd, $^{3}J_{21,22}$ = 8.9 Hz, $^{3}J_{21,20}$ = 7.4 Hz, $^{4}J_{21,23}$ = 1.2 Hz, 2 H, 21-H, 21'-H), 7.65 (dd, $^{3}J_{23,22}$ = 7.7 Hz, $^{4}J_{23,21}$ = 1.2 Hz, 2 H, 23-H, 23'-H), 7.93 (dd, $^{3}J_{20,21}$ = 7.4 Hz, $^{4}J_{20,22}$ not resolved, 2 H, 20-H, 20'-H)

^{13}C NMR ($CDCl_3$): δ = 33.9 (t, C-1, C-10), 35.4 (t, C-2, C-9), 80.6 (s, C-26, C-26'), 86.2 (s, C-25, C-25'), 93.7 (s, C-17, C-17'), 97.1 (s, C-18, C-18'), 122.5 (s, C-24, C-24'), 125.3 (s, C-4, C-5), 127.8 (d, C-22, C-22'), 128.7 (d, C-21, C-21'), 129.2 (d, C-23, C-23'), 130.0 (d, C-12, C-13), 130.2 (s, C-19, C-19'), 132.8 (d, C-20, C-20'), 133.0 (d, C-7, C-8), 139.0 (s, C-11, C-14), 145.1 (s, C-3, C-6)

IR (KBr): $\tilde{\nu}$ = 3056 cm^{-1} (w), 3018 (w), 2955 (m), 2925 (s), 2888 (m), 2850 (m), 2212 (w), 2162 (w), 1472 (s), 1452 (s), 1433 (m), 1411 (m), 1159 (m), 1097 (w), 800 (w), 755 (vs), 378 (m), 720 (m), 520 (m), 480 (w)

UV (CH_2Cl_2): λ_{max} (lg ε) = 290 nm (4.32), 310 (4.56), 324 (4.78), 347 (4.12), 354 (4.21), 364 (4.20), 380 (3.59)

MS (EI): *m/z* (%) = 454 (82) [M^{+}], 453 (84), 452 (53), 451 (42), 450 (10), 439 (62), 438 (71), 437 (62), 350 (74), 349 (79), 348 (100), 346 (50), 345 (76)

HR MS ($C_{36}H_{22}$): calcd. 454.1722; found 454.1691 ± 0.6 ppm (Δ_{rel} = 6.8 ppm)

Exp. 31: 4,5-Bis(6'-trimethylsilyl-1',5'-hexadiine-3'-ene)[2.2]paracyclophane (127)

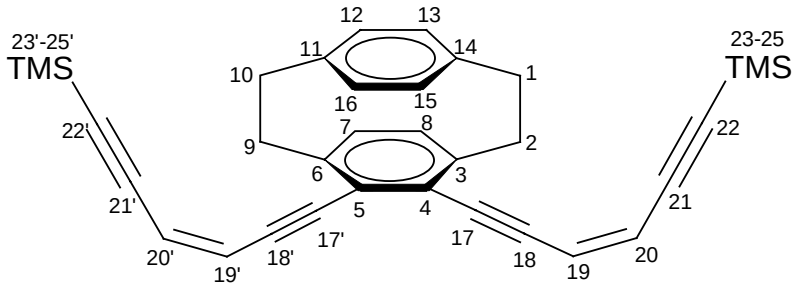

127

A solution of 67 mg (0.42 mmol) of 1-chloro-4-trimethylsilylbuten-3-yne (**175**), in 15 mL of THF and 2 mL of *n*-propylamine was deoxygenated by bubbling argon for 20 min through it. To this solution, 18 mg (0.016 mmol) of $Pd(PPh_3)_4$ and 38 mg (0.2 mmol) of CuI were added. A deoxygenated solution of 51 mg (0.2 mmol) of 4,5-diethynyl[2.2]paracyclophane (**56**) in 5 mL of THF was added by a syringe and the reaction mixture was stirred at room temp. for 24 h. The mixture was diluted with ether and filtered through a pad of silica gel. After removal of the solvents *in vacuo*, the residue was purified by column chromatography on silica gel using 10% dichloromethane and 1% triethylamine in pentane (R_f = 0.11) to yield 52 mg (0.1 mmol, 50%) of **127** as a yellow solid (m.p. 94 - 96 °C) .

^{1}H NMR ($CDCl_3$): δ = 0.25 (s, 18 H, Si(C**H**$_3$)$_3$), 2.84 (ddd, $^3J_{2a,2s}$ = 13.0 Hz, $^3J_{2a,1a}$ = 10.7 Hz, $^3J_{2a,1s}$ = 4.7 Hz ,2 H, 2-H*a*, 9-H*a*), 3.05 (ddd,$^3J_{1a,1s}$ = 12.9 Hz, $^3J_{1a,2a}$ = 10.7 Hz, $^3J_{1a,2s}$ = 2.6 Hz ,2 H, 1-H*a*, 10-H*a*), 3.35 (ddd, $^3J_{1s,1a}$ = 12.9 Hz, $^3J_{1s,2s}$ = 10.6 Hz, $^3J_{1s,2a}$ = 2.6 Hz,2 H, 1-H*s*, 10-H*s*), 3.77 (ddd, $^3J_{2s,2a}$ = 13.0 Hz, $^3J_{2s,1s}$ = 10.6 Hz, $^3J_{2s,1a}$ = 2.6 Hz, 2 H, 2-H*s*, 9-H*s*), 5.92 (d, $^3J_{19,20}$ = 11.0 Hz, 2 H, 20-H, 21'-H), 6.17 (d, $^3J_{20,19}$ = 11.0 Hz, 2 H, 19-H, 19'-H), 6.52-6.53 (m, 2 H, 12-H, 13-H), 6.54 (s, 2 H, 7-H, 8-H), 6.91-6.94 (m, 2 H, 15-H, 16-H)

^{13}C NMR ($CDCl_3$): δ = -0.1 (q, Si(**C**H$_3$)$_3$), 33.9 (t, C-2, C-9), 34.4 (t, C-1, C-10), 94.7 (s, C-18, C-18'), 96.2 (s, C-17, C-17'), 102.6 (s, C-21, C-21'), 102.9 (s, C-22, C-22'), 118.5 (d, C-20, C-20'), 120.6 (d, C-19, C-19'), 127.7 (s, C-4, C-5), 129.9 (d, C-15, C-16), 132.9 (d, C-12, C-13), 133.4 (d, C-7, C-8), 139.3 (s, C-11, C-14), 143.3 (s, C-3, C-6)

IR (ATR): $\tilde{\nu}$ = 3039 cm^{-1} (w), 2959 (m), 2932 (m), 2895 (m), 2852 (m), 2185 (m), 2130 (m), 1884 (w), 1688 (w), 1565 (w), 1500 (w), 1455 (w), 1412 (m), 1391 (m), 1248

(s), 1201 (m), 1057 (m), 1017 (m), 995 (m), 978 (m), 835 (vs), 755 (vs), 699 (s), 667 (m), 632 (s), 584 (m), 537 (m)

UV (CH_2Cl_2): λ_{max} (lg ε) = 230 nm (4.34), 251 (4.21), 315 (4.37), 361 (4.32)

MS (EI): *m/z* (%) = 500 (2) [M^+], 427 (3) [M^+-$SiMe_3$], 353 (8) [M^+-2 $SiMe_3$-H], 73 (100) [$SiMe_3^+$]

HR MS ($C_{34}H_{36}Si_2$): calc. 500.2356; found 500.2355 ± 0.9 ppm (Δ_{rel} = 0.2 ppm)

Exp. 32: 5,6-[2.2]Paracyclophano-3,7,11,13-tetradehydro[14]annulene (54)

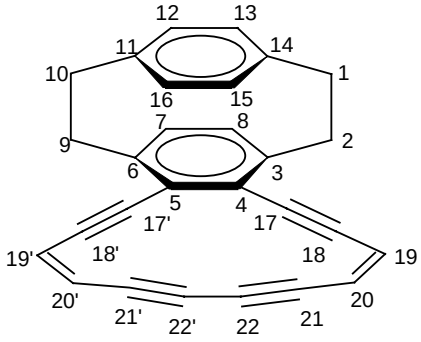

54

25 mg (0.05 mmol) of **127** in 100 mL of methanol and 100 mL of acetonitrile was subjected to general procedure E using 35 mg (0.25 mmol) of K_2CO_3 and 200 mg (1.00 mmol) of $Cu(OAc)_2 \bullet H_2O$. Purification by preparative thick layer chromatography with 20% dichloromethane and 1% triethylamine in pentane (R_f = 0.3) and extraction of the silica gel with ether and dichloromethane gave a yellow solution which turned brown upon concentration. After drying in high vacuum, 4 mg (0.01 mmol, 20%) of **54** was obtained as a brown solid.

^{1}H NMR ($CDCl_3$): δ = 3.15-3.26 (m, 6 H, 1-H*a*, 1-H*s*, 2-H*a*, 9-H*a*, 10-H*a*, 10-H*s*), 4.09-4.18 (m, 2 H, 2-H*s*, 9-H*s*), 6.00-6.01 (m, 2 H, 15-H, 16-H), 6.53 (m, 2 H, 12-H, 13-H), 6.74 (d, $^3J_{20,19}$ = 9.9 Hz, 2 H, 20-H, 20'-H), 6.79 (s, 2 H, 5-H, 6-H), 7.54 (d, $^3J_{19,20}$ = 9.9 Hz, 2 H, 19-H, 19'-H)

^{13}C NMR ($CDCl_3$): δ = 34.2 (t, C-1, C-10), 35.4 (t, C-2, C-9), 85.3 (s, C-18, C-18' or C-22, C-22'), 90.8 (s, C-17, C-17' or C-21, C-21'), 97.7 (s, C-18, C-18' or C-22, C-22'), 99.7 (s, C-17, C-17' or C-21, C-21'), 115.4 (d, C-20, C-20'), 124.6 (s, C-4, C-5), 125.9

(d, C-19, C-19'), 130.0 (d, C-15, C-16), 132.6 (d, C-12, C-13), 132.9 (d, C-7, C-8), 139.0 (s, C-11, C-14), 145.1 (s, C-3, C-6)

10.3.4 Synthesis of 4,7,12,15-tetraethynyl[2.2]paracyclophane

Exp. 33: 4,5,15,16- and 4,7,12,15-tetrabromo[2.2]paracyclophane (89) and (90)

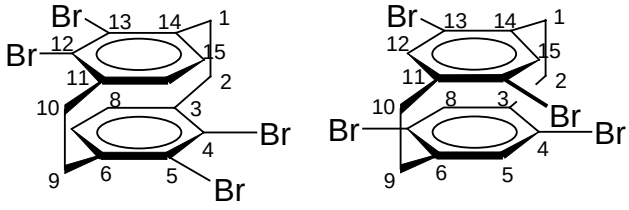

89 **90**

5.0 g (24 mmol) of [2.2]paracyclophane (**36**) was added in small portions to a mixture of 75 mg (0.3 mmol) of iodine in 15 mL of bromine in a flask wrapped with aluminum foil to exclude daylight. The reaction mixture was stirred for 8 d at room temp. and then 150 mL of 20% sodium hydroxide solution was added. The precipitate was collected by filtration and then heated in 100 mL of ethanol to reflux for 10 min. Filtration and drying *in vacuo* yielded 11.48 g (21.9 mmol, 91%; 91% lit[41]) as a mixture of **89** and **90**. To separate the isomers, the mixture was extracted with dichloromethane (3 x 30 mL) yielding a residue of 4.27 g (8.2 mmol, 34%; 43% [41]) of **89** (m.p. >280 °C[41]).

The dichloromethane filtrate was evaporated to dryness to yield 7.18 g (57%) of **89** and **90.** Column chromatography on silica gel with pentane (R_f = 0.36) gave 3.4 g (6.5 mmol, 27%) of **90** (m.p. >280 °C [41]) and 3.7 g (7.1 mmol, 30%) of a mixture of **89** and **90**.

4,5,15,16-Tetrabromo[2.2]paracyclophane (89):

^{1}H NMR ($CDCl_3$): δ = 3.05-3.14 (m, 4 H, 1-H, 2-H, 9-H, 10-H), 3.31-3.39 (m, 4 H, 1-H, 2-H, 9-H, 10-H), 7.00 (s, 4 H, 7-H, 8-H, 12-H, 13-H)

^{13}C NMR ($CDCl_3$): δ = 34.6 (t, C-1, C-2, C-9, C-10), 128.7 (d, C-7, C-8, C-12, C-13), 129.3 (s, C-4, C-5, C-15, C-16), 140.7 (s, C-3, C-6, C-11, C-14)

IR (KBr): $\tilde{\nu}$ = 2966 cm^{-1} (m), 1873 (w), 1564(w), 1434 (vs), 1371 (vs), 1314 (m), 1241 (m), 1186 (m), 1122 (m), 1061 (vs), 1047 (s), 913 (m), 889 (m), 836 (vs), 767 (m), 734 (m), 705 (s), 671 (vs)

MS (EI): *m/z* (%) = 528/526/524/522/520 (4/13/21/13/4) [M^+], 264/262/260 (44/100/50) [1/2 M^+]; 102 (48)

4,7,13,16-Tetrabromo[2.2]paracyclophane (90):

^{1}H NMR ($CDCl_3$): δ = 2.94-3.02 (m, 4 H, 1-H, 2-H, 9-H, 10-H), 3.19-3.27 (m, 4 H, 1-H, 2-H, 9-H, 10-H), 7.19 (s, 4 H, 5-H, 8-H, 12-H, 15-H)

^{13}C NMR ($CDCl_3$): δ = 32.7 (t, C-1, C-2, C-9, C-10), 125.3 (s, C-4, C-7, C-13, C-16), 134.4 (d, C-5, C-8, C-12, C-15), 140.3 (s, C-3, C-6, C-11, C-14)

IR (ATR): $\tilde{\nu}$ = 2934 cm^{-1} (m), 1574 (w), 1460 (s), 1448 (m), 1431 (m), 1358 (s), 1181 (m), 1119 (m), 1043 (vs), 963 (m), 930 (m), 881 (vs), 847 (m), 816 (m), 688 (m)

MS (EI): *m/z* (%) =528/526/524/522/520 (5/17/28/18/5) [M^+], 264/262/260 (50/100/50) [1/2 M^+], 102 (43)

Exp. 34: 4,7,13,16-Tetrakis(trimethylsilylethynyl)[2.2]paracyclophane (163)

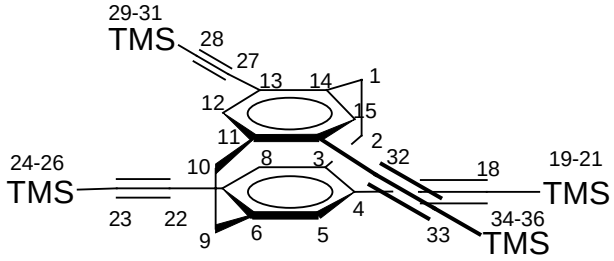

163

A solution of 524 mg (1 mmol) of 4,7,13,16-tetrabromo[2.2]paracyclophane (**90**) in 5 mL of THF and 10 mL of diisopropylamine was deoxygenated by bubbling argon for 30 min through it. 92 mg (0.08 mmol) of $Pd(PPh_3)_4$ and 30 mg (0.16 mmol) of CuI were added and the reaction mixture was heated to 40-50 °C. A solution of 0.88 mL (6 mmol) of TMSA in 5 mL of deoxygenated THF was added by a syringe pump over a period of 8 h. After 2 d of heating, the solvents were removed and the residue purified by column chromatography on silica gel using pentane to yield 58 mg (0.1 mmol, 10%) of 4,7-dibromo-13,16-bis(trimethylsilylethynyl)[2.2]paracyclophane (**166**) (R_f = 0.26; colorless solid, mp. 210 °C), 95 mg (0.16 mmol, 16%) of 4-bromo-7,13,16-tris(trimethylsilylethynyl)[2.2]paracyclophane (**165**) (R_f = 0.18; colorless solid, mp. 108 °C) and 267 mg (0.45 mmol, 45%) of 4,7,13,16-tetrakis-(trimethylsilylethynyl)[2.2]paracyclophane (**163**) (R_f = 0.12; colorless solid, mp. 118 °C).

4,7,13,16-Tetrakis(trimethylsilylethynyl)[2.2]paracyclophane (163):

^{1}H NMR ($CDCl_3$): δ = 0.31 (s, 36 H, Si(C**H**$_3$)$_3$), 2.87-2.95 (m, 4 H, 1-H, 2-H, 9-H, 10-H), 3.34-3.42 (m, 4 H, 1-H, 2-H, 9-H, 10-H), 6.98 (s, 4 H, 5-H, 8-H, 12-H, 15-H)

^{13}C NMR ($CDCl_3$): δ = 0.0 (q, Si(**C**H$_3$)$_3$, 32.1 (t, C-1, C-2, C-9, C-10), 99.4 (s, C≡**C**-SiMe$_3$), 104.7 (s, **C**≡C-SiMe$_3$), 125.1 (s, C-4, C-7, C-13, C-16), 134.4 (d, C-5, C-8, C-12, C-15), 142.2 (s, C-3, C-6, C-11, C-14)

IR (KBr): $\tilde{\nu}$ = 2958 cm^{-1} (m), 2934 (m), 2897 (w), 2852 (w), 2150 (s), 1478 (w), 1449 (w), 1392 (w), 1249 (s), 1204 (m), 1178 (w), 907 (m), 878 (vs), 841 (vs), 727 (m), 697 (m), 827 (m), 495 (w)

UV (CH_2Cl_2): 232 nm (4.72), 264 (4.35), 290 (4.31), 306 (4.46), 324 (4.48)

MS (EI): *m/z* (%) = 592 (1) [M^+], 504 (3), 438 (13), 436 (14), 357 (100), 311 (8), 309 (9), 230 (18), 103 (27)

HR MS ($^{12}C_{35}\,^{13}CH_{48}Si_4$): calc. 593.28667; found 593.28483 ± 1.0 ppm (Δ_{rel} = 3.1 ppm)

4,7-Dibromo-13,16-bis(trimethylsilylethynyl)[2.2]paracyclophane (166):

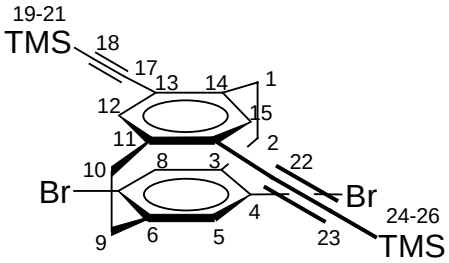

166

^{1}H NMR ($CDCl_3$): δ = 0.32 (s, 18 H, Si(C**H**$_3$)$_3$), 2.88-3.00 (m, 4 H, 1-H, 2-H, 9-H, 10-H), 3.22-3.29 (m, 2 H, 2-H, 9-H), 3.32-3.39 (m, 2 H, 1-H, 10-H), 7.02 (s, 2 H, 5-H, 8-H), 7.15 (s, 2 H, 12-H, 15-H)

^{13}C NMR ($CDCl_3$): 0.0 (q, Si(**C**H$_3$)$_3$), 31.6 (t, C-1, C-10), 33.2 (t, C-2, C-9), 100.2 (s, C≡**C**-SiMe$_3$), 104.4 (s, **C**≡C-SiMe$_3$), 125.2 (s, C-13, C-16), 125.3 (s, C-4, C-7), 133.8 (d, C-12, C-15), 134.9 (d, C-5, C-8), 140.6 (s, C-3, C-6), 141.8 (s, C-11, C-14)

IR (ATR): $\tilde{\nu}$ = 2956 cm^{-1} (m), 2937 (m), 2897 (w), 2851 (w), 2152 (m), 1479 (m), 1461 (m), 1448 (w), 1431 (w), 1410 (w), 1390 (m), 1353 (m), 1247 (s), 1206 (m), 1180 (m), 1044 (s), 966 (w), 896 (m), 835 (vs), 756 (s), 692 (s), 625 (m)

UV (CH_2Cl_2): λ_{max} (lg ε) = 228 nm (4.45), 250 (4.14), 305 (4.34), 318 (4.40)

MS (EI): *m/z* (%) = 557/559/561 (7/15/8) [M^+], 556/558/560/562 (18/41/24/2) [M^+], 296 (100), 281 (27), 223 (20), 73 (39) [$SiMe_3^+$]

$C_{26}H_{30}Br_2Si_2$ (558.50) calcd. C 55.91, H 5.41, Br 28.61, Si 10.07; found C 55.94, H 5.52

4-Bromo-7,13,16-tris(trimethylsilylethynyl)[2.2]paracyclophane (165):

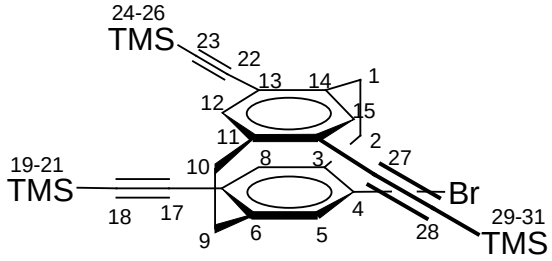

165

^{1}H NMR ($CDCl_3$): δ = 0.31 (s, 9 H, Si(C**H**$_3$)$_3$), 0.32 (s, 18 H, Si(C**H**$_3$)$_3$), 2.84-3.02 (m, 4 H, 1-H, 2-H, 9-H, 10-H), 3.21-3.30 (m, 1 H, 2-H), 3.32-3.41 (m, 3 H, 1-H, 9-H, 10-H), 6.99 (s, 1 H, 8-H), 7.02 (s, 1 H, 5-H), 7.04 (s, 1 H, 12-H), 7.10 (s, 1 H, 15-H)

^{13}C NMR ($CDCl_3$): δ = 0.0 (q, Si(**C**H$_3$)$_3$, 31.6 (t, C-1), 31.9 (t, C-9), 32.1 (t, C-10), 33.3 (t, C-2), 98.7 (s, C≡C), 99.6 (s, C≡C), 100.0 (s, C≡C), 104.2 (s, C≡C), 104.6 (s, C≡C), 124.2 (s, C-7), 125.1 (s, C-13), 125.2 (s, C-16), 127.0 (s, C-4), 133.5 (d, C-15), 134.0 (d, C-5), 134.7 (d, C-3), 135.5 (d, C-8), 138.9 (s, C-3), 142.0 (s, C-11 or C-14), 142.0 (s, C-11 or C-14), 143.9 (s, C-6)

IR (ATR): $\tilde{\nu}$ = 2956 cm^{-1} (m), 2935 (m), 2896 (w), 2852 (w), 2149 (m), 1469 (w), 1447 (w), 1391 (w), 1368 (w), 1247 (s), 1206 (w), 1183 (w), 1140 (m), 1114 (w), 902 (m), 831 (vs), 756 (s), 724 (m), 698 (s), 671 (m), 653 (m), 624 (m)

MS (EI): *m/z* (%) = 575/577 (3/3), 574/576 (6/7) [M$^+$], 495 (9), 486/488 (10/11), 407 (15), 334 (15), 296 (16), 281 (17), 223 (12), 73 (100) [SiMe$_3^+$]

Exp. 35: 4,7,13,16-Tetraethynyl[2.2]paracyclophane (164)

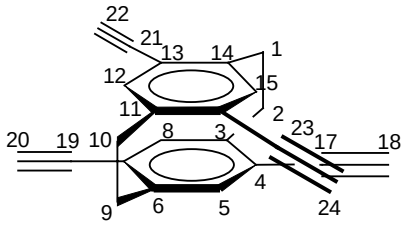

164

195 mg (0.33 mmol) of **163** in 10 mL of dichloromethane and 10 mL of methanol was subjected to general procedure D using 456 mg (3.3 mmol) of K_2CO_3. The solvents

were evaporated and the residue filtered through a short column of silica (pentane) to yield 96 mg (0.32 mmol, 97%) of 4,5,13,16-tetraethynyl[2.2]paracyclophane (**164**) as a colorless solid (m.p. 143 °C).

^{1}H NMR ($CDCl_3$): δ = 2.95-3.06 (m, 4 H, 1-H, 2-H, 9-H, 10-H), 3.37 (s, 4 H, C≡C**H**), 3.39-3.46 (m, 4 H, 1-H, 2-H, 9-H, 10-H), 7.05 (s, 4 H, 5-H, 8-H, 12-H, 15-H)

^{13}C NMR ($CDCl_3$): δ = 31.9 (t, C-1, C-2, C-9, C-10), 82.0 (C≡C-H), 82.7 (C≡C-H), 124.4 (s, C-4, C-7, C-3, C-16), 134.8 (d, C-5, C-8, C-12, C-15), 142.5 (s, C-3, C-6, C-11, C-14)

IR (KBr): $\tilde{\nu}$ = 3296 cm^{-1} (vs), 3284 (vs), 3042 (w), 3037 (w), 3013 (w), 2969 (w), 2934 (m), 2885 (w), 2851 (w), 2098 (m), 1475 (m), 1447 (m), 1431 (m), 1248 (m), 1207 (w), 1193 (m), 1166 (w), 936(w), 907 (s), 865 (m), 725 (w), 676 (m), 661 (m), 650 (s), 636 (s), 629 (m), 613 (s), 494 (m), 471 (m)

UV (CH_2Cl_2): λ_{max} (lg ε) = 232 nm (4.53), 254 (4.19), 290 (4.21), 298 (4.22), 308 (4.28)

MS (EI): *m/z* (%) = 303/304/305 (74/50/11) [M^+], 289 (59), 287 (26), 265 (18), 152 (100), 151 (89), 150 (35), 126 (18)

HR MS (C_{24} H_{15}) [M^+-H]: calc. 303.11737; found 303.11625 ± 0.5 ppm (Δ_{rel} = 3.7 ppm)

10.3.5 Synthesis of the propeller-type [2.2]paracyclophane/dehydrobenzo-annulenes

Exp. 36: 4,7,13,16-Tetrakis(4'-*tert*-butyl-2'-[trimethylsilyl]ethynyl-phenylethynyl)-[2.2]paracyclophane (167)

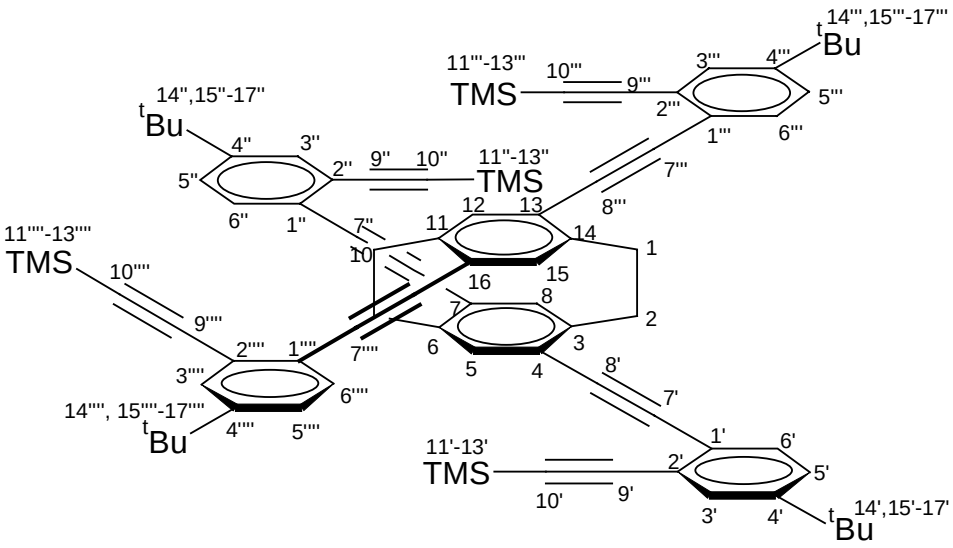

167

61 mg (0.2 mmol) of 4,7,13,16-tetraethynyl[2.2]paracyclophane (**164**) in 2 mL of THF was coupled with 357 mg (1.0 mmol) of 4-*tert*-butyl-2-[(trimethylsilyl)ethynyl]iodo-benzene (**121**) in 10 mL of THF and 12 mL of diisopropylamine as described in general procedure B using 18 mg (0.016 mmol) of $Pd(PPh_3)_4$ and 3 mg (0.016 mmol) of CuI.

Purification by preparative thick layer chromatography with 10% dichloromethane in pentane (R_f =0.07) gave 40 mg (0.03 mmol, 15%) of **167** as a light yellow solid (m.p. 96 °C).

^{1}H NMR ($CDCl_3$): δ = 0.22 (s, 36 H, Si(C**H**$_3$)$_3$), 1.35 (s, 36 H, C(C**H**$_3$)$_3$), 3.11-3.18 (m, 4 H, 1-H, 2-H, 9-H, 10-H), 3.67-3.74 (m, 4 H, 1-H, 2-H, 9-H, 10-H), 7.22 (s, 4 H, 5-H, 8-H, 12-H, 15-H), 7.33 (dd, $^3J_{5',6'}$ = 8.2 Hz, $^4J_{5',3'}$ = 2.0 Hz, 4 H, 5'-H, 5''-H, 5'''-H, 5''''-H), 7.51 (d, $^3J_{6',5'}$ = 8.2 Hz, 4 H, 6'-H, 6''-H, 6'''-H, 6''''-H), 7.55 (d, $^4J_{3',5'}$ = 2.0 Hz, 4 H, 3'-H, 3''-H, 3'''-H, 3''''-H)

^{13}C NMR ($CDCl_3$): δ = 0.1 (q, Si(**C**H$_3$)$_3$), 31.1 (q, C(**C**H$_3$)$_3$), 32.7 (t, C-1, C-2, C-9, C-10), 34.8 (s, **C**(CH$_3$)$_3$), 92.6 (s, C-8', C-8'', C-8''', C-8''''), 93.3(s, C-7', C-7'', C-7''', C-7''''), 97.6 (s, C-10', C-10'', C-10''', C-10''''), 104.3 (s, C-9', C-9'', C-9''', C-9''''),

123.5 (s, C-1', C-1", C-1'", C-1""), 124.8 (s, C-2', C-2", C-2'", C-2""), 125.4 (s, C-4, C-7, C-13, C-16), 125.7 (d, C-5', C-5", C-5'", C-5""), 129.7 (d, C-3', C-3", C-3'", C-3""), 132.2 (d, C-6', C-6", C-6'", C-6""), 135.0 (d, C-5, C-8, C-12, C-15), 141.9 (s, C-3, C-6, C-11, C-14), 151.1 (s, C-4', C-4", C-4'", C-4"")

IR (ATR): $\tilde{\nu}$ = 2958 cm^{-1} (m), 2921 (m), 2900 (m), 2864 (m), 2153 (w), 2135 (w), 1587 (w), 1540 (w), 1498 (m), 1463 (m), 1431 (m), 1392 (m)1292 (w), 1247 (m), 1199 (w), 1102 (w), 926 (m), 856 (w), 832 (vs), 830 (vs), 810 (m), 757 (m), 722 (m), 696 (m), 642 (m), 593 (m), 567 (m), 545 (m)

UV (CH_2Cl_2): λ_{max} (lg ε) = 240 nm (5.25), 250 (5.21), 268 (5.09), 312 (4.76), 332 (4.88), 374 (5.03), 386 (5.01)

MS (EI): *m/z* (%) = 1218/1219/1220 (22/15/8) [M^+], 1217 (20) [M^+-H], 1144/1145/1146 (20/20/13) [M^+-$SiMe_3$], 1072 (17) [M^+-2 $SiMe_3$], 1000 (11) [M^+-3 $SiMe_3$], 73 (100) [$SiMe_3^+$]

Exp. 37: *tert*-Butyl-annulene (157)

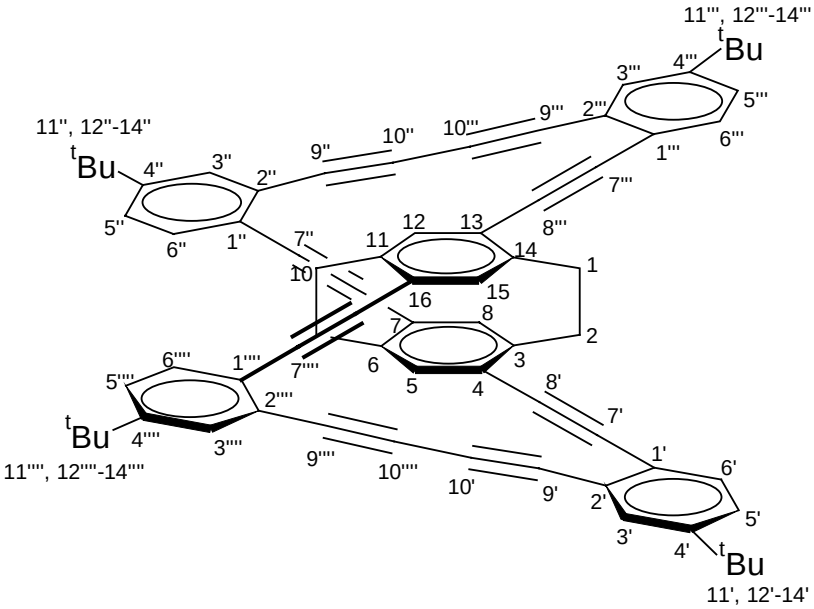

157

38 mg (0.033 mmol) of **167** in 66 mL of methanol, 66 mL of acetonitrile and 13 mL of dichloromethane was subjected to general procedure E using 46 mg (0.33 mmol) of K_2CO_3 and 265 mg (1.32 mmol) of $Cu(OAc)_2 \cdot H_2O$. Purification by preparative thick layer chromatography with 20% dichloromethane in pentane (R_f = 0.49) yielded 12 mg (0.013 mmol, 40%) of **157** as a light yellow solid (decomp. ~220 °C).

^{1}H NMR ($CDCl_3$): δ = 1.35 (s, 36 H, C(C**H**$_3$)$_3$), 3.06-3.14 (m, 4 H, 1-H, 2-H, 9-H, 10-H), 3.48-3.56 (m, 4 H, 1-H, 2-H, 9-H, 10-H), 7.18 (s, 4 H, 5-H, 8-H, 12-H, 15-H), 7.40 (dd, ^{3}J = 8.2 Hz, ^{4}J = 2.0 Hz, 4 H, 5'-H, 5''-H, 5'''-H, 5''''-H), 7.48 (d, ^{3}J = 8.2 Hz, 4 H, 6'-H, 6''-H, 6'''-H, 6''''-H), 7.55 (d, ^{4}J = 2.0 Hz, 4 H, 3'-H, 3''-H, 3'''-H, 3''''-H)

^{13}C NMR ($CDCl_3$): δ = 31.0 (q, C(**C**H$_3$)$_3$), 33.1 (t, C-1, C-2, C-9, C-10), 34.9 (s, **C**(CH$_3$)$_3$), 78.2 (s, C-10', C-10'', C-10''', C-10''''), 82.4 (s, C-9', C-9'', C-9''', C-9''''), 92.7 (s, C-7', C-7'', C-7''', C-7'''' or C-8', C-8'', C-8''', C-8'''), 92.9 (s, C-7', C-7'', C-7''', C-7'''' or C-8', C-8'', C-8''', C-8'''), 123.9 (s, C-2', C-2'', C-2''', C-2''''), 124.4 (s, C-4, C-7, C-13, C-16), 125.7 (s, C-1', C-1'', C-1''', C-1''''), 126.4 (d, C-5', C-5'', C-5''', C-5''''), 128.1 (d, C-3', C-3'', C-3''', C-3''''), 132.1 (d, C-6', C-6'', C-6''', C-6''''), 133.8 (d, C-5, C-8, C-12, C-15), 143.1 (s, C-3, C-6, C-11, C-14), 151.6 (s, C-4', C-4'', C-4''', C-4'''')

IR (ATR): $\tilde{\nu}$ = 2959 cm^{-1} (s), 2926 (m), 2902 (m), 2867 (m), 1594 (w), 1494 (s), 1462 (m), 1427(m), 1394 (m), 1363(m), 1255 (m), 1200 (m), 1127 (m), 1027 (m), 900 (m), 828 (s), 738 (m), 725(m), 712(m), 636 (m), 601 (m), 567 (m), 551 (s)

UV (CH_2Cl_2): λ_{max} (lg ε) = 232 nm (5.11), 258 (4.82), 290 (4.80), 312 (5.15), 338 (4.95), 366 (4.67), 394 (4.78)

MS (MALDI-TOF): *m*/*z* = 947.3/948.4/949.4 [M^{+}+Na], 924.3/925.4/926.4 [M^{+}]

Exp. 38: 4,7,13,16-Tetrakis(4'-*N*,*N*-dibutylamino-2'-[trimethylsilyl]ethynyl-phenylethynyl)[2.2]paracyclophane (168)

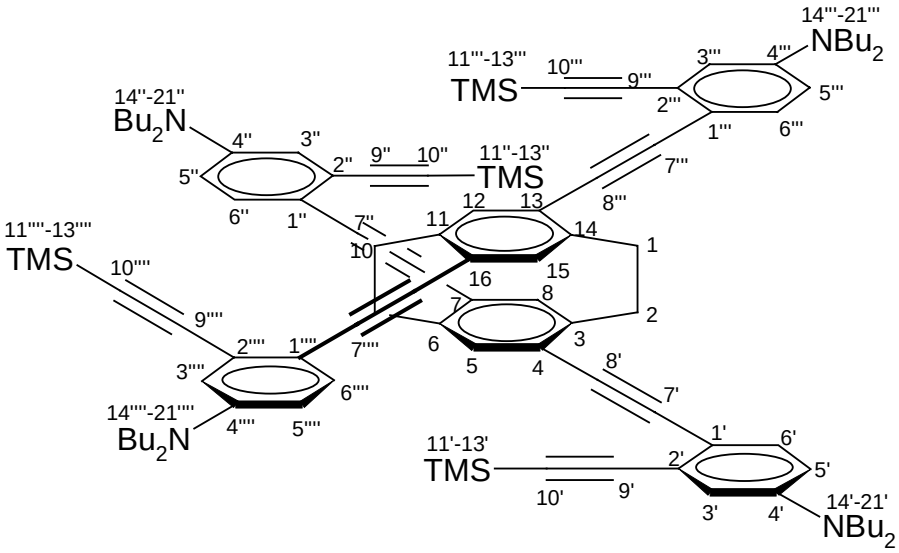

168

26 mg (0.085 mmol) of 4,7,13,16-tetraethynyl[2.2]paracyclophane (**164**) in 1 mL of THF was coupled with 172 mg (0.425 mmol) of *N*,*N*-dibutyl-4-iodo-3-[(trimethylsilyl)-ethynyl]aniline (**125**) in 5 mL of THF and 6 mL of diisopropylamine as described in general procedure B using 8 mg (0.007 mmol) of $Pd(PPh_3)_4$ and 1 mg (0.007 mmol) of CuI. Purification by preparative thick layer chromatography with 20% dichloromethane in pentane (R_f = 0.22) yielded 50 mg (0.033 mmol, 39%) of **168** as a yellow solid (m.p. 88°C).

^{1}H NMR ($CDCl_3$): δ = 0.22 (s, 36 H, Si(C**H**$_3$)$_3$), 0.97 ("t", ^3J = 7.4 Hz, 24 H, $NCH_2CH_2CH_2C$**H**$_3$), 1.37 ("six", J = 7.4 Hz, 16 H, NCH_2CH_2C**H**$_2CH_3$), 1.55-1.62 (m, 16 H, NCH_2C**H**$_2CH_2CH_3$), 3.07-3.13 (m, 4 H, 1-H, 2-H, 9-H, 10-H), 3.29 (t, J = 7.5 Hz, 16 H, NC**H**$_2CH_2CH_2CH_3$), 3.62-3.70 (m, 4 H, 1-H, 2-H, 9-H, 10-H), 6.59 (dd, $^3J_{5',6'}$ = 8.8 Hz, $^4J_{5',3'}$ = 2.6 Hz, 4 H, 5'-H, 5''-H, 5'''-H, 5''''-H), 6.75 (d, $^4J_{3',5'}$ = 2.6 Hz, 4 H, 3'-H, 3''-H, 3'''-H, 3''''-H), 7.15 (s, 4 H, 5-H, 8-H, 12-H, 15-H), 7.42 (d, $^3J_{6',5'}$ = 8.8 Hz, 4 H, 6'-H, 6''-H, 6'''-H, 6''''-H)

^{13}C NMR ($CDCl_3$): δ = 0.1 (q, Si(**C**H$_3$)$_3$), 14.0 (q, $NCH_2CH_2CH_2$**C**H$_3$), 20.3 (t, NCH_2CH_2**C**H$_2CH_3$), 29.4 (t, NCH_2**C**H$_2CH_2CH_3$), 32.8 (t, C-1, C-2, C-9, C-10), 50.6 (t, N**C**H$_2CH_2CH_2CH_3$), 91.1 (s, C-8', C-8'', C-8''', C-8''''), 93.9 (s, C-7', C-7'', C-7''', C-7''''), 96.6 (s, C-10', C-10'', C-10''', C-10''''), 105.0 (s, C-9', C-9'', C-9''', C-9''''), 112.2 (d, C-5', C-5'', C-5''', C-5''''), 113.1 (s, C-1', C-1'', C-1''', C-1''''), 115.1 (d, C-3', C-3'', C-3''',

C-3""), 125.3 (s, C-4, C-7, C-13, C-16), 125.9 (s, C-2', C-2", C-2"', C-2""), 133.6 (d, C-6', C-6", C-6"', C-6""), 134.4 (d, C-5, C-8, C-12, C-15), 141.4 (s, C-3, C-6, C-11, C-14), 147.3 (s, C-4', C-4", C-4"', C-4"")

IR (ATR): $\tilde{\nu}$ = 2956 cm^{-1} (m), 2929 (m), 2868 (m), 2193 (w), 2151 (w), 1593 (vs), 1535 (m), 1506 (s), 1463 (w), 1363 (m), 1294 (w), 1246 (m), 1224 (m), 1180 (m), 1096 (s), 939 (w), 906 (w), 836 (vs), 804 (s), 755 (m), 722 (m), 697 (m), 653 (w), 626 (m), 581 (w), 531 (w)

UV (CH_2Cl_2): λ_{max} (lg ε) = 246 nm (4.99), 262 (4.92), 358 (4.74), 422 (5.00)

MS (EI): *m/z* (%) = 1500/1501/1502/1503/1504 (18/25/20/13/7) [M^+], 1427/1428/1429 (6/7/5) [M^+-$SiMe_3$], 1277/1278/1279 (8/8/6)[M^+-3 $SiMe_3$], 73 (100) [$SiMe_3^+$]

Exp. 39: *N,N*-Dibutylamino-annulene (158)

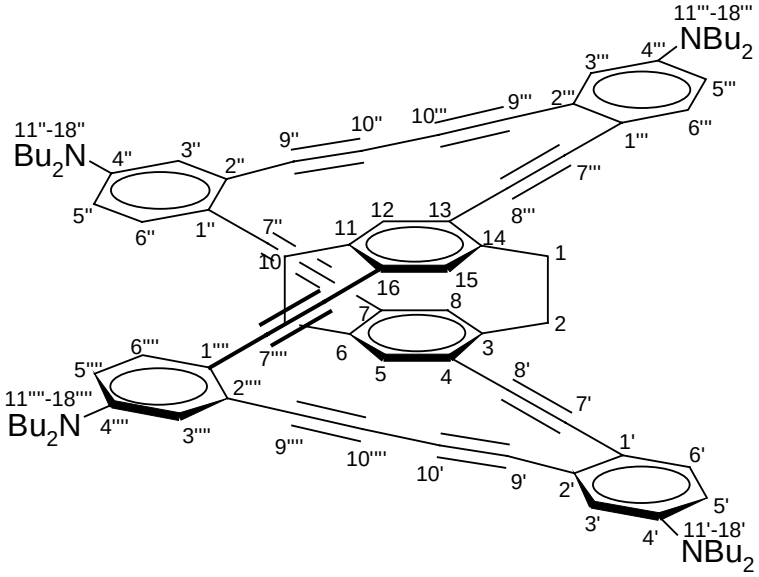

158

A solution of 38 mg (0.025 mmol) of **168** in 50 mL of methanol, 50 mL of acetonitrile and 10 mL of dichloromethane was subjected to general procedure E using 35 mg (0.25 mmol) of K_2CO_3 and 200 mg (1 mmol) of $Cu(OAc)_2 \cdot H_2O$. Purification by preparative thick layer chromatography using 20% dichloromethane in pentane (R_f = 0.6) yielded 20 mg (0.017 mmol, 66%) of **158** as a yellow solid (decomp. ~185 °C).

^{1}H NMR ($CDCl_3$): δ = 0.98 ("t", ^3J = 7.4 Hz, 24 H, $NCH_2CH_2CH_2C\mathbf{H}_3$), 1.36 ("six", *J* = 7.4 Hz, 16 H, $NCH_2CH_2C\mathbf{H}_2CH_3$), 1.54-1.70 (m, 16 H, $NCH_2C\mathbf{H}_2CH_2CH_3$), 3.05-

3.16 (m, 4 H, 1-H, 2-H, 9-H, 10-H), 3.27-3.30 (m, 16 H, NC**H**$_2$CH$_2$CH$_2$CH$_3$), 3.43-3.48 (m, 4 H, 1-H, 2-H, 9-H, 10-H), 6.61 (dd, $^3J_{5',6'}$ = 8.8 Hz, $^4J_{5',3'}$ not resolved, 4 H, 5'-H, 5''-H, 5'''-H, 5''''-H), 6.72 (d, $^4J_{3',5'}$ not resolved, 4 H, 3'-H, 3''-H, 3'''-H, 3''''-H), 7.14 (s, 4 H, 5-H, 8-H, 12-H, 15-H), 7.35 (d, $^3J_{6',5'}$ = 8.8 Hz, 4 H, 6'-H, 6''-H, 6'''-H, 6''''-H)

^{13}C NMR (CDCl$_3$): δ = 14.0 (q, NCH$_2$CH$_2$CH$_2$**C**H$_3$), 20.3 (t, NCH$_2$CH$_2$**C**H$_2$CH$_2$CH$_3$), 29.4 (t, NCH$_2$**C**H$_2$CH$_2$CH$_3$), 33.1 (t, C-1, C-2, C-9, C-10), 50.8 (t, N**C**H$_2$CH$_2$CH$_2$CH$_3$), 77.2 (s, C-10', C-10'', C-10''', C-10''''), 82.7 (s, C-9', C-9'', C-9''', C-9''''), 91.1 (s, C-8', C-8'', C-8''', C-8''''), 93.6 (s, C-7', C-7'', C-7''', C-7''''), 112.5 (d, C-5', C-5'', C-5''', C-5''''), 113.3 (s, C-3', C-3'', C-3''', C-3''''), 115.0 (d, C-1', C-1'', C-1''', C-1''''), 124.4 (s, C-4, C-7, C-13, C-16), 125.1 (s, C-2', C-2'', C-2''', C-2''''), 133.4 (d, C-5, C-8, C-12, C-15), 133.6 (d, C-6', C-6'', C-6''', C-6''''), 142.5 (s, C-3, C-6, C-11, C-14), 147.4 (s, C-4', C-4'', C-4''', C-4'''')

IR (ATR): $\tilde{\nu}$ = 2955 cm^{-1} (m), 2928 (m), 2871 (m), 2187 (w), 1593 (vs), 1533 (m), 1504 (s), 1462 (m), 1366 (m), 1252 (w), 1217 (m), 1182 (w), 1110 (w), 1093 (m), 906 (w), 843 (w), 806 (m), 713 (w)

UV (CH$_2$Cl$_2$): λ_{max} (lg ε) = 232 nm (4.93), 292 (4.76), 330 (4.97), 346 (5.00), 366 (4.82), 452 (4.80)

MS (MALDI-TOF): *m*/*z* = 1209.6/1210.7/1211.7/1212.7/1213.7 [M$^+$+H], 1208.7/1209.6/1210.7/1211.7/1212.7 [M$^+$], 1207.7/1208.7/1209.6/1210.7/1211.7 [M$^+$-H]

10.3.6 Synthesis of the unbrideged propeller type dehydrobenzoannulenes

Exp. 40: 1,4-Bis(trimethylsilylethynyl)benzene (176)

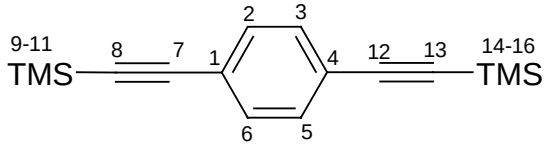

176

3.30 g (10 mmol) of 1,4-diiodobenzene was subjected to general procedure A using 40 mL of THF, 40 mL of diisopropylamine, 462 mg (0.4 mmol) of Pd(PPh$_3$)$_4$, 152 mg (0.8 mmol) of CuI and 5.7 mL (40 mmol) of TMSA. Column chromatography on silica gel

with pentane (R_f = 0.23) gave 2.52 g (9.3 mmol, 93%; ref[76] 99%) of **176** as a colorless solid (m.p. 118 °C).

^{1}H NMR ($CDCl_3$): δ = 0.25 (s, 18 H, Si(C**H**$_3$)$_3$), 7.43 (s, 4 H, 2-H, 3-H, 5-H, 6-H)

^{13}C NMR ($CDCl_3$): δ = -1.1 (q, Si(**C**H$_3$)$_3$), 96.3 (s, C≡C-TMS), 104.6 (s, C≡C-TMS), 123.1 (s, C-1, C-4), 131.7 (d, C-2, C-3, C-5, C-6)

IR (ATR): $\tilde{\nu}$ = 2956 cm^{-1} (m), 2898 (w), 2154 (s), 1491 (m), 1414 (m), 1245 (s), 1214 (m), 1102 (w), 1047 (w), 1016 (w), 825 (vs), 752 (vs), 696 (s), 626 (m), 547 (vs)

UV (CH_2Cl_2): λ_{max} (lg ε) = 264 nm (4.20), 280 (4.51), 288 (4.37), 294 (4.58)

MS (EI): *m/z* (%) = 270 (33) [M$^+$], 256 (32), 255 (100)

Exp. 41: 1,4-Diethynylbenzene (177)

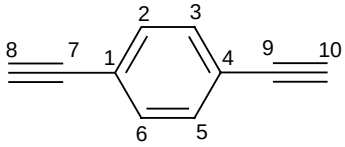

177

676 mg (2.5 mmol) of 1,4-bis(trimethylsilylethynyl)benzene (**176**) in 12 mL of methanol and 12 mL of dichloromethane was subjected to general procedure D using 1.38 g (10 mmol) of K_2CO_3. Evaporation of the solvent gave 303 mg (2.4 mmol, 96%; ref[76] 97%) of **177** as a colorless solid (m.p. 87 °C).

^{1}H NMR ($CDCl_3$): δ = 3.17 (s, 2 H, C≡C-**H**), 7.44 (s, 4 H, 2-H, 3-H, 5-H, 6-H)

^{13}C NMR ($CDCl_3$): δ = 79.0 (s, C≡C-H), 83.0 (s, C≡C-H), 122.5 (s, C-1, C-4), 132.0 (d, C-2, C-3, C-5, C-6)

IR (ATR): $\tilde{\nu}$ = 3259 cm^{-1} (vs), 2214 (w), 2103 (w), 1918 (w), 1795 (w), 1674 (w), 1493 (m), 1402 (w), 1369 (w), 1252 (m), 1105 (w), 1015 (w), 964 (w), 832 (vs), 703 (m), 674 (vs), 637 (vs), 572 (vs), 544 (vs)

UV (CH_2Cl_2): λ_{max} (lg ε) = 262 nm (4.49), 274 (4.54), 292 (3.08)

MS (EI): *m/z* (%) = 126 (100) [M$^+$]

Exp. 42: 1,4-Bis(4'-*tert*-butyl-2'-[trimethylsilyl]ethynyl-phenylethynyl)benzene (159)

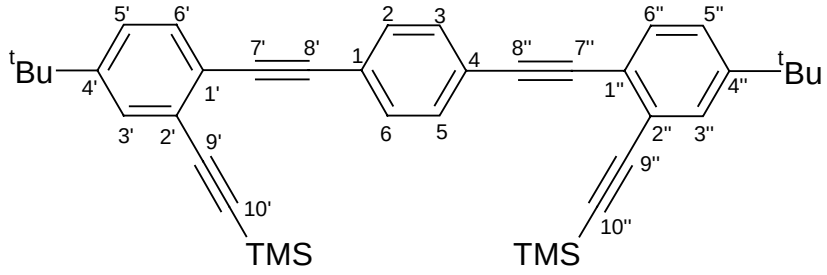

159

126 mg (1.0 mmol) of 1,2-diethynylbenzene (**177**) in 2 mL of THF was coupled with 843 mg (2.5 mmol) of 4-*tert*-butyl-2-[(trimethylsilyl)ethynyl]iodobenzene (**121**) in 5 mL of THF and 7 mL of diisopropylamine as described in general procedure B using 46 mg (0.04 mmol) of $Pd(PPh_3)_4$ and 7 mg (0.04 mmol) of CuI. Column chromatography on silica gel with 5% dichloromethane in pentane (R_f = 0.07) gave 329 mg (0.56 mmol, 56%) of **159** as a colorless solid (m.p. 190 °C).

^{1}H NMR ($CDCl_3$): δ = 0.21 (s, 18 H, Si(C**H**$_3$)$_3$), 1.24 (s, 18 H, C(C**H**$_3$)$_3$), 7.25 (dd, $^3J_{5',6'}$ = 8.2 Hz, $^4J_{5',3'}$ = 2.0 Hz, 2 H, 5'-H, 5''-H), 7.36 (d, $^3J_{6',5'}$ = 8.2 Hz, 2 H, 6'-H, 6''-H), 7.45 (d, $^4J_{3',5'}$ = 2.0 Hz, 2 H, 3'-H, 3''-H), 7.45 (s, 4 H, 2-H, 3-H, 5-H, 6-H)

^{13}C NMR ($CDCl_3$): δ = 0.1 (q, Si(**C**H$_3$)$_3$), 31.0 (q, C(**C**H$_3$)$_3$), 34.8 (s, **C**(CH$_3$)$_3$), 90.3 (s, C-7', C-7''), 92.5 (s, C-8', C-8''), 97.9 (s, C-10', C-10''), 104.0 (s, C-9', C-9''), 123.0 (s, C-1', C-1''), 123.3 (s, C-1, C-4), 125.3 (s, C-2', C-2''), 125.7 (d, C-5', C-5''), 129.3 (d, C-3', C-3''), 131.4 (d, C-6', C-6''), 131.5 (d, C-2, C-3, C-5, C-6), 151.5 (s, C-4', C-4'')

IR (ATR): $\tilde{\nu}$ = 2956 cm^{-1} (m), 2900 (w), 2867 (w), 2158 (m), 1512 (m), 1479 (w), 1462 (w), 1396 (m), 1363(w), 1243 (m), 1204 (w), 1087 (w), 927 (m), 897 (w), 835 (vs), 756 (s), 697 (m), 654(m), 640 (m)

UV (CH_2Cl_2): λ_{max} (lg ε) = 255 nm (4.49), 263 (4.63), 291 (4.16), 342 (4.63), 364 (4.47)

MS (EI): *m/z* (%) = 582/583/584 (100/54/19) [M$^+$], 567 (18), 276 (19), 221 (15), 145 (25), 73 (26) [SiMe$_3^+$]

$C_{40}H_{46}Si_2$ (582.95) calcd. C 82.41, H 7.95, Si 9.64; found C 82.13, H 8.09

Exp. 43: 1,4-Bis(4'-*tert*-butyl-2'-ethynyl-phenylethynyl)benzene (161)

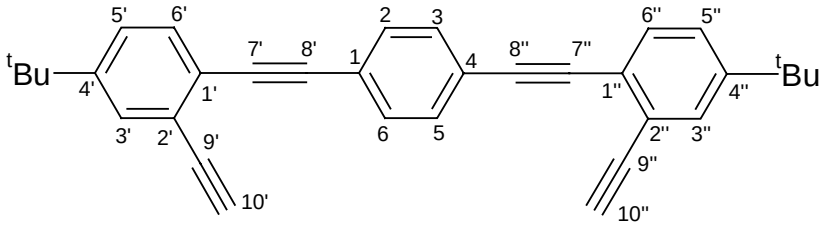

161

145 mg (0.25 mmol) of **159** in 7.5 mL of dichloromethane and 7.5 mL of methanol was subjected to general procedure D using 276 mg (2 mmol) of K_2CO_3. The solvents were removed *in vacuo* and the residue dried in high vacuum to yield 101 mg (0.23 mmol, 92%) of **161** as a colorless solid (m.p. 168 °C).

^{1}H NMR ($CDCl_3$): δ = 1.32 (s, 18 H, C(C**H**$_3$)$_3$), 3.35 (s, 2 H, C≡C-**H**), 7.36 (dd, $^3J_{5',6'}$ = 8.3, $^4J_{5',3'}$ = 2.0 Hz, 2 H, 5'-H, 5''-H) 7.47 (d, $^3J_{6',5'}$ = 8.3 Hz, 2 H, 6'-H, 6''-H), 7.52 (s, 4 H, 2-H, 3-H, 5-H, 6-H), 7.56 (d, $^4J_{3',5'}$ = 2.0 Hz, 2 H, 3'-H, 3''-H)

^{13}C NMR ($CDCl_3$): δ = 31.0 (q, C(**C**H$_3$)$_3$), 34.8 (s, **C**(CH$_3$)$_3$), 80.5 (d, C-10), 82.7 (s, C-9), 89.9 (s, C-7), 92.6 (s,C-8), 123.2 (s, C-1', C-1'' or C-1, C-4), 123.3 (s, C-1, C-4 or C-1', C-1''), 124.3 (s, C-2', C-2''), 126.0 (d, C-5', C-5''), 129.7 (d, C-3', C-3''), 131.6 (C-6', C-6''), 131.6 (d, C-2, C-3, C-5, C-6), 151.6 (s, C-4', C-4'')

IR (ATR): $\tilde{\nu}$ = 3274 cm^{-1} (s), 3061 (w), 3039 (w), 2955 (m), 2899 (m), 2861 (m), 2111 (w), 2109 (w), 1908 (w), 1783 (w), 1507 (m), 1472 (m), 1397 (m), 1361 (m), 1261 (m), 1188 (m), 1123 (w), 1098 (w), 897 (s), 828 (s), 741 (m), 670 (s), 645 (vs), 613 (m), 547 (m)

UV (CH_2Cl_2): λ_{max} (lg ε) = 286 nm (4.47), 318 (4.06), 330 (4.52), 338 (4.61), 338 (4.70), 360 (4.52)

MS (EI): *m/z* (%) = 440/439/438 (7/34/100) [M$^+$], 425/424/423 (4/18/52)

$C_{34}H_{30}$ (438.61) calcd. C 93.11%, H 6.89%; found C 93.05, H 6.91

Exp. 44: *tert*-Butyl-anulene (154)

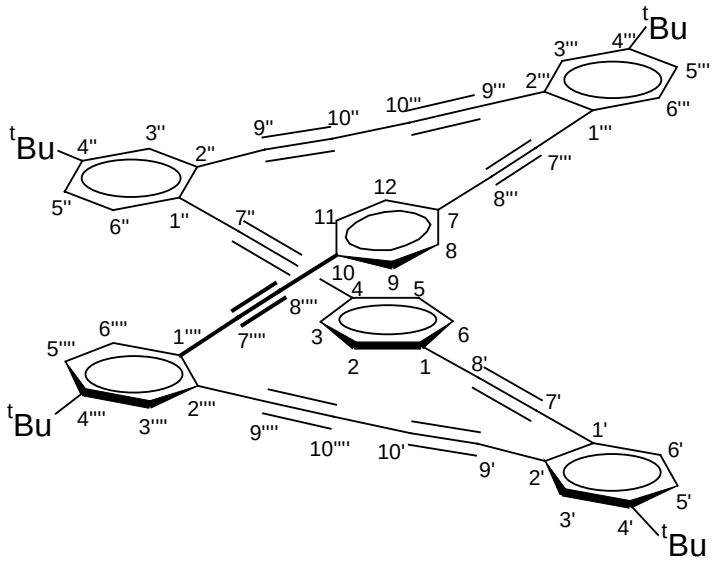

154

329 mg (0.75 mmol) of **161** in 120 mL of pyridine/ether 3:1 was dimerized as described in general procedure F using 900 mg (4.5 mmol) of $Cu(OAc)_2 \cdot H_2O$ in 255 mL of pyridine/ether (3:1). Column chromatography on silica gel with 20% dichloromethane in pentane gave 25 mg (0.03 mmol, 8%) of **154** as a colorless solid (decomposition at 170 °C). Single crystals suitable for X-ray structure analysis were obtained by slow diffusion of methanol in a dichloromethane solution of **154**.

^{1}H NMR ($CDCl_3$): δ = 1.34 (s, 36 H, C(C**H**$_3$)$_3$), 7.28 (s, 8 H, 2-H, 3-H, 5-H, 6-H, 8-H, 9-H, 11-H, 12-H), 7.38 (dd, ^3J = 8.3, ^4J = 1.9 Hz, 4 H, 5'-H, 5''-H, 5'''-H, 5''''-H), 7.44 (d, ^3J = 8.3 Hz, 4 H, 6'-H, 6''-H, 6'''-H, 6''''-H), 7.59 (d, ^4J = 1.9 Hz, 4 H, 3'-H, 3''-H, 3'''-H, 3''''-H)

^{13}C NMR ($CDCl_3$): δ = 31.0 (q, C(**C**H$_3$)$_3$), 34.8 (s, **C**(CH$_3$)$_3$), 77.5 (s, C-10', C-10'', C-10''', C-10''''), 81.6 (s, C-9', C-9'', C-9''', C-9''''), 89.3 (s, C-7', C-7'', C-7''', C-7''''), 93.9 (s, C-8', C-8'', C-8''', C-8''''), 122.6 (s, C-1, C-4, C-7, C-10), 124.6 (s, C-2', C-2'', C-2''', C-2''''), 124.6 (s, C-1', C-1'', C-1''', C-1''''), 126.4 (d, C-5', C-5'', C-5''', C-5''''), 129.3 (d, C-3', C-3'', C-3''', C-3''''), 131.1 (d, C-6', C-6'', C-6''', C-6''''), 131.5 (d, C-2, C-3, C-5, C-6, C-8, C-9, C-11, C-12), 151.5 (s, C-4', C-4'', C-4''', C-4'''')

IR (ATR): $\tilde{\nu}$ = 2957 cm^{-1} (m), 2926 (m), 2901 (m), 2866 (m), 2215 (w), 1909 (w), 1594 (w), 1512 (m), 1460 (m), 1393 (m), 1363 (m), 1254 (m), 2101 (m), 1126 (m), 1099 (m), 1018 (m), 891 (m), 828 (vs), 736 (m), 636 (m), 596 (w), 542 (m)

UV (CH_2Cl_2): λ_{max} (lg ε) = 304 nm (5.05), 330 (4.96), 360 (4.73)

MS (MALDI-TOF): *m*/*z* = 872.3/873.3/874.3 [M^+]

Exp. 45: 1,4-Bis(4'-*N*,*N*-dibutylamino-2'-[trimethylsilyl]ethynyl-phenylethynyl)-benzene (160)

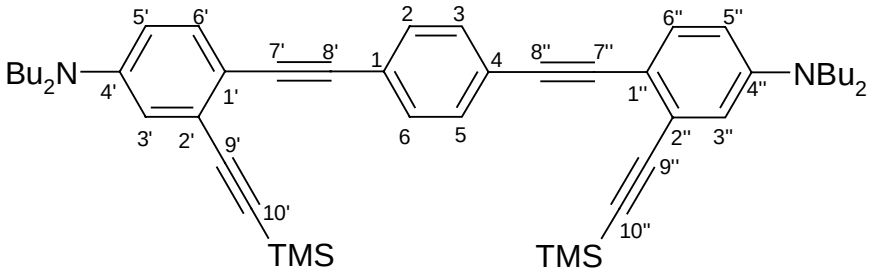

160

189 mg (1.5 mmol) of 1,2-diethynylbenzene (**177**) in 1.5 mL of THF was coupled with 1.513 g (3.75 mmol) of *N*,*N*-dibutyl-4-iodo-3-[(trimethylsilyl)ethynyl]aniline (**125**) in 4 mL of THF and 5.5 mL of diisopropylamine as described in general procedure B using 69 mg (0.06 mmol) of $Pd(PPh_3)_4$ and 11 mg (0.06 mmol) of CuI. Column chromatography on silica gel with 20% dichloromethane in pentane (R_f = 0.1) gave 428 mg (0.59 mmol, 39%) of **160** as a yellow solid (m.p. 140 - 144 °C).

^{1}H NMR ($CDCl_3$): δ = 0.29 (s, 18 H, Si(C**H**$_3$)$_3$), 0.94 ("t", ^3J = 7.4 Hz, 12 H, $NCH_2CH_2CH_2C\mathbf{H}_3$), 1.32 ("six", ^3J = 7.4 Hz, 8 H, $NCH_2CH_2C\mathbf{H}_2CH_3$), 1.52 ("q", ^3J = 7.5 Hz, 8 H, $NCH_2C\mathbf{H}_2CH_2CH_3$), 3.22 ("t", ^3J = 7.6 Hz, 8 H, $N\mathbf{C}H_2CH_2CH_2CH_3$), 6.52 (dd, $^3J_{5',6'}$ = 8.9 Hz, $^4J_{5',3'}$ = 2.7 Hz, 2 H, 5'-H, 5"-H), 6.71 (d, $^4J_{3',5'}$ = 2.7 Hz, 2 H, 3'-H, 3"-H), 7.31 (d, $^3J_{6',5'}$ = 8.9 Hz, 2 H, 6'-H, 6"-H), 7.47 (s, 4 H, 2-H, 3-H, 5-H, 6-H)

^{13}C NMR ($CDCl_3$): δ = 0.1 (q, Si(**C**H$_3$)$_3$), 13.9 (q, $NCH_2CH_2CH_2\mathbf{C}H_3$), 20.2 (t, $NCH_2CH_2\mathbf{C}H_2CH_3$), 29.3 (t, $NCH_2\mathbf{C}H_2CH_2CH_3$), 50.4 (t, $N\mathbf{C}H_2CH_2CH_2CH_3$), 90.8 (s, C-8', C-8"), 91.3 (s, C-7', C-7"), 96.6 (s, C-10', C-10"), 104.7 (s, C-9', C-9"), 111.8 (s, C-1', C-1"), 111.9 (d, C-5', C-5"), 114.6 (d, C-3', C-3"), 123.2 (s, C-1, C-4), 126.4 (s, C-2', C-2"), 130.9 (d, C-2, C-3, C-5, C-6), 132.7 (d, C-6', C-6"), 147.5 (s, C-4', C-4")

IR (ATR): $\tilde{\nu}$ = 2956 cm^{-1} (m), 2929 (m), 2894 (m), 2872 (m), 2857 (m), 2204 (m), 2152 (m), 1593 (vs), 1534 (m), 1515 (s), 1493 (m), 1463 (m), 1427 (m), 1399 (m), 1386 (m), 1295 (m), 1247 (m), 1221 (m), 1182 (m), 1097 (s), 940 (w), 905 (w), 833 (vs), 803 (s), 753 (m), 696 (w), 629 (w), 540 (w)

UV (CH_2Cl_2): λ_{max} (lg ε) = 258 nm (4.56), 266 (4.57), 300 (4.05), 360 (4.48), 402 (4.67)

MS (EI): *m/z* (%) = 724/725 (100/24) [M^+], 681 (20), 639 (16), 319 (14), 277 (15), 73 (10) [$SiMe_3^+$]

$C_{48}H_{64}N_2Si_2$ (725.22) calcd.: C 79.50, H 8.90, N 3.86, Si 7.74; found C 79.17, H 9.13, N 3.86

Exp. 46: 1,4-Bis(4'-N,N-dibutylamino-2'-ethynyl-phenylethynyl)benzene (162)

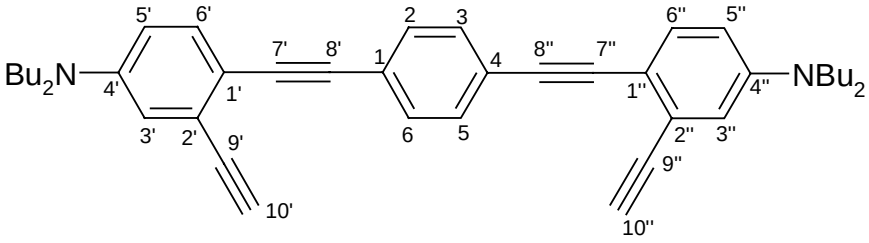

162

181 mg (0.25 mmol) of **159** in 7.5 mL of dichloromethane and 7.5 mL of methanol was subjected to general procedure D using 276 mg (2 mmol) of K_2CO_3. The solvents were removed *in vacuo* and the residue was dried in high vacuum to yield 132 mg (0.23 mmol, 91%) of **162** as a yellow solid (m.p. 128 °C).

^{1}H NMR ($CDCl_3$): δ = 0.94 ("t", *J* = 7.3 Hz, 12 H, $NCH_2CH_2CH_2C\mathbf{H}_3$), 1.33 (six, *J* = 7.5 Hz, 8 H, $NCH_2CH_2C\mathbf{H}_2CH_3$), 1.50-1.57 (m, 8 H, $NCH_2C\mathbf{H}_2CH_2CH_3$), 3.24 (t, *J* = 7.6 Hz, 8 H, $NC\mathbf{H}_2CH_2CH_2CH_3$), 3.28 (s, 2 H, 10-H), 6.55 (dd, $^3J_{5',6'}$ = 8.9 Hz, $^4J_{5',3'}$ = 2.7 Hz, 2 H, 5'-H, 5"-H), 6.74 (d, $^4J_{3',5'}$ = 2.7 Hz, 2 H, 3'-H, 3"-H), 7.32 (d, $^3J_{3',5'}$ = 8.9 Hz, 2 H, 3'-H, 3"-H), 7.45 (s, 4 H, 2-H, 3-H, 5-H, 6-H)

^{13}C NMR ($CDCl_3$): δ = 13.9 (q, $NCH_2CH_2CH_2\mathbf{C}H_3$), 20.2 (t, $NCH_2CH_2\mathbf{C}H_2CH_3$), 29.3 (t, $NCH_2\mathbf{C}H_2CH_2CH_3$), 50.6 (t, $N\mathbf{C}H_2CH_2CH_2CH_3$), 79.5 (d, C-10', C-10"), 83.3 (s, C-9', C-9"), 90.9 (s, C-7', C-7", C-8', C-8"), 111.9 (s, C-1', C-1"), 112.2 (d, C-5', C-5"), 115.0 (d, C-3), 132.2 (s, C-4, C-5), 125.4 (s, C-2', C-2"), 131.1 (d, C-2, C-3, C-5, C-6), 132.9 (d, C-6', C-6"), 147.6 (s, C-4', C-4")

IR (ATR): $\tilde{\nu}$ = 3292 cm^{-1} (m), 2957 (m), 2928 (m), 2873 (m), 2859 (m), 2201 (m), 2107 (w), 1593 (vs)m 1534 (m), 1516 (s), 1463 (m), 1425 (w), 1399 (m), 1369 (s), 1292

(m), 1257 (m), 1221 (m), 1179 (m), 1091 (s), 1015 (w), 941 (w), 880 (w), 836 (vs), 807 (vs), 746 (w), 654 (m), 627 (vs), 609 (vs), 574 (m), 541(vs)

UV (CH_2Cl_2): λ_{max} (lg ε) = 241 nm (4.58), 249 (4.56), 298 (4.17), 359 (4.58), 397 (4.80), 406 (4.78)

MS (EI): *m/z* (%) = 580/581 (100/45) [M^+], 539 (12), 537 (36), 495 (23), 395 (17), 247 (17), 226 (14), 205 (19), 198 (12), 86 (27)

$C_{42}H_{48}N_2$ (580.85) calcd.: C 86.85, H 8.33, N 4.82; found C 86.45, H 8.37, N 4.57

Exp. 47: NBu_2-Anulene (155)

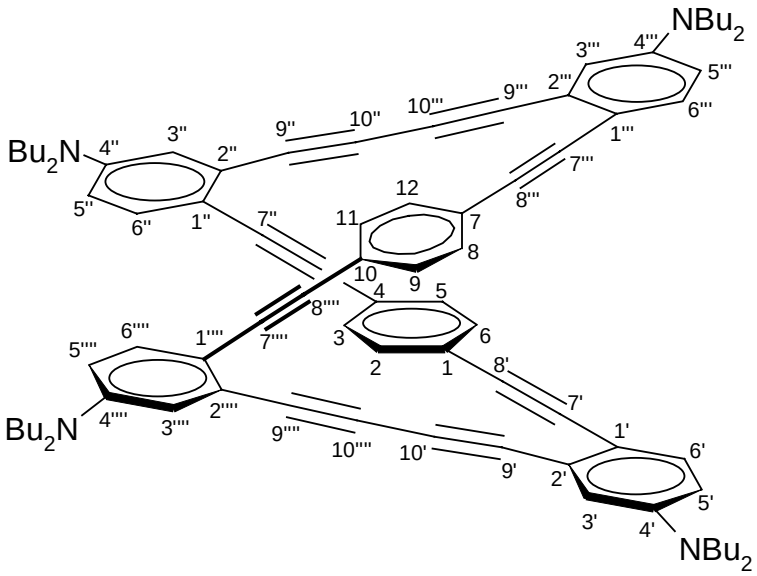

155

153 mg (0.26 mmol) of **162** in 50 mL of pyridine/ether 3:1 was dimerized as described in general procedure F using 312 mg (1.56 mmol) of $Cu(OAc)_2 \cdot H_2O$ in 125 mL of pyridine/ether (3:1). Preparative thick layer chromatography on ALOX with 20% ether in pentane (R_f = 0.33) gave 23 mg (0.02 mmol, 15%) of **155** as a yellow solid (m.p. 248-250 °C).

^{1}H NMR ($CDCl_3$): δ = 0.94 ("t", *J* = 7.3 Hz, 24 H, $NCH_2CH_2CH_2C\mathbf{H}_3$), 1.33 (six, *J* = 7.5 Hz, 16 H, $NCH_2CH_2C\mathbf{H}_2CH_3$), 1.50-1.57 (m, 16 H, $NCH_2C\mathbf{H}_2CH_2CH_3$), 3.24 (t, *J* = 7.6 Hz, 16 H, $NC\mathbf{H}_2CH_2CH_2CH_3$), 6.52 (dd, ^3J = 8.9, ^4J = 2.7 Hz, 4 H, 5'-H, 5''-H, 5'''-H, 5''''-H), 6.70 (d, ^4J = 2.7 Hz, 4 H, 3'-H, 3''-H, 3'''-H, 3''''-H), 7.15 (s, 8 H, 2-H, 3-H, 5-H, 6-H, 8-H, 9-H, 11-H, 12-H), 7.24 (d, ^3J = 8.9 Hz, 4 H, 6'-H, 6''-H, 6'''-H, 6''''-H)

^{13}C NMR ($CDCl_3$): δ = 14.0 (q, $NCH_2CH_2CH_2\mathbf{C}H_3$), 20.3 (t, $NCH_2CH_2\mathbf{C}H_2CH_3$), 29.4 (t, $NCH_2\mathbf{C}H_2CH_2CH_3$), 50.8 (t, $N\mathbf{C}H_2CH_2CH_2CH_3$), 76.8 (s, C-10', C-10", C-10"', C-10""), 81.9 (s, C-9', C-9", C-9"', C-9""), 89.9 (s, C-7', C-7", C-7"', C-7""), 92.2 (s, C-8', C-8", C-8"', C-8""), 113.7 (s, C-1', C-1", C-1"', C-1""), 112.5 (d, C-5', C-5", C-5"', C-5""), 114.5 (d, C-3', C-3", C-3"', C-3""), 122.6 (s, C-1, C-4, C-7, C-10), 125.7 (s, C-2', C-2", C-2"', C-2""), 131.0 (d, C-2, C-3, C-5, C-6, C-8, C-9, C-11, C-12), 132.4 (d, C-6', C-6", C-6"', C-6""), 147.4 (s, C-4', C-4", C-4"', C-4"")

IR (ATR): $\tilde{\nu}$ = 3078 cm^{-1} (m), 3044 (s), 2853 (m), 2208 (w), 1718 (m), 1591 (vs), 1535 (m), 1515 (s), 1493 (m), 1458 (m), 1397 (w), 1364 (s), 1279 (m), 1254 (m), 1216 (s), 1183 (w), 1124 (m), 1092 (s), 1016 (w), 926 (w), 832 (m), 804 (m), 725(m), 542 (m)

UV (CH_2Cl_2): λ_{max} (lg ε) = 234 nm (4.75), 304 (4.67), 324 (4.73), 344 (4.75), 368 (4.74), 420 (4.54)

MS (MALDI-TOF): *m/z* = 1156.7/1157.7/1158.7/1159.7 [M^+]

11 Appendix

11.1 Single crytsal X-ray structure data

Compound	**126**	**53**
Identification code	heihi	phine
Empirical formula	$C_{42}H_{40}Si_2$	$C_{40.75}H_{27}Cl_{0.5}$
Formula weight	600.92	534.35
Temperature	133(2) K	133(2) K
Crystal system	Orthorhombic	Triclinic
Space group	P 21 21 21	P(-1)
Unit cell dimensions	a = 9.3588(8) Å	a = 11.903(2) Å
	b = 12.8978(12) Å	b = 12.782(2) Å
	c = 28.840(3) Å	c = 18.785(3) Å
	α= 90°	α= 90.687(8)°
	β= 90°	β= 95.682(8)°
	γ = 90°	γ = 96.926(8)°
Volume	3481.2(5) $Å^3$	2822.5(8) $Å^3$
Z	4	4
Density (calculated)	1.147 Mg/m^3	1.257 Mg/m^3
Absorption coefficient	0.130 mm^{-1}	0.117 mm^{-1}
F(000)	1280	1120
Crystal size	0.55 x 0.55 x 0.50 mm^3	0.35 x 0.24 x 0.12 mm^3
Theta range for data collection	1.41 to 28.02°	1.09 to 26.37°
Index ranges	-11<=h<=12	-14<=h<=14
	-17<=k<=10	-15<=k<=15
	-35<=l<=38	-23<=l<=23
Reflections collected	24660	25266
Independent reflections	8401 [R(int) = 0.0250]	11502 [R(int) = 0.1195]
Completeness to theta = 28.00°	100.00%	99.80%
Data / restraints / parameters	8401 / 0 / 404	11502 / 0 / 748
Goodness-of-fit on F2	1.017	1.029
Final R indices [I>2sigma(I)]	R1 = 0.0326; wR2 = 0.0822	R1 = 0.0683; wR2 = 0.1663
R indices (all data)	R1 = 0.0381; wR2 = 0.0845	R1 = 0.1113; wR2 = 0.1862
Absolute structure parameter	0.21(7)	
Largest diff. peak and hole	0.330 and -0.165 $e.Å^{-3}$	0.593 and -1.039 $e.Å^{-3}$

4,5-Bis(2'-(trimethylsilylethynyl)phenylethynyl)[2.2]paracyclophane (126)

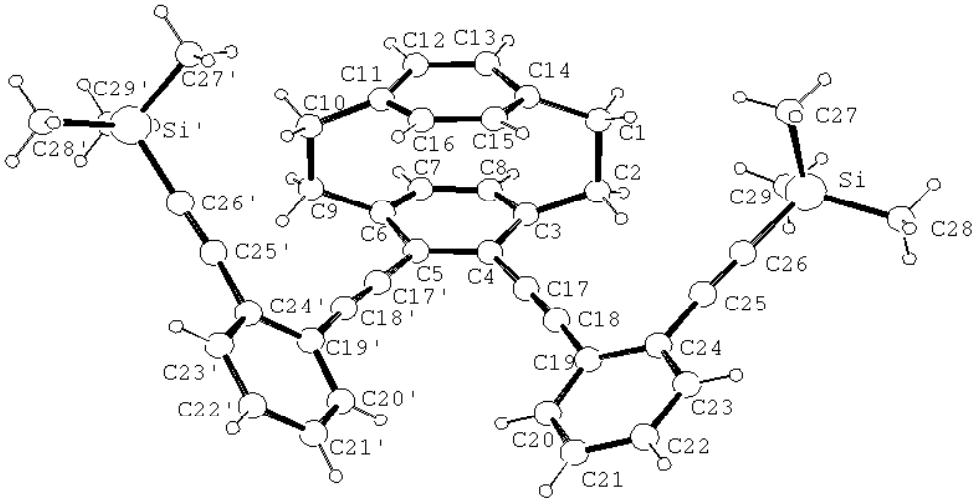

Figure 49: X-ray structure of **126**.

Table 21: Atomic coordinates (x 10^4) and equivalent isotropic displacement parameters ($Å^2$x 10^3). U(eq) is defined as one third of the trace of the orthogonalized Uij tensor.

	x	y	z	U(eq)
Si	4433.8(4)	2963.1(3)	4761.1(1)	26.6(1)
Si'	4651.0(4)	2703.1(3)	383.6(1)	29.0(1)
C(1)	2941.9(19)	1291.6(13)	3463.6(6)	38.9(4)
C(2)	4409.6(18)	695.2(12)	3549.0(5)	34.2(3)
C(3)	5050.4(15)	289.8(10)	3103.0(5)	25.2(3)
C(4)	6123.4(15)	837.7(10)	2861.3(5)	21.6(3)
C(5)	6255.9(14)	716.9(10)	2372.8(5)	22.3(3)
C(6)	5335.3(16)	34.4(11)	2135.4(5)	27.0(3)
C(7)	4523.0(16)	-650.5(10)	2399.8(5)	29.9(3)
C(8)	4386.4(16)	-526.1(11)	2873.6(5)	30.0(3)
C(9)	4989.9(17)	166.8(13)	1630.1(5)	37.4(4)
C(10)	3786.3(19)	1013.9(13)	1549.0(5)	37.5(4)
C(11)	3064.6(16)	1348.5(11)	1994.5(5)	29.1(3)
C(12)	2017.8(16)	747.1(12)	2213.2(6)	33.0(3)
C(13)	1807.8(16)	817.8(11)	2688.7(6)	33.1(3)
C(14)	2643.6(16)	1485.5(11)	2956.2(5)	29.4(3)
C(15)	3439.4(14)	2234.8(11)	2721.4(5)	27.2(3)
C(16)	3650.8(15)	2161.7(11)	2248.2(5)	27.8(3)
C(17)	6976.7(15)	1603.0(11)	3092.2(5)	23.4(3)
C(18)	7711.2(14)	2233.2(11)	3282.0(4)	23.4(3)
C(19)	8620.5(14)	3031.7(10)	3465.9(4)	21.8(3)

C(20)	9897.3(15)	3276.1(11)	3233.8(5)	27.4(3)
C(21)	10751.4(16)	4087.2(12)	3379.9(5)	30.3(3)
C(22)	10343.8(16)	4680.8(12)	3761.1(5)	30.2(3)
C(23)	9120.6(16)	4429.4(11)	4004.1(5)	26.1(3)
C(24)	8241.5(14)	3601.8(11)	3863.2(4)	22.2(3)
C(25)	6988.4(15)	3356.5(11)	4129.7(4)	24.5(3)
C(26)	5978.8(15)	3173.0(12)	4374.9(5)	28.1(3)
C(27)	2936.0(18)	3752.9(14)	4528.0(6)	44.2(4)
C(28)	4895.4(17)	3418.6(13)	5354.8(5)	36.8(4)
C(29)	4000.2(17)	1554.4(12)	4761.8(5)	31.9(3)
C(17')	7187.0(15)	1396.1(11)	2119.9(5)	23.7(3)
C(18')	7929.0(14)	1990.2(11)	1907.6(5)	24.8(3)
C(19')	8836.6(14)	2763.3(11)	1701.0(4)	23.6(3)
C(20')	10085.6(15)	3064.3(11)	1931.7(5)	27.6(3)
C(21')	10924.4(16)	3869.4(12)	1768.3(5)	31.3(3)
C(22')	10539.3(17)	4387.4(12)	1364.6(5)	32.4(3)
C(23')	9341.3(17)	4073.8(12)	1120.3(5)	30.6(3)
C(24')	8474.8(15)	3259.2(11)	1279.6(5)	25.3(3)
C(25')	7237.5(16)	2979.4(11)	1014.3(5)	27.7(3)
C(26')	6227.5(16)	2812.6(12)	764.1(5)	31.0(3)
C(27')	3121.5(19)	3298.4(16)	694.6(6)	47.5(4)
C(28')	4988(2)	3461.9(14)	-153.2(6)	43.6(4)
C(29')	4335.0(19)	1316.4(12)	235.2(5)	36.3(3)

Table 22: Bond lengths [Å] of **126**.

Si-C(26)	1.8452(15)	C(12)-C(13)	1.388(2)
Si-C(27)	1.8586(17)	C(13)-C(14)	1.396(2)
Si-C(28)	1.8608(15)	C(14)-C(15)	1.396(2)
Si-C(29)	1.8616(16)	C(15)-C(16)	1.382(2)
Si'-C(26')	1.8440(15)	C(17)-C(18)	1.1970(19)
Si'-C(27')	1.8555(18)	C(18)-C(19)	1.4373(19)
Si'-C(28')	1.8586(16)	C(19)-C(20)	1.4056(18)
Si'-C(29')	1.8626(16)	C(19)-C(24)	1.4068(19)
C(1)-C(14)	1.511(2)	C(20)-C(21)	1.382(2)
C(1)-C(2)	1.593(2)	C(21)-C(22)	1.393(2)
C(2)-C(3)	1.512(2)	C(22)-C(23)	1.381(2)
C(3)-C(8)	1.390(2)	C(23)-C(24)	1.4076(19)
C(3)-C(4)	1.4120(19)	C(24)-C(25)	1.4374(19)
C(4)-C(5)	1.4230(18)	C(25)-C(26)	1.204(2)

C(4)-C(17)	1.4337(19)	C(17')-C(18')	1.202(2)
C(5)-C(6)	1.4092(19)	C(18')-C(19')	1.4390(19)
C(5)-C(17')	1.4348(19)	C(19')-C(20')	1.3999(19)
C(6)-C(7)	1.393(2)	C(19')-C(24')	1.4146(19)
C(6)-C(9)	1.502(2)	C(20')-C(21')	1.384(2)
C(7)-C(8)	1.382(2)	C(21')-C(22')	1.390(2)
C(9)-C(10)	1.587(2)	C(22')-C(23')	1.385(2)
C(10)-C(11)	1.514(2)	C(23')-C(24')	1.404(2)
C(11)-C(16)	1.392(2)	C(24')-C(25')	1.434(2)
C(11)-C(12)	1.400(2)	C(25')-C(26')	1.209(2)

Table 23: Bond angles [°] of **126**.

C(26)-Si-C(27)	106.99(7)	C(12)-C(13)-C(14)	120.48(14)
C(26)-Si-C(28)	109.10(7)	C(15)-C(14)-C(13)	117.26(14)
C(27)-Si-C(28)	109.56(8)	C(15)-C(14)-C(1)	119.09(14)
C(26)-Si-C(29)	108.34(7)	C(13)-C(14)-C(1)	122.48(14)
C(27)-Si-C(29)	111.77(8)	C(16)-C(15)-C(14)	120.55(14)
C(28)-Si-C(29)	110.96(7)	C(15)-C(16)-C(11)	120.94(14)
C(26')-Si'-C(27')	107.34(7)	C(18)-C(17)-C(4)	178.80(15)
C(26')-Si'-C(28')	108.64(8)	C(17)-C(18)-C(19)	174.41(14)
C(27')-Si'-C(28')	108.39(9)	C(20)-C(19)-C(24)	119.01(12)
C(26')-Si'-C(29')	109.71(8)	C(20)-C(19)-C(18)	119.23(12)
C(27')-Si'-C(29')	112.70(9)	C(24)-C(19)-C(18)	121.71(12)
C(28')-Si'-C(29')	109.94(8)	C(21)-C(20)-C(19)	121.08(13)
C(14)-C(1)-C(2)	112.89(12)	C(20)-C(21)-C(22)	119.88(14)
C(3)-C(2)-C(1)	112.16(12)	C(23)-C(22)-C(21)	119.90(13)
C(8)-C(3)-C(4)	117.51(13)	C(22)-C(23)-C(24)	121.08(13)
C(8)-C(3)-C(2)	119.31(13)	C(19)-C(24)-C(23)	118.95(12)
C(4)-C(3)-C(2)	121.92(12)	C(19)-C(24)-C(25)	121.74(12)
C(3)-C(4)-C(5)	119.73(13)	C(23)-C(24)-C(25)	119.30(12)
C(3)-C(4)-C(17)	120.76(12)	C(26)-C(25)-C(24)	176.24(14)
C(5)-C(4)-C(17)	119.13(13)	C(25)-C(26)-Si	176.99(14)
C(6)-C(5)-C(4)	119.74(13)	C(18')-C(17')-C(5)	177.70(15)
C(6)-C(5)-C(17')	120.38(12)	C(17')-C(18')-C(19')	173.65(14)
C(4)-C(5)-C(17')	119.30(12)	C(20')-C(19')-C(24')	118.87(13)
C(7)-C(6)-C(5)	117.65(13)	C(20')-C(19')-C(18')	119.23(12)
C(7)-C(6)-C(9)	119.06(13)	C(24')-C(19')-C(18')	121.86(13)
C(5)-C(6)-C(9)	122.12(13)	C(21')-C(20')-C(19')	121.32(13)

C(8)-C(7)-C(6)	121.22(13)	C(20')-C(21')-C(22')	119.91(14)
C(7)-C(8)-C(3)	121.16(14)	C(23')-C(22')-C(21')	119.73(14)
C(6)-C(9)-C(10)	111.97(12)	C(22')-C(23')-C(24')	121.30(14)
C(11)-C(10)-C(9)	112.81(12)	C(23')-C(24')-C(19')	118.76(13)
C(16)-C(11)-C(12)	117.16(14)	C(23')-C(24')-C(25')	118.69(13)
C(16)-C(11)-C(10)	119.02(14)	C(19')-C(24')-C(25')	122.54(13)
C(12)-C(11)-C(10)	122.46(14)	C(26')-C(25')-C(24')	174.24(16)
C(13)-C(12)-C(11)	120.52(14)	C(25')-C(26')-Si'	174.09(15)

Table 24: Torsion angles [°] of **126**.

C(14)-C(1)-C(2)-C(3)	-10.06(18)	C(17)-C(18)-C(19)-C(24)	135.8(14)
C(1)-C(2)-C(3)-C(8)	-69.85(17)	C(24)-C(19)-C(20)-C(21)	-2.4(2)
C(1)-C(2)-C(3)-C(4)	97.00(16)	C(18)-C(19)-C(20)-C(21)	175.36(13)
C(8)-C(3)-C(4)-C(5)	14.83(19)	C(19)-C(20)-C(21)-C(22)	-0.4(2)
C(2)-C(3)-C(4)-C(5)	-152.25(14)	C(20)-C(21)-C(22)-C(23)	2.8(2)
C(8)-C(3)-C(4)-C(17)	-172.31(12)	C(21)-C(22)-C(23)-C(24)	-2.3(2)
C(2)-C(3)-C(4)-C(17)	20.6(2)	C(20)-C(19)-C(24)-C(23)	2.78(19)
C(3)-C(4)-C(5)-C(6)	-1.37(19)	C(18)-C(19)-C(24)-C(23)	-174.88(12)
C(17)-C(4)-C(5)-C(6)	-174.35(12)	C(20)-C(19)-C(24)-C(25)	-176.80(12)
C(3)-C(4)-C(5)-C(17')	169.99(12)	C(18)-C(19)-C(24)-C(25)	5.54(19)
C(17)-C(4)-C(5)-C(17')	-2.99(19)	C(22)-C(23)-C(24)-C(19)	-0.5(2)
C(4)-C(5)-C(6)-C(7)	-12.67(19)	C(22)-C(23)-C(24)-C(25)	179.12(12)
C(17')-C(5)-C(6)-C(7)	176.07(13)	C(19)-C(24)-C(25)-C(26)	151(2)
C(4)-C(5)-C(6)-C(9)	154.81(14)	C(23)-C(24)-C(25)-C(26)	-29(2)
C(17')-C(5)-C(6)-C(9)	-16.5(2)	C(24)-C(25)-C(26)-Si	53(4)
C(5)-C(6)-C(7)-C(8)	13.4(2)	C(27)-Si-C(26)-C(25)	66(2)
C(9)-C(6)-C(7)-C(8)	-154.43(14)	C(28)-Si-C(26)-C(25)	-52(2)
C(6)-C(7)-C(8)-C(3)	0.3(2)	C(29)-Si-C(26)-C(25)	-173(66)
C(4)-C(3)-C(8)-C(7)	-14.5(2)	C(6)-C(5)-C(17')-C(18')	88(4)
C(2)-C(3)-C(8)-C(7)	152.95(14)	C(4)-C(5)-C(17')-C(18')	-83(4)
C(7)-C(6)-C(9)-C(10)	86.35(17)	C(5)-C(17')-C(18')-C(19')	76(4)
C(5)-C(6)-C(9)-C(10)	-80.96(17)	C(17')-C(18')-C(19')-C(20')	45.2(14)
C(6)-C(9)-C(10)-C(11)	-10.82(19)	C(17')-C(18')-C(19')-C(24')	-132.2(13)
C(9)-C(10)-C(11)-C(16)	88.12(17)	C(24')-C(19')-C(20')-C(21')	3.4(2)
C(9)-C(10)-C(11)-C(12)	-78.18(18)	C(18')-C(19')-C(20')-C(21')	-174.10(13)
C(16)-C(11)-C(12)-C(13)	-13.6(2)	C(19')-C(20')-C(21')-C(22')	-0.8(2)
C(10)-C(11)-C(12)-C(13)	152.95(15)	C(20')-C(21')-C(22')-C(23')	-2.0(2)
C(11)-C(12)-C(13)-C(14)	-0.4(2)	C(21')-C(22')-C(23')-C(24')	2.0(2)

C(12)-C(13)-C(14)-C(15)	14.5(2)	C(22')-C(23')-C(24')-C(19')	0.7(2)
C(12)-C(13)-C(14)-C(1)	-152.94(15)	C(22')-C(23')-C(24')-C(25')	179.18(13)
C(2)-C(1)-C(14)-C(15)	-72.67(17)	C(20')-C(19')-C(24')-C(23')	-3.34(19)
C(2)-C(1)-C(14)-C(13)	94.56(17)	C(18')-C(19')-C(24')-C(23')	174.12(13)
C(13)-C(14)-C(15)-C(16)	-14.7(2)	C(20')-C(19')-C(24')-C(25')	178.22(13)
C(1)-C(14)-C(15)-C(16)	153.18(14)	C(18')-C(19')-C(24')-C(25')	-4.3(2)
C(14)-C(15)-C(16)-C(11)	0.7(2)	C(23')-C(24')-C(25')-C(26')	-0.5(16)
C(12)-C(11)-C(16)-C(15)	13.5(2)	C(19')-C(24')-C(25')-C(26')	178(67)
C(10)-C(11)-C(16)-C(15)	-153.56(14)	C(24')-C(25')-C(26')-Si'	-48(2)
C(3)-C(4)-C(17)-C(18)	129(7)	C(27')-Si'-C(26')-C(25')	-55.8(12)
C(5)-C(4)-C(17)-C(18)	-59(7)	C(28')-Si'-C(26')-C(25')	61.2(12)
C(4)-C(17)-C(18)-C(19)	73(8)	C(29')-Si'-C(26')-C(25')	-179(94)
C(17)-C(18)-C(19)-C(20)	-41.9(15)		

1,2:9,10-Dibenzo-5,6-[2.2]paracyclophano-3,7,11,13-tetradehydro[14]annulene (53)

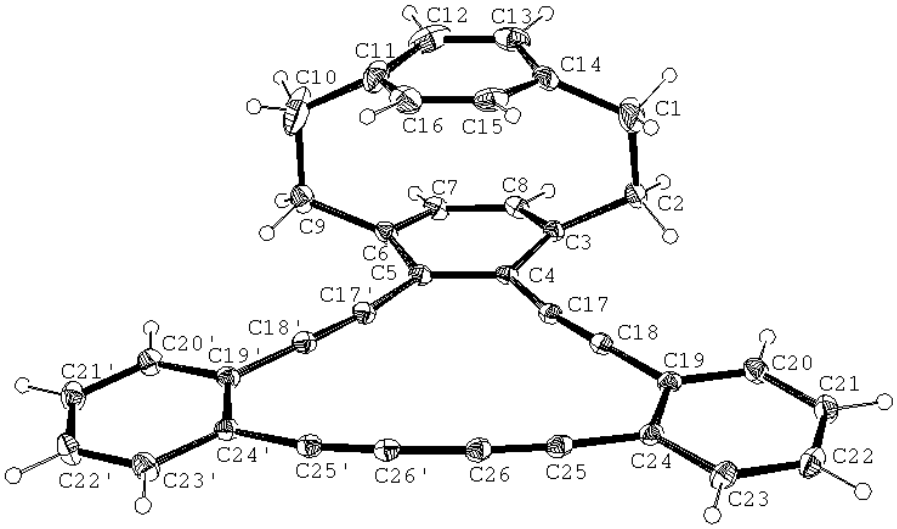

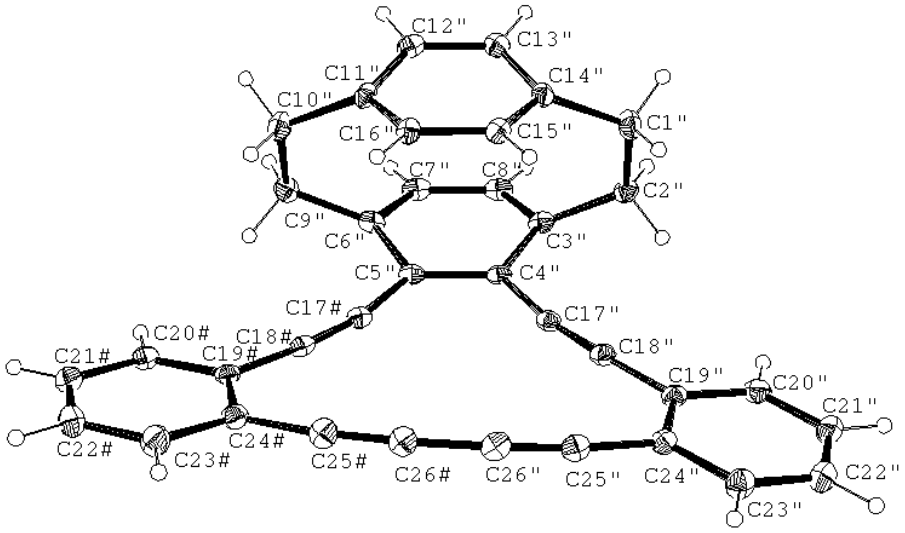

Figure 50: X-ray structure of the two inequivalent molecules of **53**, ellipsoids are drawn with 30% probability.

Table 25: Atomic coordinates (x 10^4) and equivalent isotropic displacement parameters ($Å^2$x 10^3). U(eq) is defined as one third of the trace of the orthogonalized Uij tensor.

	x	y	z	U(eq)
C(1)	3542(3)	5553(3)	7476(2)	70.9(13)
C(2)	4312(2)	6231(2)	6994.1(14)	27.9(6)
C(3)	3803(2)	7211.0(19)	6740.7(13)	21.9(6)
C(4)	2879(2)	7171.9(18)	6200.9(13)	20.0(5)
C(5)	2125(2)	7955.5(19)	6203.2(13)	21.8(6)
C(6)	2316(2)	8763.5(19)	6739.6(14)	24.6(6)
C(7)	3369(2)	8903(2)	7145.0(14)	26.7(6)
C(8)	4095(2)	8134.9(19)	7147.2(14)	24.6(6)
C(9)	1364(3)	9311(2)	6990.6(15)	33.5(7)
C(10)	822(4)	8769(3)	7620(3)	111(2)
C(11)	1235(3)	7727(3)	7823(2)	48.9(9)
C(12)	2150(3)	7679(3)	8323.5(19)	51.2(10)
C(13)	2842(3)	6888(3)	8295.8(17)	43.0(8)
C(14)	2623(3)	6116(2)	7758.0(17)	36.6(7)
C(15)	1563(3)	6039(2)	7367.5(15)	35.8(7)
C(16)	884(3)	6829(3)	7391.6(17)	41.7(8)
C(17)	2714(2)	6286(2)	5710.3(13)	22.3(6)
C(18)	2765(2)	5506.0(19)	5353.0(13)	21.9(6)
C(19)	2921(2)	4594.2(19)	4934.0(13)	22.2(6)
C(20)	3887(2)	4083(2)	5089.0(14)	27.0(6)

C(21)	4076(2)	3222(2)	4681.5(15)	30.3(6)
C(22)	3295(2)	2842(2)	4111.5(15)	32.0(7)
C(23)	2331(2)	3332(2)	3948.8(15)	28.7(6)
C(24)	2122(2)	4204.4(19)	4353.1(13)	22.4(6)
C(25)	1139(2)	4727.7(19)	4197.6(13)	23.2(6)
C(26)	400(2)	5297(2)	4143.2(13)	24.0(6)
C(17')	1111(2)	7927.2(19)	5720.4(13)	22.1(6)
C(18')	240(2)	8064.6(19)	5363.7(13)	22.7(6)
C(19')	-768(2)	8332.5(19)	4966.1(13)	22.0(6)
C(20')	-1228(2)	9249(2)	5153.3(14)	27.4(6)
C(21')	-2184(2)	9547(2)	4771.7(16)	32.2(7)
C(22')	-2717(2)	8939(2)	4189.6(16)	35.1(7)
C(23')	-2299(2)	8028(2)	3996.4(15)	30.1(6)
C(24')	-1326(2)	7711.0(19)	4375.6(13)	21.7(6)
C(25')	-867(2)	6779(2)	4192.6(13)	22.7(6)
C(26')	-332(2)	6042(2)	4140.9(13)	22.6(6)
C(1'')	9410(2)	1342(2)	7623.1(15)	33.4(7)
C(2'')	8808(2)	825(2)	6892.0(14)	28.0(6)
C(3'')	7699(2)	1249(2)	6656.2(13)	25.4(6)
C(4'')	6728(2)	1020.8(19)	7035.4(13)	21.9(6)
C(5'')	5911(2)	1745(2)	7024.6(13)	22.6(6)
C(6'')	6080(2)	2688(2)	6631.5(13)	25.6(6)
C(7'')	6882(2)	2742(2)	6139.8(14)	28.6(6)
C(8'')	7680(2)	2035(2)	6148.5(14)	28.1(6)
C(9'')	5602(2)	3681(2)	6842.6(15)	29.7(6)
C(10'')	6158(2)	4172(2)	7592.3(15)	32.8(7)
C(11'')	7250(2)	3720(2)	7843.3(14)	25.5(6)
C(12'')	8212(2)	3943(2)	7475.9(14)	28.0(6)
C(13'')	9018(2)	3243(2)	7483.3(14)	27.1(6)
C(14'')	8881(2)	2300(2)	7853.9(14)	24.4(6)
C(15'')	8050(2)	2202(2)	8332.9(13)	24.7(6)
C(16'')	7246(2)	2907(2)	8327.4(13)	24.6(6)
C(17'')	6697(2)	104(2)	7473.5(13)	22.3(6)
C(18'')	6833(2)	-686(2)	7794.6(13)	24.1(6)
C(19'')	7050(2)	-1654.5(19)	8141.0(13)	23.8(6)
C(20'')	7852(2)	-2253(2)	7896.8(15)	29.6(6)
C(21'')	8085(2)	-3176(2)	8222.6(16)	34.3(7)
C(22'')	7516(3)	-3532(2)	8799.6(16)	37.7(7)
C(23'')	6721(2)	-2963(2)	9049.8(15)	33.3(7)

C(24")	6478(2)	-2015(2)	8734.5(14)	25.1(6)
C(25")	5654(2)	-1412(2)	8971.7(14)	27.2(6)
C(26")	4985(2)	-807(2)	9075.2(14)	28.3(6)
C(17#)	4984(2)	1664.7(19)	7461.8(13)	23.2(6)
C(18#)	4190(2)	1786.5(19)	7792.7(14)	24.4(6)
C(19#)	3278(2)	2029.9(19)	8188.8(14)	23.8(6)
C(20#)	2674(2)	2876(2)	7991.2(14)	27.5(6)
C(21#)	1843(2)	3167(2)	8390.3(16)	33.3(7)
C(22#)	1579(3)	2611(2)	8995.0(17)	37.6(7)
C(23#)	2145(3)	1765(2)	9195.0(16)	35.7(7)
C(24#)	2998(2)	1461(2)	8803.2(14)	27.8(6)
C(25#)	3628(2)	610(2)	9008.3(14)	29.8(6)
C(26#)	4239(2)	-70(2)	9088.8(14)	28.9(6)
C(90)	-383(3)	4535(2)	-659.2(16)	37.4(7)
C(91)	416(3)	5422(2)	-612.9(16)	37.4(7)
C(92)	795(3)	5876(2)	51.2(17)	37.3(7)
C(93)	-177(3)	9188(2)	-503.3(16)	46.6(9)
C(94)	-907(3)	9939(3)	-526.5(17)	47.4(9)
C(95)	-735(3)	10751(3)	-19.5(18)	48.9(9)
C(96)	4738(3)	4264(2)	-548.9(15)	40.0(8)
C(97)	3971(3)	4946(2)	-416.2(16)	41.8(8)
C(98)	4237(3)	5688(2)	137.4(18)	42.9(8)
C(99)	5211(6)	567(5)	5231(3)	43.6(16)
Cl	4956.9(10)	-597.4(8)	5654.2(5)	72.3(3)

Table 26: Bond lengths [Å] of **53**.

C(1)-C(14)	1.514(4)	C(1")-C(14")	1.520(4)
C(1)-C(2)	1.550(4)	C(1")-C(2")	1.584(4)
C(2)-C(3)	1.518(3)	C(2")-C(3")	1.515(4)
C(3)-C(8)	1.388(4)	C(3")-C(8")	1.395(4)
C(3)-C(4)	1.416(3)	C(3")-C(4")	1.419(4)
C(4)-C(5)	1.423(3)	C(4")-C(5")	1.420(4)
C(4)-C(17)	1.434(3)	C(4")-C(17")	1.439(4)
C(5)-C(6)	1.417(3)	C(5")-C(6")	1.426(3)
C(5)-C(17')	1.433(4)	C(5")-C(17#)	1.434(4)
C(6)-C(7)	1.392(4)	C(6")-C(7")	1.389(4)
C(6)-C(9)	1.512(4)	C(6")-C(9")	1.516(4)
C(7)-C(8)	1.384(4)	C(7")-C(8")	1.386(4)
C(9)-C(10)	1.535(5)	C(9")-C(10")	1.584(4)

C(10)-C(11)	1.515(5)	C(10")-C(11")	1.521(4)
C(11)-C(12)	1.374(5)	C(11")-C(16")	1.389(4)
C(11)-C(16)	1.394(5)	C(11")-C(12")	1.397(4)
C(12)-C(13)	1.383(5)	C(12")-C(13")	1.388(4)
C(13)-C(14)	1.387(5)	C(13")-C(14")	1.400(4)
C(14)-C(15)	1.387(4)	C(14")-C(15")	1.398(4)
C(15)-C(16)	1.371(4)	C(15")-C(16")	1.391(4)
C(17)-C(18)	1.206(3)	C(17")-C(18")	1.202(4)
C(18)-C(19)	1.439(3)	C(18")-C(19")	1.444(4)
C(19)-C(20)	1.398(4)	C(19")-C(20")	1.401(4)
C(19)-C(24)	1.418(4)	C(19")-C(24")	1.416(4)
C(20)-C(21)	1.386(4)	C(20")-C(21")	1.381(4)
C(21)-C(22)	1.388(4)	C(21")-C(22")	1.387(4)
C(22)-C(23)	1.383(4)	C(22")-C(23")	1.375(4)
C(23)-C(24)	1.402(4)	C(23")-C(24")	1.403(4)
C(24)-C(25)	1.424(4)	C(24")-C(25")	1.420(4)
C(25)-C(26)	1.206(4)	C(25")-C(26")	1.202(4)
C(26)-C(26')	1.365(4)	C(26")-C(26#)	1.372(4)
C(17')-C(18')	1.210(4)	C(17#)-C(18#)	1.206(4)
C(18')-C(19')	1.429(4)	C(18#)-C(19#)	1.437(4)
C(19')-C(20')	1.407(4)	C(19#)-C(20#)	1.403(4)
C(19')-C(24')	1.417(3)	C(19#)-C(24#)	1.418(4)
C(20')-C(21')	1.379(4)	C(20#)-C(21#)	1.381(4)
C(21')-C(22')	1.387(4)	C(21#)-C(22#)	1.389(4)
C(22')-C(23')	1.378(4)	C(22#)-C(23#)	1.380(4)
C(23')-C(24')	1.404(4)	C(23#)-C(24#)	1.399(4)
C(24')-C(25')	1.421(3)	C(24#)-C(25#)	1.429(4)
C(25')-C(26')	1.207(3)	C(25#)-C(26#)	1.200(4)

Table 27: Bond angles [°] of **53**.

C(14)-C(1)-C(2)	114.3(2)	C(14")-C(1")-C(2")	112.7(2)
C(3)-C(2)-C(1)	112.3(2)	C(3")-C(2")-C(1")	112.9(2)
C(8)-C(3)-C(4)	118.1(2)	C(8")-C(3")-C(4")	117.9(2)
C(8)-C(3)-C(2)	118.2(2)	C(8")-C(3")-C(2")	119.6(2)
C(4)-C(3)-C(2)	122.4(2)	C(4")-C(3")-C(2")	121.3(2)
C(3)-C(4)-C(5)	119.2(2)	C(3")-C(4")-C(5")	119.5(2)
C(3)-C(4)-C(17)	117.0(2)	C(3")-C(4")-C(17")	116.7(2)
C(5)-C(4)-C(17)	123.7(2)	C(5")-C(4")-C(17")	123.5(2)
C(6)-C(5)-C(4)	119.6(2)	C(4")-C(5")-C(6")	119.3(2)

C(6)-C(5)-C(17')	117.0(2)	C(4")-C(5")-C(17#)	124.1(2)
C(4)-C(5)-C(17')	123.2(2)	C(6")-C(5")-C(17#)	116.1(2)
C(7)-C(6)-C(5)	117.9(2)	C(7")-C(6")-C(5")	117.6(2)
C(7)-C(6)-C(9)	118.3(2)	C(7")-C(6")-C(9")	119.6(2)
C(5)-C(6)-C(9)	122.5(2)	C(5")-C(6")-C(9")	121.6(2)
C(8)-C(7)-C(6)	120.7(2)	C(8")-C(7")-C(6")	121.3(2)
C(7)-C(8)-C(3)	121.2(2)	C(7")-C(8")-C(3")	120.5(2)
C(6)-C(9)-C(10)	113.4(2)	C(6")-C(9")-C(10")	113.3(2)
C(11)-C(10)-C(9)	115.0(3)	C(11")-C(10")-C(9")	112.0(2)
C(12)-C(11)-C(16)	116.7(3)	C(16")-C(11")-C(12")	117.6(2)
C(12)-C(11)-C(10)	121.3(4)	C(16")-C(11")-C(10")	120.8(3)
C(16)-C(11)-C(10)	120.2(4)	C(12")-C(11")-C(10")	120.0(2)
C(11)-C(12)-C(13)	121.4(3)	C(13")-C(12")-C(11")	120.5(2)
C(12)-C(13)-C(14)	120.4(3)	C(12")-C(13")-C(14")	120.8(3)
C(15)-C(14)-C(13)	116.6(3)	C(15")-C(14")-C(13")	117.0(2)
C(15)-C(14)-C(1)	118.8(3)	C(15")-C(14")-C(1")	120.7(2)
C(13)-C(14)-C(1)	123.1(3)	C(13")-C(14")-C(1")	120.9(2)
C(16)-C(15)-C(14)	121.2(3)	C(16")-C(15")-C(14")	120.7(2)
C(15)-C(16)-C(11)	120.6(3)	C(11")-C(16")-C(15")	120.7(2)
C(18)-C(17)-C(4)	168.2(3)	C(18")-C(17")-C(4")	169.3(3)
C(17)-C(18)-C(19)	175.5(3)	C(17")-C(18")-C(19")	175.8(3)
C(20)-C(19)-C(24)	118.5(2)	C(20")-C(19")-C(24")	118.5(2)
C(20)-C(19)-C(18)	120.0(2)	C(20")-C(19")-C(18")	120.0(2)
C(24)-C(19)-C(18)	121.5(2)	C(24")-C(19")-C(18")	121.5(2)
C(21)-C(20)-C(19)	121.2(3)	C(21")-C(20")-C(19")	121.2(3)
C(20)-C(21)-C(22)	120.2(3)	C(20")-C(21")-C(22")	120.1(3)
C(23)-C(22)-C(21)	119.7(3)	C(23")-C(22")-C(21")	120.0(3)
C(22)-C(23)-C(24)	121.1(3)	C(22")-C(23")-C(24")	121.1(3)
C(23)-C(24)-C(19)	119.2(2)	C(23")-C(24")-C(19")	119.1(2)
C(23)-C(24)-C(25)	122.4(2)	C(23")-C(24")-C(25")	122.7(2)
C(19)-C(24)-C(25)	118.3(2)	C(19")-C(24")-C(25")	118.1(2)
C(26)-C(25)-C(24)	169.2(3)	C(26")-C(25")-C(24")	169.3(3)
C(25)-C(26)-C(26')	171.9(3)	C(25")-C(26")-C(26#)	171.3(3)
C(18')-C(17')-C(5)	169.1(3)	C(18#)-C(17#)-C(5")	167.9(3)
C(17')-C(18')-C(19')	174.4(3)	C(17#)-C(18#)-C(19#)	174.9(3)
C(20')-C(19')-C(24')	117.9(2)	C(20#)-C(19#)-C(24#)	118.3(2)
C(20')-C(19')-C(18')	119.8(2)	C(20#)-C(19#)-C(18#)	120.2(2)
C(24')-C(19')-C(18')	122.3(2)	C(24#)-C(19#)-C(18#)	121.4(2)
C(21')-C(20')-C(19')	121.4(3)	C(21#)-C(20#)-C(19#)	121.3(3)

C(20')-C(21')-C(22')	120.2(3)	C(20#)-C(21#)-C(22#)	120.1(3)
C(23')-C(22')-C(21')	120.0(3)	C(23#)-C(22#)-C(21#)	119.8(3)
C(22')-C(23')-C(24')	120.8(3)	C(22#)-C(23#)-C(24#)	121.1(3)
C(23')-C(24')-C(19')	119.6(2)	C(23#)-C(24#)-C(19#)	119.4(3)
C(23')-C(24')-C(25')	122.5(2)	C(23#)-C(24#)-C(25#)	122.6(3)
C(19')-C(24')-C(25')	117.8(2)	C(19#)-C(24#)-C(25#)	118.1(2)
C(26')-C(25')-C(24')	168.1(3)	C(26#)-C(25#)-C(24#)	170.1(3)
C(25')-C(26')-C(26)	171.5(3)	C(25#)-C(26#)-C(26")	170.9(3)

Table 28: Torsion angles [°] of **53**.

C(14)-C(1)-C(2)-C(3)	-15.4(5)	C(14")-C(1")-C(2")-C(3")	-11.5(3)
C(1)-C(2)-C(3)-C(8)	92.2(3)	C(1")-C(2")-C(3")-C(8")	98.4(3)
C(1)-C(2)-C(3)-C(4)	-74.6(4)	C(1")-C(2")-C(3")-C(4")	-69.0(3)
C(8)-C(3)-C(4)-C(5)	-14.9(3)	C(8")-C(3")-C(4")-C(5")	-15.5(4)
C(2)-C(3)-C(4)-C(5)	151.9(2)	C(2")-C(3")-C(4")-C(5")	152.2(2)
C(8)-C(3)-C(4)-C(17)	169.7(2)	C(8")-C(3")-C(4")-C(17")	170.8(2)
C(2)-C(3)-C(4)-C(17)	-23.6(3)	C(2")-C(3")-C(4")-C(17")	-21.6(3)
C(3)-C(4)-C(5)-C(6)	0.5(3)	C(3")-C(4")-C(5")-C(6")	0.1(4)
C(17)-C(4)-C(5)-C(6)	175.7(2)	C(17")-C(4")-C(5")-C(6")	173.4(2)
C(3)-C(4)-C(5)-C(17')	-174.1(2)	C(3")-C(4")-C(5")-C(17#)	-171.3(2)
C(17)-C(4)-C(5)-C(17')	1.0(4)	C(17")-C(4")-C(5")-C(17#)	2.0(4)
C(4)-C(5)-C(6)-C(7)	14.4(4)	C(4")-C(5")-C(6")-C(7")	15.2(4)
C(17')-C(5)-C(6)-C(7)	-170.7(2)	C(17#)-C(5")-C(6")-C(7")	-172.7(2)
C(4)-C(5)-C(6)-C(9)	-152.4(2)	C(4")-C(5")-C(6")-C(9")	-152.1(2)
C(17')-C(5)-C(6)-C(9)	22.6(4)	C(17#)-C(5")-C(6")-C(9")	20.0(3)
C(5)-C(6)-C(7)-C(8)	-15.2(4)	C(5")-C(6")-C(7")-C(8")	-15.4(4)
C(9)-C(6)-C(7)-C(8)	152.1(3)	C(9")-C(6")-C(7")-C(8")	152.1(3)
C(6)-C(7)-C(8)-C(3)	0.7(4)	C(6")-C(7")-C(8")-C(3")	-0.1(4)
C(4)-C(3)-C(8)-C(7)	14.5(4)	C(4")-C(3")-C(8")-C(7")	15.7(4)
C(2)-C(3)-C(8)-C(7)	-152.8(2)	C(2")-C(3")-C(8")-C(7")	-152.1(2)
C(7)-C(6)-C(9)-C(10)	-76.8(4)	C(7")-C(6")-C(9")-C(10")	-101.2(3)
C(5)-C(6)-C(9)-C(10)	89.9(4)	C(5")-C(6")-C(9")-C(10")	65.8(3)
C(6)-C(9)-C(10)-C(11)	-6.6(6)	C(6")-C(9")-C(10")-C(11")	15.1(3)
C(9)-C(10)-C(11)-C(12)	90.6(5)	C(9")-C(10")-C(11")-C(16")	-97.8(3)
C(9)-C(10)-C(11)-C(16)	-73.8(5)	C(9")-C(10")-C(11")-C(12")	67.7(3)
C(16)-C(11)-C(12)-C(13)	14.1(5)	C(16")-C(11")-C(12")-C(13")	13.1(4)
C(10)-C(11)-C(12)-C(13)	-150.7(3)	C(10")-C(11")-C(12")-C(13")	-152.8(2)
C(11)-C(12)-C(13)-C(14)	-0.2(5)	C(11")-C(12")-C(13")-C(14")	0.4(4)
C(12)-C(13)-C(14)-C(15)	-14.4(4)	C(12")-C(13")-C(14")-C(15")	-13.5(4)

C(12)-C(13)-C(14)-C(1)	151.2(3)	C(12")-C(13")-C(14")-C(1")	152.9(2)
C(2)-C(1)-C(14)-C(15)	91.6(4)	C(2")-C(1")-C(14")-C(15")	95.3(3)
C(2)-C(1)-C(14)-C(13)	-73.7(4)	C(2")-C(1")-C(14")-C(13")	-70.6(3)
C(13)-C(14)-C(15)-C(16)	15.1(4)	C(13")-C(14")-C(15")-C(16")	13.1(4)
C(1)-C(14)-C(15)-C(16)	-151.1(3)	C(1")-C(14")-C(15")-C(16")	-153.3(2)
C(14)-C(15)-C(16)-C(11)	-1.3(4)	C(12")-C(11")-C(16")-C(15")	-13.5(4)
C(12)-C(11)-C(16)-C(15)	-13.4(4)	C(10")-C(11")-C(16")-C(15")	152.4(2)
C(10)-C(11)-C(16)-C(15)	151.7(3)	C(14")-C(15")-C(16")-C(11")	0.3(4)
C(24)-C(19)-C(20)-C(21)	0.9(4)	C(24")-C(19")-C(20")-C(21")	0.2(4)
C(18)-C(19)-C(20)-C(21)	-178.1(2)	C(18")-C(19")-C(20")-C(21")	179.3(3)
C(19)-C(20)-C(21)-C(22)	-0.7(4)	C(19")-C(20")-C(21")-C(22")	0.4(4)
C(20)-C(21)-C(22)-C(23)	0.5(4)	C(20")-C(21")-C(22")-C(23")	-0.2(4)
C(21)-C(22)-C(23)-C(24)	-0.4(4)	C(21")-C(22")-C(23")-C(24")	-0.6(4)
C(22)-C(23)-C(24)-C(19)	0.6(4)	C(22")-C(23")-C(24")-C(19")	1.2(4)
C(22)-C(23)-C(24)-C(25)	179.8(2)	C(22")-C(23")-C(24")-C(25")	179.2(3)
C(20)-C(19)-C(24)-C(23)	-0.8(4)	C(20")-C(19")-C(24")-C(23")	-1.0(4)
C(18)-C(19)-C(24)-C(23)	178.2(2)	C(18")-C(19")-C(24")-C(23")	179.9(2)
C(20)-C(19)-C(24)-C(25)	179.9(2)	C(20")-C(19")-C(24")-C(25")	-179.1(2)
C(18)-C(19)-C(24)-C(25)	-1.1(3)	C(18")-C(19")-C(24")-C(25")	1.8(4)
C(24')-C(19')-C(20')-C(21')	-0.8(4)	C(24#)-C(19#)-C(20#)-C(21#)	1.4(4)
C(18')-C(19')-C(20')-C(21')	178.5(2)	C(18#)-C(19#)-C(20#)-C(21#)	-175.8(2)
C(19')-C(20')-C(21')-C(22')	0.1(4)	C(19#)-C(20#)-C(21#)-C(22#)	-0.9(4)
C(20')-C(21')-C(22')-C(23')	0.8(4)	C(20#)-C(21#)-C(22#)-C(23#)	-0.2(4)
C(21')-C(22')-C(23')-C(24')	-0.9(4)	C(21#)-C(22#)-C(23#)-C(24#)	0.8(5)
C(22')-C(23')-C(24')-C(19')	0.2(4)	C(22#)-C(23#)-C(24#)-C(19#)	-0.4(4)
C(22')-C(23')-C(24')-C(25')	-179.9(3)	C(22#)-C(23#)-C(24#)-C(25#)	177.9(3)
C(20')-C(19')-C(24')-C(23')	0.6(4)	C(20#)-C(19#)-C(24#)-C(23#)	-0.7(4)
C(18')-C(19')-C(24')-C(23')	-178.6(2)	C(18#)-C(19#)-C(24#)-C(23#)	176.4(2)
C(20')-C(19')-C(24')-C(25')	-179.3(2)	C(20#)-C(19#)-C(24#)-C(25#)	-179.0(2)
C(18')-C(19')-C(24')-C(25')	1.5(4)	C(18#)-C(19#)-C(24#)-C(25#)	-1.9(4)

Compound	**144**
Identification code	hinuba
Empirical formula	$C_{28}H_{34}Si_2$
Formula weight	426.37
Temperature	133(2) K
Crystal system	Monoclinic
Space group	P21/c
Unit cell dimensions	a = 11.1670(12) Å
	b = 9.4422(10) Å
	c = 23.557(3) Å
	α= 90°
	β= 96.044(2)°
	γ = 90°
Volume	2470.0(5) $Å^3$
Z	4
Density (calculated)	1.148 Mg/m^3
Absorption coefficient	0.156 mm^{-1}
F(000)	920
Crystal size	0.30 x 0.30 x 0.08 mm^3
Theta range for data collection	1.74 to 28.28°
Index ranges	-14<=h<=14
	-12<=k<=12
	-31<=l<=31
Reflections collected	24721
Independent reflections	6136 [R(int) = 0.1022]
Completeness to theta = 28.00°	99.90%
Absorption correction	None
Data / restraints / parameters	6136 / 0 / 277
Goodness-of-fit on F2	1.148
Final R indices [I>2sigma(I)]	R1 = 0.1132; wR2 = 0.2649
R indices (all data)	R1 = 0.1442; wR2 = 0.2780
Largest diff. peak and hole	0.729 and -0.553 $e.Å^{-3}$

8,9-Bis(trimethylsilyl)[2.2](1,4)biphenylenoparacyclophane (144)

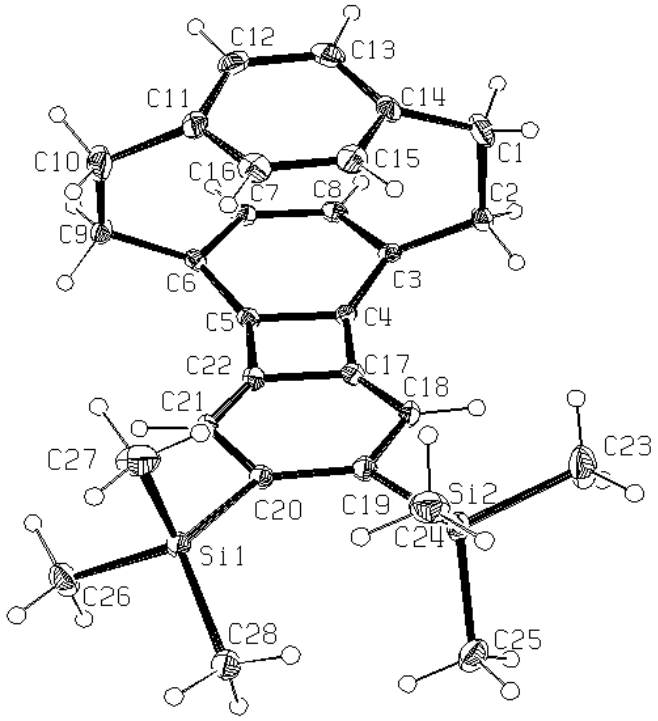

Figure 51: X-ray structure of **144**. Ellipsoids are drawn with 30% probability.

Table 29: Atomic coordinates (x 10^4) and equivalent isotropic displacement parameters ($Å^2$x 10^3). U(eq) is defined as one third of the trace of the orthogonalized Uij tensor.

	x	y	z	U(eq)
C(1)	3137(5)	3274(7)	2176(3)	42.5(16)
C(2)	1804(5)	3100(5)	2306(2)	24.7(10)
C(3)	1244(4)	4467(5)	2482.6(19)	18.3(9)
C(4)	1168(4)	4849(5)	3038.3(19)	18.0(9)
C(5)	1178(4)	6303(5)	3220.9(19)	19.4(9)
C(6)	1271(4)	7409(5)	2854.1(19)	19.7(9)
C(7)	1013(4)	7009(5)	2264.7(19)	21.7(9)
C(8)	992(4)	5607(5)	2088.1(19)	22.2(10)
C(9)	1859(5)	8824(5)	3015(2)	25.3(10)
C(10)	3260(6)	8761(7)	3085(3)	47.9(17)
C(11)	3762(5)	7400(6)	2859(3)	30.3(12)
C(12)	3795(5)	7179(6)	2282(2)	32.1(12)
C(13)	3778(5)	5813(7)	2062(2)	33.0(12)

C(14)	3701(5)	4645(6)	2410(3)	30.5(12)
C(15)	3922(5)	4869(6)	2999(2)	30.0(11)
C(16)	3945(5)	6222(6)	3225(2)	31.5(12)
C(17)	1477(5)	4377(5)	3649.0(19)	22.4(10)
C(18)	1798(5)	3291(5)	4018(2)	26.1(11)
C(19)	2084(5)	3628(5)	4614(2)	25.3(11)
C(20)	2046(5)	5056(5)	4806.1(19)	23.3(10)
C(21)	1771(5)	6162(5)	4396(2)	23.3(10)
C(22)	1487(4)	5809(5)	3834(2)	21.5(9)
Si(1)	2421.4(14)	5781.6(15)	5554.5(5)	24.6(3)
Si(2)	2509.1(15)	2011.2(15)	5076.6(6)	27.7(4)
C(23)	2810(8)	486(6)	4598(3)	55(2)
C(24)	3954(6)	2244(7)	5549(2)	39.2(14)
C(25)	1244(6)	1485(6)	5489(2)	35.4(13)
C(26)	1520(7)	7450(6)	5624(2)	39.2(15)
C(27)	4052(6)	6270(8)	5643(3)	45.0(16)
C(28)	2010(6)	4673(6)	6162(2)	34.2(13)

Table 30: Bond lengths [Å] of **144**.

C(1)-C(14)	1.517(8)	C(13)-C(14)	1.382(8)
C(1)-C(2)	1.560(8)	C(14)-C(15)	1.401(8)
C(2)-C(3)	1.511(7)	C(15)-C(16)	1.383(8)
C(3)-C(4)	1.369(6)	C(17)-C(18)	1.367(7)
C(3)-C(8)	1.431(7)	C(17)-C(22)	1.421(7)
C(4)-C(5)	1.438(6)	C(18)-C(19)	1.443(7)
C(4)-C(17)	1.511(6)	C(19)-C(20)	1.425(7)
C(5)-C(6)	1.366(7)	C(19)-Si(2)	1.906(5)
C(5)-C(22)	1.523(6)	C(20)-C(21)	1.434(7)
C(6)-C(7)	1.438(6)	C(20)-Si(1)	1.897(5)
C(6)-C(9)	1.519(7)	C(21)-C(22)	1.368(7)
C(7)-C(8)	1.387(7)	Si(1)-C(27)	1.868(7)
C(9)-C(10)	1.557(8)	Si(1)-C(28)	1.868(5)
C(10)-C(11)	1.521(8)	Si(1)-C(26)	1.886(6)
C(11)-C(12)	1.379(8)	Si(2)-C(25)	1.865(6)
C(11)-C(16)	1.408(8)	Si(2)-C(24)	1.873(7)
C(12)-C(13)	1.390(8)	Si(2)-C(23)	1.881(6)

Table 31: Bond angles [°] of **144**.

C(14)-C(1)-C(2)	112.8(4)	C(15)-C(16)-C(11)	119.9(5)
C(3)-C(2)-C(1)	113.3(4)	C(18)-C(17)-C(22)	121.7(4)
C(4)-C(3)-C(8)	113.2(4)	C(18)-C(17)-C(4)	147.7(5)
C(4)-C(3)-C(2)	123.9(4)	C(22)-C(17)-C(4)	90.3(4)
C(8)-C(3)-C(2)	121.5(4)	C(17)-C(18)-C(19)	118.1(4)
C(3)-C(4)-C(5)	122.6(4)	C(20)-C(19)-C(18)	120.4(4)
C(3)-C(4)-C(17)	143.3(4)	C(20)-C(19)-Si(2)	126.2(4)
C(5)-C(4)-C(17)	90.2(4)	C(18)-C(19)-Si(2)	113.3(4)
C(6)-C(5)-C(4)	122.6(4)	C(19)-C(20)-C(21)	119.1(4)
C(6)-C(5)-C(22)	144.0(4)	C(19)-C(20)-Si(1)	128.7(4)
C(4)-C(5)-C(22)	89.2(4)	C(21)-C(20)-Si(1)	112.0(3)
C(5)-C(6)-C(7)	112.9(4)	C(22)-C(21)-C(20)	119.1(4)
C(5)-C(6)-C(9)	125.1(4)	C(21)-C(22)-C(17)	121.4(4)
C(7)-C(6)-C(9)	120.5(4)	C(21)-C(22)-C(5)	148.1(5)
C(8)-C(7)-C(6)	122.3(4)	C(17)-C(22)-C(5)	90.4(4)
C(7)-C(8)-C(3)	121.8(4)	C(27)-Si(1)-C(28)	111.6(3)
C(6)-C(9)-C(10)	113.3(4)	C(27)-Si(1)-C(26)	107.9(3)
C(11)-C(10)-C(9)	113.5(5)	C(28)-Si(1)-C(26)	103.0(3)
C(12)-C(11)-C(16)	117.8(5)	C(27)-Si(1)-C(20)	108.1(3)
C(12)-C(11)-C(10)	121.5(6)	C(28)-Si(1)-C(20)	117.5(2)
C(16)-C(11)-C(10)	119.2(6)	C(26)-Si(1)-C(20)	108.4(2)
C(11)-C(12)-C(13)	120.5(5)	C(25)-Si(2)-C(24)	112.0(3)
C(14)-C(13)-C(12)	121.2(5)	C(25)-Si(2)-C(23)	107.6(3)
C(13)-C(14)-C(15)	116.8(5)	C(24)-Si(2)-C(23)	104.4(3)
C(13)-C(14)-C(1)	121.0(6)	C(25)-Si(2)-C(19)	110.8(3)
C(15)-C(14)-C(1)	120.7(5)	C(24)-Si(2)-C(19)	113.1(3)
C(16)-C(15)-C(14)	121.0(5)	C(23)-Si(2)-C(19)	108.7(2)

Table 32: Torsion angles [°] of **144**.

C(14)-C(1)-C(2)-C(3)	16.1(7)	C(3)-C(4)-C(17)-C(18)	-17.1(13)
C(1)-C(2)-C(3)-C(4)	-97.2(6)	C(5)-C(4)-C(17)-C(18)	-171.9(8)
C(1)-C(2)-C(3)-C(8)	68.6(6)	C(3)-C(4)-C(17)-C(22)	154.8(7)
C(8)-C(3)-C(4)-C(5)	-16.7(7)	C(5)-C(4)-C(17)-C(22)	0.1(4)
C(2)-C(3)-C(4)-C(5)	150.2(5)	C(22)-C(17)-C(18)-C(19)	3.7(8)
C(8)-C(3)-C(4)-C(17)	-166.3(6)	C(4)-C(17)-C(18)-C(19)	174.2(7)
C(2)-C(3)-C(4)-C(17)	0.6(10)	C(17)-C(18)-C(19)-C(20)	-0.9(8)
C(3)-C(4)-C(5)-C(6)	-0.3(8)	C(17)-C(18)-C(19)-Si(2)	179.8(4)

C(17)-C(4)-C(5)-C(6)	162.0(5)	C(18)-C(19)-C(20)-C(21)	-2.7(8)
C(3)-C(4)-C(5)-C(22)	-162.4(5)	Si(2)-C(19)-C(20)-C(21)	176.5(4)
C(17)-C(4)-C(5)-C(22)	-0.1(4)	C(18)-C(19)-C(20)-Si(1)	-178.0(4)
C(4)-C(5)-C(6)-C(7)	16.6(7)	Si(2)-C(19)-C(20)-Si(1)	1.2(8)
C(22)-C(5)-C(6)-C(7)	165.1(6)	C(19)-C(20)-C(21)-C(22)	3.6(8)
C(4)-C(5)-C(6)-C(9)	-149.5(5)	Si(1)-C(20)-C(21)-C(22)	179.6(4)
C(22)-C(5)-C(6)-C(9)	-1.1(10)	C(20)-C(21)-C(22)-C(17)	-1.0(8)
C(5)-C(6)-C(7)-C(8)	-16.0(7)	C(20)-C(21)-C(22)-C(5)	-176.6(7)
C(9)-C(6)-C(7)-C(8)	150.9(5)	C(18)-C(17)-C(22)-C(21)	-2.8(8)
C(6)-C(7)-C(8)-C(3)	-1.0(8)	C(4)-C(17)-C(22)-C(21)	-177.8(5)
C(4)-C(3)-C(8)-C(7)	17.2(7)	C(18)-C(17)-C(22)-C(5)	174.9(5)
C(2)-C(3)-C(8)-C(7)	-150.0(5)	C(4)-C(17)-C(22)-C(5)	-0.1(4)
C(5)-C(6)-C(9)-C(10)	76.0(7)	C(6)-C(5)-C(22)-C(21)	22.5(13)
C(7)-C(6)-C(9)-C(10)	-89.2(6)	C(4)-C(5)-C(22)-C(21)	176.3(8)
C(6)-C(9)-C(10)-C(11)	12.4(8)	C(6)-C(5)-C(22)-C(17)	-153.8(7)
C(9)-C(10)-C(11)-C(12)	77.0(7)	C(4)-C(5)-C(22)-C(17)	0.1(4)
C(9)-C(10)-C(11)-C(16)	-88.6(7)	C(19)-C(20)-Si(1)-C(27)	91.1(6)
C(16)-C(11)-C(12)-C(13)	12.1(8)	C(21)-C(20)-Si(1)-C(27)	-84.5(5)
C(10)-C(11)-C(12)-C(13)	-153.7(5)	C(19)-C(20)-Si(1)-C(28)	-36.2(6)
C(11)-C(12)-C(13)-C(14)	1.4(8)	C(21)-C(20)-Si(1)-C(28)	148.2(4)
C(12)-C(13)-C(14)-C(15)	-14.3(8)	C(19)-C(20)-Si(1)-C(26)	-152.3(5)
C(12)-C(13)-C(14)-C(1)	152.4(5)	C(21)-C(20)-Si(1)-C(26)	32.1(5)
C(2)-C(1)-C(14)-C(13)	-98.7(7)	C(20)-C(19)-Si(2)-C(25)	76.8(5)
C(2)-C(1)-C(14)-C(15)	67.4(7)	C(18)-C(19)-Si(2)-C(25)	-103.9(4)
C(13)-C(14)-C(15)-C(16)	14.0(8)	C(20)-C(19)-Si(2)-C(24)	-49.8(6)
C(1)-C(14)-C(15)-C(16)	-152.7(5)	C(18)-C(19)-Si(2)-C(24)	129.4(4)
C(14)-C(15)-C(16)-C(11)	-0.9(8)	C(20)-C(19)-Si(2)-C(23)	-165.2(5)
C(12)-C(11)-C(16)-C(15)	-12.3(8)	C(18)-C(19)-Si(2)-C(23)	14.0(5)
C(10)-C(11)-C(16)-C(15)	153.9(5)		

Compound	**164**	**154**
Identification code	hinfort	hinhalt
Empirical formula	$C_{24}H_{16}$	$C_{68}H_{56}$
Formula weight	304.37	873.13
Temperature	133(2) K	133(2) K
Crystal system	Orthorhombic	Monoclinic
Space group	Pca21	C2/c
Unit cell dimensions	a = 13.7087(16) Å	a = 24.185(3) Å
	b = 9.4745(12) Å	b = 14.024(2) Å
	c = 12.7205(16) Å	c = 16.621(2) Å
	α= 90°	α= 90°
	β= 90°	β= 111.143(5)°
	γ = 90°	γ = 90°
Volume	1652.2(4) $Å^3$	5258.1(12) $Å^3$
Z	4	4
Density (calculated)	1.224 Mg/m^3	1.103 Mg/m^3
Absorption coefficient	0.069 mm^{-1}	0.062 mm^{-1}
F(000)	640	1856
Crystal size	0.20 x 0.20 x 0.13 mm^3	0.45 x 0.30 x 0.30 mm^3
Theta range for data collection	2.15 to 30.03°	1.71 to 30.03°
Index ranges	-18<=h<=19	-34<=h<=34,
	-13<=k<=12	-19<=k<=19
	-17<=l<=17	-23<=l<=23
Reflections collected	18176	29739
Independent reflections	2524 [R(int) = 0.0298]	7679 [R(int) = 0.0797]
Completeness to theta = 28.00°	100.00%	99.80%
Absorption correction	None	None
Data / restraints / parameters	2524 / 7 / 233	7679 / 0 / 313

4,7,13,16-Tetraethynyl[2.2]paracyclophane (164)

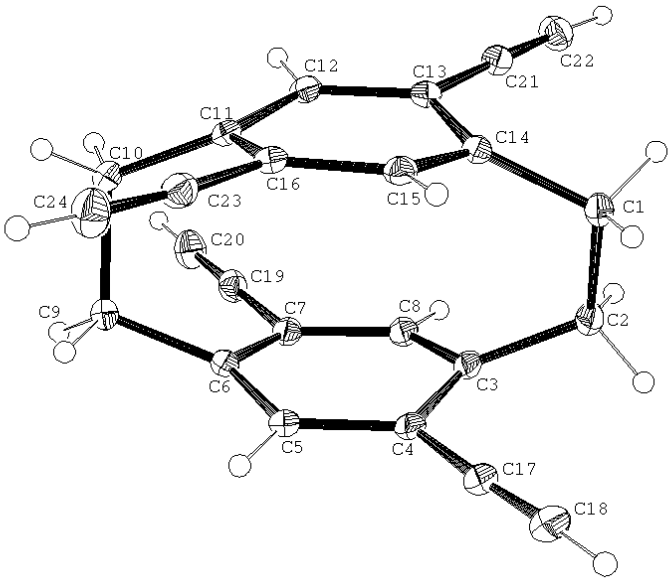

Figure 52: X-ray crystal structure of **164**, ellipsoids are drawn with 30% probability.

Table 33: Atomic coordinates (x 10^4) and equivalent isotropic displacement parameters ($Å^2$x 10^3). U(eq) is defined as one third of the trace of the orthogonalized Uij tensor.

	x	y	z	U(eq)
C(1)	5045.0(12)	4556.2(16)	1885.2(13)	25.4(3)
C(2)	5715.5(12)	5320.0(16)	1037.3(12)	26.1(3)
C(3)	6077.8(12)	6731.8(15)	1430.1(11)	23.3(3)
C(4)	5426.0(11)	7867.4(16)	1589.4(11)	23.5(3)
C(5)	5648.6(11)	8897.1(15)	2345.6(11)	22.7(3)
C(6)	6510.3(10)	8837.0(14)	2927.9(12)	21.8(3)
C(7)	7246.8(11)	7905.9(15)	2577.0(12)	23.4(3)
C(8)	7012.2(11)	6857.0(15)	1839.9(11)	24.3(3)
C(9)	6552.1(11)	9478.3(15)	4011.9(12)	23.4(3)
C(10)	6477.4(11)	8316.3(16)	4903.9(12)	24.1(3)
C(11)	5968.0(11)	6995.3(16)	4511.9(11)	21.2(3)
C(12)	6500.4(10)	5801.1(15)	4233.8(12)	22.4(3)
C(13)	6145.3(11)	4830.9(14)	3491.2(12)	21.8(3)
C(14)	5246.6(10)	5097.3(15)	2985.3(12)	21.7(3)
C(15)	4638.2(10)	6098.8(15)	3442.6(12)	22.1(3)
C(16)	4975.9(11)	7028.1(15)	4213.1(12)	21.8(3)
C(17)	4481.9(13)	7841.3(16)	1100.0(12)	27.0(3)
C(18)	3705.7(13)	7747.6(19)	679.5(14)	33.0(4)
C(19)	8182.0(12)	7890.5(16)	3091.0(13)	26.9(3)

C(20)	8947.1(13)	7870.8(19)	3528.6(17)	34.1(4)
C(21)	6740.5(11)	3669.9(15)	3146.4(13)	25.5(3)
C(22)	7199.0(13)	2682.8(18)	2848.5(15)	32.5(3)
C(23)	4357.3(11)	8115.3(17)	4638.5(13)	25.4(3)
C(24)	3892.4(12)	9022(2)	5051.4(15)	33.4(4)

Table 34: Bond lengths [Å] of **164**.

C(1)-C(14)	1.516(2)	C(11)-C(16)	1.413(2)
C(1)-C(2)	1.591(2)	C(12)-C(13)	1.405(2)
C(2)-C(3)	1.512(2)	C(13)-C(14)	1.413(2)
C(3)-C(8)	1.388(2)	C(13)-C(21)	1.438(2)
C(3)-C(4)	1.413(2)	C(14)-C(15)	1.391(2)
C(4)-C(5)	1.404(2)	C(15)-C(16)	1.396(2)
C(4)-C(17)	1.436(2)	C(16)-C(23)	1.440(2)
C(5)-C(6)	1.395(2)	C(17)-C(18)	1.194(2)
C(6)-C(7)	1.413(2)	C(18)-H(18)	0.92(2)
C(6)-C(9)	1.508(2)	C(19)-C(20)	1.188(2)
C(7)-C(8)	1.404(2)	C(20)-H(20)	0.945(18)
C(7)-C(19)	1.439(2)	C(21)-C(22)	1.189(2)
C(9)-C(10)	1.584(2)	C(22)-H(22)	0.950(19)
C(10)-C(11)	1.517(2)	C(23)-C(24)	1.192(2)
C(11)-C(12)	1.392(2)	C(24)-H(24)	0.945(18)

Table 35: Bond angles [°] of **164**.

C(14)-C(1)-C(2)	111.51(11)	C(16)-C(11)-C(10)	120.89(13)
C(3)-C(2)-C(1)	111.60(12)	C(11)-C(12)-C(13)	121.39(13)
C(8)-C(3)-C(4)	117.68(13)	C(12)-C(13)-C(14)	119.44(13)
C(8)-C(3)-C(2)	120.20(14)	C(12)-C(13)-C(21)	120.59(13)
C(4)-C(3)-C(2)	120.88(14)	C(14)-C(13)-C(21)	119.50(13)
C(5)-C(4)-C(3)	119.34(14)	C(15)-C(14)-C(13)	117.02(13)
C(5)-C(4)-C(17)	120.32(14)	C(15)-C(14)-C(1)	120.50(13)
C(3)-C(4)-C(17)	119.63(14)	C(13)-C(14)-C(1)	121.28(13)
C(6)-C(5)-C(4)	121.29(14)	C(14)-C(15)-C(16)	121.66(13)
C(5)-C(6)-C(7)	117.56(13)	C(15)-C(16)-C(11)	119.61(13)
C(5)-C(6)-C(9)	120.07(13)	C(15)-C(16)-C(23)	121.31(13)
C(7)-C(6)-C(9)	120.88(13)	C(11)-C(16)-C(23)	118.80(13)
C(8)-C(7)-C(6)	119.29(13)	C(18)-C(17)-C(4)	176.57(18)
C(8)-C(7)-C(19)	120.03(14)	C(17)-C(18)-H(18)	177.3(19)

C(6)-C(7)-C(19)	119.95(13)	C(20)-C(19)-C(7)	179.01(19)
C(3)-C(8)-C(7)	121.52(14)	C(19)-C(20)-H(20)	178.5(16)
C(6)-C(9)-C(10)	111.87(11)	C(22)-C(21)-C(13)	177.34(17)
C(11)-C(10)-C(9)	111.56(11)	C(21)-C(22)-H(22)	177(2)
C(12)-C(11)-C(16)	117.02(13)	C(24)-C(23)-C(16)	175.15(17)
C(12)-C(11)-C(10)	120.83(13)	C(23)-C(24)-H(24)	177.8(15)

Table 36: Torsion angles [°] of **164**.

C(14)-C(1)-C(2)-C(3)	-22.48(19)	C(6)-C(9)-C(10)-C(11)	-24.21(17)
C(1)-C(2)-C(3)-C(8)	99.47(16)	C(9)-C(10)-C(11)-C(12)	101.60(16)
C(1)-C(2)-C(3)-C(4)	-67.52(19)	C(9)-C(10)-C(11)-C(16)	-65.22(17)
C(8)-C(3)-C(4)-C(5)	-15.2(2)	C(16)-C(11)-C(12)-C(13)	14.3(2)
C(2)-C(3)-C(4)-C(5)	152.14(13)	C(10)-C(11)-C(12)-C(13)	-152.98(13)
C(8)-C(3)-C(4)-C(17)	174.41(13)	C(11)-C(12)-C(13)-C(14)	2.4(2)
C(2)-C(3)-C(4)-C(17)	-18.3(2)	C(11)-C(12)-C(13)-C(21)	174.59(13)
C(3)-C(4)-C(5)-C(6)	1.3(2)	C(12)-C(13)-C(14)-C(15)	-16.71(19)
C(17)-C(4)-C(5)-C(6)	171.67(13)	C(21)-C(13)-C(14)-C(15)	171.06(14)
C(4)-C(5)-C(6)-C(7)	13.9(2)	C(12)-C(13)-C(14)-C(1)	150.83(13)
C(4)-C(5)-C(6)-C(9)	-152.29(13)	C(21)-C(13)-C(14)-C(1)	-21.40(19)
C(5)-C(6)-C(7)-C(8)	-15.24(19)	C(2)-C(1)-C(14)-C(15)	99.59(16)
C(9)-C(6)-C(7)-C(8)	150.85(13)	C(2)-C(1)-C(14)-C(13)	-67.52(17)
C(5)-C(6)-C(7)-C(19)	174.53(13)	C(13)-C(14)-C(15)-C(16)	14.3(2)
C(9)-C(6)-C(7)-C(19)	-19.4(2)	C(1)-C(14)-C(15)-C(16)	-153.31(13)
C(4)-C(3)-C(8)-C(7)	13.9(2)	C(14)-C(15)-C(16)-C(11)	2.5(2)
C(2)-C(3)-C(8)-C(7)	-153.53(14)	C(14)-C(15)-C(16)-C(23)	176.33(14)
C(6)-C(7)-C(8)-C(3)	1.4(2)	C(12)-C(11)-C(16)-C(15)	-16.78(19)
C(19)-C(7)-C(8)-C(3)	171.63(14)	C(10)-C(11)-C(16)-C(15)	150.53(13)
C(5)-C(6)-C(9)-C(10)	102.02(15)	C(12)-C(11)-C(16)-C(23)	169.23(13)
C(7)-C(6)-C(9)-C(10)	-63.72(17)	C(10)-C(11)-C(16)-C(23)	-23.5(2)

tert-Butyl-annulene (154)

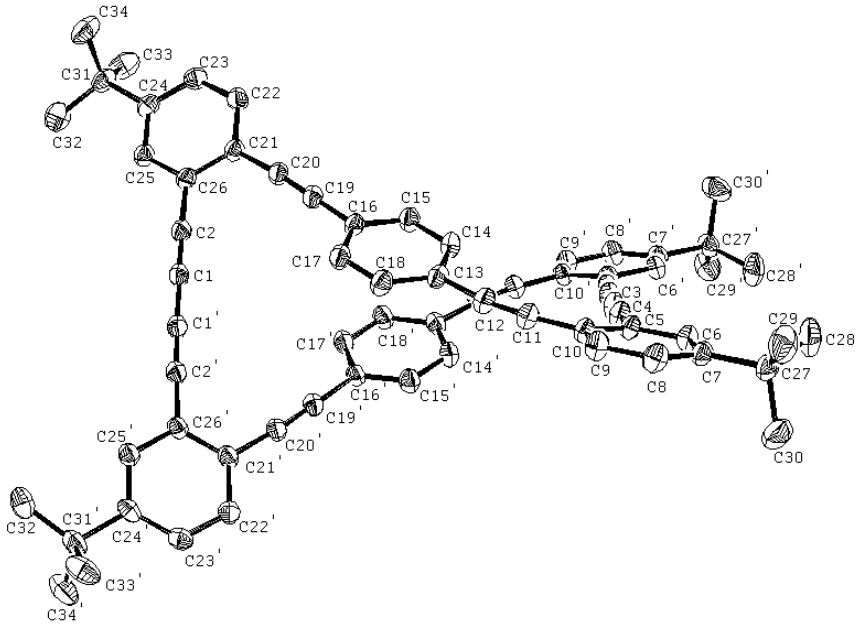

Figure 53: X-ray crystal structure of **154** (side view). Ellipsoids are drawn with 50% probability.

Table 37: Atomic coordinates (x 10^4) and equivalent isotropic displacement parameters ($Å^2$x 10^3). U(eq) is defined as one third of the trace of the orthogonalized Uij tensor.

	x	y	z	U(eq)
C(1)	303.6(5)	8551.7(8)	2626.2(8)	31.6(3)
C(2)	834.3(5)	8540.8(8)	2847.7(8)	30.4(3)
C(3)	-146.2(6)	946.2(9)	2784.6(9)	35.4(3)
C(4)	-399.4(6)	912.0(8)	3289.1(9)	33.6(3)
C(5)	-710.6(5)	817.6(8)	3868.0(8)	28.6(3)
C(6)	-884.5(5)	-90.6(8)	4036.4(8)	30.7(3)
C(7)	-1208.2(5)	-224.1(8)	4570.4(8)	30.7(3)
C(8)	-1355.8(6)	586.4(9)	4934.4(9)	35.8(3)
C(9)	-1176.2(6)	1491.7(9)	4796.5(9)	35.1(3)
C(10)	-852.1(5)	1626.0(8)	4260.5(8)	29.4(3)
C(11)	-638.6(6)	2540.6(8)	4119.2(8)	31.8(3)
C(12)	-407.1(6)	3245.5(9)	3982.3(8)	33.4(3)
C(13)	-59.9(5)	4012.3(8)	3835.4(8)	30.6(3)
C(14)	418.2(6)	3786.6(9)	3588.4(8)	33.5(3)
C(15)	786.6(6)	4492.9(9)	3490.4(8)	33.1(3)
C(16)	679.8(5)	5447.4(8)	3624.8(8)	30.2(3)
C(17)	189.6(6)	5677.8(9)	3846.0(9)	35.3(3)
C(18)	-173.1(6)	4967.2(9)	3953.8(9)	34.9(3)

C(19)	1073.7(6)	6183.0(8)	3561.7(9)	32.5(3)
C(20)	1399.9(5)	6812.3(8)	3530.5(8)	30.9(3)
C(21)	1748.4(5)	7616.9(8)	3471.4(8)	29.2(3)
C(22)	2367.0(6)	7580.1(9)	3756.7(9)	36.8(3)
C(23)	2691.0(6)	8373.4(9)	3703.7(9)	37.7(3)
C(24)	2419.7(5)	9236.4(9)	3367.8(8)	31.6(3)
C(25)	1805.9(5)	9275.5(8)	3083.8(8)	30.6(3)
C(26)	1465.1(5)	8481.9(8)	3130.7(8)	27.2(2)
C(27)	-1407.0(6)	-1224.0(9)	4725.5(9)	37.2(3)
C(28)	-1012.0(8)	-2000.6(10)	4560.2(13)	59.3(5)
C(29)	-1380.3(9)	-1327.7(12)	5649.4(10)	56.1(4)
C(30)	-2042.2(8)	-1380.0(13)	4113.0(12)	63.2(5)
C(31)	2801.7(6)	10099.4(10)	3336.7(9)	38.5(3)
C(32)	2424.5(7)	10960.7(10)	2893.5(12)	53.4(4)
C(33)	3205.9(7)	9837.6(12)	2839.3(11)	54.8(4)
C(34)	3189.2(8)	10361.3(12)	4262.0(10)	55.2(4)

Table 38: Bond lengths [Å] of **154**.

C(1)-C(2)	1.2009(17)	C(15)-C(16)	1.3965(16)
C(1)-C(1)#1	1.374(2)	C(16)-C(17)	1.3999(18)
C(2)-C(26)	1.4276(17)	C(16)-C(19)	1.4333(16)
C(3)-C(4)	1.2044(17)	C(17)-C(18)	1.3813(17)
C(3)-C(3)#1	1.370(2)	C(19)-C(20)	1.1974(16)
C(4)-C(5)	1.4257(17)	C(20)-C(21)	1.4328(16)
C(5)-C(6)	1.4008(16)	C(21)-C(22)	1.3978(17)
C(5)-C(10)	1.4104(16)	C(21)-C(26)	1.4078(16)
C(6)-C(7)	1.3918(17)	C(22)-C(23)	1.3818(17)
C(7)-C(8)	1.3933(18)	C(23)-C(24)	1.3938(18)
C(7)-C(27)	1.5342(16)	C(24)-C(25)	1.3870(17)
C(8)-C(9)	1.3874(17)	C(24)-C(31)	1.5347(16)
C(9)-C(10)	1.3955(17)	C(25)-C(26)	1.4038(15)
C(10)-C(11)	1.4333(16)	C(27)-C(29)	1.521(2)
C(11)-C(12)	1.1978(16)	C(27)-C(30)	1.522(2)
C(12)-C(13)	1.4385(16)	C(27)-C(28)	1.537(2)
C(13)-C(18)	1.3950(17)	C(31)-C(34)	1.529(2)
C(13)-C(14)	1.3957(18)	C(31)-C(32)	1.533(2)
C(14)-C(15)	1.3806(16)	C(31)-C(33)	1.535(2)

Symmetry transformations used to generate equivalent atoms: #1 -x,y,-z+1/2

Table 39: Bond angles [°] of **154**.

C(2)-C(1)-C(1)#1	179.27(9)	C(17)-C(18)-C(13)	120.54(12)
C(1)-C(2)-C(26)	177.10(13)	C(20)-C(19)-C(16)	177.90(14)
C(4)-C(3)-C(3)#1	177.67(9)	C(19)-C(20)-C(21)	175.24(13)
C(3)-C(4)-C(5)	176.69(13)	C(22)-C(21)-C(26)	118.31(10)
C(6)-C(5)-C(10)	119.87(10)	C(22)-C(21)-C(20)	122.12(11)
C(6)-C(5)-C(4)	119.27(11)	C(26)-C(21)-C(20)	119.56(10)
C(10)-C(5)-C(4)	120.85(10)	C(23)-C(22)-C(21)	120.72(12)
C(7)-C(6)-C(5)	121.88(11)	C(22)-C(23)-C(24)	121.93(12)
C(6)-C(7)-C(8)	117.28(11)	C(25)-C(24)-C(23)	117.52(11)
C(6)-C(7)-C(27)	120.84(11)	C(25)-C(24)-C(31)	122.73(12)
C(8)-C(7)-C(27)	121.86(11)	C(23)-C(24)-C(31)	119.75(11)
C(9)-C(8)-C(7)	122.03(11)	C(24)-C(25)-C(26)	121.84(11)
C(8)-C(9)-C(10)	120.68(11)	C(25)-C(26)-C(21)	119.69(11)
C(9)-C(10)-C(5)	118.21(10)	C(25)-C(26)-C(2)	120.99(11)
C(9)-C(10)-C(11)	122.95(11)	C(21)-C(26)-C(2)	119.31(10)
C(5)-C(10)-C(11)	118.79(10)	C(29)-C(27)-C(30)	109.07(13)
C(12)-C(11)-C(10)	172.09(13)	C(29)-C(27)-C(7)	110.82(11)
C(11)-C(12)-C(13)	172.24(13)	C(30)-C(27)-C(7)	108.72(11)
C(18)-C(13)-C(14)	119.00(11)	C(29)-C(27)-C(28)	108.06(13)
C(18)-C(13)-C(12)	122.51(11)	C(30)-C(27)-C(28)	108.73(14)
C(14)-C(13)-C(12)	118.47(11)	C(7)-C(27)-C(28)	111.40(11)
C(15)-C(14)-C(13)	120.68(11)	C(34)-C(31)-C(32)	109.67(13)
C(14)-C(15)-C(16)	120.29(12)	C(34)-C(31)-C(24)	108.27(11)
C(15)-C(16)-C(17)	119.09(11)	C(32)-C(31)-C(24)	112.12(11)
C(15)-C(16)-C(19)	120.80(11)	C(34)-C(31)-C(33)	108.71(12)
C(17)-C(16)-C(19)	120.08(11)	C(32)-C(31)-C(33)	108.30(12)
C(18)-C(17)-C(16)	120.34(11)	C(24)-C(31)-C(33)	109.73(11)

Symmetry transformations used to generate equivalent atoms: #1 -x,y,-z+1/2

Table 40: Torsion angles [°] of **154**.

C(10)-C(5)-C(6)-C(7)	1.45(19)	C(20)-C(21)-C(22)-C(23)	-178.93(13)
C(4)-C(5)-C(6)-C(7)	-177.59(12)	C(21)-C(22)-C(23)-C(24)	0.0(2)
C(5)-C(6)-C(7)-C(8)	0.12(18)	C(22)-C(23)-C(24)-C(25)	0.0(2)
C(5)-C(6)-C(7)-C(27)	178.41(11)	C(22)-C(23)-C(24)-C(31)	179.08(12)
C(6)-C(7)-C(8)-C(9)	-1.81(19)	C(23)-C(24)-C(25)-C(26)	0.14(19)

C(27)-C(7)-C(8)-C(9)	179.92(12)	C(31)-C(24)-C(25)-C(26)	-178.96(12)
C(7)-C(8)-C(9)-C(10)	1.9(2)	C(24)-C(25)-C(26)-C(21)	-0.21(18)
C(8)-C(9)-C(10)-C(5)	-0.31(19)	C(24)-C(25)-C(26)-C(2)	178.98(12)
C(8)-C(9)-C(10)-C(11)	-177.82(12)	C(22)-C(21)-C(26)-C(25)	0.19(18)
C(6)-C(5)-C(10)-C(9)	-1.33(18)	C(20)-C(21)-C(26)-C(25)	179.05(11)
C(4)-C(5)-C(10)-C(9)	177.69(12)	C(22)-C(21)-C(26)-C(2)	-179.02(12)
C(6)-C(5)-C(10)-C(11)	176.29(11)	C(20)-C(21)-C(26)-C(2)	-0.16(18)
C(4)-C(5)-C(10)-C(11)	-4.69(18)	C(6)-C(7)-C(27)-C(29)	143.61(14)
C(18)-C(13)-C(14)-C(15)	2.18(19)	C(8)-C(7)-C(27)-C(29)	-38.18(18)
C(12)-C(13)-C(14)-C(15)	-176.05(12)	C(6)-C(7)-C(27)-C(30)	-96.53(16)
C(13)-C(14)-C(15)-C(16)	-1.00(19)	C(8)-C(7)-C(27)-C(30)	81.68(16)
C(14)-C(15)-C(16)-C(17)	-1.02(19)	C(6)-C(7)-C(27)-C(28)	23.26(17)
C(14)-C(15)-C(16)-C(19)	177.28(12)	C(8)-C(7)-C(27)-C(28)	-158.53(13)
C(15)-C(16)-C(17)-C(18)	1.85(19)	C(25)-C(24)-C(31)-C(34)	116.44(15)
C(19)-C(16)-C(17)-C(18)	-176.46(12)	C(23)-C(24)-C(31)-C(34)	-62.64(17)
C(16)-C(17)-C(18)-C(13)	-0.7(2)	C(25)-C(24)-C(31)-C(32)	-4.68(18)
C(14)-C(13)-C(18)-C(17)	-1.34(19)	C(23)-C(24)-C(31)-C(32)	176.24(13)
C(12)-C(13)-C(18)-C(17)	176.81(12)	C(25)-C(24)-C(31)-C(33)	-125.06(14)
C(26)-C(21)-C(22)-C(23)	-0.1(2)	C(23)-C(24)-C(31)-C(33)	55.86(17)

Symmetry transformations used to generate equivalent atoms: #1 -x,y,-z+1/2

12 References

[1] O. Schlenk, *Angew. Chem.* **1925**, *38*, 782-783.

[2] R. Willstätter, E. Waser, *Ber. Dtsch. Chem. Ges.* **1911**, *44*, 3423-3445.

[3] W. Reppe, O. Schlichting, K. Klager, T. Toepel, *Liebigs Ann. Chem.* **1948**, *560*, 1-92.

[4] W. Reppe, O. Schlichting, H. Meister, *Liebigs Ann. Chem.* **1948**, *560*, 93-104.

[5] A. W. Krebs, *Angew. Chem.* **1965**, *77*, 966; *Angew. Chem. Int. Ed. Engl.* **1965**, *4*, 954.

[6] R. A. G. de Graaft, S. Gorter, C. Romers, H. N. C. Wong, F. Sondheimer, *J. Chem. Soc. Perkin Trans. 2*, **1981**, 478-480.

[7] G. Eglinton, A. R. Galbraith, *Proc. Chem. Soc.* **1957**, 350.

[8] O. M. Behr, G. Eglinton, R. A. Raphael, *Chem.& Ind.* 1959, 699-700.

[9] O. M. Behr, G. Eglinton, A. R. Galbraith, R. A. Raphael, *J. Chem. Soc.* **1960**, 3614-3625.

[10] H. A. Staab, K. Neunhoeffer, *Synthesis* **1974**, 424.

[11] S. Takahashi, Y. Kuroyama, K. Sonogashira, N. Hagigara, *Synthesis* **1980**, 627-630.

[12] a) K. Kodo, S. Yasuda, T. Sakaguchi, M. Miya, *J. Chem. Soc., Chem. Commun.* **1995**, 55-56; b) M. B. Nielsen, F. Diederich in *Modern Arene Chemistry* ed. D. Astruc, Wiley VCH, Weinheim **2002**, 196-216

[13] K. P. Baldwin, A. J. Matzger, D. A. Scheinman, C. A. Tessier, K. P. C. Vollhardt, W. J. Youngs, *Synlett* **1995**, 1215-1218.

[14] M. Laskoski, W. Steffen, J. G. M. Morton, M. D. Smith, U. H. F. Bunz, *J. Am. Chem. Soc.* **2002**, *124*, 13814-13818.

[15] M. M. Haley, S. C. Brand, J. J. Pak, *Angew. Chem.* **1997**, *109*, 864-866; *Angew. Chem. Int. Ed. Engl.* **1997**, 836-838.

[16] M. Laskoski, M. D. Smith, J. G. M. Morton, U. H. F. Bunz, *J. Org. Chem.* **2001**, *66*, 5174-5181.

[17] L. T. Scott, M. A. Kirms, H. Günther, H. von Puttkammer, *J. Am. Chem. Soc.* **1983**, *105*, 1372-1373.

[18] M. Laskoski, G. Roidl, M. D. Smith, U. H. F. Bunz, *Angew. Chem.* **2001**, *113*, 1508-1511; *Angew. Chem. Int. Ed. Engl.* **2001**, 1460-1463.

[19] M. Laskoski, W. Steffen, M. D. Smith, U. H. F. Bunz, *Chem. Commun.* **2001**, 691-692.

[20] S. K. Collins, G. P. A. Yap, A. G. Fallis, *Org. Lett.* **2000**, *2*, 3189-3192.

[21] M. A. Heuft, S. K. Collins, A. G. Fallis, *Org. Lett.* **2003**, *3*, 2883-2886.

[22] Y. Rubin, T. C. Parker, S. I. Kahn, C. L. Holliman, S. W. McElvany, *J. Am. Chem. Soc.* **1996**, *118*, 5308-5309.

[23] C. J. Brown, A. C. Farthing, *Nature* **1949**, *164*, 915.

[24] D. J. Cram, H. Steinberg, *J. Am. Chem. Soc.* **1951**, *73*, 5691-5704.

[25] H. E. Winberg, F. S. Fawcett, *Org. Synth. Coll. Vol. V*, J. Wiley and Sons, New York, N. Y. **1973**, 883-886.

[26] F. Vögtle, *Angew. Chem.* **1969**, *81*, 258-259; *Angew. Chem. Int. Ed. Engl.* **1969**, *8*, 274.

[27] V. Boeckelheide, *Topics Curr. Chem.* **1983**, *113*, 87-143.

[28] H. A. Staab, M. Haenel, *Tetrahedron Lett.* **1970**, 3585-3588.

[29] H. Hopf, *Angew. Chem.* **1972**, *84*, 471-472; *Angew. Chem. Int. Ed. Engl.* **1972**, *11*, 419-420.

[30] C. J. Brown, *J. Chem. Soc.* **1953**, 3265-3270.

[31] a) H. Steinberg, D. J. Cram, *J. Am. Chem. Soc.* **1952**, *74*, 5388-5391; b) D. J. Cram, N. L. Allinger, *J. Am. Chem. Soc.* **1954**, *76*, 726-731; c) N. L. Allinger, D. J. Cram, *J. Am. Chem. Soc.* **1954**, *76*, 2362-2367; d) J. Abell, D. J. Cram, *J. Am. Chem. Soc.* **1954**, *76*, 4406-4412; e) D. J. Cram, N. L. Allinger, H. Steinberg, *J. Am. Chem. Soc.* **1954**, *76*, 6132-6141; f) D. J. Cram, J. Abell, *J. Am. Chem. Soc.* **1955**, *77*, 1179-1186; g) D. J. Cram, R. W. Kierstead, *J. Am. Chem. Soc.* **1955**, *77*, 1186-1190; h) D. J. Cram, M. Cordon, *J. Am. Chem. Soc.* **1955**, *77*, 4090-4094; i) D. J. Cram, N. L. Allinger, *J. Am. Chem. Soc.* **1955**, 77, 6289-6294.

[32] H. J. Reich, D. J. Cram, *J. Am. Chem. Soc.* **1969**, *91*, 3505-3516.

[33] A. J. Boydston, L. Bondarenko, I. Dix, T. J. R. Weakley, H. Hopf, M. M. Haley, *Angew. Chem.* **2001**, 3074-3077; *Angew. Chem. Int. Ed.* **2001**, *40*, 2986-2989.

[34] S. Hentschel, *Dissertation* **1989**, TU Braunschweig.

[35] E. J. Corey, P. L. Fuchs, *Tetrahedron Lett* **1972**, *36*, 3769-3772.

[36] J. Hillmer, *Dissertation* **1991**, TU Braunschweig.

[37] S. Müller, B. Liepold, G. J. Roth, H. J. Bestmann, *Synlett* **1996**, 521-522.

[38] L. Bondarenko, I. Dix, H. Hinrichs, H. Hopf, *Synthesis* **2004**, 2751-2759.

[39] I. Dix, *Dissertation* **2000**, TU Braunschweig.

[40] H. J. Reich, D. J. Cram, *J. Am. Chem. Soc.* **1969**, 3527-3533.

[41] B. König, *Dissertation* **1991**, Universität Hamburg; B. König, B. Knieriem, A. de Meijere, *Chem. Ber.* **1993**, *126*, 1643-1650.

[42] H. Hinrichs, *Diplomarbeit* **2000**, TU Braunschweig.

[43] H. Hopf, D. G. Barrett, *Liebigs Ann.* **1995**, 449-452.

[44] D. J. Cram, A. C. Day, *J. Org. Chem.* **1966**, *31*, 1227-1232.

[45] L. Ernst, L. Wittkowski, *Eur. J. Org. Chem.* **1999**, *7*, 1653-1664.

[46] K. Krohn, H. Rieger, H. Hopf, D. Barrett, P. G. Jones, D. Döring, *Chem. Ber.* **1990**, *123*, 1729-1732.

[47] N. A. Powell, S. D. Rychnovsky, *Tetrahedron Lett.* **1996**, *37*, 7901-7904.

[48] K. Lonsdale, H. J. Milledge, K. V. K. Rao, *Proc. R. Soc. London, A* **1960**, *255*, 82-100.

[49] L. Ernst, *Liebigs Ann.* **1995**, 13-17.

[50] H. Friebolin, *Ein- und zweidimensionale NMR-Spektroskopie*, VCH Weinheim, **1988**.

[51] H. Günther, *NMR-Spektroskopie, 3. Auflage*, Georg Thieme Verlag, Stuttgart **1992**.

[52] J. M. Kehoe, J. H. Kiley, J. J. English, C. A. Johnson, R. C. Petersen, M. M. Haley, *Org. Lett.* **2000**, *2*, 969-972.

[53] W. B. Wan, M. M. Haley, *J. Org. Chem.* **2001**, *66*, 3893-3901.

[54] J. J. Pak, T. J. R. Weakley, M. M. Haley, *J. Am. Chem. Soc.* **1999**, 121, 8182-8192.

[55] J. Zhang, D. J. Pesak, J. L. Ludwick, J. S. Moore, *J. Am. Chem. Soc.* **1994**, *116*, 4227-4239.

[56] S. Kajigaeshi, T. Kakinami, H. Yamasaki, S. Fujisaki, T. Okamoto, *Bull. Chem. Soc. Jpn.* **1988**, *61*, 600-602.

[57] D. Chemin, G. Linstrumelle, *Tetrahedron* **1994**, *50*, 5335-5344.

[58] M. Hesse, H. Meier, B. Zeeh, *Spektrokopische Methoden in der organischen Chemie, 5. Auflage*, Georg Thieme Verlag, Stuttgart **1995**.

[59] A. J. Matzger, K. P. C. Vollhardt, *Tetrahedron Lett.* **1998**, *39*, 6791-6794.

[60] W. B. Wan, R. C. Chiechi, T. J. R. Weakley, M. M. Haley, *Eur. J. Org. Chem.* **2001**, 3485-3490.

[61] N. J. Turro, *Modern Molecular Photochemistry*, University Science Books, Sausalito, **1991**.

[62] M. Kasha, *Disc. Faraday Soc.* **1950**, *9*, 14-21.

[63] F. H. Allen, O. Kennard, D. G. Watson, L. Brammer, A. G. Orpen, *J. Chem. Soc. Perkin Trans. II* **1987**, S1-S19.

[64] J. Grunenberg, personal communication.

[65] K. P. C. Vollhardt, *Angew. Chem.* **1984**, *96*, 525-541; *Angew. Chem. Int. Ed. Engl.* **1984**, *23*, 539-555.

[66] R. Gleiter, D. Kratz, *Angew. Chem.* **1990**, *102*, 304-307; *Angew. Chem. Int. Ed. Engl.* **1990**, 276-279.

[67] D. R. McAlister, J. E. Bercaw, R. G. Bergman, *J. Am. Chem. Soc.* **1977**, 1666-1668.

[68] C. N. Iverson, W. D. Jones, *Organometallics* **2001**, 5745-5750.

[69] O. Bastiansen, M. Traetteberg, *Tetrahedron* **1962**, *17*, 147.

[70] K. Kuchitsu, *J. Chem. Phys.* **1968**, *83*, 64.

[71] T. C. W. Mak, J. Trotter, *J. Chem. Soc.* **1962**, 1-8.

[72] D. Holmes, S. Kumaraswamy, A. J. Matzger, K. P. C. Vollhardt, *Chem. Eur. J.* **1999**, *5*, 3399-3412.

[73] R. R. Jones, R. G. Bergman, *J. Am. Chem. Soc.* **1972**, *94*, 660-661.

[74] R. G. Bergman, *Acc. Chem. Res.* **1973**, *6*, 25-31.

[75] D. J. Cram, C. K. Dalton, G. R. Knox, *J. Am. Chem. Soc.* **1963**, *85*, 1088-1093.

[76] J. A. Tour, A. M. Rawlett, M. Kozaki, Y. Yao, R. C. Jagessar, S. M. Dirk, D. W. Price, M. A. Reed, C.-W. Zhou, J. Chen, W. Wang, I. Campbell, *Chem. Eur. J.* **2001**, *23*, 5118-5134.

[77] M. Nimtz, personal communication.

[78] R. Herges, D. Geuenich, *J. Phys. Chem. A* **2001**, *105*, 3214-4220.

[79] A. Lüttringhaus, H. Gralheer, *Ann. Chem.* **1941**, 67-98.

[80] a) D. J. Cram, W. J. Wechter, R. W. Kierstead, *J. Am. Chem. Soc.* **1958**, *80*, 3126. b) D. J. Cram, R. A. Reeves, *J. Am. Chem. Soc.* **1958**, *80*, 3094.

[81] R. S. Cahn, C. K. Ingold, *J. Chem. Soc.* **1951**, 612-622.

[82] R. S. Cahn, C. K. Ingold, V. Prelog, *Experientia* **1956**, *12*, 81.

[83] R. S. Cahn, C. K. Ingold, V. Prelog, *Angew. Chem.* **1966**, 413-447; *Angew. Chem. Int. Ed. Engl.* **1966**, *5*, 385-415.

[84] Y. Okamoto, personal communication.

[85] C. Schulz, *Dissertation* **2000**, TU Braunschweig.

[86] D. Pamperin, C. Schulz, H. Hopf, C. Syldatk, M. Pietsch, *Eur. J. Org. Chem.* **1998**, 1441-1445.